

**RĪGAS TEHNISKĀ UNIVERSITĀTE**

Materiālzinātnes un lietišķās ķīmijas fakultāte  
Organiskās ķīmijas tehnoloģijas institūts

**RIGA TECHNICAL UNIVERSITY**

Faculty of Materials Science and Applied Chemistry  
Institute of Technology of Organic Chemistry

**Aleksandrs Pustenko**

Doktora studiju programmas “Ķīmija” doktorants  
Doctoral Student of the Study Programme “Chemistry”

**JAUNA VEIDA OĢĻSKĀBES ANHIDRĀŽU  
INHIBITORU SINTĒZE**

**Promocijas darbs**

**SYNTHESIS OF A NEW TYPE OF CARBONIC  
ANHYDRASES INHIBITORS**

**Doctoral Thesis**

Zinātniskais vadītājs  
asociētais profesors *Dr. chem.*  
RAIVIS ŽALUBOVSKIS

Scientific supervisor  
Associate Professor *Dr. chem.*  
RAIVIS ŽALUBOVSKIS

RTU Izdevniecība / RTU Press  
Rīga 2020 / Riga 2020

Pustenko, A. Jauna veida ogļskābes anhidrāžu inhibitoru sintēze. Promocijas darbs. Rīga: RTU Izdevniecība, 2020. 102 lpp.

Pustenko, A. Synthesis of a New Type of Carbonic Anhydrases Inhibitors. Doctoral Thesis. Riga: RTU Press, 2020. 102 p.

Iespiests saskaņā ar RTU promocijas padomes “P-01” 2020. gada 12. jūnija lēmumu, protokols Nr. 1.

Published in accordance with the decision of the Promotion Council “P-01” of 26 June 2020, Minutes No. 1.

# PROMOCIJAS DARBS IZVIRZĪTS ZINĀTNES DOKTORA GRĀDA IEGŪŠANAI RĪGAS TEHNISKAJĀ UNIVERSITĀTĒ

Promocijas darbs zinātnes doktora (*Ph. D.*) grāda iegūšanai tiek publiski aizstāvēts 2020. gada 30. septembrī Rīgas Tehniskās universitātes Materiālzinātnes un lietišķās ķīmijas fakultātē, Rīgā, Paula Valdena ielā 3, 272. auditorijā.

## OFICIĀLIE RECENZENTI

Docente *Dr. chem.* Jeļena Kirilova,  
Daugavpils Universitāte, Latvija

Profesors *Dr. chem. Jean-Yves Winum*,  
Monpeljē Universitāte (*Université de Montpellier*), Francija (*French Republic*)

Vadošais pētnieks *Dr. chem.* Kaspars Traskovskis,  
Rīgas Tehniskā universitāte, Latvija

## APSTIPRINĀJUMS

Apstiprinu, ka esmu izstrādājis šo promocijas darbu, kas iesniegts izskatīšanai Rīgas Tehniskajā universitātē zinātnes doktora grāda (*Ph. D.*) iegūšanai. Promocijas darbs zinātniskā grāda iegūšanai nav iesniegts nevienā citā universitātē.

Aleksandrs Pustenko ..... (paraksts)

Datums: .....

Promocijas darbs sagatavots kā tematiski vienota zinātnisko publikāciju kopa. Tajā ir kopsavilkums un piecas publikācijas. Publikācijas uzrakstītas angļu valodā, to kopējais apjoms ir 39 lpp.

# SATURS

<b>PROMOCIJAS DARBA VISPĀRĒJS RAKSTUROJUMS .....</b>	<b>5</b>
Tēmas aktualitāte .....	5
Promocijas darba mērķis .....	5
Promocijas darba uzdevumi.....	6
Zinātniskā novitāte un galvenie rezultāti.....	6
Darba struktūra un apjoms.....	6
Darba aprobācija un publikācijas .....	6
<b>PROMOCIJAS DARBA GALVENIE REZULTĀTI.....</b>	<b>8</b>
1. 3 <i>H</i> -1,2-Benzoksatiepīna-2,2-dioksīda atvasinājumu sintēze.....	10
1.1. 3 <i>H</i> -1,2-Benzoksatiepīna-2,2-dioksīda 1,2,3-triazolilatvasinājumu sintēze .....	12
1.2. 3 <i>H</i> -1,2-Benzoksatiepīna-2,2-dioksīda 7-acilaminoatvasinājumu sintēze.....	14
1.3. 3 <i>H</i> -1,2-Benzoksatiepīna-2,2-dioksīda arilatvasinājumu sintēze.....	15
2. Imidazolidīn-2,4-diona atvasinājumu sintēze.....	22
<b>SECINĀJUMI.....</b>	<b>25</b>
<b>LITERATŪRAS SARAKSTS.....</b>	<b>26</b>
<b>PATEICĪBAS .....</b>	<b>29</b>
<b>PIELIKUMI.....</b>	<b>58</b>

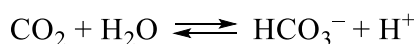
# PROMOCIJAS DARBA VISPĀRĒJS RAKSTUROJUMS

## Tēmas aktualitāte

Pēc Pasaules Veselības organizācijas datiem 2018. gadā pasaulē tika reģistrēti 9,6 miljoni onkoloģisko saslimšanu izraisīti nāves gadījumi un 18,1 miljoni jaunu onkoloģisko saslimšanas gadījumu. Katrs piektais vīrietis un katra sestā sieviete dzīves laikā saslimst ar vēzi [1]. Eiropā, kur dzīvo ~9 % no visiem pasaules iedzīvotājiem, 2018. gadā reģistrēti 23,4 % no visiem onkoloģisko saslimšanu gadījumiem, tai skaitā 20,3 % no visiem nāves gadījumiem, tāpēc ir ļoti svarīgi nepārtraukti attīstīt un pilnveidot onkoloģisko slimību ārstēšanas iespējas [1].

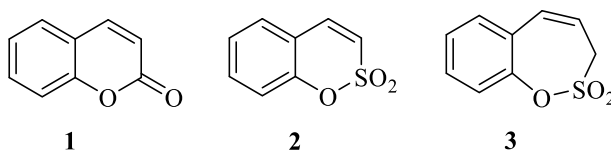
Mūsdienās ir zināmi vairāk nekā 300 dažādi enzīmi, kuriem cinks ir nozīmīgs kofaktors. Šie enzīmi organismā veic bioloģiski nozīmīgas funkcijas, to darbība ir tieši saistīta ar epiģenētiskās kontroles mehānismiem šūnās, kuru regulēšanas traucējumi ir viens no galvenajiem vēža rašanās cēloņiem [2].

Pēdējā desmitgadē pastiprināta uzmanība pievērsta cinku saturošiem metalloenzīmiem – ogļskābes anhidrāzēm (CA, EC 4.2.1.1), kas organismā katalizē apgriezenisku oglekļa dioksīda hidratāciju.



Tiek uzskatīts, ka no šobrīd zināmajām 15 cilvēka  $\alpha$ -ogļskābes anhidrāžu izoformām, CA IX un CA XII tiek paaugstināti ekspresētas hipoksijai pakļautajās vēža šūnās, nodrošinot optimālu pH to izdzīvošanai un attīstībai. Lai apturētu vēža šūnu attīstību un izvairītos no nevēlamām blaknēm, jānodrošina selektīva CA IX un CA XII izoformu inhibēšana.

Literatūrā [3] zināms, ka kumarīna **1** atvasinājumiem piemīt selektīva CA IX un CA XII inhibēšanas spēja. Mūsu grupā tika sintezēti sulfokumarīna **2** atvasinājumi, kas izrādījās selektīvi CA IX un CA XII inhibitori [4]. Balstoties uz šīm zināšanām, tika sintezēti benzoksatiepīna-2,2-dioksīda **3** atvasinājumi, kas ir sulfokumarīna atvasinājumi ar paplašinātu ciklu.

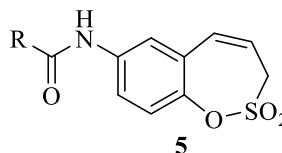
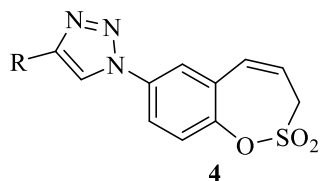


## Promocijas darba mērķis

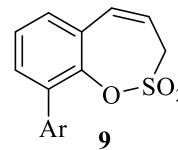
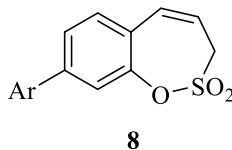
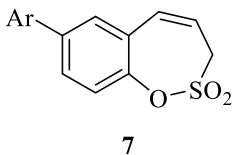
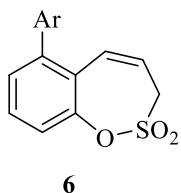
Izveidot jaunus, efektīvus un selektīvus CA IX un CA XII inhibitorus, no kuriem nākotnē, iespējams, varētu tikt izstrādāts jaunas paaudzes pretvēža līdzeklis.

## Promocijas darba uzdevumi

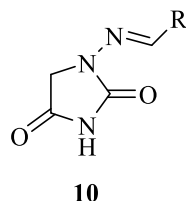
1. Izstrādāt 3*H*-1,2-benzoksatiepīna-2,2-dioksīda **3** atvasinājumu iegūšanas metodes.
2. Iegūt 3*H*-1,2-benzoksatiepīna-2,2-dioksīda 7-triazolil- **4** un 7-acilaminoatvasinājumus **5**.



3. Iegūt 6-, 7-, 8- un 9-aizvietotus 3*H*-1,2-benzoksatiepīna-2,2-dioksīda arilatvasinājumus **6–9**.



4. Iegūt 1-imidazolidīn-2,4-diona atvasinājumus **10**.



5. Izvērtēt sintezēto savienojumu CA inhibēšanas aktivitātes.

## Zinātniskā novitāte un galvenie rezultāti

Ir atrasta jauna, selektīva CA IX un CA XII inhibitoru klase – 3*H*-1,2-benzoksatiepīna-2,2-dioksīdi. Sintezēta virkne 3*H*-1,2-benzoksatiepīna-2,2-dioksīda triazolil-, acilamino- un arilatvasinājumu.

Atklājām, ka furagīns, klīnikā lietots antibakteriālais līdzeklis, ir selektīvs CA IX un CA XII inhibitors. Attīstot šo virzienu, tika sintezēta virkne imidazolidīn-2,4-diona atvasinājumu. Visiem promocijas darbā iegūtajiem produktiem noteikta cilvēka CA (I, II, IX un XII) izoformu inhibēšanas aktivitāte.

## Darba struktūra un apjoms

Promocijas darbs sagatavots kā tematiski vienota zinātnisko publikāciju kopa par ogļskābes anhidrāzes inhibitoru sintēzi.

## Darba aprobācija un publikācijas

Promocijas darba rezultāti izklāstīti piecās zinātniskajās publikācijās, publikāciju kopējā ietekmes faktoru summa – 16,9. Darba rezultāti prezentēti sešās konferencēs.

## Zinātniskās publikācijas

1. Pustenko, A., Nocentini, A., Gratteri, P., Bonardi, A., Vozny, I., Žalubovskis, R., Supuran, C. T. The antibiotic furagin and its derivatives are isoform-selective human carbonic anhydrase inhibitors. *J. Enzyme Inhib. Med. Chem.* **2020**, *35*, 1011–1020.
2. Pustenko, A., Nocentini, A., Balašova, A., Krasavin, M., Žalubovskis, R., Supuran, C. T. 7-acylamino-3H-1,2-benzoxathiepine 2,2-dioxides as new isoform-selective carbonic anhydrase IX and XII inhibitors. *J. Enzyme Inhib. Med. Chem.* **2020**, *35*, 650–656.
3. Pustenko, A., Nocentini, A., Balašova, A., Alafeefy, A., Krasavin, M., Žalubovskis, R., Supuran, C. T. Aryl derivatives of 3H-1,2-benzoxathiepine 2,2-dioxide as carbonic anhydrase inhibitors. *J. Enzyme Inhib. Med. Chem.* **2020**, *35*, 245–254.
4. Pustenko, A., Stepanovs, D., Žalubovskis, R., Vullo, D., Kazaks, A., Leitans, J., Tars, K., Supuran, C. 3H-1,2-benzoxathiepine 2,2-dioxides: a new class of isoform-selective carbonic anhydrase inhibitors. *J. Enzyme Inhib. Med. Chem.* **2017**, *32*, 767–775.
5. Pustenko, A., Žalubovskis, R. Recent advances in sultone synthesis (microreview). *Chem. Heterocycl. Compd.* **2017**, *53*, 1283–1285.

## Darba rezultāti prezentēti sešās zinātniskajās konferencēs

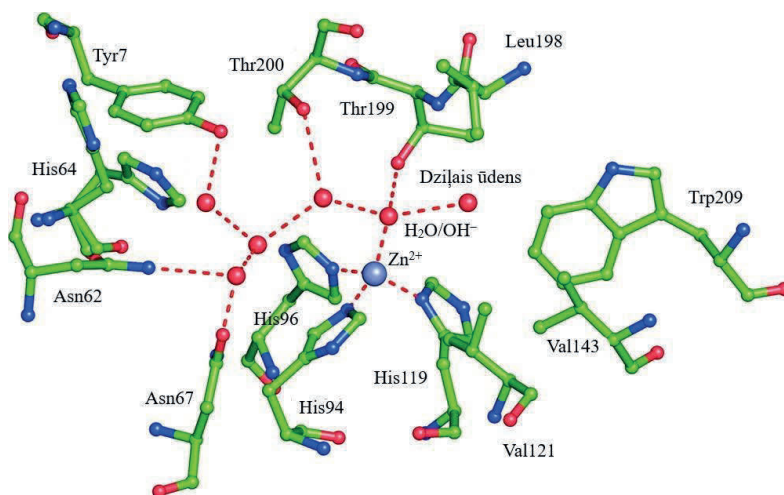
1. Žalubovskis, R., Grandāne, A., Ivanova, J., Balode, A., Pustenko, A., Domraceva, I., Tārs, K., Leitāns, J. Challenging design and synthesis of inhibitors of carbonic anhydrases. *International Conference on Organic Synthesis Balticum Organicum Syntheticum (BOS-2016)*. Riga, Latvia, July 3–6, **2016**.
2. Pustenko, A. Carbonic Anhydrases: Inhibitor Synthesis. *10<sup>th</sup> Paul Walden Symposium on Organic Chemistry*, Riga, Latvia, June 15–16, **2017**.
3. Žalubovskis, R., Ivanova, J., Pustenko, A., Grandane, A., Domraceva, I., Tars, K., Supuran, C., T. Inhibitors of Carbonic Anhydrases—challenges of design and synthesis. *3<sup>rd</sup> Satellite Meeting on Carbonic Anhydrase “New Trend in Carbonic Anhydrases Research”*, Montecatini Terme, Italy, May 24–27, **2017**.
4. Pustenko, A., Ivanova, J., Grandane, A., Vozny, I., Žalubovskis, R. Towards Novel Inhibitors of Cancer Associated Enzymes. *11<sup>th</sup> International Conference on Carbonic Anhydrases*, Bucharest, Romania, June 27–30, **2018**.
5. Pustenko, A., Balašova, A. Carbonic Anhydrases: Inhibitor Synthesis. *11<sup>th</sup> Paul Walden Symposium on Organic Chemistry*, Riga, Latvia, September 19–20, **2019**.
6. Pustenko, A., Balašova, A., Kapura, V., Žalubovskis, R. Inhibitors of cancer associated enzymes – design and synthesis. *4<sup>th</sup> Satellite Meeting on Carbonic Anhydrases*, Parma, Italy, November 14–17, **2019**.

## PROMOCIJAS DARBA GALVENIE REZULTĀTI

Lai labāk izprastu promocijas darbā paveikto, sākotnēji jāaplūko mērķenzīmu ogļskābes anhidrāzes (CA). Ogļskābes anhidrāzes ir metalloenzīmi, kas katalizē apgriezenisku oglekļa dioksīda hidratāciju. Ogļskābes anhidrāzes tika atklātas 1933. gadā, kopš tā laika tās ir plaši pētītas. Mūsdienās ogļskābes anhidrāzes iedala astoņās dažādās klasēs:  $\alpha$ ,  $\beta$ ,  $\gamma$ ,  $\delta$ ,  $\xi$ ,  $\eta$ ,  $\theta$  un  $\iota$  [5], [6].  $\alpha$ -CA ir visplašāk pētītā klase, jo šīs klases ogļskābes anhidrāzes sastopamas zīdītājos.  $\beta$ -CA sastopamas augstākajos augos un dažos prokariotos.  $\gamma$ -CA sastopamas arheobaktērijās (*Archea*) un cianobaktērijās.  $\delta$ - un  $\xi$ -CA sastopamas tikai aļģēs, savukārt  $\eta$ -CA – tikai vienšūņos [7].  $\alpha$ -,  $\beta$ - un  $\delta$ -CA aktīvajā centrā satur Zn(II) jonus,  $\gamma$ -CA satur Fe(II) jonus,  $\xi$ -CA satur Co(II) jonus un  $\iota$ -CA satur Mn(II) jonus [5, 6]. Daudzos organismos CA piedalās vitāli svarīgu fizioloģisko procesu norisē, kas saistīti ar pH regulēšanu un CO<sub>2</sub> homeostāzes nodrošināšanu [7].

Cilvēkos ir zināmas 15  $\alpha$ -CA izoformas. CA I, II, III, VII un XIII atrodas citosolā, CA IV, IX, XII un XIV ir piesaistītas membrānai, CA VA un VB atrodas mitohondrijā, savukārt CA VI atrodas siekalās un mātes pienā [8], [9]. Jāatzīmē, ka visām  $\alpha$ -CA izoformām, izņemot CA VB, ir zināma 3D struktūra. Neatkarīgi no dažādā novietojuma šūnā visas  $\alpha$ -CA izoformas ir strukturāli līdzīgas, tās ir monomēras, izņemot CA IX, CA XII un CA VI – tās ir dimēras [8].

$\alpha$ -CA aktīvais centrs ir novietots konusveida dobumā, kas ir aptuveni 12 Å plats un 13 Å dziļš. Cinka jons ir novietots dobuma apakšā, tas ir saistīts ar ligandiem – 3 histidīna atlikumiem (His119, His94 un His 96), ūdens molekulu / hidroksīdjonu (1. att.) [7], [8].



1. att. CAII aktīvā centra struktūra [8].

Zn<sup>2+</sup> jons ar ūdenraža saitēm ir saistīts ar treonīna (Thr199) hidroksilgupu un divām pretēji novietotām ūdens molekulām. Ūdens molekulu, kas novietota hidrofobajā daļā, sauc par "dziļo ūdeni" ("deep water"), to ieskauj Val121, Val143, Leu198 un Trp207. Otra ūdens molekula novietota hidrofilajā daļā, aktīvā centra ieejā, un to ieskauj Asn62, His64 un Asn67.



Hidrofobais un hidrofilais apgabals skaidrojams ar substrāta ( $\text{CO}_2$ ) un tā hidratācijas produktu ( $\text{H}^+$  un  $\text{HCO}_3^-$ ) dažādo ķīmisko dabu [8]. Makkenna (*McKenna*) ar līdzstrādniekiem parādīja, ka  $\text{CO}_2$  molekula saistās enzīma hidrofobajā daļā, savukārt hidratācijas produkti – enzīma hidrofilajā daļā [10].

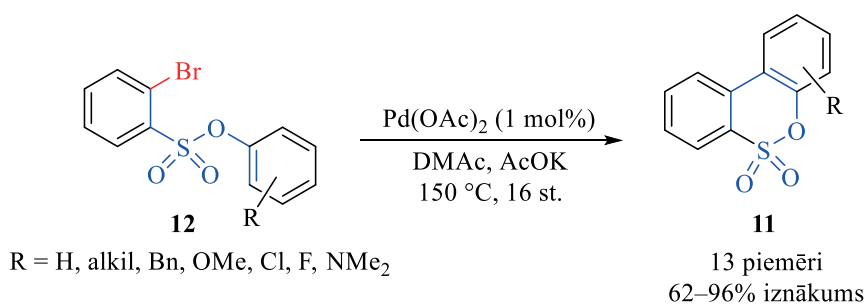
Jāatzīmē, ka visām līdz šim kristalizētajām cilvēka CA izoformām cinka jons ir saistīts ar trīs histidīna atlikumiem (His119, His94 un His 96) un tām visām ir novērota hidrofobā un hidrofilā daļa [7]. Balstoties uz šīm zināšanām par mērķenzīmu, tiek konstruēti un izstrādāti inhibitori.

Mūsdienās ir zināmi vairāki  $\alpha$ -CA inhibīcijas mehānismi. Sulfonamīdi ( $\text{RSO}_2\text{NH}_2$ ), sulfamāti ( $\text{ROSO}_2\text{NH}_2$ ), sulfamīdi ( $\text{RNHSO}_2\text{NH}_2$ ), karboksilāti ( $\text{RCO}_2^-$ ), ureāti un fosfonāti ( $\text{R}'\text{PO}(\text{OR})_2$ ) saistās ar enzīma aktīvajā centrā esošo cinka jonu un veido papildu H-saites ar Thr199. Fenoli un poliamīdi koordinējas ar ūdens molekulu / hidroksīdjonu, kas saistīts pie cinka. Kumarīni un to izostēri nosedz ieeju aktīvajā centrā, tādējādi CA aktivatori nevar piesaistīties pie enzīma [11], [12].

3*H*-1,2-Benzoksatiepīna-2,2-dioksīds ir uzskatāms par sultonu. Termins “sultoni” pirmo reizi tika lietots 1888. gadā. Mūsdienās sultoni tiek plaši izmantoti medicīnas ķīmijā kā enzīmu inhibitori, tiem piemīt pretvīrusu iedarbība. Labākās sultonu iegūšanas metodes ir pārejas metālu katalīze, ciklopievienošanās reakcijas un *Diels–Alder* tipa reakcijas [13].

Promocijas darba izstrādes laikā tika apkopota un vēlāk arī publicēta jaunākā informācija par pārejas metālu katalizētām sultonu sintēzes metodēm. Sultonus iespējams iegūt pallādija, rodija, vara, zelta un rutēnija katalizētās reakcijās, tuvāk tiks aplūkotas dažas no šīm metodēm.

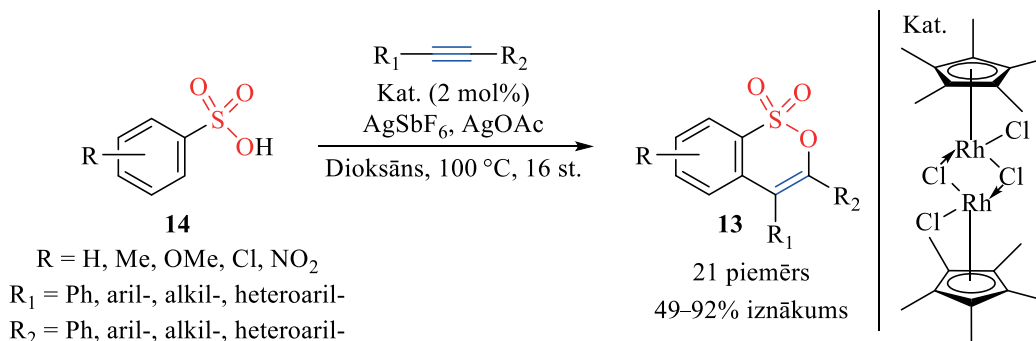
Doucets (*Doucet*) un līdzstrādnieki publicēja pallādija katalizētu sultonu **11** sintēzes metodi (2. att.), kā izejvielu izmantojot 2-brombenzosulfonskābes fenilesteri **12** [14].



2. att. Pallādija katalizēta sultonu **11** sintēze.

Jāatzīmē, ka reakcija ir atkarīga no aizvietotāja R dabas. Izmantojot elektrononus aizvietotājus, reakcijas produktu iznākums palielinās, savukārt, izmantojot elektronakceptorus aizvietotājus ( $\text{NO}_2$ ,  $\text{CO}_2\text{Bu}$ ,  $\text{CF}_3$ ), attiecīgie sultoni neveidojas. Visos gadījumos sultoni **11** tika iegūti ar augstu reģioselektivitāti.

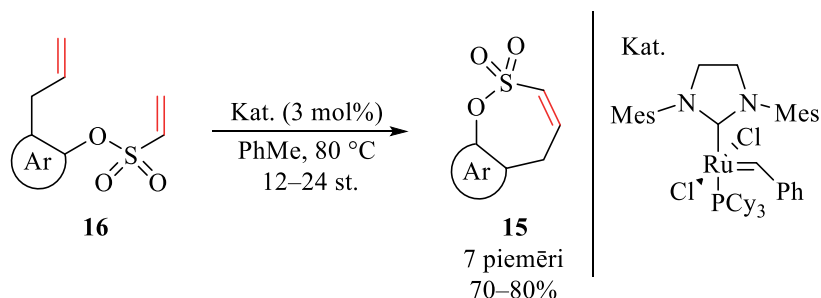
Li (*Li*) un līdzstrādnieki izstrādāja efektīvu Rh(III) katalizētu sultonu **13** sintēzes metodi no arilsulfonskābēm **14** un alkīniem (3. att.) [15].



3. att. Rodija katalizēta sultonu **13** sintēze.

Šajā metodē iespējams izmantot alkīnus gan ar elektrondonoriem, gan ar elektronakceptoriem aizvietotājiem. Jāatzīmē, ka, izmantojot alkīnu ar elektrondonoriem aizvietotājiem, reakcijas produkta iznākums ir augstāks. Izmantojot nesimetriskus alkīnus, attiecīgie sultoni tika iegūti ar ļoti labu reģioselektivitāti.

Mondals (*Mondal*) un līdzstrādnieki publicēja efektīvu sultonu **15** sintēzes metodi no attiecīgajiem diolefiniem **16**, tos ciklizējot (4. att.) [16]. Diolefini **16** tika ciklizēti, izmantojot rutēnija katalizētu olefīnu cikla saslēgšanas metatēzes reakciju. Jāatzīmē, ka, izmantojot Grabsa (*Grubbs*) pirmās paaudzes rutēnija katalizatoru, sultoni **15** neveidojās. Izmantojot Grabsa otrās paaudzes rutēnija katalizatoru, sultoni **15** tika iegūti ar labiem iznākumiem.



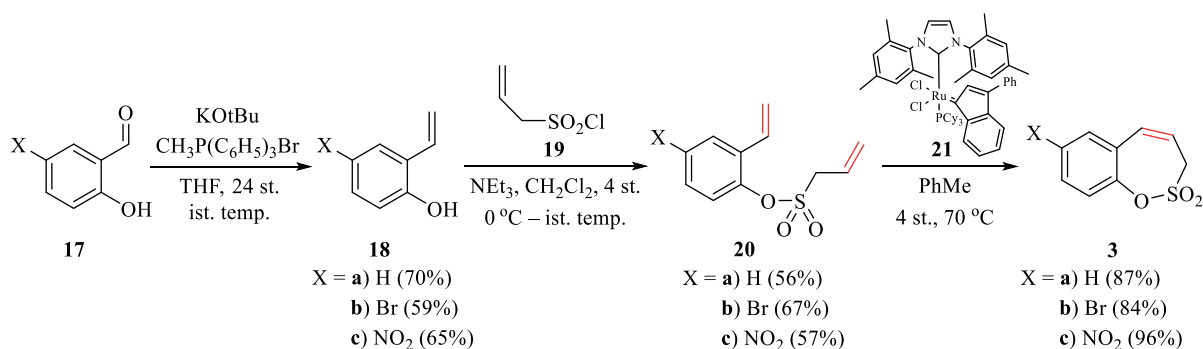
4. att. Rutēnija katalizēta sultonu **15** sintēze.

Izanalizējot literatūrā pieejamo informāciju, benzoksatiepīna-2,2-dioksīda **3** atvasinājumus nolēmām iegūt rutēnija katalizētā olefīnu cikla saslēgšanas metatēzes reakcijā. Izmantojot cikla saslēgšanas metatēzes reakciju, iespējams iegūt sultonus ar elektrondonoriem un elektronakceptoriem aizvietotājiem. Reakcijas produktu iznākumi parasti ir augsti.

### 1. 3*H*-1,2-Benzoksatiepīna-2,2-dioksīda atvasinājumu sintēze

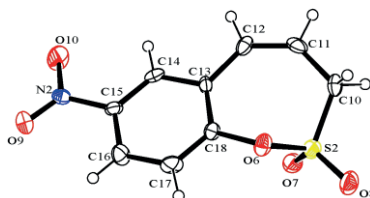
Pētījuma sākumā tika izstrādāta sintēzes metode. Sintēzi sākām no 5-aizvietota 2-hidroksibenzaldehīda **17**, tam veicot Vitiga reakciju, ieguvām olefīnus **18** (5. att.). Olefīnus **18** apstrādājām ar sulfonilhlorīdu **19**, iegūstot diolefinus **20** ar pieņemamiem iznākumiem (56–67 %). Sulfonilhlorīds **19** ir komerciāli pieejams, taču dārgs reaģents. To veiksmīgi ieguvām,  $Na_2SO_3$  vārot ar alilbromīdu, pēc tam iegūto nātrija sāli apstrādājām ar  $POCl_3$ . Jāatzīmē, ka sulfonilhlorīds **19** gaisā nav stabils, tāpēc to ieguvām lielākā daudzumā, lai attīrīšanu veiktu vakuumdestilācijas ceļā. Izmantojot nedestilētu sulfonilhlorīdu **19**, reakcijas produktu

iznākums būtiski samazinās. Kā galvenā stadija benzoksatiepīna-2,2-dioksīda iegūšanā tika izvēlēta diolefīna **20** ciklizācija, izmantojot olefīnu cikla saslēgšanas metatēzes reakciju. Ciklizāciju veiksmīgi veicām, izmantojot komerciāli pieejamo Grabsa otrās paaudzes katalizatora atvasinājumu **21**. Veiksmīgi ieguvām attiecīgos 7- aizvietotus 3*H*-1,2-benzoksatiepīna-2,2-dioksīdus **3** ar augstiem iznākumiem (84–96 %).



5. att. Benzoksatiepīna-2,2-dioksīda atvasinājumu **3a–3c** iegūšana.

Darba gaitā veiksmīgi izdevās iegūt 7-nitro-3*H*-1,2-benzoksatiepīna-2,2-dioksīda **3c** monokristālu, kas bija pietiekami kvalitatīvs struktūras noteikšanai, izmantojot monokristāla rentgendifraktometriju. Latvijas Organiskās sintēzes institūta Fizikāli organiskās ķīmijas laboratorijā tika iegūta rentgendifrakcijas aina, kas ir neapšaubāms savienojuma **3c** struktūras pierādījums (6. att.).

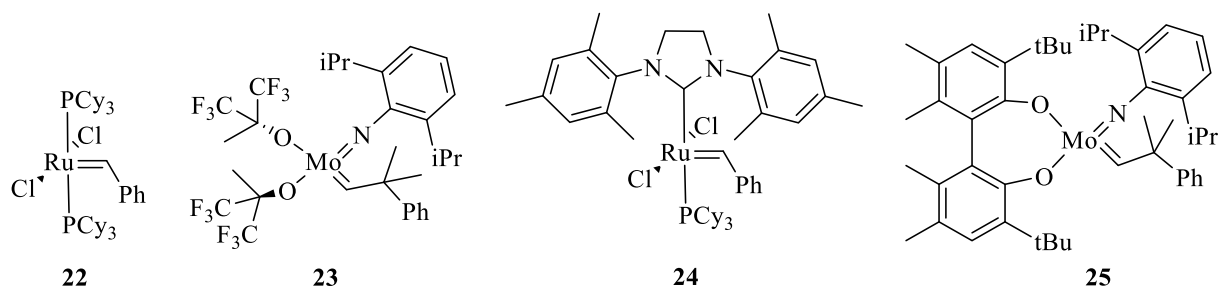


6. att. 7-Nitro-3*H*-1,2-benzoksatiepīna-2,2-dioksīda **3c** rentgenstruktūra.

Jāatzīmē, ka mūsdienās ir zināmi daudzi un dažādi cikla saslēgšanas metatēzes reakcijas katalizatori. Galvenokārt izmanto rutēnija un molibdēna katalizatorus. Pagājušā gadsimta 90. gados tika izstrādāti un komercializēti pirmās paaudzes katalizatori. Zināmākie no tiem ir Grabsa pirmās paaudzes katalizators **22** un Šroka (*Schrock*) katalizators **23** (7. att.). Diemžēl pirmās paaudzes katalizatoriem nepiemīt augsta funkcionālo grupu tolerance un selektivitāte, tie ir gaisa un mitruma jutīgi [17]. 1999. gada augustā Grabs publicēja rakstu, kurā ir apskatīti jauni, efektīvāki olefīnu cikla saslēgšanas metatēzes rutēnija katalizatori [18]. Mūsdienās tos pazīst kā Grabsa otrās paaudzes katalizatorus. Otrās paaudzes rutēnija katalizatori ir efektīvāki, tiem piemīt paaugstināta termiskā stabilitāte, katalītiskā aktivitāte, gaisa un mitrumizturība. Tas tika panākts, tricikloheksilfosfīna ligandu aizstājot ar *N*-heterociklisku karbēna ligandu [17], [19]. Zināmākais no šiem katalizatoriem ir Grabsa otrās paaudzes katalizators **24** (7. att.). Attīstot molibdēna katalizatorus, izstrādāja Šroka–Hoveidas (*Schrock–Hoveyda*) katalizatoru **25** (7. att.), kam piemīt augstāka funkcionālo grupu tolerance un selektivitāte nekā Šroka katalizatoram **23**. Tiek uzskatīts, ka molibdēna katalizatori tolerē

amīnus un fosfīnus, bet netolerē substrātus ar karboksil-, hidroksi-, un aldehīdgrupām. Savukārt rutēnija katalizatori netolerē amīnus un fosfīnus, bet tolerē substrātus ar karboksil-, hidroksi-, un aldehīdgrupām [17].

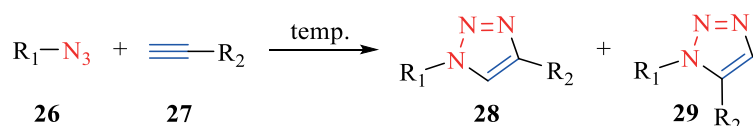
Otrās paaudzes rutēnija katalizatori ir termiski stabili, ar labu funkcionālo grupu toleranci, gaisa un mitrumizturību, tāpēc nolēmām izmantot komerciāli pieejamo otrās paaudzes katalizatora atvasinājumu **21**.



7. att. Olefīnu metatēzes reakcijas katalizatoru piemēri.

### 1.1. 3*H*-1,2-Benzoksatiepīna-2,2-dioksīda 1,2,3-triazolilatvasinājumu sintēze

Lai labāk izprastu struktūras–aktivitātes likumsakarības, nolēmām sintezēt 1,4-diaizvietotus benzoksatiepīna-2,2-dioksīda 1,2,3-triazolilatvasinājumus **4**. Mihaels (*Michael*) 1893. gadā publicēja pirmo 1,2,3-triazolu sintēzi no dietilacetilēndikarboksilāta un fenilazīda [20]. Neskatoties uz to, 1,2,3-triazolu sintēzi vairāk saista ar Huisgēna (*Huisgen*) vārdu. 20. gadsimta 60. gados viņš strādāja pie 1,3-dipolārajām ciklopievienošanās reakcijām, tai skaitā 1,2,3-triazolu sintēzes. Nodarbojās ar reakcijas mehānisma un kinētikas pētījumiem [21]. Kopš tā laika zināms, ka azīdu **26** reakcijās ar alkīniem **27** paaugstinātā temperatūrā veidojas reģioizomēru – 1,4- **28** un 1,5-diaizvietotu **29** 1,2,3-triazolu maisījums (8. att.).

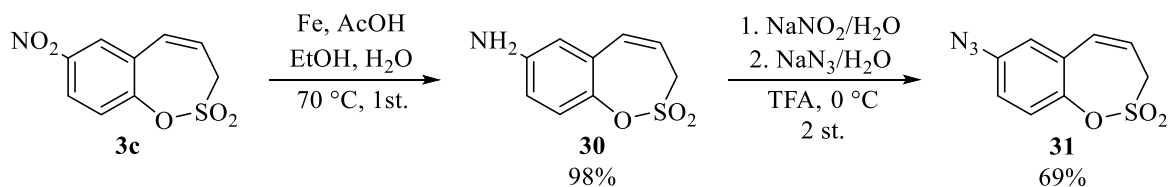


8. att. 1,2,3-Triazolilatvasinājumu veidošanās.

Mūsdienās ir izstrādātas metodes selektīvai 1,4- vai 1,5-diaizvietotu 1,2,3-triazolilatvasinājumu sintēzei. 2002. gadā Mendals (*Mendal*) un līdzstrādnieki [22] un Šarpless (*Sharpless*) un līdzstrādnieki [23] neatkarīgi viens no otra publicēja rakstus, kur aprakstīta Cu(I) katalizēta azīda-alkīna ciklopievienošanās, selektīvi veidojot 1,4-diaizvietotus 1,2,3-triazolilatvasinājumus. Jāatzīmē, ka Šarplesa izstrādātajā protokolā [23] tika izmantots CuSO<sub>4</sub>, ko *in situ* reducēja ar nātrija askorbātu, veidojot Cu(I) nevis Cu(0). Selektīvu 1,5-diaizvietotu 1,2,3-triazolilatvasinājumu veidošanos iespējams panākt, izmantojot dažādus rutēnija katalizatorus [21], [24].

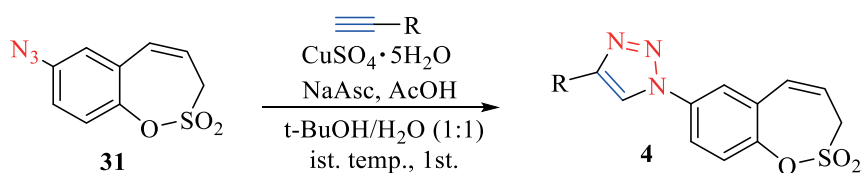
Turpinot darbu, nitroatvasinājumu **3c** veiksmīgi reducējām ar Fe(0), ar labu iznākumu iegūstot aminoatvasinājumu **30** (9. att.). No aminoatvasinājuma **30** ar pieņemamu iznākumu (69 %) pagatavoja azidoatvasinājumu **31** (9. att.), ko tālāk izmantoja kā izejvielu 1,4-

diaizvietotu 1,2,3-triazolilatvasinājumu sintēzē. Apstrādājot aminoatvasinājumu **30** ar NaNO<sub>2</sub> skābā vidē, *in situ* veidojas diazonija sāls, kuram reaģējot ar NaN<sub>3</sub>, veidojas azīds **31**. Jāatzīmē, ka no NaN<sub>3</sub> skābā vidē veidojas HN<sub>3</sub> (slāpekļūdeņražskābe), kas ir viegli gaistošs, toksisks savienojums. Tāpēc reakcija jāveic 0 °C temperatūrā.



9. att. Benzoksatiepīna-2,2-dioksīda azidoatvasinājuma **31** iegūšana.

Selektīvai 1,4-diaizvietotu 1,2,3-triazolilatvasinājumu **4** iegūšanai izvēlējāmies izmantot Cu(I) katalizētu reakciju starp azīdu **31** un dažādiem alkīniem (10. att.). Cu(I) ieguvām no CuSO<sub>4</sub>, to *in situ* reducējot ar nātrija askorbātu, līdzīgi kā Šarpleša rakstā [23]. Kā šķīdinātāju lietojām *t*-BuOH/H<sub>2</sub>O maisījumu attiecībā 1 : 1. Ar labiem iznākumiem tika iegūta rinda 1,4-diaizvietotu 1,2,3-triazolilatvasinājumu **4a–4j** (1. tabula). Jāatzīmē, ka tika izmantota etiķskābes piedeva. Ir pierādīts, ka vājas organiskas skābes (etiķskābe, benzoskābe) atvieglo vara eliminēšanos pēc 1,3-dipolārās ciklopievienošanās, tādējādi paaugstinot reakcijas ātrumu [25].



10. att. 1,4-Diaizvietotu 1,2,3-triazolu **4a–4j** sintēze.

1. tabula

Benzoksatiepīna-2,2-dioksīda 1,2,3-triazolilatvasinājumus **4** sintēze, CA inhibēšanas rezultāti

N. p. k.	R	4, iznākums, %	K <sub>I</sub> <sup>*</sup> , μM			
			hCA I	hCA II	hCA IX	hCA XII
1.	C <sub>6</sub> H <sub>5</sub>	<b>4a</b> , 95	>50	>50	1,71	>50
2.	4-ClC <sub>6</sub> H <sub>4</sub>	<b>4b</b> , 74	>50	>50	3,59	>50
3.	3-OMeC <sub>6</sub> H <sub>4</sub>	<b>4c</b> , 51	>50	>50	2,56	>50
4.	4-FC <sub>6</sub> H <sub>4</sub>	<b>4d</b> , 66	>50	>50	1,75	>50
5.	4-OCF <sub>3</sub> C <sub>6</sub> H <sub>4</sub>	<b>4e</b> , 83	>50	5,77	0,34	1,72
6.	3-FC <sub>6</sub> H <sub>4</sub>	<b>4f</b> , 74	>50	>50	1,15	>50
7.	2-NH <sub>2</sub> C <sub>6</sub> H <sub>4</sub>	<b>4g</b> , 57	>50	>50	0,46	2,32
8.	CH <sub>2</sub> OH	<b>4i</b> , 81	>50	>50	0,87	>50
9.	4-CF <sub>3</sub> C <sub>6</sub> H <sub>4</sub>	<b>4j</b> , 85	>50	>50	0,43	>50
10.	AAZ <sup>*</sup>	–	0,25	0,012	0,025	0,006

\* 10. rindā parādīta acetazolamīda (AAZ) dažādu CA izoformu inhibēšanas spēja.

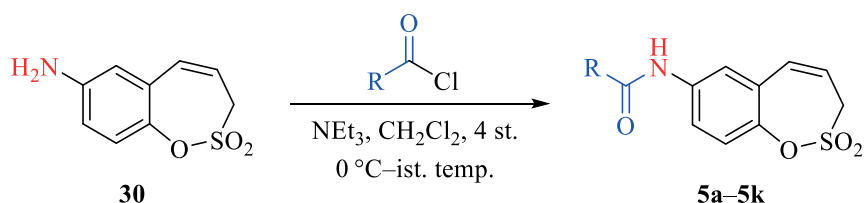
Promocijas darbā sintezētajiem savienojumiem Florences Universitātē profesora C. T. Supurāna (*Supuran*) grupā tika noteiktas cilvēka ogļskābes anhidrāžu (CA I, CA II, CA IX un CA XII) inhibēšanas aktivitātes. Visos gadījumos kā salīdzināšanas standarts izmantots 5-acetamido-1,3,4-tiadiazol-2-sulfonamīds (acetazolamīds, AAZ), kas ir izoformu neselektīvs inhibitors. Jāatzīmē, ka citosolisko CA izoformu CA I un CA II inhibēšana ir nevēlama, jo tās ir plaši sastopamas cilvēka organismā (nemērķenzīmi). Savukārt uz šūnu membrānas virsmas saistītās CA izoformas CA IX un CA XII ir mērķenzīmi, jo audzēju šūnās tās tiek pastiprināti ekspresētas.

Kā redzams 1. tabulā, neviens no triazolilatvasinājumiem neinhibē citosoliskās CA I un CA II, izņemot savienojumu **4e**, kam piemīt vāja CA II inhibitorā aktivitāte ( $K_I = 5,77 \mu\text{M}$ ) (5. rinda). Triazolilatvasinājumi **4a–4j** inhibē CA IX, inhibitorā aktivitāte ir 0,43–3,59  $\mu\text{M}$ , kas ir vājāka par acetazolamīda CA IX inhibēšanas aktivitāti. Vislabākos rezultātus uzrādīja triazolilatvasinājumi **4e**, **4g–4j**. Savienojums **4i** satur hidroksimetilgrupu triazolilgredzenā, tā CA IX inhibēšanas konstante ir  $K_I = 0,87 \mu\text{M}$  (8. rinda). Arilgrupu saturošajiem triazolīem **4e**, **4g** un **4j**, kas satur 4-trifluormetoksi-, 2-amino- un 4-trifluoraizvietotājus fenilgredzenā  $K_I$  ir 0,34  $\mu\text{M}$ ; 0,46  $\mu\text{M}$  un 0,43  $\mu\text{M}$  attiecīgi (5., 7. un 9. rinda).

Septiņi no deviņiem triazolilatvasinājumiem neinhibē CA XII,  $K_I > 50 \mu\text{M}$  (1.–4. rinda, 6. rinda un 8.–9. rinda). Atlikušie divi savienojumi **4e** un **4g** ir vāji CA XII inhibitori –  $K_I = 1,72 \mu\text{M}$  un 2,32  $\mu\text{M}$ . No bioloģiskajiem rezultātiem izriet, ka 1,4-diazvietotie 1,2,3-triazolilatvasinājumi **4a–4j** ir selektīvi CA IX inhibitori.

## 1.2. 3H-1,2-Benzoksatiepīna-2,2-dioksīda 7-acilaminoatvasinājumu sintēze

Lai paplašinātu savienojumu klāstu bioloģisko aktivitāšu pētījumiem, tika nolemts iegūt benzoksatiepīna-2,2-dioksīda 7-acilaminoatvasinājumus **5**. Tos sekmīgi ieguva no aminoatvasinājuma **30** reakcijās ar dažādiem acilchlorīdiem (11. att., 2. tab.).



11. att. Benzoksatiepīna-2,2-dioksīda 7-acilaminoatvasinājumu **5** sintēze.

Neviens no produktiem **5a–5g** neinhibē citosoliskās CA I un CA II ( $K_I > 100\,000 \text{ nM}$ ). Savukārt visi produkti **5a–5g** inhibē mērķenzīmus CA IX un CA XII nanomolārās koncentrācijās. Produkts **5i** uzrāda lielisku gan CA IX, gan arī CA XII inhibēšanas spēju –  $K_I = 19,7 \text{ nM}$  un 8,7 nM (8. rinda). Tas ir aktīvāks CA IX inhibitors nekā medicīnā lietotais acetazolamīds, kam CA IX  $K_I = 25 \text{ nM}$ . Produktiem **5a–5g** un **5j–5k** piemīt vājāka bioloģiskā aktivitāte uz CA IX un CA XII nekā acetazolamīdam ( $K_I = 25 \text{ nM}$  un 5,7 nM), to inhibēšanas konstantes ir 45,4–353,3 nM un 40,3–643,7 nM attiecīgi (1.–7., 9., 10. rinda).

Benzoksatiepīna-2,2-dioksīda 7-acilaminoatvasinājumu **5** sintēze, CA inhibēšanas rezultāti

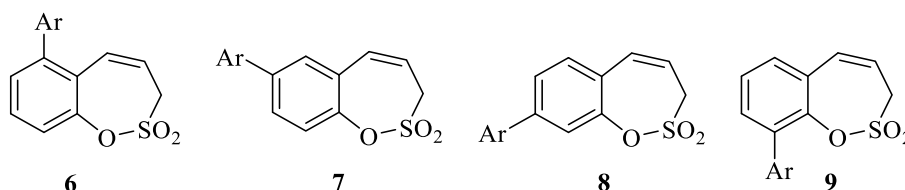
N. p. k.	R	5, iznākums, %	$K_1^*$ , nM			
			hCA I	hCA II	hCA IX	hCA XII
1.	CH <sub>3</sub>	<b>5a</b> , 70	>100 000	>100 000	61,8	162,5
2.	C <sub>6</sub> H <sub>5</sub>	<b>5b</b> , 72	>100 000	>100 000	208,6	370,1
3.	4-CH <sub>3</sub> C <sub>6</sub> H <sub>4</sub>	<b>5c</b> , 73	>100 000	>100 000	83	309,3
4.	4-BrC <sub>6</sub> H <sub>4</sub>	<b>5d</b> , 59	>100 000	>100 000	353,3	140,7
5.	2-IC <sub>6</sub> H <sub>4</sub>	<b>5e</b> , 88	>100 000	>100 000	45,4	643,7
6.	2-BrC <sub>6</sub> H <sub>4</sub>	<b>5f</b> , 82	>100 000	>100 000	66,8	96,2
7.	2-FC <sub>6</sub> H <sub>4</sub>	<b>5g</b> , 79	>100 000	>100 000	74,6	40,3
8.	2-CF <sub>3</sub> C <sub>6</sub> H <sub>4</sub>	<b>5i</b> , 87	>100 000	>100 000	19,7	8,7
9.	2-tienil	<b>5j</b> , 81	>100 000	>100 000	177,5	73,2
10.	2-furil	<b>5k</b> , 81	>100 000	>100 000	210,1	134,4
11.	*AAZ	–	250	12	25	5,7

\* 10. rindā parādīta acetazolamīda (AAZ) dažādu CA izoformu inhibēšanas spēja.

Produkts **5d**, kas satur 4-bromfenilgrupu, ir mazāk aktīvs CA IX inhibitors (CA IX  $K_1 = 353,3$  nM, 4. rinda) nekā savienojums **5f**, kas satur 2-bromfenilgrupu (CA IX  $K_1 = 66,8$  nM, 6. rinda). Iespējams, fenilkarboksiamīdatvasinājumi, kas satur aizvietotāju fenilgrupas otrajā pozīcijā, ir aktīvāki nekā savienojumi, kas satur aizvietotāju fenilgrupas 4. pozīcijā. Ja neaizvietotu fenilgrupu (savienojums **5b**, 2. rinda) aizvieto ar metilgrupu (savienojums **5a**, 1. rinda), CA IX inhibitorā aktivitāte palielinās. Savukārt, ja neaizvietotu fenilgrupu (savienojums **5b**, 2. rinda) aizvieto ar pieclocekļu heterociklu (**5j** un **5g**), CA IX inhibitorā aktivitāte būtiski nemainās –  $K_1$  vērtības 117,5 nM un 210,1 nM attiecīgi (9. un 10. rinda).

### 1.3. 3H-1,2-Benzoksatiepīna-2,2-dioksīda arilatvasinājumu sintēze

Lai gūtu priekšstatu par struktūras-aktivitātes likumsakarībām un paplašinātu savienojumu klāstu, tika nolemts sintezēt benzoksatiepīna-2,2-dioksīda arilatvasinājumus **6–9** (12. att.).



12. att. Benzoksatiepīna-2,2-dioksīda arilatvasinājumu **6–9** vispārējās struktūrformulas.

Arilatvasinājumus izvēlējamies iegūt Pd katalizētas Suzuki–Mijauras šķērssametnāšanas reakcijas ceļā attiecīgo halogēnatvasinājumu reakcijās ar arilborskābēm.

Suzuki–Mijauras šķērssametnāšanas reakcijā galvenokārt tiek izmantoti pallādijs un niķeļa katalizatori. Pallādijs katalizatoru gadījumā reaģētspējīgākie ir ariljodīdi, kam seko triflāti un bromīdi. Izmantojot arilhlorīdus, reakcijas produktu iznākums būtiski samazinās. Tas skaidrojams ar oksidējošās pievienošanās (pirmās katalītiskā cikla stadijas) ātruma palēnināšanos [26]. Visbiežāk izmantotie pallādijs katalizatori Suzuki–Mijauras šķērssametnāšanas reakcijā ir pallādijs katalizatori ar fosfina ligandiem: Pd(PPh<sub>3</sub>)<sub>4</sub>, Pd(dppf)Cl<sub>2</sub>, Pd(PPh<sub>3</sub>)<sub>2</sub>Cl<sub>2</sub>, jo tie ir termiski izturīgi un komerciāli pieejami [26], [27].

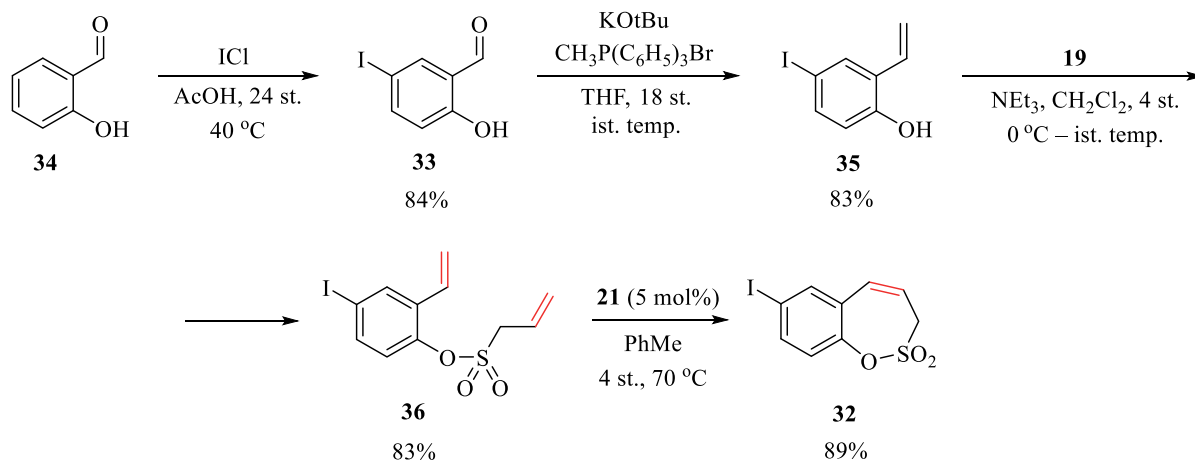
Niķeļa katalizatoru attīstība ir veicinājusi mazāk reaģētspējīgu elektrofilu, piemēram, arilhlorīdu, fluorīdu, esteru, nitrilu un arilamīdu, izmantošanu Suzuki–Mijauras šķērssametnāšanas reakcijā [28]. Tomēr, neskatoties uz šīm priekšrocībām, praksē vairāk izmanto tieši pallādijs katalīzi. Parasti niķeļa katalizētas Suzuki–Mijauras šķērssametnāšanas reakcijās nepieciešams liels katalizatora iesvars (3–10 mol %), un tās ir jutīgas pret reakcijas apstākļiem. Ļoti svarīga ir bāzes un šķīdinātāja izvēle. Lielākoties izmanto THF, dioksānu vai toluolu apvienojumā ar slikti šķīstošu neorganisko bāzi, piemēram, K<sub>3</sub>PO<sub>4</sub> vai K<sub>2</sub>CO<sub>3</sub> [28]. Hidroksīdu [29], kā arī ūdens izmantošana [30] deaktivē niķeļa katalizatorus, un reakcijas produktu iznākums samazinās.

Turpretī pallādijs katalizētā Suzuki–Mijauras šķērssametnāšanas reakcijā izmanto gan organiskās, gan neorganiskās bāzes, piemēram, Na/K<sub>3</sub>PO<sub>4</sub>, Na/Cs/K<sub>2</sub>CO<sub>3</sub>, Na/KOH, Na/KOt-Bu, NaOEt, NaOMe. Svarīgi atzīmēt, ka reakcija nenorisinās bez bāzes klātbūtnes. Kā šķīdinātāju parasti izmanto organisko šķīdinātāju maisījumā ar ūdeni. Visbiežāk lietotie organiskie šķīdinātāji ir dioksāns, THF, DMF un toluols [31].

Šķērssametnāšanas reakcijas attīstību lielā mērā ir sekmējusi organobora atvasinājumu vājā nukleofilā daba un stabilitāte. Tie ir komerciāli pieejami, kā arī ir izstrādātas vairākas metodes to iegūšanai. Šķērssametnāšanu iespējams veikt ar labu ķīmisko, reģio- un stereoselektivitāti.

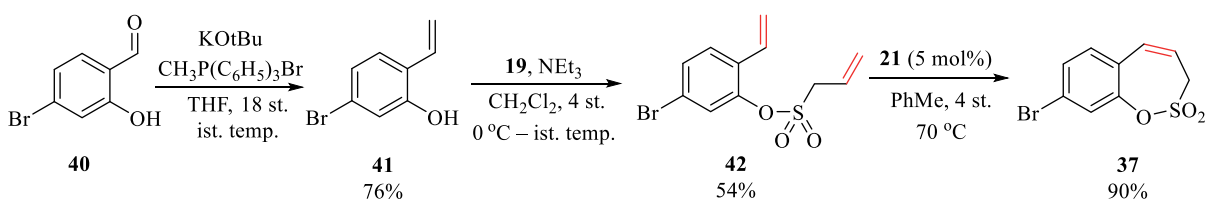
Mērķsavienojumu **6–9** sintēzi sākām ar izejvielu iegūšanu. Pallādijs katalizētā Suzuki–Mijauras šķērssametnāšanas reakcijā jodīdi reaģē aktīvāk nekā bromīdi, tāpēc nolēmām iegūt 7-jodatvasinājumu **32**. Jāatzīmē, ka jodsalicilaldehīds **33**, lai arī komerciāli pieejams, tomēr ir dārgs reaģents. To veiksmīgi ieguva no salicilaldehīda **34**, to apstrādājot ar joda monohlorīdu skābā vidē. Tālāk jodsalicilaldehīdam **33** veica vitīgu reakciju, iegūstot olefīnu **35**, ko veiksmīgi sulfonilēja ar sulfonilhlorīdu **19**, iegūstot diolefīnu **36**. Diolefīnu ciklizēja izmantojot rutēnija katalizatoru **21**, ar labu reakcijas produktu iznākumu iegūstot 7-jodatvasinājumu **32** (13.att.).



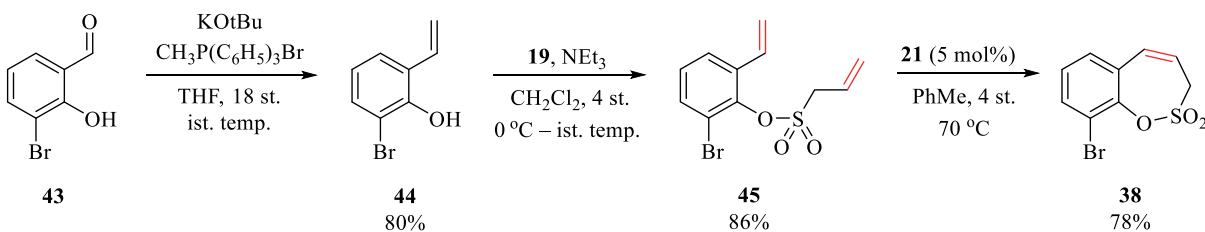


13. att. 7-Jod-3H-1,2-benzoksatiepīna-2,2-dioksīda (**32**) sintēze.

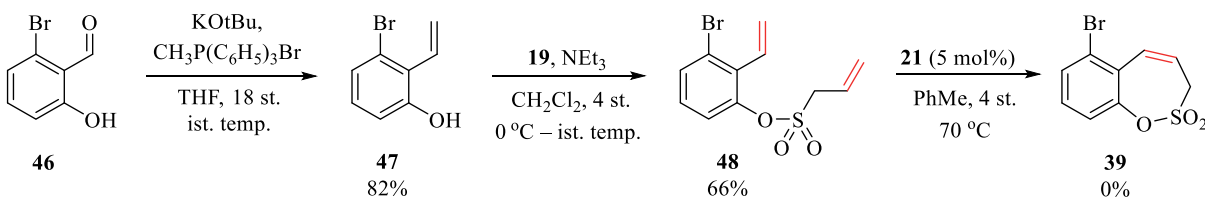
3-, 4- un 6-bromsalicilaldehīdi ir komerciāli pieejami, un nav ērtas sintēzes metodes attiecīgo jodsalicilaldehīdu iegūšanai, tāpēc nolēmām sintetēt bromatvasinājumus **37–39** (14.–16. att.).



14. att. 8-Brom-3H-1,2-benzoksatiepīna-2,2-dioksīda (**37**) sintēze.

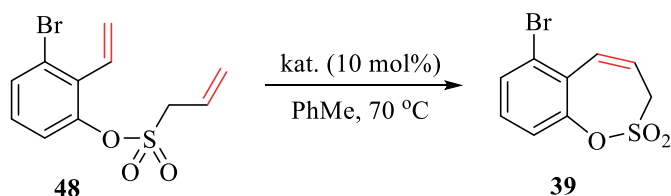


15. att. 9-Brom-3H-1,2-benzoksatiepīna-2,2-dioksīda (**38**) sintēze.



16. att. 6-Brom-3H-1,2-benzoksatiepīna-2,2-dioksīda (**39**) sintēze.

Bromatvasinājumus **37**, **38** ieguva līdzīgi kā jodatvasinājumu **32**. Attiecīgajam salicilaldehīdam veica Vitiga reakciju, iegūstot olefīnu. Olefīnu sulfonilēja ar sulfonilhlorīdu **19**, iegūstot attiecīgo diolefīnu, kuru veiksmīgi ciklizēja izmantojot iepriekš izstrādātos ciklizācijas apstākļus, savienojumu **39** iegūt neizdevās. Veicānēlielu reakcijas apstākļu optimizāciju (17. att., 3. tab.).



17. att. Diolefīna **48** cikla saslēgšanas metatēzes reakcijas apstākļu optimizācija.

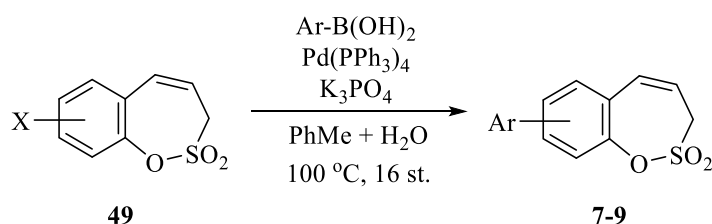
3. tabula

Diolefīna **48** cikla saslēgšanas metatēzes reakcijas apstākļu optimizācijas rezultāti

N. p. k.	Katalizators	Laiks, st.	Iznākums, %
1.	<b>21</b>	40	–
2.	<b>23</b>	16	–
3.	<b>25</b>	16	–

Izmantojot iepriekš lietoto katalizatoru **21**, palielinot reakcijas laiku un divreiz palielinot katalizatoru iesvaru, produkta veidošanos nenovēroja (1. rinda). Izvēlējamies izmēģināt Šroka (*Schrock*) katalizatorus **23** un **25**, jo tiek uzskatīts, ka molibdēna katalizatori ir aktīvāki par rutēnija katalizatoriem. Diemžēl produktu **39** iegūt neizdevās, iespējams, tas neveidojās stērisko traucējumu dēļ.

Arilatvasinājumus **7–9** tika sekmīgi sintezēti pallādijs katalizētā Suzuki–Mijauras šķerssametināšanas reakcijā, kā katalizatoru izmantojot pallādijs tetrakis ( $\text{Pd}(\text{PPh}_3)_4$ ) (18. att., 4.–6. tab.). Reakcijas veiksmīgai norisei bija nepieciešama paaugstināta temperatūra un ūdens piedeva. Bez ūdens piedevas reakcijas produktu iznākums būtiski samazinās.



18. att. Optimizētie Suzuki–Mijauras sametināšanas reakcijas apstākļi.

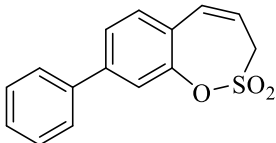
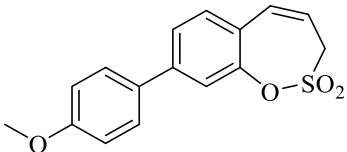
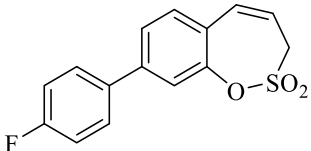
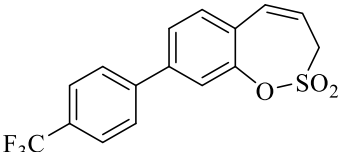
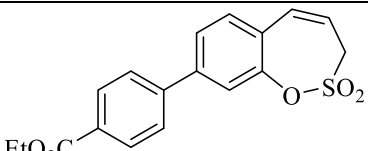
7-Aril-3H-1,2-benzoksatiēpīna-2,2-dioksīda **7** atvasinājumu sintēze, CA inhibēšanas rezultāti

N. p. k.	Produkta Nr., iznākums, %	Produkts	$K_1^*$ , nM	
			hCA IX	hCA XII
1.	<b>7a</b> , 56		654,8	1376
2.	<b>7b</b> , 61		407,6	2934
3.	<b>7c</b> , 44		330,8	890,5
4.	<b>7d</b> , 66		221,4	4017
5.	<b>7e</b> , 44		620,8	2398

\* CA I un CA II  $K_1 > 100 \mu\text{M}$ . Kā standarts izmantots AAZ, tā CA IX  $K_1 = 25 \text{ nM}$  un CA XII  $K_1 = 5,7 \text{ nM}$ .

Kā redzams 4. tabulā, 7-arilaizvietoti benzoksatiēpīna-2,2-dioksīda atvasinājumi **7a–7e** iegūti ar labiem (1., 2., 4. rinda) un vidējiem (3., 5. rinda) iznākumiem. 7-Arilatvasinājumi **7a–7e** neinhibē citosoliskās CA I un CA II, savukārt inhibē mērķenzīmus CA IX un CA XII. Savienojumi **7a–7e** spēcīgāk inhibē CA IX ( $K_1 = 221,4–654,8 \text{ nM}$ ) nekā CA XII ( $K_1 = 890,5–4017 \text{ nM}$ ).

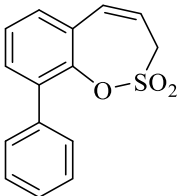
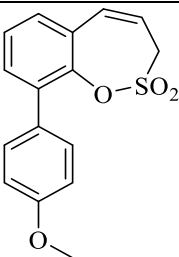
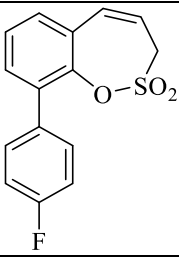
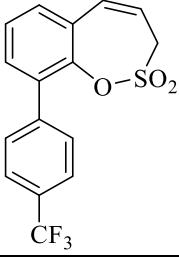
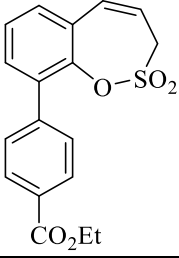
8-Aril-3H-1,2-benzoksatiepīna-2,2-dioksīda **8** atvasinājumu sintēze, CA inhibēšanas rezultāti

N. p. k.	Produkta Nr., iznākums, %	Produkts	$K_1^*$ , nM	
			hCA IX	hCA XII
1.	<b>8a</b> , 44		104,8	473,2
2.	<b>8b</b> , 44		63,1	168,6
3.	<b>8c</b> , 41		95,2	77,9
4.	<b>8d</b> , 46		44,0	247,8
5.	<b>8e</b> , 38		79,8	289,3

\* CA I un CA II  $K_1 > 100 \mu\text{M}$ . Kā standarts izmantots AAZ, tā CA IX  $K_1 = 25 \text{ nM}$  un CA XII  $K_1 = 5,7 \text{ nM}$ .

Kā redzams 5. tabulā, 8-arilaizvietoti benzoksatiepīna-2,2-dioksīda atvasinājumi **8a–8e** iegūti ar vidējiem iznākumiem. 8-Arilatvasinājumi **8a–8e** neinhibē citosoliskās CA I un CA II, savukārt inhibē mērķenzīmus CA IX un CA XII. Savienojumi **8a–8e** spēcīgāk inhibē CA IX ( $K_1 = 44,0\text{--}104,8 \text{ nM}$ ) nekā CA XII ( $K_1 = 77,9\text{--}473,2 \text{ nM}$ ).

9-aril-3*H*-1,2-benzoksatiepīna-2,2-dioksīda **9** atvasinājumu sintēze, CA inhibēšanas rezultāti

N. p. k.	Produkta Nr., iznākums, %	Produkts	$K_1^*$ , $\mu\text{M}$	
			hCA IX	hCA IX
1.	<b>9a</b> , 42		21,1	>100
2.	<b>9b</b> , 40		60,9	>100
3.	<b>9c</b> , 39		33,7	>100
4.	<b>9d</b> , 44		47,1	>100
5.	<b>9e</b> , 36		16,4	>100

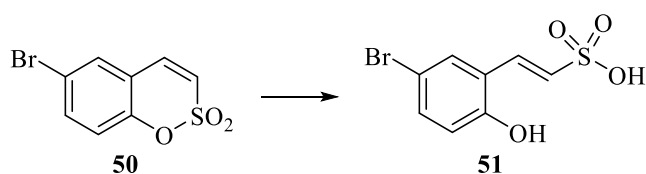
\* CA I un CA II  $K_1 > 100 \mu\text{M}$ . Kā standarts izmantots AAZ, tā CA IX  $K_1 = 25 \text{ nM}$  un CA XII  $K_1 = 5,7 \text{ nM}$ .

Kā redzams 6. tabulā, 9-arilaizvietoti benzoksatiepīna-2,2-dioksīda atvasinājumi **9a–9e** iegūti ar vidējiem iznākumiem. 9-Arilatvasinājumi **9a–9e** neinhibē citosoliskās CA I un CA II un mērķenzīmu CA XII. Tie vāji inhibē CA IX,  $K_1 = 16,4–60,9 \mu\text{M}$ .

Jāatzīmē, ka netika novērota arilborskābju aizvietotāju ietekme uz Suzuki–Mijauras sametināšanas reakcijas norisi. Visos gadījumos produkti **7–9** tika iegūti ar līdzīgiem iznākumiem.

Salīdzinot 7-aril- (4. tab.), 8-aril- (5. tab.) un 9-arilsavienojumu (6. tab.) bioloģiskās aktivitātes, tika secināts, ka visaktīvākie CA IX un CA XII inhibitori ir 8-arilatvasinājumi **8a–8e**, kam seko 7-arilatvasinājumi **7a–7e**. 9-Arilatvasinājumi **9a–9e** vāji inhibē CA IX un neinhē CA XII. Vislabākais CA IX inhibitors ir 8-(4-(trifluormetil)fenil)-benzoksatiepīna-2,2-dioksīds (**8d**) (5. tab., 4. rinda), savukārt vislabākais CA XII inhibitors ir 8-(4-fluorfenil)-3*H*-1,2-benzoksatiepīna-2,2-dioksīds (**8c**) (4. tab., 3. rinda). 7-Arilatvasinājumi **7a–7e** un 8-arilatvasinājumi **8a–8e** ir selektīvi CA IX inhibitori.

Lai izprastu benzoksatiepīna-2,2-dioksīda mijiedarbību ar CA, Latvijas Biomedicīnas pētījumu centrā K. Tāra grupā tika veikti benzoksatiepīna-2,2-dioksīdu un cilvēka CA IX kokristalizācijas mēģinājumi. Diemžēl līdz šim brīdim enzīma-inhibitora kokristālu iegūt nav izdevies. Jāatzīmē, ka iepriekš mūsu grupā izstrādātajam un sintezētajam sulfokumarīna atvasinājumam **50** Latvijas Biomedicīnas pētījumu centrā K. Tāra vadībā izdevās iegūt CA II / CA IX mimētiķa-sulfokumarīna kokristālu [4a]. Izpētot kokristāla struktūru, secinājām, ka aktīvajā centrā notikusi sulfokumarīna cikla atvēršanās, veidojot vinilsulfonskābi **51** (19. att.). Kumarīniem notiek analoga cikla atvēršanās, veidojot attiecīgos kanēļskābes atvasinājumus [3].

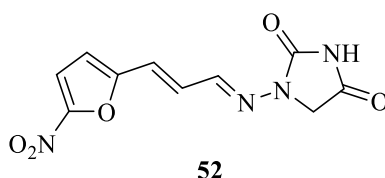


19. att. Sulfokumarīna cikla atvēršanās enzīma aktīvajā centrā.

Benzoksatiepīna-2,2-dioksīda-mērķenzīma kokristāla mums nav, tāpēc varam tikai izteikt minējumus par inhibēšanas mehānismu. Iespējams, ka oksatiepīna-2,2-dioksīda cikls enzīma aktīvajā centrā atveras līdzīgi kā sulfokumarīnu gadījumā.

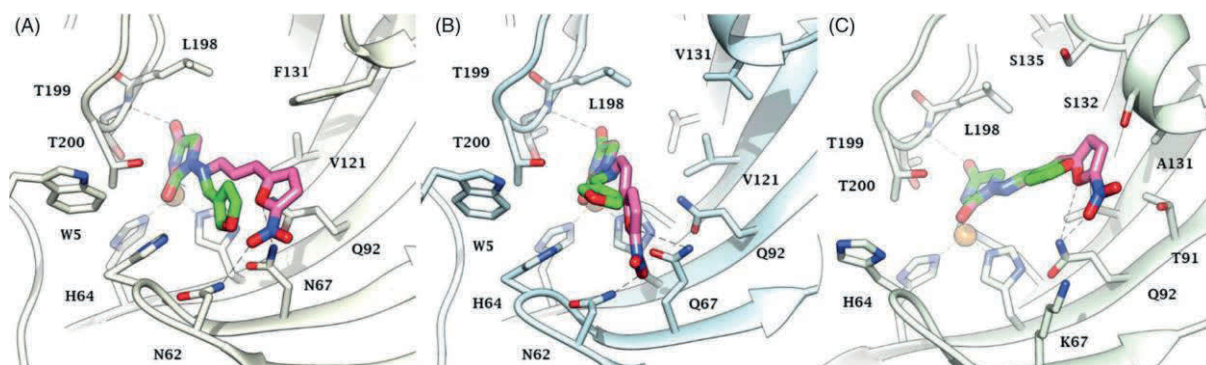
## 2. Imidazolidīn-2,4-diona atvasinājumu sintēze

Promocijas darba iztrādes beigu posmā atklājām, ka furagīns **52** (20. att.), klīnikā lietots antibakteriālais līdzeklis, ir selektīvs CA IX un CA XII inhibitors. Furagīns tiek pieskaitīts pie nitrofurāna preparātiem. Iekšķīgi to lieto pret urīnceļu infekcijām, arīgi – ķirurģijā un ginekoloģijā [32].



20. att. Furagīna struktūrformula.

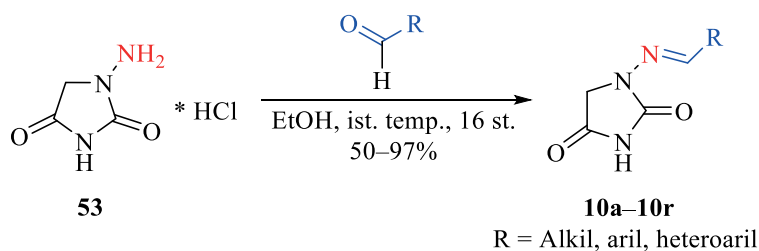
Lai gūtu priekšstatu par to, kā furagīns saistās ar dažādām cilvēka CA izoformām (CA II, CA IX un CA XII), mūsu sadarbības partneri no Florences Univesitātes veica molekulārās modelēšanas (21. att.) un molekulārās dinamikas simulāciju eksperimentus.



21. att. Paredzamās furagīna (rozā) un imidazolidīn-2,4-diona atvasinājuma **10f** (zaļā) orientācijas enzīmu (A) CA II, (B) CA IX un (C) CA XII aktīvajā centrā.

No molekulārās modelēšanas eksperimentiem var secināt, ka imidazolidīn-2,4-diona funkcija ir cinku saistošā grupa. Molekulārās dinamikas simulāciju eksperimenti 100 nanosekunžu robežās parāda, ka furagīns veido spēcīgu H-saites mijiedarbību ar mērķenzīmiem CA IX un CA XII. Savukārt ar CA II furagīns neveido spēcīgu H-saites mijiedarbību, tāpēc tas ir selektīvs CA IX un CA XII inhibitors.

Ņemot vērā iegūtos rezultātus, tika nolemts attīstīt šo virzienu, sintezējot virkni imidazolidīn-2,4-diona atvasinājumu **10a–10r** (22. att., 7. tab.). Savienojumus **10a–10r** veiksmīgi tika iegūti 1-aminoimidazolidīna-2,4-diona hidrohlorīda **53** reakcijās ar izvēlētajiem aldehīdiem.



22. att. Imidazolidīn-2,4-diona atvasinājumu **10a–10r** sintēze.

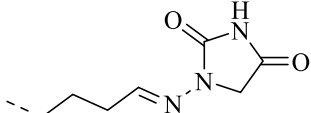
Kā redzams 7. tabulā, iegūta virkne savienojumu ar alkil- **10h** un **10i** (8.–9. rinda), aril- **10a–10c**, **10g** un **10j–10l** (1.–4., 7., 10.–12. rinda), heteroaril- **10f** un **10m–10p** (6. un 13.–16. rinda) aizvietotajiem. Neatkarīgi no aizvietotāja dabas reakcijas produkti tika iegūti ar labiem un ļoti labiem iznākumiem (50–97 %). Jāatzīmē, ka visus savienojumus **10a–10r** izdevās veiksmīgi attīrīt, izmantojot kristalizāciju no etanola, papildu attīrīšana ar kolonnu hromatogrāfiju nebija nepieciešama.

Visiem sintezētajiem imidazolidīn-2,4-diona atvasinājumiem **10a–10r** tika noteiktas bioloģiskās aktivitātes uz dažādām CA izoformām, iegūtie rezultāti apkopoti 7. tabulā. Visi imidazolidīn-2,4-diona atvasinājumi **10a–10r** ir vāji citosoliskās CA I inhibitori,  $K_I = 16\ 800\text{--}100\ 000\ \text{nM}$ . Tie labāk inhibēja CA II nekā CA I ( $K_I = 620\text{--}59\ 000\ \text{nM}$ ). Savienojumi **10a**, **10f**, **10g** un **10n** (1., 6.–7. un 14. rinda), kas satur neaizvietotas fenil- vai heteroarilgrupas, izrādījās visspēcīgākie CA II inhibitori ( $K_I = 540\text{--}900\ \text{nM}$ ). Atlikušie savienojumi uzrādīja zemu CA II inhibitoro aktivitāti –  $K_I = 3100\text{--}59\ 000\ \text{nM}$ . Jāatzīmē, ka savienojums **10k**

(11. rinda), kas satur dihidroksifenilgrupu, izrādījās gandrīz trīs reizes vājāks CA II inhibitors par otru vājāko inhibitoru **10h** (8. rinda).

7. tabula

Imidazolidīn-2,4-diona atvasinājumu **10a–10r** iznākumi, CA inhibēšanas rezultāti

N. p. k.	Produkta Nr., iznākums, %	R	$K_I^*$ , nM			
			CA I	CA II	CA IX	CA XII
1.	<b>10a</b> , 90	C <sub>6</sub> H <sub>5</sub>	39 600	900	3500	5600
2.	<b>10b</b> , 80	4-OCH <sub>3</sub> -C <sub>6</sub> H <sub>4</sub>	57 600	6400	1200	4700
3.	<b>10c</b> , 82	4-NO <sub>2</sub> -C <sub>6</sub> H <sub>4</sub>	>100 000	11 100	7400	2800
4.	<b>10d</b> , 95	4-(CO <sub>2</sub> CH <sub>3</sub> )-C <sub>6</sub> H <sub>4</sub>	>100 000	8300	4900	930
5.	<b>10e</b> , 50		19 100	4000	1100	160
6.	<b>10f</b> , 89	3-furil	16 800	710	850	1700
7.	<b>10g</b> , 90	4-(OCH <sub>2</sub> C <sub>6</sub> H <sub>5</sub> )-C <sub>6</sub> H <sub>4</sub>	>100 000	540	350	910
8.	<b>10h</b> , 81	CHCH(CO <sub>2</sub> C <sub>2</sub> H <sub>5</sub> )	45 900	23 600	810	440
9.	<b>10i</b> , 72	CHC(CH <sub>3</sub> ) <sub>2</sub>	28 800	16 500	2900	880
10.	<b>10j</b> , 71	CHCH(4-OCH <sub>3</sub> -C <sub>6</sub> H <sub>4</sub> )	>100 000	3100	400	360
11.	<b>10k</b> , 93	2,4-(OH) <sub>2</sub> -C <sub>6</sub> H <sub>3</sub>	>100 000	59 900	5800	150
12.	<b>10l</b> , 88	4-(B(OH) <sub>2</sub> )-C <sub>6</sub> H <sub>4</sub>	90 700	14 200	7300	230
13.	<b>10m</b> , 95	2-piridil	51 800	4200	4500	1300
14.	<b>10n</b> , 90	3-piridil	45 600	620	2300	3200
15.	<b>10o</b> , 91	4-piridil	26 600	3300	1600	810
16.	<b>10p</b> , 97	5-imidazolil	9600	12 400	560	350
17.	Furagīns ( <b>52</b> )*	–	>100 000	9600	260	57
18.	AAZ*	–	250	12	25	6

\* 17. rindā parādīta furagīna **52** dažādu CA izoformu inhibēšanas spēja, 18. rindā parādīta acetazolamīda (AAZ) dažādu CA izoformu inhibēšanas spēja.

Savienojumi **10f–10h** (6.–8. rinda), **10j** (10. rinda), **10p** (16. rinda) un furagīns **50** (17. rinda) mērķenzīmu CA IX inhibēja nanomolārās koncentrācijās –  $K_I = 260–850$  nM. Efektīvākais CA IX inhibitors no šiem savienojumiem izrādījās furagīns **50**. Atlikušie savienojumi uzrādīja par kārtu zemāku CA IX inhibitoro aktivitāti ( $K_I = 1100–7300$  nM). Vērojama zināma likumsakarība, ka savienojumi, kas satur vinilgrupu **10h** (8. rinda), **10j** (10. rinda) vai mazu heteroarilaizvietotāju **10f** (6. rinda) un **10p** (16. rinda) ir labāki CA IX inhibitori nekā pārējie atvasinājumi. Izņēmums ir savienojums **10g** (7. rinda), kas fenilgredzenā satur ētera grupu.

Vislabāk no visām pārbaudītajām izoformām tika inhibēta CA XII, vislabākais inhibitors bija furagīns **52** (17. rinda),  $K_I = 57$  nM. Par kārtu mazāka inhibitorā aktivitāte tika novērota savienojumiem **10d** un **10e** (4.–5. rinda), **10g–10l** (7.–12. rinda), **10o** un **10p** (14.–15. rinda), CA XII  $K_I = 150–930$  nM.



## SECINĀJUMI

1. Rutēnija katalizēta olefīnu cikla saslēgšanas metatēzes reakcija ir piemērota *3H*-1,2-benzoksatiepīna-2,2-dioksīda un tā atvasinājumu iegūšanai.
2. Olefīnu cikla saslēgšanas metatēzes reakcija, izmantojot gan rutēnija, gan molibdēna katalizatoru, nav piemērota 6-brom-*3H*-1,2-benzoksatiepīna-2,2-dioksīda sintēzei.
3. *3H*-1,2-Benzoksatiepīna-2,2-dioksīdi, kas 7. vietā satur triazolil-, acilamino- vai arilatvasinājumus, ir selektīvi un efektīvi hipoksijai pakļautajās šūnās ekspresēto CA IX un CA XII izoformu inhibitori.
4. 8-Aril *3H*-1,2-benzoksatiepīna-2,2-dioksīdi CA IX un CA XII izoformas inhibē visefektīvāk, salīdzinot ar atbilstošajiem 7- un 9-aril *3H*-1,2-benzoksatiepīna-2,2-dioksīdiem.
5. Furagīns un sintezētie imidazolidīn-2,4-diona atvasinājumi ir selektīvi un efektīvi hipoksijai pakļautajās šūnās ekspresēto CA IX un CA XII izoformu inhibitori.

## LITERATŪRAS SARAKSTS

1. International Agency for Research on Cancer: Latest Global Cancer Data. <https://www.who.int/cancer/PRGlobocanFinal.pdf>
2. Supuran, C. T., Winum, J. Y. (2009) In: Wang, B. (eds) Drug design of zinc-enzyme inhibitors: functional, structural, and disease applications. John Wiley & Sons: Hoboken, New Jersey, pp. 3–13.
3. Maresca, A., Temperini, C., Vu, H., Pham, N. B., Poulsen, S., Scozzafava, A., Quinn, R. J., Supuran, C. T. Non-Zinc Mediated Inhibition of Carbonic Anhydrases: Coumarins Are a New Class of Suicide Inhibitors. *J. Am. Chem. Soc.* **2009**, *131*, 3057–3062.
4. a) Tars, K., Vullo, D., Kazaks, A., Leitans, J., Lends, A., Grandane, A., Žalubovskis, R., Scozzafava, A., Supuran, C., T. Sulfocoumarins (1,2-benzoxathiine 2,2-dioxides): a class of potent and isoform-selective inhibitors of tumor-associated carbonic anhydrases. *J. Med. Chem.* **2013**, *56*, 293–300. b) Grandane, A., Tanc, M., Žalubovskis, R., Supuran, C., T. 6-Triazolyl-substituted sulfocoumarins are potent, selective inhibitors of the tumor-associated carbonic anhydrases IX and XII. *Bioorg. Med. Chem. Lett.* **2014**, *24*, 1256–1260. c) Grandane, A., Tanc, M., Žalubovskis, R., Supuran, C., T. Synthesis of 6-tetrazolyl-substituted sulfocoumarins acting as highly potent and selective inhibitors of the tumor-associated carbonic anhydrase isoforms IX and XII. *Bioorg. Med. Chem.* **2014**, *22*, 1522–1528.
5. Nocentini, A., Supuran, C. T. Advances in the structural annotation of human carbonic anhydrases and impact on future drug discovery. *Expert Opin. Ther. Pat.* **2018**, *28*, 745–754.
6. Jensen, E. L., Clement, R., Kosta, A., Maberly, S. C., Gontero, B. A new widespread subclass of carbonic anhydrase in marine phytoplankton. *ISME J.* **2019**, *13*, 2094–2106.
7. Supuran, C. T. Structure and function of carbonic anhydrases. *Biochem. J.* **2016**, *473*, 2023–2032.
8. Alterio, V., Di Fiore, A., D'Ambrosio, K., Supuran, C. T., Simone, G. Multiple Binding Modes of Inhibitors to Carbonic Anhydrases: How to Design Specific Drugs Targeting 15 Different Isoforms? *Chem. Rev.* **2012**, *112*, 4421–4468.
9. Supuran, C. T. Carbonic anhydrases: novel therapeutic applications for inhibitors and activators. *Nat. Rev. Drug. Discov.* **2008**, *7*, 168–181.
10. Domsic, J. F., Avvaru, B. S., Kim, C. U., Gruner, S. M., Agbandje-McKenna, M., Silverman, D. N., McKenna, R. Entrapment of Carbon Dioxide in the Active Site of Carbonic Anhydrase II. *J. Biol. Chem.* **2008**, *283*, 30766–30771.
11. Supuran, C. T. How many carbonic anhydrase inhibition mechanisms exist? *J. Enzyme Inhib. Med. Chem.* **2016**, *31*, 345–360.
12. Lomelino, C. L., Supuran, C. T., McKenna, R. Non-Classical Inhibition of Carbonic Anhydrase. *Int. J. Mol. Sci.* **2016**, *17*, 1150.
13. Mondal, S. Recent Developments in the Synthesis and Application of Sultones. *Chem. Rev.* **2012**, *112*, 5339–5355.

14. Bheeter, C. B., Bera, J. K., Doucet, H. Palladium- Catalysed Intramolecular Direct Arylation of 2- Bromobenzenesulfonic Acid Derivatives. *Adv. Synth. Catal.* **2012**, *354*, 3533–3538.
15. Qi, Z., Wang, M., Li, X. Rh(III)-Catalyzed synthesis of sultones through C–H activation directed by a sulfonic acid group. *Chem. Commun.* **2014**, *50*, 9776–9778.
16. Mondal, S., Debnath, S. Ring-closing metathesis in the synthesis of fused sultones. *Tetrahedron Lett.* **2014**, *55*, 1577–1580.
17. Hoveyda, A., Zhugralin, A. The remarkable metal-catalysed olefin metathesis reaction. *Nature* **2007**, *450*, 243–251.
18. Scholl, M., Ding, S., Lee, C. W., Grubbs, R. Synthesis and Activity of a New Generation of Ruthenium-Based Olefin Metathesis Catalysts Coordinated with 1,3-Dimesityl-4,5-dihydroimidazol-2-ylidene Ligands. *Org. Lett.* **1999**, *6*, 953–956.
19. Lozano-Vila, A., Monsaert, S., Bajek, A., Verpoort, F. Ruthenium-Based Olefin Metathesis Catalysts Derived from Alkynes. *Chem. Rev.* **2010**, *110*, 4865–4909.
20. Huisgen, R. 1,3-Dipolar Cycloadditions Past and Future. *Angew. Chem., Int. Ed. Engl.* **1963**, *2*, 565–632.
21. Johansson, R., Beke-Somfai, T., Stalsmeden, A., Kann, N. Ruthenium-Catalyzed Azide Alkyne Cycloaddition Reaction: Scope, Mechanism, and Applications. *Chem. Rev.* **2016**, *116*, 14726–14768.
22. Tornøe, C., Christensen, C., Meldal, M. Peptidotriazoles on Solid Phase: [1,2,3]-Triazoles by Regiospecific Copper(I)-Catalyzed 1,3-Dipolar Cycloadditions of Terminal Alkynes to Azides. *J. Org. Chem.* **2002**, *67*, 3057–3064.
23. Rostovtsev, V., Green, L., Fokin, V., Sharpless, B. A Stepwise Huisgen Cycloaddition Process: Copper(I)-Catalyzed Regioselective Ligation of Azides and Terminal Alkynes. *Angew. Chem. Int. Ed.* **2002**, *41*, 2595–2599.
24. Zhang, L., Chen, X., Xue, P., Sun, H., Williams, I., Sharpless, B., Fokin, V., Jia, G. Ruthenium-Catalyzed Cycloaddition of Alkynes and Organic Azides. *J. Am. Chem. Soc.* **2005**, *127*, 15998–15999.
25. Shao, C., Wang, X., Xu, J., Zhao, J., Zhang, Q., Hu, Y. Carboxylic Acid-Promoted Copper(I)-Catalyzed Azide-Alkyne Cycloaddition. *J. Org. Chem.* **2010**, *75*, 7002–7005.
26. Jana, R., Pathak, T., Sigman, M. Advances in Transition Metal (Pd,Ni,Fe)-Catalyzed Cross-Coupling Reactions Using Alkyl-organometallics as Reaction Partners. *Chem. Rev.* **2011**, *111*, 1417–1492.
27. Buchwald, S., Martin, R. Palladium-Catalyzed Suzuki-Miyaura Cross-Coupling Reactions Employing Dialkylbiaryl Phosphine Ligands. *Acc. Chem. Res.* **2008**, *41*, 1461–1473.
28. Payard, P., A., Perego, L., A., Coifini, I., Grimaud, L., Taming Nickel-Catalyzed Suzuki-Miyaura Coupling: A Mechanistic Focus on Boron-to-Nickel Transmetalation. *ACS Catal.* **2018**, *8*, 4812–4823.
29. Saito, S., Sakai, M., Miyaura, N. A Synthesis of Biaryls v/a Nickei(0).Catalyzed Cross-Coupling Reaction of Chloroarenes with Phenylboronic Acids. *Tetrahedron Lett.* **1996**, *37*, 2993–2996.

30. Saito, S., Oh-tani, S., Miyaura, N. Synthesis of Biaryls via a Nickel(0)-Catalyzed Cross-Coupling Reaction of Chloroarenes with Arylboronic Acids. *J. Org. Chem.* **1997**, *62*, 8024–8030.
31. Maluenda, I., Navarro, O. Recent Developments in the Suzuki-Miyaura Reaction: 2010–2014. *Molecules* **2015**, *20*, 7528–7557.
32. Slapšyte, G., Jankauskiene, A., Mierauskiene, J., Lazutka, J., R. Cytogenetic analysis of children under long-term antibacterial therapy with nitroheterocyclic compound furagin. *Mutat. Res.* **2001**, *491*, 25–30.

## PATEICĪBAS

Paldies zinātniskajam vadītājam Raivim Žalubovskim par sniegtajām zinātniskajām konsultācijām visu šo gadu laikā!

Pateicība Florences Universitātes (Itālija) profesoram Klaudiu T. Supurānam (*Claudiu T. Supuran*) un viņa grupai par ogļskābes anhidrāžu izoformu inhibēšanas noteikšanu un *In Silico* pētījumiem.

Paldies Latvijas Organiskās sintēzes institūta Fizikāli organiskās ķīmijas laboratorijas kolektīvam par KMR, IS spektru uzņemšanu un AIMS veikšanu!

Aleksandrs Pustenko

# **DOCTORAL THESIS PROPOSED TO RIGA TECHNICAL UNIVERSITY FOR THE PROMOTION TO THE SCIENTIFIC DEGREE OF DOCTOR OF SCIENCE**

To be granted the scientific degree of Doctor of Science (Ph. D.), the present Doctoral Thesis has been submitted for the defence at the open meeting of RTU Promotion Council on 30 September 2020 at the Faculty of Materials Science and Applied Chemistry of Riga Technical University, Riga, 3 Paula Valdena Street, Room 272.

## **OFFICIAL REVIEWERS**

Assistant professor Dr. chem. Jeļena Kirilova  
Daugavpils University, Latvia

Professor Dr. chem. Jean-Yves Winum  
Université de Montpellier, France

Lead Researcher Dr. chem. Kaspars Traskovskis  
Riga Technical University, Latvia

## **DECLARATION OF ACADEMIC INTEGRITY**

I hereby declare that the Doctoral Thesis submitted for the review to Riga Technical University for the promotion to the scientific degree of Doctor of Science (Ph. D.) is my own. I confirm that this Doctoral Thesis had not been submitted to any other university for the promotion to a scientific degree.

Aleksandrs Pustenko ..... (signature)

Date: .....

The Doctoral Thesis has been prepared as a thematically united collection of scientific publications. It consists of a summary and five scientific publications. Publications have been written in English, their total volume is 39 pages.

# CONTENTS

<b>GENERAL OVERVIEW OF THE THESIS .....</b>	<b>32</b>
Introduction .....	32
The aim of the dissertation .....	32
Objectives .....	33
Scientific novelty and main results.....	33
Structure of the Thesis .....	33
Publications and approbation of the Thesis .....	34
<b>MAIN RESULTS OF THE DOCTORAL THESIS .....</b>	<b>35</b>
1. Synthesis of 3 <i>H</i> -1,2-benzoxathiepine 2,2-dioxide derivatives .....	37
1.1. Synthesis of 3 <i>H</i> -1,2-benzoxathiepine 2,2-dioxide 1,2,3-triazolyl derivatives.....	39
1.2. Synthesis of 7-acylamino-3 <i>H</i> -1,2-benzoxathiepine 2,2-dioxides .....	41
1.3. Synthesis of 3 <i>H</i> -1,2-benzoxathiepine 2,2-dioxide aryl derivatives .....	42
2. Synthesis of imidazolidine-2,4-dione derivative .....	49
<b>CONCLUSIONS.....</b>	<b>53</b>
<b>REFERENCES .....</b>	<b>54</b>
<b>ACKNOWLEDGEMENTS.....</b>	<b>57</b>
<b>PUBLICATIONS .....</b>	<b>58</b>

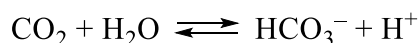
# GENERAL OVERVIEW OF THE THESIS

## Introduction

According to the World Health Organization, in 2018, 9.6 million deaths due to oncological diseases and 18.1 million new oncological cases were registered worldwide. One in 5 men and one in 6 women develop cancer in their lifetime [1]. In Europe, where ~9 % of the world's population lived in 2018, 23.4 % of all oncological diseases were registered, including 20.3 % of all deaths [1]. Therefore, it is very important to continuously develop and improve cancer treatment.

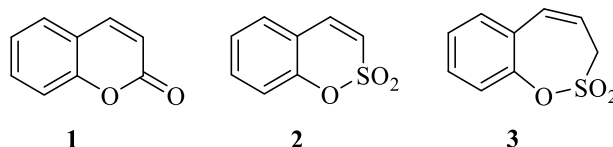
Today, more than 300 different enzymes are known for which zinc is an important cofactor. These enzymes perform various biologically important functions in human organism. Their activity is directly related to epigenetic control mechanisms in cells, the deregulation of which is one of the main causes of cancer [2].

In the last decade, increased attention has been paid to zinc-containing metalloenzymes carbonic anhydrases (CA, EC 4.2.1.1), which catalyze the reversible hydration of carbon dioxide in the living organisms.



From currently known 15 human  $\alpha$ -carbonic anhydrase isoforms, CA IX and CA XII are thought to be over expressed in hypoxic cancer cells providing an optimal pH for their survival and development. To stop the development of cancer cells and avoid unwanted side effects, selective inhibition of CA IX and CA XII isoforms must be developed.

In the literature [3] it has been shown that coumarin **1** derivatives are selective CA IX and CA XII inhibitors. In our group, sulfocoumarin **2** derivatives were synthesized, which proved to be selective inhibitors of CA IX and CA XII [4]. Therefore, we decided to synthesize benzoxathiepine-2,2-dioxide **3** derivatives, which are sulfocoumarin derivatives with an extended cycle.



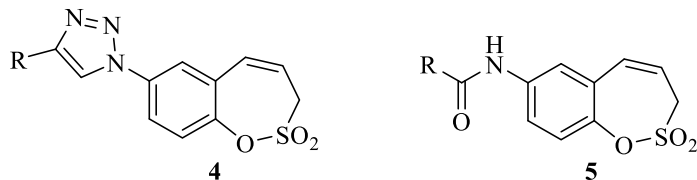
## The aim of the dissertation

To develop new, effective and selective inhibitors of CA IX and CA XII, from which a new generation of anticancer agent could be developed in the future.

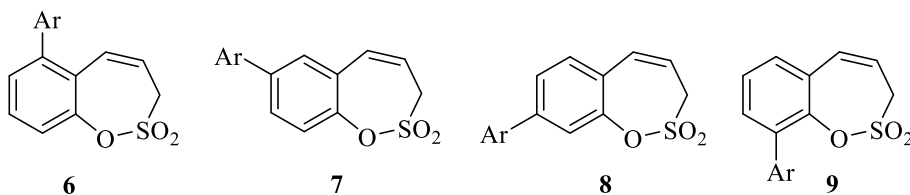


## Objectives

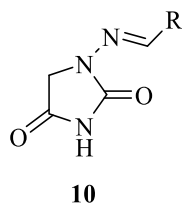
1. To develop synthesis method of 3*H*-1,2-benzoxathiepine 2,2-dioxide **3** derivative.
2. To synthesize 3*H*-1,2-benzoxathiepine 2,2-dioxide 7-triazolyl **4** and 7-acylamino **5** derivatives.



3. To synthesize 6-, 7-, 8- and 9-substituted 3*H*-1,2-benzoxathiepine 2,2-dioxide aryl derivatives **6–9**.



4. To synthesize 1-imidazolidine-2,4-dione derivatives **10**.



5. To evaluate inhibitory activities of synthesized compounds against hCA isoforms.

## Scientific novelty and main results

A new, selective class of CA IX and CA XII inhibitors – 3*H*-1,2-benzoxathiepine 2,2-dioxides, has been found. A series of 3*H*-1,2-benzoxathiepine 2,2-dioxide triazolyl, acylamino and aryl derivatives was synthesized.

We discovered that furagin, a clinically used antibacterial agent, is a selective inhibitor of CA IX and CA XII. Developing this concept, we synthesized a series of imidazolidine-2,4-dione derivatives.

Inhibitory activity on relevant human CA isoforms (I, II, IX, and XII) was determined for all products synthesized within the scope of the Doctoral Thesis.

## Structure of the Thesis

The Thesis is a summary of scientific publications focused on carbonic anhydrase inhibitor synthesis.

## Publications and approbation of the Thesis

Main results of Thesis were summarized in four scientific publications and a review article. Total IF sum is 16.9. Results of the research were presented at six conferences.

### Scientific publications

1. Pustenko, A., Nocentini, A., Gratteri, P., Bonardi, A., Vozny, I., Žalubovskis, R., Supuran, C. T. The antibiotic furagin and its derivatives are isoform-selective human carbonic anhydrase inhibitors. *J. Enzyme Inhib. Med. Chem.* **2020**, *35*, 1011–1020.
2. Pustenko, A., Nocentini, A., Balašova, A., Krasavin, M., Žalubovskis, R., Supuran, C. T. 7-acylamino-3H-1,2-benzoxathiepine 2,2-dioxides as new isoform-selective carbonic anhydrase IX and XII inhibitors. *J. Enzyme Inhib. Med. Chem.* **2020**, *35*, 650–656.
3. Pustenko, A., Nocentini, A., Balašova, A., Alafeefy, A., Krasavin, M., Žalubovskis, R., Supuran, C. T. Aryl derivatives of 3H-1,2-benzoxathiepine 2,2-dioxide as carbonic anhydrase inhibitors. *J. Enzyme Inhib. Med. Chem.* **2020**, *35*, 245–254.
4. Pustenko, A., Stepanovs, D., Žalubovskis, R., Vullo, D., Kazaks, A., Leitans, J., Tars, K., Supuran, C. T. 3H-1,2-benzoxathiepine 2,2-dioxides: a new class of isoform-selective carbonic anhydrase inhibitors. *J. Enzyme Inhib. Med. Chem.* **2017**, *32*, 767–775.
5. Pustenko, A., Žalubovskis, R. Recent advances in sultone synthesis (microreview). *Chem. Heterocycl. Compd.* **2017**, *53*, 1283–1285.

### Results of the research were presented at the following conferences

1. Žalubovskis, R., Grandāne, A., Ivanova, J., Balode, A., Pustenko, A., Domraceva, I., Tārs, K., Leitāns, J. Challenging design and synthesis of inhibitors of carbonic anhydrases. *International Conference on Organic Synthesis Balticum Organicum Syntheticum (BOS-2016)*. Riga, Latvia, July 3–6, **2016**.
2. Pustenko, A. Carbonic Anhydrases: Inhibitor Synthesis. *10<sup>th</sup> Paul Walden Symposium on Organic Chemistry*, Riga, Latvia, June 15–16, **2017**.
3. Žalubovskis, R., Ivanova, J., Pustenko, A., Grandane, A., Domraceva, I., Tars, K., Supuran, C. T. Inhibitors of Carbonic Anhydrases—challenges of design and synthesis. *3<sup>rd</sup> Satellite Meeting on Carbonic Anhydrase “New Trend in Carbonic Anhydrases Research”*, Montecatini Terme, Italy, May 24–27, **2017**.
4. Pustenko, A., Ivanova, J., Grandane, A., Vozny, I., Žalubovskis, R. Towards Novel Inhibitors of Cancer Associated Enzymes. *11<sup>th</sup> International Conference on Carbonic Anhydrases*, Bucharest, Romania, June 27–30, **2018**.
5. Pustenko, A., Balašova, A. Carbonic Anhydrases: Inhibitor Synthesis. *11<sup>th</sup> Paul Walden Symposium on Organic Chemistry*, Riga, Latvia, September 19–20, **2019**.
6. Pustenko, A., Balašova, A., Kapura, V., Žalubovskis, R. Inhibitors of cancer associated enzymes – design and synthesis. *4<sup>th</sup> Satellite Meeting on Carbonic Anhydrases*, Parma, Italy, November 14–17, **2019**.

## MAIN RESULTS OF THE DOCTORAL THESIS

To better understand the results of this Doctoral Thesis, first, we will take a look at the target enzyme – carbonic anhydrases (CA). CAs are metalloenzymes which catalyze reversible carbon dioxide hydration. CAs were discovered in 1933 and since then they have been extensively studied. Today at least 8 genetic families of CA are known:  $\alpha$ ,  $\beta$ ,  $\gamma$ ,  $\delta$ ,  $\xi$ ,  $\eta$ ,  $\theta$ , and  $\iota$  [5], [6]. The  $\alpha$ -CAs are the most widely studied class because it is found in mammals. The  $\beta$ -CAs are found in higher plants and in some prokaryotes. The  $\gamma$ -CAs are found in cyanobacteria and *Archaea*. The  $\delta$  and  $\xi$ -CA are found only in marine diatoms, whereas the  $\eta$ -CAs in protozoa [7]. The  $\alpha$ -,  $\beta$ -, and  $\delta$ -CAs contain Zn(II) in the active site, the  $\gamma$ -CAs contain Fe(II) ions,  $\xi$  contain Co(II) ions and  $\iota$  contain Mn(II) ions [5], [6]. In many organisms, the CAs are involved in vital physiological processes – pH regulation and providing of CO<sub>2</sub> homeostasis [7].

In humans, 15  $\alpha$ -CA isoforms have been described. CA I, II, III, VII, and XIII are found in cytosol, CA IV, IX, XII, and XIV are membrane bound, CA VA and VB are found in mitochondria, CA VI is found in saliva and breast milk [8], [9]. It should be noted, that all  $\alpha$ -CA isoforms, except CA VB, have a known 3D structure. Regardless of the different subcellular localization, all  $\alpha$ -CA isoforms are structurally similar, they are monomers, except for CA IX, CA XII, and CA VI – which are dimers [8].

The active site of  $\alpha$ -CAs is located in a conical cavity that is approximately 12 Å wide and 13 Å deep. Zinc ion is placed at the bottom of the cavity and it is bound to ligands – 3 histidine residues (His119, His94, and His96), water molecule / hydroxide ion (Fig. 1) [7], [8].

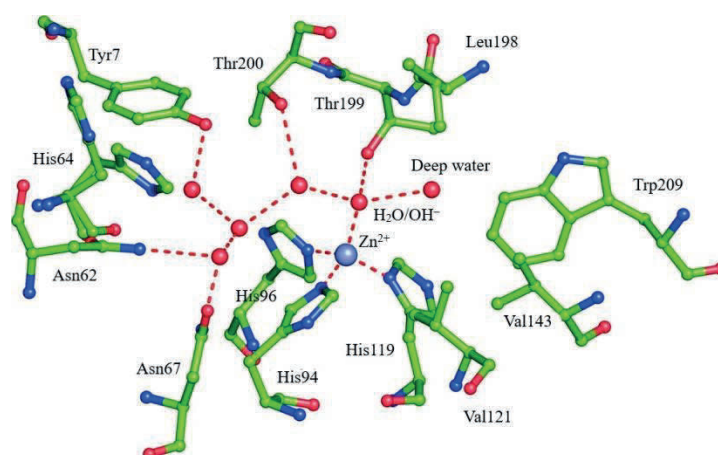


Fig. 1. Active site structure of human CAII [8].

Zn<sup>2+</sup> ion with hydrogen bonds is bonded with threonine (Thr199) hydroxyl group and two opposite water molecules. The water molecule located in hydrophobic part is called “deep water” and is surrounded by Val121, Val143, Leu198, and Trp207. The second water molecule is located in hydrophilic part, in the entrance of active site, and is surrounded by Asn62, His64, and Asn67.

The hydrophobic and hydrophilic regions can be explained by the different chemical nature of the substrate ( $\text{CO}_2$ ) and its hydration products ( $\text{H}^+$  and  $\text{HCO}_3^-$ ) [8]. McKenna with co-workers showed that the  $\text{CO}_2$  molecule binds in the hydrophobic part of the enzyme, while the hydration products bind in the hydrophilic part of the enzyme [10].

It should be noted, that for all human CA isoforms crystallized so far, the zinc ion is bound to three histidine residues (His119, His94, and His96), and all of them have a hydrophobic and hydrophilic parts [7]. Inhibitors are designed and developed based on this knowledge about target enzyme.

Nowadays several  $\alpha$ -CAs inhibition mechanisms are known. Sulphonamides ( $\text{RSO}_2\text{NH}_2$ ), sulfamates ( $\text{ROSO}_2\text{NH}_2$ ), sulfamides ( $\text{RNHSO}_2\text{NH}_2$ ), carboxylates ( $\text{RCO}_2^-$ ), urates, and phosphonates ( $\text{R}'\text{PO}(\text{OR})_2$ ) bind to the zinc ion located in the active site and form additional H-bonds with Thr199. Phenols and polyamides coordinate with water molecule / hydroxide ion, which is bound to zinc. Coumarins and their isosteres block the active site entrance, so CA activators cannot bind to the enzyme [11], [12].

In general, 3*H*-1,2-benzoxathiepine 2,2-dioxide is a sultone. The term “sultone” was first used in 1888 by Endermann. Nowadays sultones are widely used in medicinal chemistry as enzyme inhibitors, they exhibit antiviral activity. The most powerful sultone synthesis methods include transition metal catalyzed reaction, cycloaddition reactions, and Diels-Alder type reactions [13].

In the process of development of the Doctoral Thesis, the latest information on transition metal-catalyzed sultone synthesis methods was summarized and published in a review article. Sultones can be synthesized using palladium, rhodium, copper, gold and ruthenium catalyzed reactions, we will take a closer look at some of these methods.

Doucet with co-workers reported palladium catalyzed, phosphine free sultone **11** synthesis method using 2-bromobenzenesulfonic acid phenyl esters **12** as a starting material (Fig. 2) [14].

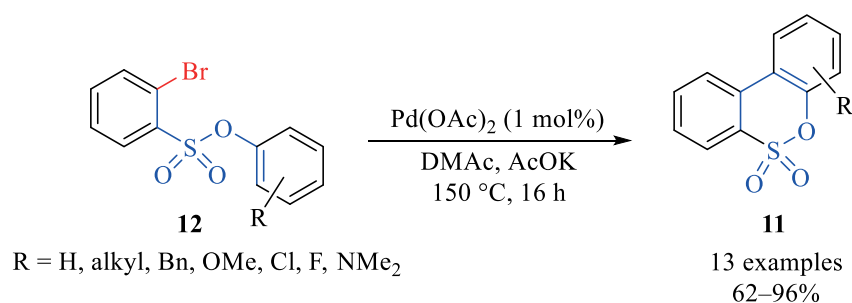


Fig. 2. Palladium catalyzed sultone **11** synthesis.

It should be noted, that substituent R has a strong influence on the reaction outcome. Using electron donor substituents, the yield of reaction products increases, while using electron acceptor substitutes ( $\text{NO}_2$ ,  $\text{CO}_2\text{Bu}$ ,  $\text{CF}_3$ ) corresponding sultones do not form. In all cases when reaction occurred high product regioselectivity was observed.

Li with co-workers reported efficient Rh(III) catalyzed sultone **13** synthesis method by coupling aryl sulfonic acids **14** with internal alkynes (Fig. 3) [15].

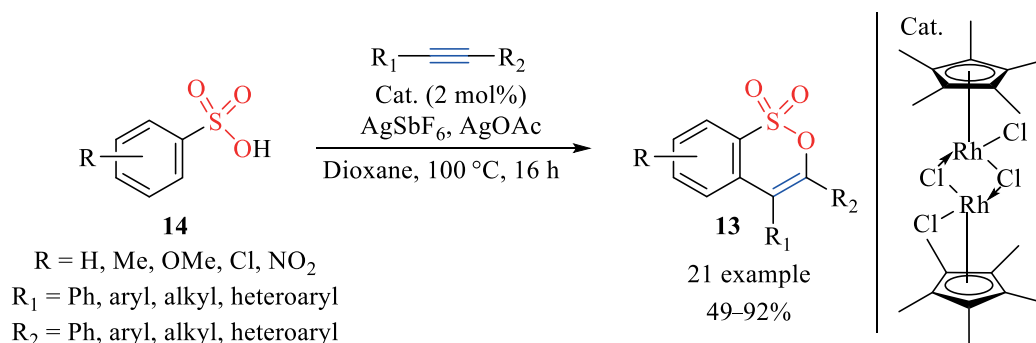


Fig. 3. Rhodium catalyzed sultone **13** synthesis.

Alkynes with both electron donor and electron acceptor substituents can be used in this method, but reaction product yield is higher using alkynes with electron donor substituents. In case of unsymmetrical alkynes, product regioselectivity is very high.

Mondal with co-workers reported convenient sultone **15** synthesis method by cyclization of corresponding diolefines **16** via Ru-catalyzed ring closing metathesis (RCM) (Fig. 4) [16]. Using Grubbs 1<sup>st</sup> generation catalyst, no sultone **15** formation was observed. Changing catalyst to Grubbs 2<sup>nd</sup> generation catalyst, sultones **15** were synthesized in good yields.

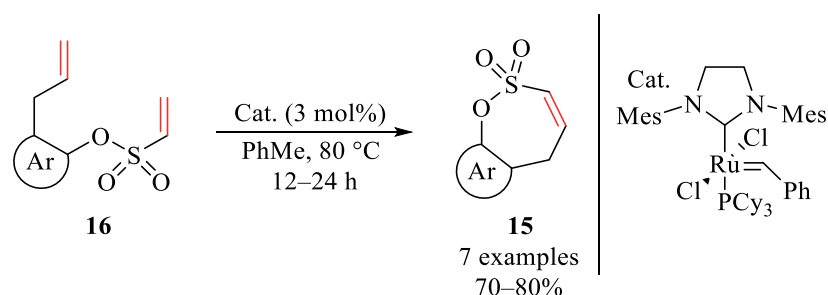


Fig. 4. Ruthenium catalyzed sultone **15** synthesis.

After summarizing the information available in the literature, we decided to synthesize benzoxathiepine 2,2-dioxide **3** derivatives in a ruthenium catalyzed olefin ring closing metathesis reaction.

## 1. Synthesis of 3*H*-1,2-benzoxathiepine 2,2-dioxide derivatives

We started our research with the development of synthesis method. At first, in Wittig reaction from 5-substituted 2-hydroxybenzaldehydes **17** we prepared corresponding olefins **18** (Fig. 5). Olefins **18a–18c** were sulfonated with sulfonyl chloride **19** to give diolefins **20** in moderate yields (56–67 %). Sulfonyl chloride **19**, although commercially available, is an expensive reagent. Therefore it was successfully synthesized by boiling allyl bromide with Na<sub>2</sub>SO<sub>3</sub>, then obtained sodium salt was treated with POCl<sub>3</sub>. It should be noted, that sulfonyl chloride **19** is air sensitive, therefore, we obtained it in larger quantities and purified by vacuum distillation. Using non-distilled sulfonyl chloride **19**, the yield of reaction products was significantly reduced. Cyclization of diolefin **20** using olefin ring closing metathesis reaction was chosen as the key step in synthesis of benzoxathiepine-2,2-dioxide. Cyclization

was successfully performed using a commercially available Grubbs 2<sup>nd</sup> generation catalyst derivative **21**. We obtained corresponding 7-substituted 3*H*-1,2-benzoxathiepine 2,2-dioxides **3** in good yields (84–96 %).

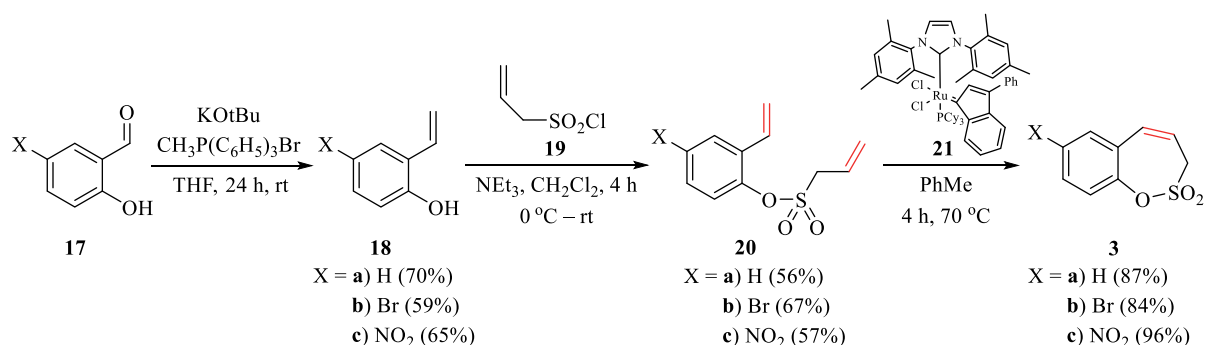


Fig. 5. Synthesis of 3*H*-1,2-benzoxathiepine 2,2-dioxide derivatives **3a–3c**.

7-Nitro-3*H*-1,2-benzoxathiepine 2,2-dioxide **3c** mono crystal, which was of sufficient quality for structure determination using single crystal X-ray diffraction was obtained. In the laboratory of Physical Organic Chemistry of the Latvian Institute of Organic Synthesis, an X-ray pattern was obtained. X-ray pattern is an unequivocal proof of the structure of compound **3c** (Fig. 6).

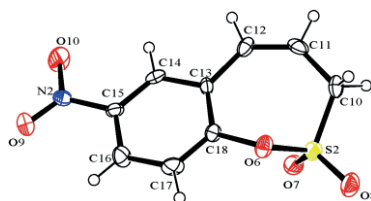


Fig. 6. 7-Nitro-3*H*-1,2-benzoxathiepine 2,2-dioxide **3c** X-ray structure.

It should be noted, that nowadays a lot of different olefin ring closing metathesis reaction catalysts are known. Mostly ruthenium and molybdenum catalysts are used. In 1990s, first generation catalysts were developed and commercialized. The best known ones are Grubbs 1<sup>st</sup> generation catalyst **22** and Schrock's catalyst **23** (Fig. 7). Unfortunately, 1<sup>st</sup> generation catalysts do not exceed high functional group tolerance and selectivity; they are air and moisture sensitive [17]. In August 1999, Grubbs published a paper in which he described new, more efficient ruthenium olefin ring closing metathesis reaction catalysts [18]. Today they are known as Grubbs 2<sup>nd</sup> generation catalysts. 2<sup>nd</sup> generation ruthenium catalysts are more efficient, they have increased thermal stability, catalytic activity, air and moisture resistance. That was achieved by replacing the tricyclohexylphosphine ligand with an N-heterocyclic carbene (NHCs) ligand [17], [19]. The best known of these catalysts is Grubbs 2<sup>nd</sup> generation catalyst **24** (Fig. 7). Continuing the development of molybdenum catalysts, Schrock–Hoveyda catalyst **25** (Fig. 7) was developed. It has a higher functional group tolerance and selectivity than the Schrock's catalyst **23**. In general molybdenum catalysts tolerate amines and phosphines, but do not tolerate substrates with carboxyl, hydroxy, and

aldehyde groups. Ruthenium catalysts, on the other hand, do not tolerate amines and phosphines, but tolerate substrates with carboxyl, hydroxy, and aldehyde groups [17].

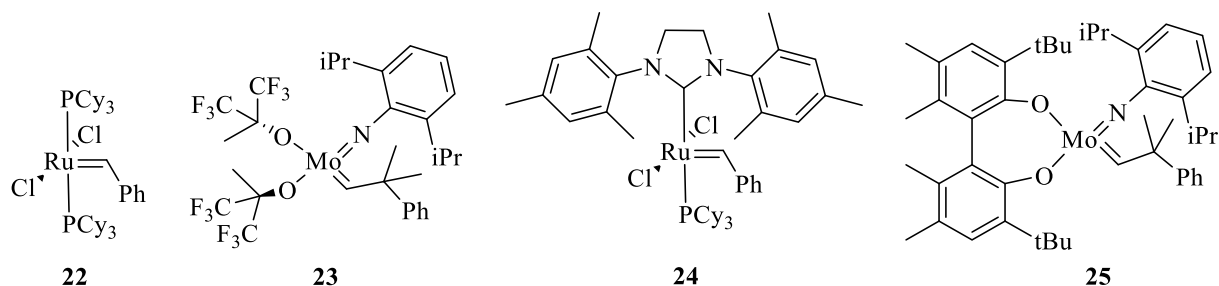


Fig. 7. Some olefin ring closing metathesis reaction catalysts.

Since 2<sup>nd</sup> generation ruthenium catalysts are thermally stable, with good functional group tolerance, air and moisture resistance, we decided to use a commercially available 2<sup>nd</sup> generation catalyst derivative **21**.

### 1.1. Synthesis of 3*H*-1,2-benzoxathiepine 2,2-dioxide 1,2,3-triazolyl derivatives

To better understand structure–activity relationship (SAR) we decided to synthesize 1,4-disubstituted benzoxathiepine-2,2-dioxide 1,2,3-triazolyl derivatives **4**. Michael, in 1893, published the first ever synthesis of 1,2,3-triazoles from diethyl acetylenedicarboxylate and phenyl azide [20]. Despite this, the synthesis of 1,2,3-triazoles is more related with Huisgen. In the 1960s, he worked on 1,3-dipolar cycloaddition reactions, including the synthesis of 1,2,3-triazoles, studied the reaction mechanism and kinetics [21]. Since then, it has been known that the reaction of azides **26** with alkynes **27** at high temperature forms a mixture of regioisomers – 1,4- **28** and 1,5-disubstituted **29** 1,2,3-triazoles (Fig. 8).

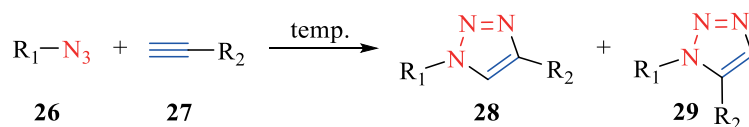


Fig. 8. Synthesis of 1,2,3-triazoles.

Nowadays, there are methods for selective synthesis of 1,4- or 1,5-disubstituted 1,2,3-triazolyl derivatives. In 2002, Mendal with co-workers [22] and Sharpless with co-workers [23] independently of each other published papers describing Cu (I) catalyzed azide-alkyne cycloaddition to selectively form 1,4-disubstituted 1,2,3-triazole derivatives. It should be noted, that in the protocol developed by Sharpless [23] CuSO<sub>4</sub> was used, which was reduced *in situ* with sodium ascorbate to selectively form Cu(I) instead of Cu(0). Selective formation of 1,5-disubstituted 1,2,3-triazolyl derivatives can be achieved using various ruthenium catalysts [21], [24].

Continuing the work, we successfully reduced nitro derivative **3c** with Fe(0), obtaining the amino derivative **30** (Fig. 9). From amino derivative **30** in decent yield (69 %) we synthesized azide derivative **31** (Fig. 9.), which was further used as a starting material in the synthesis of 1,4-disubstituted 1,2,3-triazolyl derivatives. Treatment of amino derivative **30** with NaNO<sub>2</sub> in

acid medium *in situ* produces diazonium salt, which then reacts with NaN<sub>3</sub> to form azide **31**. It should be noted, that from NaN<sub>3</sub> in acid medium HN<sub>3</sub> (hydrazoic acid) forms, which is a volatile, toxic compound. Therefore, the reaction must be carried out at 0 °C temperature.

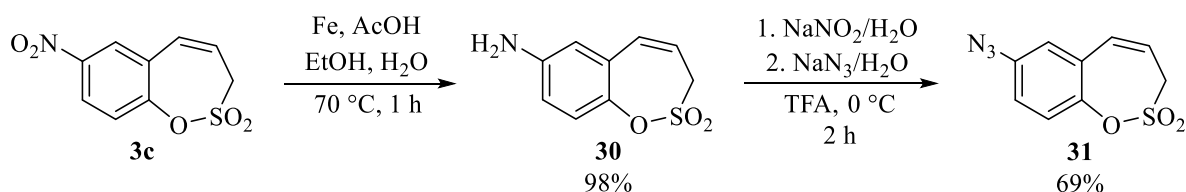


Fig. 9. Synthesis of 3*H*-1,2-benzoxathiepine 2,2-dioxide azido derivative **31**.

For selective synthesis of 1,4-disubstituted 1,2,3-triazolyl derivatives we chose to use a Cu(I) catalyzed reaction between azide **31** and various alkynes (Fig. 10). Cu(I) was obtained from CuSO<sub>4</sub> by *in situ* reduction with sodium ascorbate, similar like in Scharpless article [23]. As a solvent, we chose to use a 1 : 1 mixture of *t*-BuOH/H<sub>2</sub>O. With good yields we synthesized a series of 1,4-disubstituted 1,2,3-triazole derivatives **4a–4j**. It should be noted, that we decided to use acetic acid additive. It has been proven, that weak organic acid additive (acetic, benzoic acid) facilitates the elimination of copper after 1,3-dipolar cycloaddition, thus increasing the reaction rate [25].

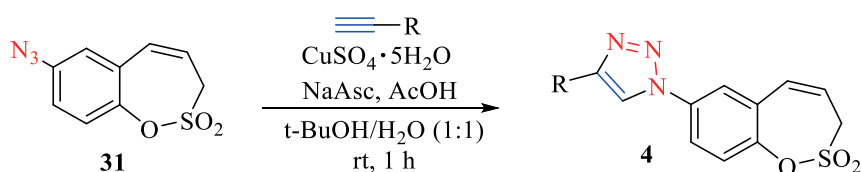


Fig. 10. Synthesis of 1,4-disubstituted 1,2,3-triazole derivatives **4**.

Table 1

Synthesis of benzoxathiepine-2,2-dioxide 1,2,3-triazolyl derivatives **4**, CA inhibition results

Entry	R	<b>4</b> , yield, %	$K_I^*$ , $\mu\text{M}$			
			hCA I	hCA II	hCA IX	hCA XII
1	C <sub>6</sub> H <sub>5</sub>	<b>4a</b> , 95	>50	>50	1.71	>50
2	4-ClC <sub>6</sub> H <sub>4</sub>	<b>4b</b> , 74	>50	>50	3.59	>50
3	3-OMeC <sub>6</sub> H <sub>4</sub>	<b>4c</b> , 51	>50	>50	2.56	>50
4	4-FC <sub>6</sub> H <sub>4</sub>	<b>4d</b> , 66	>50	>50	1.75	>50
5	4-OCF <sub>3</sub> C <sub>6</sub> H <sub>4</sub>	<b>4e</b> , 83	>50	5.77	0.34	1.72
6	3-FC <sub>6</sub> H <sub>4</sub>	<b>4f</b> , 74	>50	>50	1.15	>50
7	2-NH <sub>2</sub> C <sub>6</sub> H <sub>4</sub>	<b>4g</b> , 57	>50	>50	0.46	2.32
8	CH <sub>2</sub> OH	<b>4i</b> , 81	>50	>50	0.87	>50
9	4-CF <sub>3</sub> C <sub>6</sub> H <sub>4</sub>	<b>4j</b> , 85	>50	>50	0.43	>50
10	AAZ*	–	0.25	0.012	0.025	0.006

\* Different CA isoform inhibition of acetazolamide (AAZ, Entry 10).



For the compounds synthesized within the scope of the Doctoral Thesis, inhibitory activities of human carbonic anhydrases (CA I, CA II, CA IX, and CA XII) were determined at University of Florence in Prof. C. T. Supuran's group. In all cases, 5-acetamido-1,3,4-thiadiazole-2-sulfonamide (acetazolamide, AAZ), a non-selective isoform inhibitor, was used as a reference standard.

It should be noted, that inhibition of the cytosolic CA isoforms CA I and CA II is undesirable because they are widespread in the human body (off-target enzymes). On the other hand, transmembrane isoforms (CA IX and CA XII) are drug targets, because they are overexpressed in tumour cells.

As shown in Table 1, all synthesized triazole derivatives do not inhibit cytosolic CA I and CA II, except compound **4e**, which showed a moderate inhibitory profile against CA II ( $K_I = 5.77 \mu\text{M}$ , *Entry 5*). Tumour associated isoform CA IX was inhibited by all triazole derivatives **4a–4j**, with  $K_{IS}$  ranging between  $0.43 \mu\text{M}$  and  $3.59 \mu\text{M}$ . Four compounds **4e**, **4g–4j** showed submicromolar CA IX inhibitory activity. Compound **4i** contains a hydroxymethyl group in the triazolyl ring, its CA IX inhibition constant is  $K_I = 0.87 \mu\text{M}$  (*Entry 8*). For phenyl group containing triazoles **4e**, **4g**, and **4j** substituted with 4-trifluoromethoxy-, 2-amino-, or 4-trifluoromethyl substituents on the aryl fragment  $K_{IS}$  are  $0.34 \mu\text{M}$ ;  $0.46 \mu\text{M}$  and  $0.43 \mu\text{M}$  (*Entry 5, 7, 9*).

Seven out of nine triazole derivatives do not inhibit CA XII,  $K_I > 50 \mu\text{M}$  (*Entry 1–4, 6, 8–9*). Remaining two compounds **4e** and **4g** are moderate CA XII inhibitors –  $K_I = 1.72$  and  $2.32 \mu\text{M}$  (*Entry 5, 7*). Based on biological results, we can conclude that 1,4-disubstituted 1,2,3-triazole derivatives **4a–4j** are selective CA IX inhibitors.

## 1.2. Synthesis of 7-acylamino-3H-1,2-benzoxathiepine 2,2-dioxides

Continuing development of the work, we decided to synthesize 7-acylamino-3H-1,2-benzoxathiepine 2,2-dioxide derivatives **5** to better understand SAR. 7-Acylamino derivatives were successfully synthesized from amino derivative **30** in reactions with various acyl chlorides (Fig. 11, Table 2).

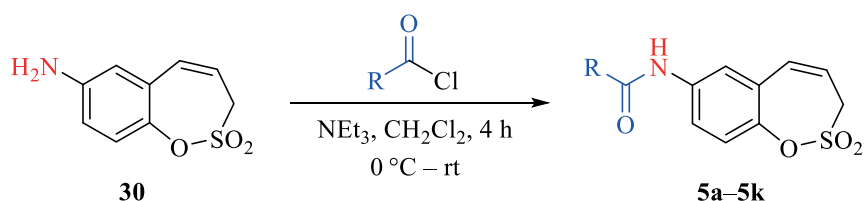


Fig. 11. 7-Acylamino-3H-1,2-benzoxathiepine 2,2-dioxide **5** synthesis.

As shown in Table 2, all synthesized products **5a–5g** do not inhibit cytosolic (off-target) CA I and CA II ( $K_I > 100\,000 \text{ nM}$ ). On the other hand, they inhibit target enzymes CA IX and CA XII in nanomolar concentrations. Derivative **5i** is the most active CA IX and CA XII inhibitor –  $K_I = 19.7 \text{ nM}$  and  $8.7 \text{ nM}$  (*Entry 8*), it is even more active than AAZ (*Entry 11*).

Table 2

Synthesis of 7-acylamino benzoxathiepine 2,2-dioxide derivatives **5**, CA inhibition results

Entry	R	Product No., yield, %	$K_I^*$ , nM			
			hCA I	hCA II	hCA IX	hCA XII
1	CH <sub>3</sub>	<b>5a</b> , 70	>100 000	>100 000	61.8	162.5
2	C <sub>6</sub> H <sub>5</sub>	<b>5b</b> , 72	>100 000	>100 000	208.6	370.1
3	4-CH <sub>3</sub> C <sub>6</sub> H <sub>4</sub>	<b>5c</b> , 73	>100 000	>100 000	83	309.3
4	4-BrC <sub>6</sub> H <sub>4</sub>	<b>5d</b> , 59	>100 000	>100 000	353.3	140.7
5	2-IC <sub>6</sub> H <sub>4</sub>	<b>5e</b> , 88	>100 000	>100 000	45.4	643.7
6	2-BrC <sub>6</sub> H <sub>4</sub>	<b>5f</b> , 82	>100 000	>100 000	66.8	96.2
7	2-FC <sub>6</sub> H <sub>4</sub>	<b>5g</b> , 79	>100 000	>100 000	74.6	40.3
8	2-CF <sub>3</sub> C <sub>6</sub> H <sub>4</sub>	<b>5i</b> , 87	>100 000	>100 000	19.7	8.7
9	2-thienyl	<b>5j</b> , 81	>100 000	>100 000	177.5	73.2
10	2-furyl	<b>5k</b> , 81	>100 000	>100 000	210.1	134.4
11	AAZ*	–	250	12	25	5.7

\* Different CA isoform inhibition of acetazolamide (AAZ, Entry 10).

Compounds **5a–5g** and **5j–5k** exhibit weaker biological activity on CA IX and CA XII than AAZ (Entry 11), their inhibition constants are 45.4–353.3 and 40.3–643.7 nM (Entry 1–7, 9, 10). Compound **5d**, which contains 4-bromophenyl substituent, is less active CA IX inhibitor (CA IX  $K_I = 353.3$  nM, Entry 4) than compound **5f**, which contains 2-bromophenyl substituent (CA IX  $K_I = 66.8$  nM, Entry 6). In general, compounds containing substituents in second position of phenyl ring are more active than the compounds containing substituent in fourth position of phenyl ring. If unsubstituted phenyl group (**5b**, Entry 2) is replaced by methyl group (**5a**, Entry 1), increases inhibitory activity on target enzymes. If unsubstituted phenyl group (**5b**, Entry 2) is replaced by five membered heterocycle **5j** (Entry 9) and **5g** (Entry 10), the target enzyme inhibitory activity does not change significantly.

### 1.3. Synthesis of 3H-1,2-benzoxathiepine 2,2-dioxide aryl derivatives

To gain a better understanding about SAR and expand the range of compounds, we decided to synthesize benzoxathiepine-2,2-dioxide aryl derivatives **6–9** (Fig. 12).

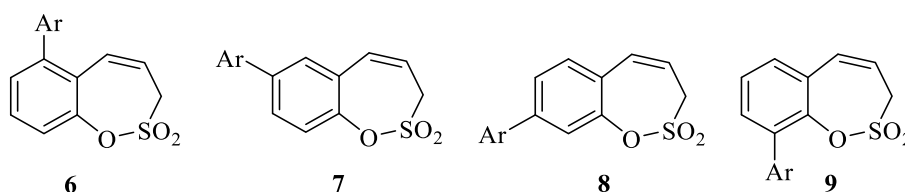


Fig. 12. General structures of benzoxathiepine-2,2-dioxide aryl derivatives **6–9**.

We decided to synthesize benzoxathiepine-2,2-dioxide aryl derivatives by palladium catalyzed Suzuki–Miyaura cross-coupling reaction, from corresponding benzoxathiepine-2,2-dioxide halogen derivatives and aryl boronic acids.

In general, palladium and nickel catalysts are mainly used in Suzuki–Miyaura cross-coupling reaction. In the case of palladium catalysts, the most reactive are aryl iodides, followed by triflates and bromides. The use of aryl chlorides significantly reduces the reaction product yield. Oxidative addition (the first stage of the catalytic cycle) in most cases is the limiting step, its speed decreases in order  $I \gg OTf \approx Br \gg Cl$  [26]. The most commonly used palladium catalysts in the Suzuki–Miyaura cross-coupling reaction are palladium catalysts with phosphine ligands:  $Pd(PPh_3)_4$ ,  $Pd(dppf)Cl_2$ ,  $Pd(PPh_3)_2Cl_2$ , they are thermally stable and commercially available [26], [27].

The development of nickel catalysts has contributed to the use of less reactive electrophiles such as aryl chlorides, fluorides, esters, nitriles and aryl amides Suzuki–Miyaura cross-coupling reaction [28]. However, despite these advantages, palladium catalysis is more widely used in practical synthesis than nickel catalysis. Generally, nickel catalyzed Suzuki–Miyaura cross-coupling reactions require high catalyst loading (3–10 mol %), and they are sensitive to reaction conditions. The choice of base and solvent is very crucial. Mostly THF, dioxane or toluene is used in combination with a poorly soluble inorganic base such as  $K_3PO_4$  or  $K_2CO_3$  [28]. Alkali hydroxides [29], water addition [30] deactivates nickel catalysts and the reaction product yield decreases.

In palladium catalyzed Suzuki–Miyaura cross-coupling reaction both – inorganic and organic bases such as  $Na/K_3PO_4$ ,  $Na/Cs/K_2CO_3$ ,  $Na/KOH$ ,  $Na/KOt-Bu$ ,  $NaOEt$ ,  $NaOMe$  can be used. It is important to note that the role of base is crucial, cross-coupling reaction will not proceed without the presence of a base. Mainly organic solvent is used in mixture with water. Commonly used organic solvents are dioxane, THF, DMF, and toluene [31].

Weak nucleophilic nature and stability of organoboron compounds contributed to the development of cross-coupling reaction. Organoboron compounds are commercially available, several methods have been developed to synthesize them. Cross-coupling can be done with good chemical, regio- and stereoselectivity.

We started target compound **6–9** synthesis with preparation of starting materials. In palladium catalyzed Suzuki–Miyaura cross-coupling reaction iodides react more actively than bromides, therefore we decided to synthesize 7-iodo derivative **32**. It should be noted, that iodosalicylaldehyde **33**, although commercially available, is an expensive reagent. It was successfully synthesized from salicylaldehyde **34** treating it with iodine monochloride in acid medium (Fig. 13). Next, we performed Wittig reaction on iodosalicylaldehyde **33** to yield olefin **35**. Olefin **35** was successfully sulfonylated with sulfonyl chloride **19** to give diolefin **36**. Diolefin **36** was successfully cyclised using ruthenium olefin ring-closing metathesis catalyst **21** to give 7-iodo derivative **32** in good yield.

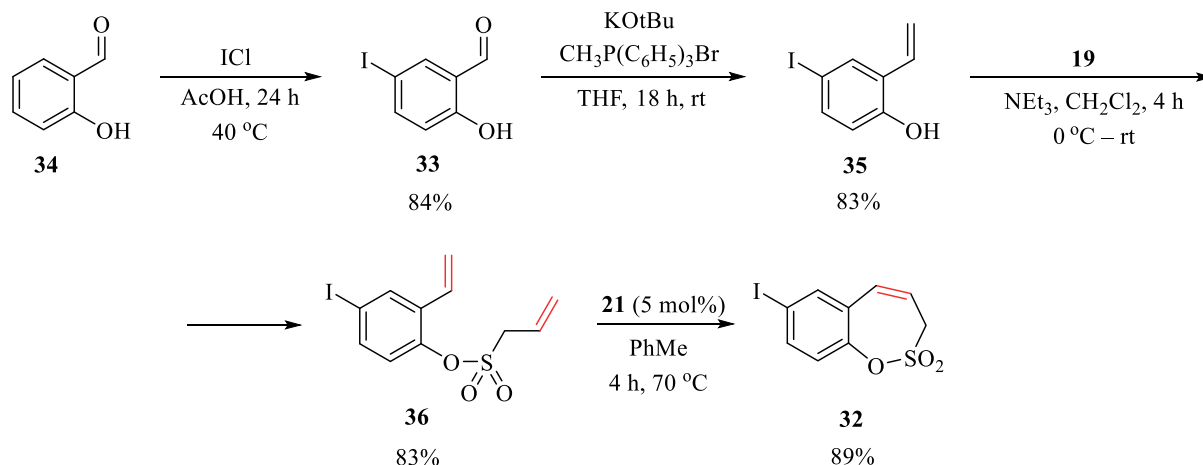


Fig. 13. Synthesis of 7-iodo-3*H*-1,2-benzoxathiepine 2,2-dioxide **32**.

As 3-, 4-, and 6-bromosalicylaldehydes are commercially available and there is no convenient synthesis method for preparation of corresponding iodosalicylaldehydes, we decided to synthesize bromo derivatives **37–39** (Fig. 14–16).

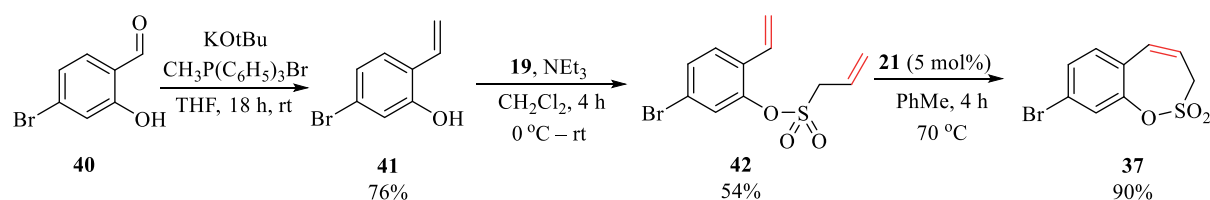


Fig. 14. Synthesis of 8-bromo-3*H*-1,2-benzoxathiepine 2,2-dioxide **37**.

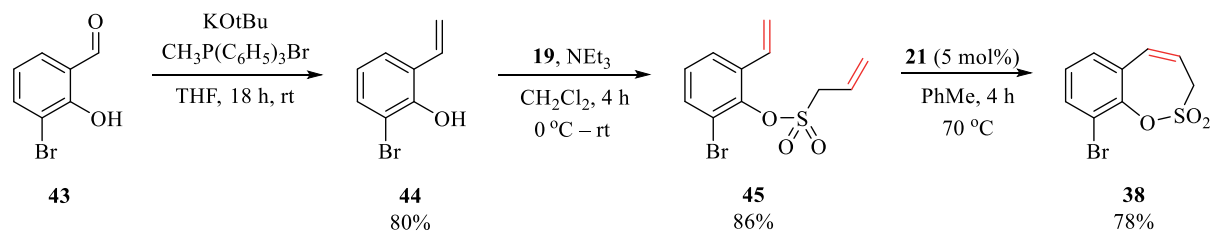


Fig. 15. Synthesis of 9-bromo-3*H*-1,2-benzoxathiepine 2,2-dioxide **38**.

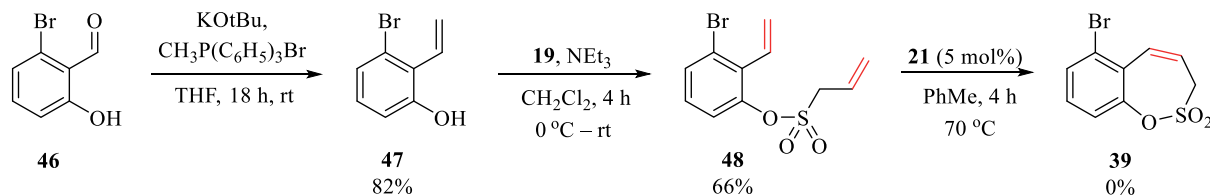


Fig. 16. Synthesis of 6-bromo-3*H*-1,2-benzoxathiepine 2,2-dioxide **39**.

Bromo derivatives **37** and **38** were obtained similarly to iodine derivative **32**. At first we performed Wittig reaction on the corresponding salicylaldehyde to obtain corresponding olefin. The olefin was sulfonylated with sulfonyl chloride **19** to give the corresponding diolefin, which was successfully cyclized using ruthenium ring-closing metathesis catalyst **21**. Unfortunately using the previously developed cyclization conditions, compound **39** was not obtained. We performed a small optimization of the reaction conditions (Fig. 17 and Table 3).

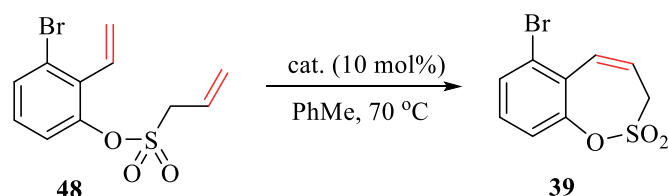


Fig. 17. Optimization of diolefin **48** ring-closing metathesis reaction conditions.

Table 3

Optimization Results of Diolefin **48** Ring-Closing Metathesis Reaction Conditions

Entry	Catalyst	Time, h	Yield, %
1	<b>21</b>	40	–
2	<b>23</b>	16	–
3	<b>25</b>	16	–

Using previously used catalyst **21**, increasing reaction time and twice increasing the amount of catalyst, no product formation was observed (*Entry 1*). We decided to try Schrock's molybdenum catalysts **23** (*Entry 2*) and **25** (*Entry 3*), because in general molybdenum catalysts are more active than ruthenium catalysts. Unfortunately, even by changing the catalyst the desired product **39** was not forming. Most likely it is due to steric factors.

Benzoxathiepine 2,2-dioxide aryl derivatives **7–9** were successfully synthesized in a palladium catalyzed Suzuki–Miyaura cross-coupling reaction using palladium tetrakis ( $\text{Pd}(\text{PPh}_3)_4$ ) as a catalyst (Fig. 18, Tables 4–6). The reaction required heating and addition of water. Without water additive yield of reaction products decreased significantly.

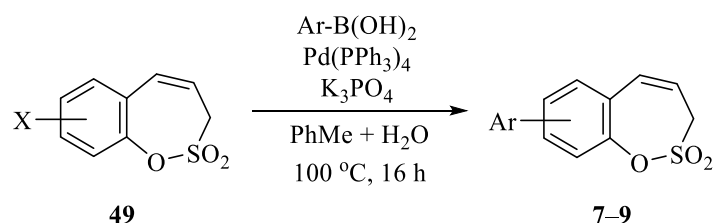
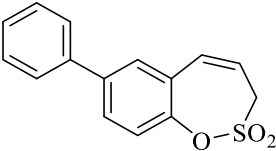
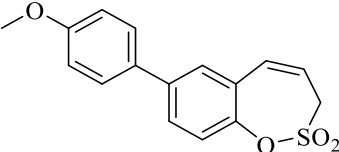
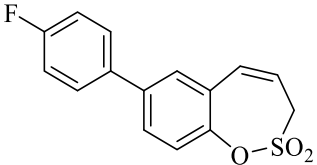
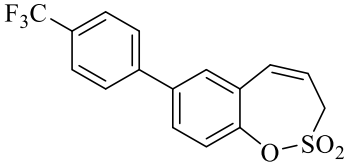
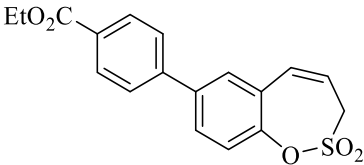


Fig. 18. Optimized Suzuki–Miyaura cross-coupling reaction conditions.

Table 4

Synthesis of 7-aryl-3H-1,2-benzoxathiepine 2,2-dioxide derivatives **7**, CA inhibition results

Entry	Product No., yield, %	Product	$K_I^*$ , nM	
			hCA IX	hCA XII
1	<b>7a</b> , 56		654.8	1376
2	<b>7b</b> , 61		407.6	2934
3	<b>7c</b> , 44		330.8	890.5
4	<b>7d</b> , 66		221.4	4017
5	<b>7e</b> , 44		620.8	2398

\* For compounds **7a–7e** hCA I and hCA II  $K_I > 100 \mu\text{M}$ . AAZ used as a standard CA inhibitor, its hCAI  $K_I = 0.25 \text{ nM}$ , hCAII  $K_I = 0.012 \text{ nM}$ , CA IX  $K_I = 25 \text{ nM}$ , and CA XII  $K_I = 5.7 \text{ nM}$ .

As shown in Table 4, 7-aryl substituted benzoxathiepine 2,2-dioxide derivatives **7a–7c** were obtained in good (*Entry* 1, 2 and 4) and moderate yields (*Entry* 3 and 5). 7-aryl derivatives **7a–7c** do not inhibit cytosolic (off-target) CA I and CA II. On the other hand, 7-aryl derivatives **7a–7c** inhibit target enzymes CA IX ( $K_I = 221.4–654.8 \text{ nM}$ ) and CA XII ( $K_I = 890.5–4017 \text{ nM}$ ), they are more effective CA IX than CA XII inhibitors.

Table 5

Synthesis of 8-aryl-3*H*-1,2- benzoxathiepine 2,2-dioxide derivatives **8**, CA inhibition results

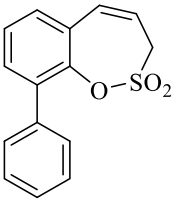
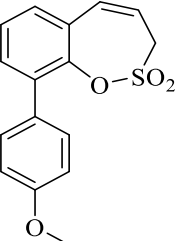
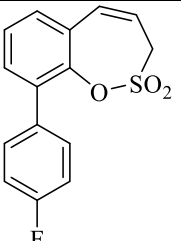
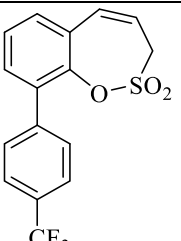
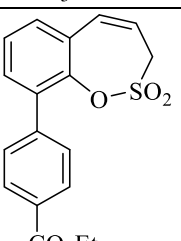
Entry	Product No., yield, %	Product	$K_I^*$ , nM	
			hCA IX	hCA XII
1	<b>8a</b> , 44		104.8	473.2
2	<b>8b</b> , 44		63.1	168.6
3	<b>8c</b> , 41		95.2	77.9
4	<b>8d</b> , 46		44.0	247.8
5	<b>8e</b> , 38		79.8	289.3

\* For compounds **8a–8e** hCA I and hCA II  $K_I > 100 \mu\text{M}$ . AAZ used as a standard CA inhibitor, its hCAI  $K_I = 0.25 \text{ nM}$ , hCAII  $K_I = 0.012 \text{ nM}$ , CA IX  $K_I = 25 \text{ nM}$ , and CA XII  $K_I = 5.7 \text{ nM}$ .

As shown in Table 5, 8-aryl substituted benzoxathiepine 2,2-dioxide derivatives **8a–8c** were obtained in moderate yields. 8-aryl derivatives **8a–8c** do not inhibit cytosolic (off-target) CA I and CA II. However, 8-aryl derivatives **8a–8c** inhibit target enzymes CA IX ( $K_I = 44.0\text{--}104.8 \text{ nM}$ ) and CA XII ( $K_I = 77.9\text{--}473.2 \text{ nM}$ ).

Table 6

Synthesis of 9-aryl-3*H*-1,2-benzoxathiepine 2,2-dioxide derivatives **9**, CA inhibition results

Entry	Product No., yield, %	Product	$K_1^*$ , $\mu\text{M}$	
			hCA IX	hCA IX
1	<b>9a</b> , 42		21.1	>100
2	<b>9b</b> , 40		60.9	>100
3	<b>9c</b> , 39		33.7	>100
4	<b>9d</b> , 44		47.1	>100
5	<b>9e</b> , 36		16.4	>100

\* For compounds **9a–9e** hCA I and hCA II  $K_1 > 100 \mu\text{M}$ . AAZ used as a standard CA inhibitor, its hCAI  $K_1 = 0.25 \text{ nM}$ , hCAII  $K_1 = 0.012 \text{ nM}$ , CA IX  $K_1 = 25 \text{ nM}$ , and CA XII  $K_1 = 5.7 \text{ nM}$ .

As shown in Table 6, 9-aryl substituted benzoxathiepine 2,2-dioxide derivatives **9a–9c** were obtained in moderate yields. 9-aryl derivatives **9a–9c** do not inhibit cytosolic (off-target) CA I, CA II, and cancer associated (target) isoform CA XII. They poorly inhibit other cancer associated isoform CA IX ( $K_1 = 16.4\text{--}60.9 \mu\text{M}$ ).



It should be noted, that no effect of aryl boronic acid substituent was observed on Suzuki–Miyaura cross-coupling reaction. In all cases, products **7–9** were obtained in similar yields.

Comparing 7-aryl (Table 4), 8-aryl (Table 5), and 9-aryl (Table 6) benzoxathiepine 2,2-dioxide biological activities, we conclude that the most active cancer associated isoform (CA IX and CA XII) inhibitors are 8-aryl derivatives **8a–8e** (Table 5), followed by 7-aryl derivatives **7a–7e** (Table 4). 9-aryl derivatives **9a–9e** exhibit very weak inhibitory activity on CA IX and they do not inhibit CA XII.

7-aryl derivatives **7a–7e** (Table 4) are more selective CA IX inhibitors than 8-aryl derivatives **8a–8e** (Table 5), but best inhibitory activity on CA IX was observed for compound **8d** (Table 5, *Entry 4*), the best CA XII inhibitor was compound **8c** (Table 4, *Entry 3*).

In order to understand the interaction of benzoxathiepine 2,2-dioxide with CA, Professor K. Tars' group at Latvian Biomedical Research and Study Centre performed co-crystallization experiments of benzoxathiepine 2,2-dioxide and human CA IX. Unfortunately, the enzyme-inhibitor cocrystal has not been obtained so far. It should be noted, that the sulfocoumarin derivative **50** previously developed and synthesized in our group was successfully cocrystallized with CA II / CA IX mimetic under the supervision of K. Tars [4a].

Examining the structure of the cocrystal, we concluded that the sulfocoumarin ring has opened in the active site of enzyme forming vinylsulfonic acid **51** (Fig. 19). Coumarins undergo an analogous ring opening forming corresponding cinnamic acid derivatives [3].

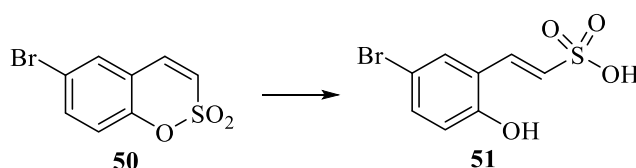


Fig. 19. Sulfocoumarin ring opening in CA II / CA IX mimic active site.

Since we do not have a benzoxathiepine 2,2-dioxide-target enzyme cocrystal, we can only guess the mechanism of inhibition. It is possible that oxathiepine 2,2-dioxide ring opens in the active site of the enzyme in a similar way to sulfocoumarins.

## 2. Synthesis of imidazolidine-2,4-dione derivative

In the final stage of the Doctoral Thesis, we discovered that furagin **52** (Fig. 20), an antibacterial drug used in clinics, is a selective inhibitor of tumour associated CA IX and CA XII. Furagin, nitrofurantoin analog, is used in the therapy of urinary tract infections [32].

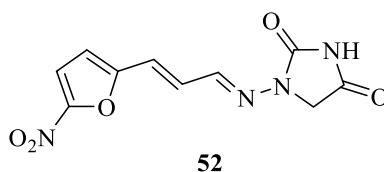


Fig. 20. Furagin structure.

To better understand how furagin binds to different CA isoforms (CA II, CA IX, and CA XII), our collaboration partners from the University of Florence performed molecular modelling (Fig. 21) and molecular dynamics simulation experiments.

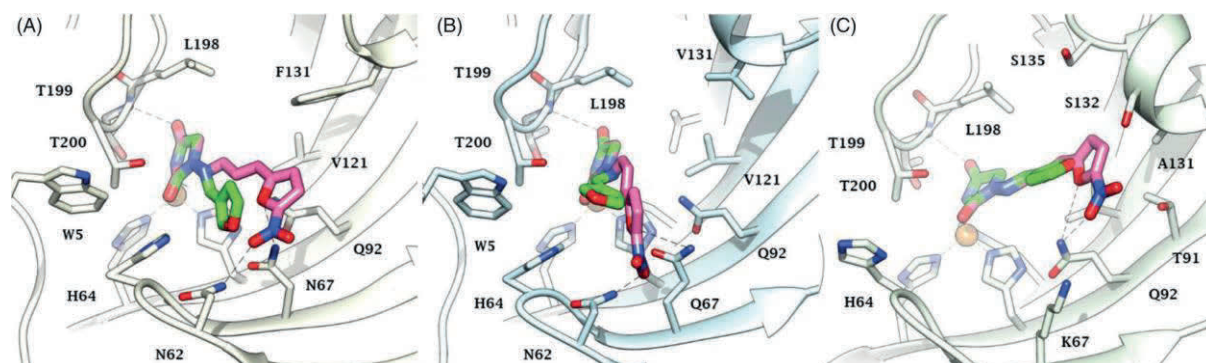


Fig. 21. Predicted docking orientations of furagin (pink) imidazolidine-2,4-dione (green) to (A) CA II, (B) CA IX, and (C) CA XII.

From the molecular modelling experiments we conclude that imidazolidine-2,4-dione function is a zinc binding group. Molecular dynamics simulation experiments in the range of 100 nanoseconds show that furagin forms a strong H-bond interaction with target enzymes CA IX and CA XII. In contrast, furagin does not form a strong H-bond interaction with CA II, that is why it is a selective inhibitor of CA IX and CA XII.

Based on docking and molecular simulation experiments, we decided to develop this direction by synthesizing a series of imidazolidine-2,4-dione derivatives **10a–10r** (Fig. 22 and Table 7). Imidazolidine-2,4-dione derivatives **10a–10r** were successfully synthesized by reaction of 1-aminoimidazolidine-2,4-dione hydrochloride **53** with various aldehydes.

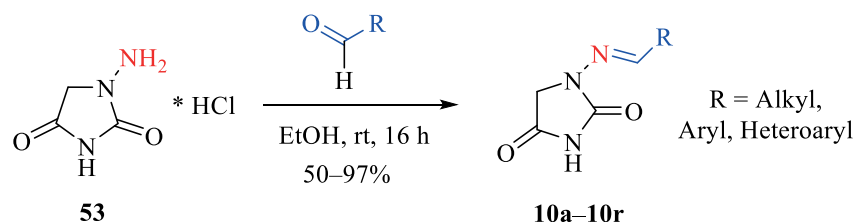
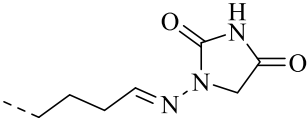


Fig. 22. Synthesis of imidazolidine-2,4-dione derivative **10a–10r**.

As shown in Table 7, a number of compounds with alkyl **10h** and **10i** (Entry 8–9), aryl **10a–10c**, **10g** and **10j–10l** (Entry 1–4, 7, 10–12), heteroaryl substituents **10f** and **10m–10p** (Entry 6 and 13–16) were obtained. Regardless of the type of substituent, all reaction products were obtained in good and very good yield 50–97 %. It should be noted, that all compounds **10a–10r** were successfully purified by crystallization from ethanol, no further purification by column chromatography was required.

Table 7

Imidazolidine-2,4-dione derivative **10a–10r** synthesis, CA inhibition results

Entry	Product No., yield, %	R	$K_I^*$ , nM			
			CA I	CA II	CA IX	CA XII
1	<b>10a</b> , 90	C <sub>6</sub> H <sub>5</sub>	39 600	900	3500	5600
2	<b>10b</b> , 80	4-OCH <sub>3</sub> -C <sub>6</sub> H <sub>4</sub>	57 600	6400	1200	4700
3	<b>10c</b> , 82	4-NO <sub>2</sub> -C <sub>6</sub> H <sub>4</sub>	>100 000	11 100	7400	2800
4	<b>10d</b> , 95	4-(CO <sub>2</sub> CH <sub>3</sub> )-C <sub>6</sub> H <sub>4</sub>	>100 000	8300	4900	930
5	<b>10e</b> , 50		19 100	4000	1100	160
6	<b>10f</b> , 89	3-furanyl	16 800	710	850	1700
7	<b>10g</b> , 90	4-(OCH <sub>2</sub> C <sub>6</sub> H <sub>5</sub> )-C <sub>6</sub> H <sub>4</sub>	>100 000	540	350	910
8	<b>10h</b> , 81	CHCH(CO <sub>2</sub> C <sub>2</sub> H <sub>5</sub> )	45 900	23 600	810	440
9	<b>10i</b> , 72	CHC(CH <sub>3</sub> ) <sub>2</sub>	28 800	16 500	2900	880
10	<b>10j</b> , 71	CHCH(4-OCH <sub>3</sub> -C <sub>6</sub> H <sub>4</sub> )	>100 000	3100	400	360
11	<b>10k</b> , 93	2,4-(OH) <sub>2</sub> -C <sub>6</sub> H <sub>3</sub>	>100 000	59 900	5800	150
12	<b>10l</b> , 88	4-(B(OH) <sub>2</sub> )-C <sub>6</sub> H <sub>4</sub>	90 700	14 200	7300	230
13	<b>10m</b> , 95	2-pyridyl	51 800	4200	4500	1300
14	<b>10n</b> , 90	3-pyridyl	45 600	620	2300	3200
15	<b>10o</b> , 91	4-pyridyl	26 600	3300	1600	810
16	<b>10p</b> , 97	5-imidazolyl	9600	12 400	560	350
17	Furagin ( <b>52</b> )*	–	>100 000	9600	260	57
18	AAZ*	–	250	12	25	6

\* Row 17 shows the ability of furagin **52** to inhibit different CA isoforms; Row 18 shows the ability of acetazolamide (AAZ) to inhibit different CA isoforms.

Inhibition activities of various CA isoforms were determined for all synthesized imidazolidine-2,4-dione derivatives **10a–10r**, see Table 7 for the obtained results. All tested imidazolidine-2,4-dione derivatives **10a–10r** exhibited weak inhibitory effect on cytosolic CA I isoform,  $K_I = 16\,800\text{--}100\,000$  nM. The physiologically relevant isoform, CA II, was better inhibited,  $K_I = 620\text{--}59\,000$  nM. Compounds **10a**, **10f**, **10g**, and **10n** (Entry 1, 6–7, and 14) containing unsubstituted phenyl moiety, or heteroaryl group showed the best inhibitory activities,  $K_I = 540\text{--}900$  nM. The rest of the compounds showed weaker inhibitory effect of CA II,  $K_I = 3100\text{--}59\,000$  nM. It should be noted, that the compound **10k** (Entry 11), having dihydroxyphenyl substituent, proved to be almost a three times weaker CA II inhibitor, than the second weakest CA II inhibitor **10h** (Entry 8).

Compounds **10f–10h** (Entry 6–8), **10j** (Entry 10), **10p** (Entry 16), and furagin (Entry 17) inhibited cancer associated target enzyme CA IX at nanomolar concentrations ( $K_I = 260\text{--}850$  nM), the strongest inhibition was observed for furagin. The rest of imidazolidine-2,4-dione derivatives showed one order weaker CA IX inhibition activities,  $K_I = 1100\text{--}7300$  nM.

Certain pattern can be observed, compounds containing vinyl substituent **10h** (Entry 8), **10j** (Entry 10) and furagin (Entry 17) or small heteroaryl substituent **10f** (Entry 6) and **10p**

(Entry 16) are better CA IX inhibitors than the rest of compounds, except in the case of compound **10g** (Entry 7), containing ether moiety.

Of all the isoforms studied, the other cancer associated isoform CA XII was inhibited best. The best inhibitor was furagin (Entry 17),  $K_I = 57$  nM. One order weaker CA XII inhibition compared to furagin was observed for compounds **10d** and **10e** (Entry 4–5), **10g–10l** (Entry 7–12), **10o** and **10p** (Entry 14–15), CA XII,  $K_I = 150–930$  nM.

In summary, we have showed that furagin and imidazolidine-2,4-dione derivatives are potential CA inhibitors. Good selectivity against cancer associated isoforms (CA IX and CA IX) compared to cytosolic ones (CA I and CA II) was observed for furagin and compound **10h**.

## CONCLUSIONS

1. The ruthenium-catalyzed olefin ring closing metathesis reaction is suitable for the preparation of 3*H*-1,2-benzoxathiepine 2,2-dioxide and its derivatives.
2. The olefin ring closing metathesis reaction using both ruthenium and molybdenum catalysts is not suitable for the synthesis of 6-bromo-3*H*-1,2-benzoxathiepine-2,2-dioxide.
3. 3*H*-1,2-Benzoxathiepine 2,2-dioxides containing triazolyl, acylamino, or aryl derivatives at 7<sup>th</sup> position are selective and effective inhibitors of tumour associated CA isoforms – CA IX and CA XII.
4. 8-Aryl 3*H*-1,2-benzoxathiepine 2,2-dioxides are the most effective CA IX and CA XII inhibitors compared to the corresponding 7- and 9-aryl 3*H*-1,2-benzoxathiepine 2,2-dioxides.
5. Furagin and the synthesized imidazolidine-2,4-dione derivatives are selective and effective inhibitors of tumour associated CA isoforms – CA IX and CA XII.

## REFERENCES

1. International Agency for Research on Cancer: Latest Global Cancer Data. <https://www.who.int/cancer/PRGlobocanFinal.pdf>
2. Supuran, C. T., Winum, J. Y. (2009) In: Wang, B. (eds) Drug design of zinc-enzyme inhibitors: functional, structural, and disease applications. John Wiley & Sons: Hoboken, New Jersey, pp. 3–13.
3. Maresca, A., Temperini, C., Vu, H., Pham, N. B., Poulsen, S., Scozzafava, A., Quinn, R. J., Supuran, C. T. Non-Zinc Mediated Inhibition of Carbonic Anhydrases: Coumarins Are a New Class of Suicide Inhibitors. *J. Am. Chem. Soc.* **2009**, *131*, 3057–3062.
4. a) Tars, K., Vullo, D., Kazaks, A., Leitans, J., Lends, A., Grandane, A., Žalubovskis, R., Scozzafava, A., Supuran, C. T. Sulfocoumarins (1,2-benzoxathiine 2,2-dioxides): a class of potent and isoform-selective inhibitors of tumor-associated carbonic anhydrases. *J. Med. Chem.* **2013**, *56*, 293–300. b) Grandane, A., Tanc, M., Žalubovskis, R., Supuran, C. T. 6-Triazolyl-substituted sulfocoumarins are potent, selective inhibitors of the tumor-associated carbonic anhydrases IX and XII. *Bioorg. Med. Chem. Lett.* **2014**, *24*, 1256–1260. c) Grandane, A., Tanc, M., Žalubovskis, R., Supuran, C. T. Synthesis of 6-tetrazolyl-substituted sulfocoumarins acting as highly potent and selective inhibitors of the tumor-associated carbonic anhydrase isoforms IX and XII. *Bioorg. Med. Chem.* **2014**, *22*, 1522–1528.
5. Nocentini, A., Supuran, C. T. Advances in the structural annotation of human carbonic anhydrases and impact on future drug discovery. *Expert Opin. Ther. Pat.* **2018**, *28*, 745–754.
6. Jensen, E. L., Clement, R., Kosta, A., Maberly, S. C., Gontero, B. A new widespread subclass of carbonic anhydrase in marine phytoplankton. *ISME J.* **2019**, *13*, 2094–2106.
7. Supuran, C. T. Structure and function of carbonic anhydrases. *Biochem. J.* **2016**, *473*, 2023–2032.
8. Alterio, V., Di Fiore, A., D'Ambrosio, K., Supuran, C. T., Simone, G. Multiple Binding Modes of Inhibitors to Carbonic Anhydrases: How to Design Specific Drugs Targeting 15 Different Isoforms? *Chem. Rev.* **2012**, *112*, 4421–4468.
9. Supuran, C. T. Carbonic anhydrases: novel therapeutic applications for inhibitors and activators. *Nat. Rev. Drug. Discov.* **2008**, *7*, 168–181.
10. Domsic, J. F., Avvaru, B. S., Kim, C. U., Gruner, S. M., Agbandje-McKenna, M., Silverman, D. N., McKenna, R. Entrapment of Carbon Dioxide in the Active Site of Carbonic Anhydrase II. *J. Biol. Chem.* **2008**, *283*, 30766–30771.
11. Supuran, C. T. How many carbonic anhydrase inhibition mechanisms exist? *J. Enzyme Inhib. Med. Chem.* **2016**, *31*, 345–360.
12. Lomelino, C. L., Supuran, C. T., McKenna, R. Non-Classical Inhibition of Carbonic Anhydrase. *Int. J. Mol. Sci.* **2016**, *17*, 1150.
13. Mondal, S. Recent Developments in the Synthesis and Application of Sultones. *Chem. Rev.* **2012**, *112*, 5339–5355.

14. Bheeter, C. B., Bera, J. K., Doucet, H. Palladium- Catalysed Intramolecular Direct Arylation of 2- Bromobenzenesulfonic Acid Derivatives. *Adv. Synth. Catal.* **2012**, *354*, 3533–3538.
15. Qi, Z., Wang, M., Li, X. Rh(III)-Catalyzed synthesis of sultones through C–H activation directed by a sulfonic acid group. *Chem. Commun.* **2014**, *50*, 9776–9778.
16. Mondal, S., Debnath, S. Ring-closing metathesis in the synthesis of fused sultones. *Tetrahedron Lett.* **2014**, *55*, 1577–1580.
17. Hoveyda, A., Zhugralin, A. The remarkable metal-catalysed olefin metathesis reaction. *Nature* **2007**, *450*, 243–251.
18. Scholl, M., Ding, S., Lee, C. W., Grubbs, R. Synthesis and Activity of a New Generation of Ruthenium-Based Olefin Metathesis Catalysts Coordinated with 1,3-Dimesityl-4,5-dihydroimidazol-2-ylidene Ligands. *Org. Lett.* **1999**, *6*, 953–956.
19. Lozano-Vila, A., Monsaert, S., Bajek, A., Verpoort, F. Ruthenium-Based Olefin Metathesis Catalysts Derived from Alkynes. *Chem. Rev.* **2010**, *110*, 4865–4909.
20. Huisgen, R. 1,3-Dipolar Cycloadditions Past and Future. *Angew. Chem., Int. Ed. Engl.* **1963**, *2*, 565–632.
21. Johansson, R., Beke-Somfai, T., Stalsmeden, A., Kann, N. Ruthenium-Catalyzed Azide Alkyne Cycloaddition Reaction: Scope, Mechanism, and Applications. *Chem. Rev.* **2016**, *116*, 14726–14768.
22. Tornøe, C., Christensen, C., Meldal, M. Peptidotriazoles on Solid Phase: [1,2,3]-Triazoles by Regiospecific Copper(I)-Catalyzed 1,3-Dipolar Cycloadditions of Terminal Alkynes to Azides. *J. Org. Chem.* **2002**, *67*, 3057–3064.
23. Rostovtsev, V., Green, L., Fokin, V., Sharpless, B. A Stepwise Huisgen Cycloaddition Process: Copper(I)-Catalyzed Regioselective Ligation of Azides and Terminal Alkynes. *Angew. Chem. Int. Ed.* **2002**, *41*, 2595–2599.
24. Zhang, L., Chen, X., Xue, P., Sun, H., Williams, I., Sharpless, B., Fokin, V., Jia, G. Ruthenium-Catalyzed Cycloaddition of Alkynes and Organic Azides. *J. Am. Chem. Soc.* **2005**, *127*, 15998–15999.
25. Shao, C., Wang, X., Xu, J., Zhao, J., Zhang, Q., Hu, Y. Carboxylic Acid-Promoted Copper(I)-Catalyzed Azide-Alkyne Cycloaddition. *J. Org. Chem.* **2010**, *75*, 7002–7005.
26. Jana, R., Pathak, T., Sigman, M. Advances in Transition Metal (Pd,Ni,Fe)-Catalyzed Cross-Coupling Reactions Using Alkyl-organometallics as Reaction Partners. *Chem. Rev.* **2011**, *111*, 1417–1492.
27. Buchwald, S., Martin, R. Palladium-Catalyzed Suzuki-Miyaura Cross-Coupling Reactions Employing Dialkylbiaryl Phosphine Ligands. *Acc. Chem. Res.* **2008**, *41*, 1461–1473.
28. Payard, P. A., Perego, L. A., Coifini, I., Grimaud, L. Taming Nickel-Catalyzed Suzuki-Miyaura Coupling: A Mechanistic Focus on Boron-to-Nickel Transmetalation. *ACS Catal.* **2018**, *8*, 4812–4823.
29. Saito, S., Sakai, M., Miyaura, N. A Synthesis of Biaryls v/a Nickei(0).Catalyzed Cross-Coupling Reaction of Chloroarenes with Phenylboronic Acids. *Tetrahedron Lett.* **1996**, *37*, 2993–2996.

30. Saito, S., Oh-tani, S., Miyaura, N. Synthesis of Biaryls via a Nickel(0)-Catalyzed Cross-Coupling Reaction of Chloroarenes with Arylboronic Acids. *J. Org. Chem.* **1997**, *62*, 8024–8030.
31. Maluenda, I., Navarro, O. Recent Developments in the Suzuki-Miyaura Reaction: 2010–2014. *Molecules* **2015**, *20*, 7528–7557.
32. Slapšyte, G., Jankauskiene, A., Mierauskiene, J., Lazutka, J. R. Cytogenetic analysis of children under long-term antibacterial therapy with nitroheterocyclic compound furagin. *Mutat. Res.* **2001**, *491*, 25–30.



## ACKNOWLEDGEMENTS

Firstly, I would like to thank my supervisor Raivis Žalubovskis.

Secondly, I also want to warmly thank Professor of Florence University (Italy) Claudiu T. Supuran and his research group for carbonic anhydrase inhibition determination and *In Silico* studies.

Finally, I would like to express my appreciation to the Laboratory of Physical Organic Chemistry of the Latvian Institute of Organic Synthesis for NMR and IR spectrum recording.

Aleksandrs Pustenko

## **PIELIKUMI / PUBLICATIONS**

Pustenko, A., Žalubovskis, R. Recent advances in sultone synthesis (microreview). *Chem. Heterocycl. Compd.* **2017**, *53*, 1283–1285.

Reprinted with permission from Springer Science Business Media.

Copyright © 2017, Springer Science Business Media, LLC, part of Springer Nature

# HETEROCYCLES IN FOCUS

## Recent advances in sultone synthesis (microreview)

Aleksandrs Pustenko<sup>1,2\*</sup>, Raivis Žalubovskis<sup>1</sup>

<sup>1</sup> Latvian Institute of Organic Synthesis,  
21 Aizkraukles St., Riga LV-1006, Latvia; e-mail: aleksandrspustenko@gmail.com

<sup>2</sup> Institute of Technology of Organic Chemistry,  
Faculty of Materials Science and Applied Chemistry, Riga Technical University,  
3/7 Paula Valdena St., Riga LV-1048, Latvia

Published in Khimiya Geterotsiklicheskikh Soedinenii,  
2017, 53(12), 1283–1285

Submitted May 23, 2017  
Accepted August 27, 2017



This microreview summarizes recent advances in sultone synthesis, focusing on the transition metal-catalyzed reactions reported from 2012 to 2017.

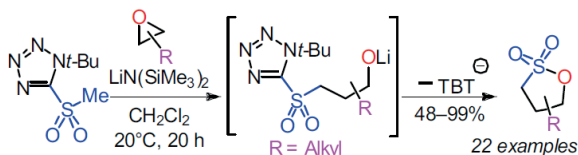
### Introduction

Sultones, the internal esters of hydroxysulfonic acids, sulfur analogs of lactones, are among the oldest known sulfur heterocycles as the term "sultone" was introduced by Endermann in 1888.<sup>1</sup> Nowadays sultones are demanded scaffolds in medicinal chemistry research,<sup>1–3</sup> as they exhibit skin sensitization, antiviral, and enzyme inhibitory activities.<sup>1,3–7</sup> They also have broad application in organic

synthesis, as they are key intermediates in many natural product syntheses.<sup>8</sup> Most sultones reported in literature are 4–7-membered rings, but few are larger.<sup>1</sup> The most powerful sultone synthesis methodologies include, among others, various transition metal-catalyzed reactions,<sup>1,5,8–10</sup> cycloaddition reactions,<sup>11,12</sup> Diels–Alder-type reactions,<sup>4,13</sup> and the use of ionic liquids as sulfonating agents.<sup>2,14</sup>

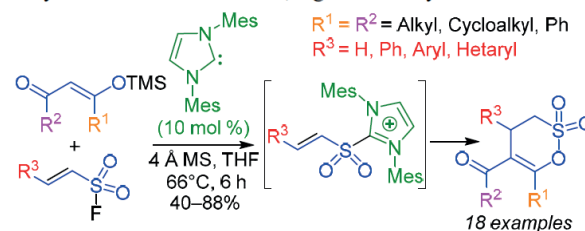
### Julia–Kocienski reaction

First literature example of homologous Julia–Kocienski reaction of epoxides with sulfones, which provides access to  $\gamma$ -sultones in one-pot stereocontrolled manner, was reported by Bray and coworkers.<sup>15</sup> Method has good functional group tolerance: substrates with protected alcohols and amines, ketones, halogens, and even terminal epoxides in the side chain can be used. In case of a bis-epoxide even with five equivalents of base only the monosultonylated product was obtained. Most likely formation of the first ring slows down formation of the second one.



### N-Heterocyclic carbene catalysis

N-Heterocyclic carbene-catalyzed (NHC) procedure of  $\delta$ -sultone synthesis using TMS enol ethers and  $\alpha,\beta$ -unsaturated sulfonyl fluorides via  $\alpha,\beta$ -unsaturated sulfonyl azolium intermediates was reported by Lupton and coworkers.<sup>16</sup> Reaction is moderately sensitive to electronic effects of starting materials: electron-poor sulfonyl fluorides are more efficiently converted to corresponding sultones than electron-rich ones. In this convenient procedure, both aliphatic and aromatic TMS enol ethers can be used. In the case of an unsymmetric TMS enol ethers, regioselectivity is moderate.



**Aleksandrs Pustenko** was born in 1992 in Bauska, Latvia. He received his M.Sc. degree in chemistry in 2016 at the University of Latvia. Since September 2016 he is a PhD student under supervision of Dr. Chem. R. Žalubovskis at the Latvian Institute of Organic Synthesis. His research mainly focuses on novel carbonic anhydrase inhibitor design and synthesis.

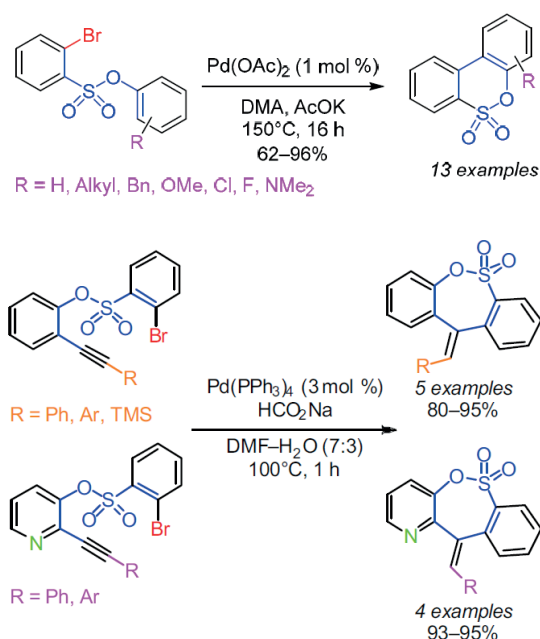


**Raivis Žalubovskis** was born in 1975 in Riga, Latvia. He received his PhD in 2006 under supervision of Prof. Christina Moberg at the KTH Royal Institute of Technology, Sweden. Currently he is research group leader at the Latvian Institute of Organic Synthesis. One of his current scientific activities is related to the synthesis of sultones as potential carbonic anhydrase inhibitors.

### Palladium catalysis

Palladium-catalyzed phosphine-free intramolecular direct arylation of 2-bromobenzenesulfonic acid phenyl esters was first reported by Doucet and coworkers.<sup>17</sup> Using this procedure biarylsulfones can be obtained in good and excellent yields. Unfortunately, substituents on the phenol moiety have a strong influence on the reaction outcome. Electron-donating substituents accelerate the reaction, whereas substrates with electron-withdrawing substituents ( $\text{NO}_2$ ,  $\text{CO}_2\text{Bu}$ ,  $\text{CF}_3$ ) do not undergo ring closure. In all cases when reaction occurred high regioselectivity was observed.

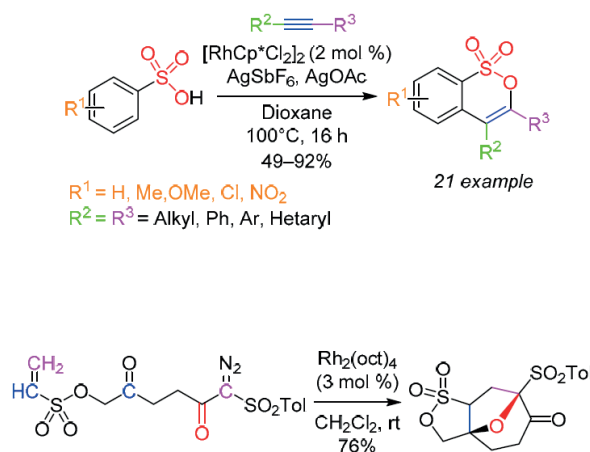
An efficient regioselective Pd(0)-catalyzed intramolecular Heck-type cyclization strategy for the synthesis of fused seven-membered sultones was reported by Mondal and coworkers.<sup>18</sup> However no examples with aliphatic or aromatic substituents containing electron-withdrawing groups are reported. It is interesting that in the case of dibenzo-fused sultones the exocyclic double bond conformation is opposite to that of benzopyrido-fused sultones. Authors explain it using DFT calculations of possible reaction mechanism. In case of benzopyrido-fused sultones, Pd–N interaction dominates over the steric interaction.



### Rhodium catalysis

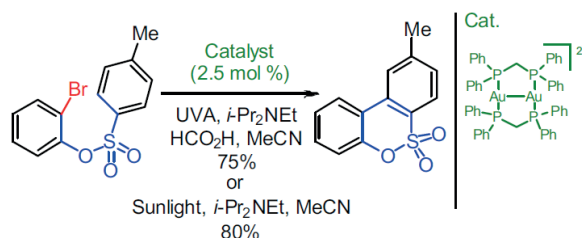
A new access to sultones using Rh(III)-catalyzed coupling of arylsulfonic acids with internal alkynes, where sulfonic acid assisted C–H activation at the *ortho* position, was reported by Li and coworkers.<sup>19</sup> Under these reaction conditions, alkynes with electron-donating and electron-withdrawing substituents can be used. Moreover, electron-donating substituents provide higher yields. In case of unsymmetrical alkynes, product yields are moderate, but regioselectivity is very high.

An effective rhodium-catalyzed carbene cyclization–cycloaddition cascade (CCCC) reaction of vinylsulfonate giving polycyclic sultone in good yield and diastereoselectivity was reported by Metz and coworkers.<sup>20</sup> Rhodium carbenoid obtained from diazoketone moiety undergoes addition to ketone and forms carbonyl ylide. The 1,3-dipolar cycloaddition to the vinyl sulfone moiety of the latter completes the reaction sequence.



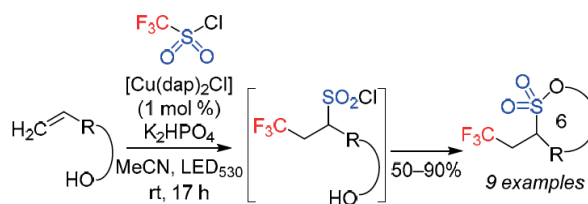
### Gold catalysis

Barriault and coworkers have reported a straightforward heterocycle synthesis using dimeric phosphine–gold catalyst.<sup>21</sup> The authors have demonstrated a light-enabled reductive radical reaction of unactivated alkyl and aryl bromides where the gold complex acts as a photocatalyst. This reaction can be carried out using UVA or sunlight and it is suitable for the synthesis of benzosultones and other heterocycles. Intermolecular transformations are also possible.



### Copper catalysis

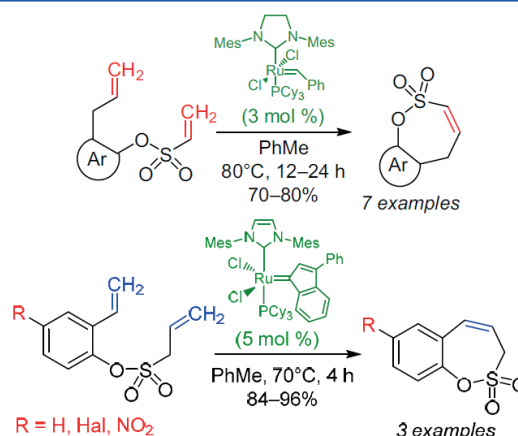
Simple photoredox-catalyzed procedure for the synthesis of sultones in moderate to excellent yields using copper catalyst was reported by Reiser and coworkers.<sup>22</sup> Using this reaction procedure, aliphatic, spirocyclic, as well as annulated  $\delta$ -sultones can be prepared even on gram scale. Unfortunately, the method has a poor regio- and diastereo-selectivity. It is sensitive to steric effects, and substitution at the double bond or next to it leads to increasing extent of  $\text{CF}_3\text{Cl}$  addition.



### Ruthenium catalysis

Mondal and coworkers reported a convenient synthetic strategy toward seven-membered sultones fused with a heterocycle or various carbocycles *via* Ru-catalyzed ring closing metathesis (RCM).<sup>8</sup> Using 1st generation Grubbs catalyst no sultone formation was observed. Changing catalyst to 2nd generation Grubbs catalyst sultones were obtained in good to excellent yields.

An efficient Ru-catalyzed olefin RCM example of seven-membered sultone synthesis was reported by our group.<sup>7</sup> Using 2nd generation Grubbs catalyst indenylidene variation it was possible to synthesize seven-membered benzo-fused sultones with excellent yields and functional group tolerance.



### References

- Mondal, S. *Chem. Rev.* **2012**, *112*, 5339.
- Rad-Moghadam, K.; Hassani, S. A. R. M.; Roudsari, S. T. *J. Mol. Liq.* **2016**, *218*, 275.
- Xu, H.-W.; Zhao, L.-J.; Lui, H.-F.; Zhao, D.; Luo, J.; Xie, X.-P.; Liu, W.-S.; Zheng, J.-X.; Dai, G.-F.; Liu, H.-M.; Liu, L.-H.; Liang, Y.-B. *Bioorg. Med. Chem. Lett.* **2014**, *24*, 2388.
- Ghandi, M.; Nazeri, M. T.; Kubicki, M. *Tetrahedron*, **2013**, *69*, 4979.
- Mondal, S.; Debnath, S.; Pal, S.; Das, A. *Synthesis* **2015**, 3423.
- (a) Tars, K.; Vullo, A.; Kazaks, A.; Leitans, J.; Lends, A.; Grandane, A.; Zalubovskis, R.; Scozzafava, A.; Supuran, C. T. *J. Med. Chem.* **2013**, *56*, 293. (b) Grandane, A.; Tanc, M.; Zalubovskis, R.; Supuran, C. T. *Bioorg. Med. Chem.* **2014**, *22*, 1522. (c) Grandane, A.; Tanc, M.; Zalubovskis, R.; Supuran, C. T. *Bioorg. Med. Chem. Lett.* **2014**, *24*, 1256.
- Pustenko, A.; Stepanovs, D.; Zalubovskis, R.; Vullo, D.; Kazaks, A.; Leitans, J.; Tars, K.; Supuran, C. *J. Enzyme Inhib. Med. Chem.* **2017**, *32*, 767.
- Mondal, S.; Debnath, S. *Tetrahedron Lett.* **2014**, *55*, 1577.
- Li, F.; Liu, T.-X.; Wang, W.-G. *Org. Lett.* **2012**, *14*, 2176.
- Li, F.; Jiang, T.; Cai, H.; Wang, G. *Chin. J. Chem.* **2012**, *30*, 2041.
- Ghandi, M.; Taheri, A.; Bozcheloei, A. H.; Abbasi, A.; Kia, R. *Tetrahedron* **2012**, *68*, 3641.
- Alcaide, B.; Almendros, P.; Aragoncillo, C.; Fernández, I.; Gomez-Campillos, G. *Chem.–Eur. J.* **2016**, *22*, 285.
- Moghaddam, F. M.; Khodabakhshi, M. R.; Kiamehr, M.; Ghahremannejad, Z. *Tetrahedron Lett.* **2013**, *54*, 2685.
- Moghadam, K. R.; Roudsari, S. T.; Sheykhan, M. *Synlett* **2014**, 827.
- Smith, G. M. T.; Bruton, P. M.; Bray, C. D. *Angew. Chem., Int. Ed.* **2015**, *127*, 15451.
- Ungureanu, A.; Levens, A.; Candish, L.; Lupton, D. W. *Angew. Chem., Int. Ed.* **2015**, *127*, 11946.
- Bheeter, C. B.; Bera, J. K.; Doucet, H. *Adv. Synth. Catal.* **2012**, *354*, 3533.
- Mondal, S.; Debnath, S.; Das, B. *Tetrahedron* **2015**, *71*, 476.
- Qi, Z.; Wang, M.; Li, X. *Chem. Commun.* **2014**, *50*, 9776.
- Groß, T.; Herrmann, T.; Shi, B.; Jäger, A.; Chiu, P.; Metz, P. *Tetrahedron*, **2015**, *71*, 5925.
- Revol, G.; McCallum, T.; Morin, M.; Gagosz, F.; Barriault, L. *Angew. Chem., Int. Ed.* **2013**, *52*, 13342.
- Rawner, T.; Knorn, M.; Lutsker, E.; Hossain, A.; Reiser, O. *J. Org. Chem.* **2016**, *81*, 7139.

Pustenko, A., Stepanovs, D., Žalubovskis, R., Vullo, D., Kazaks, A., Leitans, J., Tars, K., Supuran, C. T. 3*H*-1,2-benzoxathiepine 2,2-dioxides: a new class of isoform-selective carbonic anhydrase inhibitors. *J. Enzyme Inhib. Med. Chem.* **2017**, *32*, 767–775.

Reprinted with permission from Taylor & Francis Group.  
Copyright © 2017, Taylor & Francis Group.

## 3*H*-1,2-benzoxathiepine 2,2-dioxides: a new class of isoform-selective carbonic anhydrase inhibitors

Aleksandrs Pustenko<sup>a,b</sup>, Dmitrijs Stepanovs<sup>a</sup>, Raivis Žalubovskis<sup>a</sup>, Daniela Vullo<sup>c</sup>, Andris Kazaks<sup>d</sup>, Janis Leitans<sup>d</sup>, Kaspars Tars<sup>e</sup> and Claudiu T. Supuran<sup>f</sup>

<sup>a</sup>Latvian Institute of Organic Synthesis, Riga, Latvia; <sup>b</sup>Institute of Technology of Organic Chemistry, Faculty of Materials Science and Applied Chemistry, Riga Technical University, Riga, Latvia; <sup>c</sup>Dipartimento di Chimica, Laboratorio di Chimica Bioinorganica, Polo Scientifico, Università degli Studi di Firenze, Sesto Fiorentino, Florence, Italy; <sup>d</sup>Latvian Biomedical Research and Study Centre, Riga, Latvia; <sup>e</sup>Faculty of Biology, Department of Molecular Biology, University of Latvia, Riga, Latvia; <sup>f</sup>Dipartimento Neurofarba, Sezione di Scienze Farmaceutiche e Nutraceutiche, Università degli Studi di Firenze, Sesto Fiorentino, Florence, Italy

### ABSTRACT

A new chemotype with carbonic anhydrase (CA, EC 4.2.1.1) inhibitory action has been discovered, the homo-sulfocoumarins (3*H*-1,2-benzoxathiepine 2,2-dioxides) which have been designed considering the (sulfo)coumarins as lead molecules. An original synthetic strategy of a panel of such derivatives led to compounds with a unique inhibitory profile and very high selectivity for the inhibition of the tumour associated (CA IX/XII) over the cytosolic (CA I/II) isoforms. Although the CA inhibition mechanism with these new compounds is unknown for the moment, we hypothesize that it may be similar to that of the sulfocoumarins, i.e. hydrolysis to the corresponding sulfonic acids which thereafter anchor to the zinc-coordinated water molecule within the enzyme active site.

### ARTICLE HISTORY

Received 15 March 2017  
Revised 1 April 2017  
Accepted 4 April 2017

### KEYWORDS

Carbonic anhydrase;  
sulfocoumarin; homo-  
sulfocoumarins; inhibitor

### Introduction

Sulfocoumarins (1,2-benzoxathiine 2,2-dioxides) such as derivatives of type **A** were discovered by our groups to act as inhibitors of the metalloenzyme carbonic anhydrase (CA, EC 4.2.1.1)<sup>1,2</sup>. A large series of sulfocoumarins derivatives, among which compounds of type **B**, were thereafter reported, by using click chemistry or other conventional drug design approaches (Figure 1)<sup>3–6</sup>.

A salient feature of this type of CA inhibitor (CAI) was the fact that they showed a very pronounced isoform selectivity for inhibiting tumour-associated CA isoforms (CA IX and XII) over the widespread, cytosolic ones CA I and II<sup>1–3</sup>. This has been explained when the mechanism of CA inhibition with sulfocoumarins was elucidated, by using kinetic and X-ray crystallographic experiments<sup>1</sup>. Indeed, in the X-ray crystal structure of the adduct of a CA II/IX mimic complexed with the 6-bromosulfocoumarin **A2** (**A**, R = Br) (Figure 1), the 2-dihydroxy-5-bromophenyl-vinyl sulfonic acid **D** was observed within the enzyme active site, probably due to the CA-mediated hydrolysis of **A2** to the *cis*-sulfonic acid **C** which was thereafter isomerized to the more stable *trans*-derivative **D** (Scheme 1)<sup>1</sup>.

This inhibition mechanism is similar to the one observed earlier for coumarins<sup>7,8</sup> the class of CAIs which constituted the lead compounds for the discovery of sulfocoumarins. Finding isoform-selective CAIs for the 15 different human CA isoforms is a challenging task<sup>9,10</sup>, but coumarins and sulfocoumarins (and several families of sulfonamides) do show such properties, which make them of great interest for the design of pharmacological agents useful as diuretics, antiglaucoma, anticonvulsant and/or antitumor drugs<sup>9–13</sup>.

Here, we report the homo-sulfocoumarins or 3*H*-1,2-benzoxathiepine 2,2-dioxides, which can be considered as homologs of

sulfocoumarins or 1,2-benzoxathiine 2,2-dioxides<sup>1</sup>, where oxathiine ring was expanded by one carbon to form an oxathiepine ring. To the best of our knowledge, there is no reported method for the synthesis of 3*H*-1,2-benzoxathiepine 2,2-dioxides in the literature. The general strategy for the formation of oxathiepine ring reported in this paper involves a ruthenium-catalysed olefin metathesis as a key step.




### Materials and methods

#### Chemistry

Reagents, starting materials and solvents were obtained from commercial sources and used as received. Thin-layer chromatography was performed on silica gel, spots were visualized with UV light (254 and 365 nm). Melting points were determined on an OptiMelt automated melting point system. IR spectra were measured on Shimadzu FTIR IR Prestige-21 spectrometer. NMR spectra were recorded on Varian Mercury (400 MHz) spectrometer with chemical shifts values ( $\delta$ ) in ppm relative to TMS using the residual DMSO-*d*<sub>6</sub> signal (<sup>1</sup>H 2.50; <sup>13</sup>C 39.52) or CDCl<sub>3</sub> signal (<sup>1</sup>H 7.26; <sup>13</sup>C 77.16) as an internal standard. HRMS data were obtained with a Q-TOF micro high resolution mass spectrometer with ESI (ESI+/ESI). Elemental analyses were performed on a CARLO ERBA ELEMENTAL ANALYZER EA 1108.

#### General procedure for the synthesis of 4-substituted 2-ethenylphenoles (2*a*–*c*)<sup>14</sup>

To a stirred solution of methyltriphenylphosphonium bromide (2.64 eq.) in dry THF (5 ml/1 mmol of corresponding aldehyde),

CONTACT Raivis Žalubovskis  raivis@osi.lv  claudiu.supuran@unifi.it  Dipartimento Neurofarba, Sezione di Scienze Farmaceutiche e Nutraceutiche, Università degli Studi di Firenze, Sesto Fiorentino, Florence, Italy

© 2017 The Author(s). Published by Informa UK Limited, trading as Taylor & Francis Group.

This is an Open Access article distributed under the terms of the Creative Commons Attribution License (<http://creativecommons.org/licenses/by/4.0/>), which permits unrestricted use, distribution, and reproduction in any medium, provided the original work is properly cited.



was added tBuOK (2.86–3.12 eq.) in several portions over 20 min. Reaction mixture was stirred for 1 h at RT. Corresponding 2-hydroxybenzaldehyde (1 eq.) was added and stirring continued at room temperature for 24 h. Reaction mixture was diluted with CH<sub>2</sub>Cl<sub>2</sub> (5 ml/1 mmol aldehyde). Organic layer was collected and washed with water (2 × 20 ml) and brine (2 × 20 ml), dried over Na<sub>2</sub>SO<sub>4</sub>, solvent was driven off in vacuum. The crude product was purified by column chromatography (silica gel, EtOAc/PhMe 1:5).

#### 2-Ethenylphenol (2a)

Compound **2a** was prepared according to the general procedure from methyltriphenylphosphonium bromide (18.88 g, 52.9 mmol), tBuOK (6.42 g, 57.2 mmol) and 2-hydroxybenzaldehyde (2.44 g, 20.0 mmol) as yellowish at room temperature melting solid (1.67 g, 70%). <sup>1</sup>H NMR (400 MHz, CDCl<sub>3</sub>) δ = 5.37 (dd, 1H, *J* = 11.3, 1.3 Hz), 5.42 (s, 1H), 5.76 (dd, 1H, *J* = 17.8, 1.3 Hz), 6.81 (dd, 1H, *J* = 8.1, 1.1 Hz), 6.90–6.96 (m, 1H), 6.98 (dd, 1H, *J* = 17.8, 11.3 Hz), 7.12–7.18 (m, 1H), 7.41 (dd, 1H, *J* = 7.7, 1.7 Hz).

#### 4-Bromo-2-ethenylphenol (2b)

Compound **2b** was prepared according to the general procedure from methyltriphenylphosphonium bromide (13.22 g, 37.0 mmol), tBuOK (4.90 g, 43.7 mmol) and 5-bromo-2-hydroxybenzaldehyde (2.81 g, 14.0 mmol) as yellowish at room temperature melting solid (1.64 g, 59%). <sup>1</sup>H NMR (400 MHz, CDCl<sub>3</sub>) δ = 4.98 (s, 1H), 5.40 (dd, 1H, *J* = 11.3, 1.0 Hz), 5.74 (dd, 1H, *J* = 17.8, 1.0 Hz), 6.68 (d, 1H, *J* = 8.6 Hz), 6.85 (dd, 1H, *J* = 17.8, 8.6 Hz), 7.23 (dd, 1H, *J* = 8.6, 2.4 Hz), 7.49 (d, 1H, *J* = 2.4 Hz).

#### 2-Ethenyl-4-nitrophenol (2c)

Compound **2c** was prepared according to the general procedure from methyltriphenylphosphonium bromide (28.31 g, 79.3 mmol), tBuOK (9.60 g, 85.6 mmol) and 5-nitro-2-hydroxybenzaldehyde (5 g, 30 mmol) as yellow at room temperature melting solid (3.23 g, 65%). <sup>1</sup>H NMR (400 MHz, CDCl<sub>3</sub>) δ = 5.43 (dd, 1H, *J* = 11.3, 1.1 Hz), 5.87 (dd, 1H, *J* = 17.8, 1.1 Hz), 6.92–7.00 (m, 2H), 7.96 (dd, 1H, *J* = 8.9, 2.6 Hz), 8.31 (d, 1H, *J* = 2.6 Hz), 8.82 (s, 1H).

#### Prop-2-ene-1-sulfonyl chloride (3)<sup>15</sup>

To a solution of 3-bromoprop-1-ene (24.2 g, 0.20 mol) in water (140 ml) was added Na<sub>2</sub>SO<sub>3</sub> (30 g, 0.24 mol) and the reaction mixture was stirred overnight. To a solution of 3-bromoprop-1-ene (24.2 g, 0.20 mol) in water (140 ml) was added Na<sub>2</sub>SO<sub>3</sub> (30 g, 0.24 mol) and the reaction

mixture was refluxed overnight. After cooling to room temperature, reaction mixture was washed with Et<sub>2</sub>O (3 × 35 ml). Aqueous phase was concentrated. Crude white solid was dried under high vacuum at 110 °C for 4 h. To the white solid at 0 °C POCl<sub>3</sub> (80 ml) was added, and mixture was refluxed for 4 h. After cooling to room temperature dry THF (60 ml) was added and reaction mixture was vigorously stirred for 10 min and filtered. Filter cake was suspended in dry THF (60 ml), suspension was vigorously stirred for 10 min and filtered. Filtrates were combined and solvent was carefully driven off on rotary evaporator. Residue was distilled in vacuum (10 mbar) and fraction with boiling point 38–42 °C was collected, to give prop-2-ene-1-sulfonyl chloride (**3**) as colourless oil (18.8 g, 67%).

#### General procedure for the synthesis of 4-substituted 2-ethenyl prop-2-ene-1-sulfonates (4a–c)

To a stirred solution of corresponding 2-ethenylphenol **2** (1 eq.) in CH<sub>2</sub>Cl<sub>2</sub> (10 ml/20 mmol phenol) at 0 °C was added prop-2-ene-1-sulfonyl chloride (**3**) (1.6 eq.) and Et<sub>3</sub>N (1.5 eq.). Reaction mixture was stirred overnight (20 h) at room temperature. Water (10 ml/20 mmol phenol) was added, reaction mixture was extracted with EtOAc (3 × 10 ml/20 mmol phenol), combined organic extracts were washed with brine (2 × 10 ml/20 mmol olefin), dried over Na<sub>2</sub>SO<sub>4</sub>, filtered and solvent was driven off in vacuum. The crude product was purified by column chromatography (silica gel, CH<sub>2</sub>Cl<sub>2</sub>/PhMe 3:2).

#### 2-Ethenylphenyl prop-2-ene-1-sulfonate (4a)

Compound **4a** was prepared according to the general procedure from 2-ethenylphenol (**2a**) (0.50 g, 4.16 mmol), prop-2-ene-1-sulfonyl chloride (**3**) (0.94 g, 6.69 mmol) and Et<sub>3</sub>N (0.87 ml, 6.23 mmol) as colourless oil (0.52 g, 56%). IR (film, cm<sup>-1</sup>) ν<sub>max</sub> = 1368 (S=O), 1178 (S=O), 1154 (S=O); <sup>1</sup>H NMR (400 MHz, CDCl<sub>3</sub>) δ = 3.96–4.00 (m, 2H), 5.37–5.41 (m, 1H), 5.48–5.54 (m, 2H), 5.79 (dd, 1H, *J* = 17.6, 0.9 Hz), 5.90–6.01 (m, 1H), 6.99 (dd, 1H, *J* = 17.6, 11.0 Hz), 7.23–7.34 (m, 2H), 7.57–7.62 (m, 1H); <sup>13</sup>C NMR (100 MHz, CDCl<sub>3</sub>) δ = 55.6, 117.3, 122.8, 123.9, 125.4, 126.9, 127.4, 129.2, 130.3, 131.3, 146.5; HRMS (ESI) *m/z* [M – 1]<sup>-</sup> calcd for C<sub>11</sub>H<sub>11</sub>O<sub>3</sub>S: 223.0429, found 223.0435.

#### 4-Bromo-2-ethenylphenyl prop-2-ene-1-sulfonate (4b)

#### 4-Bromo-2-ethenylphenyl prop-2-ene-1-sulfonate (4b)

Compound **4b** was prepared according to the general procedure from 4-bromo-2-ethenylphenol (**2b**) (0.50 g, 2.51 mmol), prop-2-ene-1-sulfonyl chloride (**3**) (0.57 g, 4.05 mmol) and Et<sub>3</sub>N (0.52 ml, 3.76 mmol) as colourless oil (0.51 g, 67%). IR (film, cm<sup>-1</sup>) ν<sub>max</sub> = 1364 (S=O), 1170 (S=O), 1154 (S=O); <sup>1</sup>H NMR (400 MHz, CDCl<sub>3</sub>) δ = 4.00 (dt, 2H, *J* = 7.4, 0.9 Hz), 5.46 (d, 1H, *J* = 11.0 Hz), 5.51–5.59 (m, 2H), 5.81 (d, 1H, *J* = 17.6 Hz), 5.91–6.03 (m, 1H), 6.92 (dd, 1H, *J* = 17.6, 11.0 Hz), 7.22 (d, 1H, *J* = 8.6 Hz), 7.41 (dd, 1H, *J* = 8.6, 2.4 Hz), 7.73 (d, 1H, *J* = 2.4 Hz); <sup>13</sup>C NMR (100 MHz, CDCl<sub>3</sub>) δ = 55.7, 118.6, 121.0, 123.7, 124.6, 125.7, 129.2, 129.8, 132.0, 133.3.

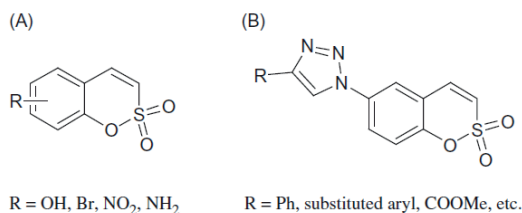
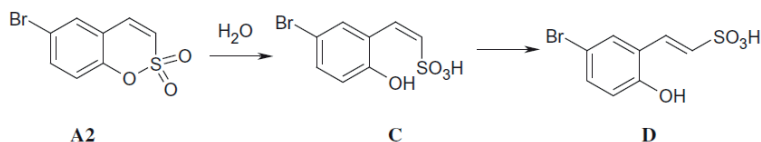


Figure 1. Chemical structure of sulfocoumarins A and B.



Scheme 1. Active site, CA-mediated hydrolysis of A2 to D<sup>1</sup>.

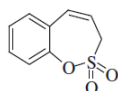
145.3; HRMS (ESI)  $m/z$   $[M - 1]^-$  calcd for  $C_{11}H_{10}BrO_3S$ : 300.9534, found 300.9537.

#### 2-Ethenyl-4-nitrophenyl prop-2-ene-1-sulfonate (**4c**)

Compound **4c** was prepared according to the general procedure from 2-ethenyl-4-nitrophenol (**2c**) (0.32 g, 1.94 mmol), prop-2-ene-1-sulfonyl chloride (**3**) (0.44 g, 3.13 mmol) and  $Et_3N$  (0.41 ml, 2.96 mmol) as yellowish oil (0.30 g, 57%). IR (film,  $cm^{-1}$ )  $\nu_{max}$  = 1350 (S=O), 1159 (S=O);  $^1H$  NMR (400 MHz,  $CDCl_3$ )  $\delta$  = 4.01 (dt, 2H,  $J$  = 7.2, 0.9 Hz), 5.54–5.63 (m, 3H), 5.93–6.05 (m, 2H), 6.99 (dd, 1H,  $J$  = 17.6, 11.0 Hz), 7.53 (d, 1H,  $J$  = 9.0 Hz), 8.16 (dd, 1H,  $J$  = 9.0, 2.8 Hz), 8.48 (d, 1H,  $J$  = 2.8 Hz);  $^{13}C$  NMR (100 MHz,  $CDCl_3$ )  $\delta$  = 56.3, 120.2, 122.4, 123.4, 123.8, 124.0, 126.2, 128.6, 132.8, 146.5, 150.2; HRMS (ESI)  $m/z$   $[M - 1]^-$  calcd for  $C_{11}H_{10}NO_3S$ : 268.0280, found 268.0280.

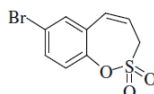
#### General procedure for the synthesis of 7-substitued 3H-1,2-benzoxathiepine 2,2-dioxides (6a–c)

To a stirred solution of corresponding 4-substitued 2-ethenyl prop-2-ene-1-sulfonate (1 eq.) in dry toluene (10 ml/0.2 g **4**), was added Ru-catalyst **5** (tricyclohexylphosphine[1,3-bis(2,4,6-trimethylphenyl)imidazol-2-ylidene][3-phenyl-1H-inden-1-ylidene]ruthenium(II) dichloride, CAS Nr. 254972–49-1) (0.05 eq.). Reaction mixture was stirred at 70 °C for 4 h. Solvent was driven off in vacuum and the crude product was purified by column chromatography (silica gel, Hex/EtOAc 4:1) with following re-crystallization from EtOAc/Hex. Compound **6c** was purified by column chromatography (silica gel,  $CH_2Cl_2$ /Hex 2:1).



#### 3H-1,2-benzoxathiepine 2,2-dioxide (6a)

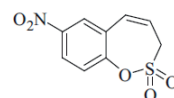
Compound **5a** was prepared according to the general procedure from 2-ethenylphenyl prop-2-ene-1-sulfonate (**4a**) (100 mg, 0.45 mmol), Ru-catalyst **5** (21 mg, 0.022 mmol) as white solid (76 mg, 87%). Mp 131–132 °C. IR (film,  $cm^{-1}$ )  $\nu_{max}$  = 1369 (S=O), 1176 (S=O);  $^1H$  NMR (400 MHz,  $CDCl_3$ )  $\delta$  = 4.01 (dd, 2H,  $J$  = 6.3, 1.2 Hz), 5.96–6.03 (m, 1H), 6.90 (d, 1H,  $J$  = 10.9 Hz), 7.31–7.37 (m, 3H), 7.41–7.46 (m, 1H);  $^{13}C$  NMR (100 MHz,  $CDCl_3$ )  $\delta$  = 51.2, 119.5, 123.0, 127.3, 128.4, 130.6, 130.8, 132.9, 147.8; HRMS (ESI)  $m/z$   $[M - 1]^-$  calcd for  $C_9H_9O_3S$ : 195.0116, found 195.0115.



#### 7-Bromo-3H-1,2-benzoxathiepine 2,2-dioxide (6b)

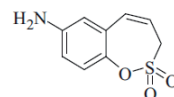
Compound **5b** was prepared according to the general procedure from 4-bromo-2-ethenylphenyl prop-2-ene-1-sulfonate (**4b**) (100 mg, 0.33 mmol), Ru-catalyst **5** (16 mg, 0.017 mmol) as yellowish solid (76 mg, 84%). Mp 129.3–130.3 °C. IR (film,  $cm^{-1}$ )  $\nu_{max}$  = 1360 (S=O), 1170 (S=O), 1154 (S=O);  $^1H$  NMR (400 MHz,  $CDCl_3$ )  $\delta$  = 4.03 (dd, 2H,  $J$  = 6.3, 0.9 Hz), 5.99–6.06 (m, 1H), 6.81 (d, 1H,  $J$  = 11.0 Hz), 7.22 (d, 1H,  $J$  = 8.6 Hz), 7.47 (d, 1H,  $J$  = 2.4 Hz), 7.54

(dd, 1H,  $J$  = 8.6, 2.4 Hz);  $^{13}C$  NMR (100 MHz,  $CDCl_3$ )  $\delta$  = 51.4, 120.5, 120.9, 124.7, 130.2, 131.6, 133.5, 133.6, 146.7; Anal. Calcd for  $C_9H_7BrO_3S$  (275.12): C 39.29, H 2.56, found C 39.19, H 2.59.



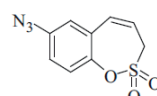
#### 7-Nitro-3H-1,2-benzoxathiepine 2,2-dioxide (6c)

Compound **5c** was prepared according to the general procedure from 2-ethenyl-4-nitrophenyl prop-2-ene-1-sulfonate (**4c**) (100 mg, 0.37 mmol), catalyst **5** (18 mg, 0.019 mmol) as yellowish solid (86 mg, 96%). Mp 130–131 °C. IR (film,  $cm^{-1}$ )  $\nu_{max}$  = 1375 (S=O), 1351 (S=O), 1170 (S=O), 1161 (S=O);  $^1H$  NMR (400 MHz,  $CDCl_3$ )  $\delta$  = 4.18 (dd, 2H,  $J$  = 5.8, 1.2 Hz), 6.05–6.12 (m, 1H), 6.89 (d, 1H,  $J$  = 11.3 Hz), 7.48 (d, 1H,  $J$  = 8.9 Hz), 8.24 (d, 1H,  $J$  = 2.6 Hz), 8.28 (dd, 1H,  $J$  = 8.9, 2.6 Hz);  $^{13}C$  NMR (100 MHz,  $CDCl_3$ )  $\delta$  = 52.4, 121.6, 124.3, 125.6, 126.8, 129.4, 130.8, 151.3; Anal. Calcd for  $C_9H_7NO_5S$  (241.22): C 44.81, H 2.92, N 5.81, found C 44.70, H 2.95, N 5.79.



#### 7-Amino-3H-1,2-benzoxathiepine 2,2-dioxide (7)

To a solution of 7-nitro-3H-1,2-benzoxathiepine 2,2-dioxide (**6c**) (250 mg, 1.04 mmol) in EtOH (4.3 ml) and  $H_2O$  (2.8 ml) AcOH (0.06 ml, 1.04 mmol) was added following by iron powder (350 mg, 6.27 mmol) at room temperature. Resulting suspension was stirred at 75 °C for 1 h. It was cooled to room temperature, EtOAc (50 ml) was added and washed with sat. aq.  $NaHCO_3$  ( $5 \times 30$  ml). Organic layer was dried over  $Na_2SO_4$  and concentrated in vacuum. Re-crystallized of the crude product from EtOAc/Hex afforded **7** (220 mg, 98%) as yellowish solid. Mp 170–171 °C. IR (film,  $cm^{-1}$ )  $\nu_{max}$  = 3465 (N–H), 3382 (N–H), 1358 (S=O), 1163 (S=O);  $^1H$  NMR (400 MHz,  $CDCl_3$ )  $\delta$  = 3.72–3.85 (br s, 2H), 3.92 (dd, 2H,  $J$  = 6.3, 1.0 Hz), 5.93–6.00 (m, 1H), 6.53 (d, 1H,  $J$  = 2.9 Hz), 6.68 (dd, 1H,  $J$  = 8.8, 2.6 Hz), 6.80 (d, 1H,  $J$  = 10.6 Hz), 7.12 (d, 1H,  $J$  = 8.8 Hz);  $^{13}C$  NMR (100 MHz,  $CDCl_3$ )  $\delta$  = 50.5, 115.0, 116.8, 119.8, 123.8, 133.4, 140.4, 145.5; HRMS (ESI)  $m/z$   $[M + H]^+$  calcd for  $C_9H_{10}NO_3S$ : 212.0381, found 212.0364.

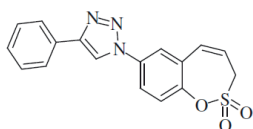


#### 7-Azido-3H-1,2-benzoxathiepine 2,2-dioxide (8)

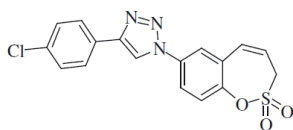
To a solution of 7-amino-3H-1,2-benzoxathiepine 2,2-dioxide (**7**) (220 mg, 1.03 mmol) in trifluoroacetic acid (1.3 ml) at 0 °C, slowly was added  $NaNO_2$  (80 mg, 1.12 mmol). After 30 min stirring at 0 °C, solution of  $NaN_3$  (67 mg, 1.03 mmol) in water (3 ml) was added. Mixture was stirring at 0 °C for 1 h. Collection of solid precipitate and drying in vacuum afforded **8** (170 mg, 69%) as brown solid. IR (film,  $cm^{-1}$ )  $\nu_{max}$  = 2116 ( $N_3$ ), 1374 (S=O), 1369 (S=O), 1167 (S=O);  $^1H$  NMR (400 MHz,  $CDCl_3$ )  $\delta$  = 4.01 (dd, 2H,  $J$  = 6.3, 1.2 Hz), 5.99–6.07 (m, 1H), 6.83 (d, 1H,  $J$  = 10.9 Hz), 6.94 (d, 1H,  $J$  = 2.8 Hz), 7.06 (dd, 1H,  $J$  = 8.9, 2.8 Hz), 7.32 (d, 1H,  $J$  = 8.9 Hz);  $^{13}C$  NMR (100 MHz,  $CDCl_3$ )  $\delta$  = 51.2, 120.5, 120.8, 120.9, 124.5, 129.8, 132.0, 139.2, 144.5.

**General procedure for the synthesis of 1,4-disubstitutedtriazoly compound (9–17)**

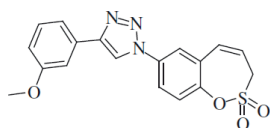
To a solution of corresponding alkyne (1 eq.) in tBuOH/H<sub>2</sub>O 1:1 mixture (10 ml) 7-azido-3H-1,2-benzoxathiepine 2,2-dioxide (**8**) (1 eq.), CuSO<sub>4</sub>·5H<sub>2</sub>O (2 eq.) and sodium ascorbate (4 eq.) were added and reaction mixture was stirred at room temperature for 10 min. AcOH (19–21 eq.) was added and mixture was stirred for additional 30 min. Solvent was driven off in vacuum and the crude product was purified by reversed phase chromatography (C-18, H<sub>2</sub>O–MeCN gradient MeCN 10–90%).

**1-(2,2-Dioxido-3H-1,2-benzoxathiepin-7-yl)-4-phenyl-1H-1,2,3-triazole (9)**

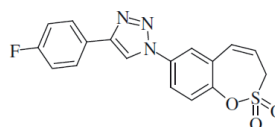
Compound **9** was prepared according to the general procedure from phenylacetylene (13 mg, 0.13 mmol), azide **8** (30 mg, 0.13 mmol), CuSO<sub>4</sub>·5H<sub>2</sub>O (65 mg, 0.26 mmol), sodium ascorbate (103 mg, 0.52 mmol), AcOH (0.14 ml, 2.45 mmol) as white solid (41 mg, 95%). Mp 203–204 °C. IR (KBr, cm<sup>-1</sup>)  $\nu_{\max}$ =1368 (S=O), 1171 (S=O); <sup>1</sup>H NMR (400 MHz, DMSO-d<sub>6</sub>)  $\delta$ =4.61 (dd, 2H, *J*=5.9, 1.2 Hz), 6.09–6.16 (m, 1H), 7.02 (d, 1H, *J*=11.3 Hz), 7.37–7.43 (m, 1H), 7.48–7.54 (m, 2H), 7.63 (d, 1H, *J*=8.8 Hz), 7.92–7.97 (m, 2H), 8.04 (dd, 1H, *J*=8.8, 2.6 Hz), 8.13 (d, 1H, *J*=2.6 Hz), 9.35 (s, 1H); <sup>13</sup>C NMR (100 MHz, DMSO-d<sub>6</sub>)  $\delta$ =51.7, 119.9, 121.6, 122.1, 122.7, 124.0, 125.3, 128.4, 129.1, 129.6, 130.0, 130.1, 135.0, 146.3, 147.5; HRMS (ESI) *m/z* [M+H]<sup>+</sup> calcd for C<sub>17</sub>H<sub>14</sub>N<sub>3</sub>O<sub>3</sub>S: 340.0756, found 340.0755.

**4-(4-Chlorophenyl)-1-(2,2-dioxido-3H-1,2-benzoxathiepin-7-yl)-1H-1,2,3-triazole (10)**

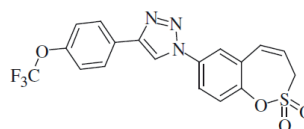
Compound **10** was prepared according to the general procedure from 1-chloro-4-ethynylbenzene (17 mg, 0.12 mmol), azide **8** (29 mg, 0.12 mmol), CuSO<sub>4</sub>·5H<sub>2</sub>O (61 mg, 0.24 mmol), sodium ascorbate (97 mg, 0.49 mmol), AcOH (0.13 ml, 2.27 mmol) as yellowish solid (34 mg, 74%). Mp 191–192 °C. IR (KBr, cm<sup>-1</sup>)  $\nu_{\max}$ =1369 (S=O), 1356 (S=O), 1168 (S=O); <sup>1</sup>H NMR (400 MHz, DMSO-d<sub>6</sub>)  $\delta$ =4.61 (dd, 2H, *J*=5.9, 1.2 Hz), 6.09–6.16 (m, 1H), 7.01 (d, 1H, *J*=11.5 Hz), 7.55–7.61 (m, 2H), 7.63 (d, 1H, *J*=8.9 Hz), 7.92–7.98 (m, 2H), 8.02 (dd, 1H, *J*=8.9, 2.7 Hz), 8.11 (d, 1H, *J*=2.7 Hz), 9.38 (s, 1H); <sup>13</sup>C NMR (100 MHz, DMSO-d<sub>6</sub>)  $\delta$ =51.7, 120.3, 121.6, 122.1, 122.7, 124.1, 127.0, 129.0, 129.1, 129.6, 130.1, 132.8, 135.0, 146.3, 146.4; HRMS (ESI) *m/z* [M+H]<sup>+</sup> calcd for C<sub>17</sub>H<sub>13</sub>ClN<sub>3</sub>O<sub>3</sub>S: 374.0366, found 374.0366.

**1-(2,2-Dioxido-3H-1,2-benzoxathiepin-7-yl)-4-(3-methoxyphenyl)-1H-1,2,3-triazole (11)**

Compound **11** was prepared according to the general procedure from 3-ethynylanisole (17 mg, 0.13 mmol), azide **8** (30 mg, 0.13 mmol), CuSO<sub>4</sub>·5H<sub>2</sub>O (63 mg, 0.25 mmol), sodium ascorbate (100 mg, 0.50 mmol), AcOH (0.14 ml, 2.45 mmol) as yellowish solid (24 mg, 51%). Mp 210–211 °C. IR (KBr, cm<sup>-1</sup>)  $\nu_{\max}$ =1372 (S=O), 1162 (S=O); <sup>1</sup>H NMR (400 MHz, DMSO-d<sub>6</sub>)  $\delta$ =3.84 (s, 3H), 4.61 (dd, 2H, *J*=5.8, 1.2 Hz), 6.09–6.16 (m, 1H), 6.94–6.99 (m, 1H), 7.02 (d, 1H, *J*=11.5 Hz), 7.39–7.45 (m, 1H), 7.48–7.55 (m, 2H), 7.63 (d, 1H, *J*=8.9 Hz), 8.03 (dd, 1H, *J*=8.9, 2.7 Hz), 8.12 (d, 1H, *J*=2.7 Hz), 9.36 (s, 1H); <sup>13</sup>C NMR (100 MHz, DMSO-d<sub>6</sub>)  $\delta$ =51.7, 55.2, 110.6, 114.1, 117.6, 120.1, 121.6, 122.1, 122.6, 124.0, 129.6, 130.1, 130.2, 131.4, 135.0, 146.3, 147.4, 159.8; HRMS (ESI) *m/z* [M+H]<sup>+</sup> calcd for C<sub>18</sub>H<sub>16</sub>N<sub>3</sub>O<sub>4</sub>S: 370.0862, found 370.0876.

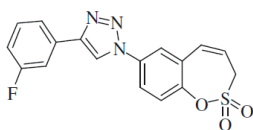
**1-(2,2-Dioxido-3H-1,2-benzoxathiepin-7-yl)-4-(4-fluorophenyl)-1H-1,2,3-triazole (12)**

Compound **12** was prepared according to the general procedure from 1-ethynyl-4-fluorobenzene (30 mg, 0.25 mmol), azide **8** (60 mg, 0.25 mmol), CuSO<sub>4</sub>·5H<sub>2</sub>O (126 mg, 0.50 mmol), sodium ascorbate (200 mg, 1.02 mmol), AcOH (0.28 ml, 5.05 mmol) as yellowish solid (60 mg, 66%). Mp 200–201 °C. IR (KBr, cm<sup>-1</sup>)  $\nu_{\max}$ =1369 (S=O), 1167 (S=O); <sup>1</sup>H NMR (400 MHz, DMSO-d<sub>6</sub>)  $\delta$ =4.61 (d, 2H, *J*=5.4 Hz), 6.07–6.17 (m, 1H), 7.01 (d, 1H, *J*=11.3 Hz), 7.30–7.71 (m, 2H), 7.63 (d, 1H, *J*=8.8 Hz), 7.94–8.05 (m, 3H), 8.11 (s, 1H), 9.34 (s, 1H); <sup>13</sup>C NMR (100 MHz, DMSO-d<sub>6</sub>)  $\delta$ =51.7, 116.1 (d, *J*=21.9 Hz), 119.9, 121.6, 122.1, 122.7, 124.1, 126.6, 127.4 (d, *J*=8.3 Hz), 129.7, 130.1, 135.0, 146.3, 146.6, 162.1 (d, *J*=245.3 Hz); HRMS (ESI) *m/z* [M+H]<sup>+</sup> calcd for C<sub>17</sub>H<sub>13</sub>FN<sub>3</sub>O<sub>3</sub>S: 358.0662, found 358.0656.

**1-(2,2-Dioxido-3H-1,2-benzoxathiepin-7-yl)-4-[4-(trifluoromethoxy)phenyl]-1H-1,2,3-triazole (13)**

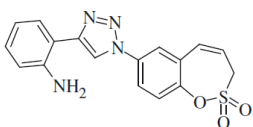
Compound **13** was prepared according to the general procedure from 4-(trifluoromethoxy) phenylacetylene (40 mg, 0.21 mmol), azide **8** (50 mg, 0.21 mmol), CuSO<sub>4</sub>·5H<sub>2</sub>O (105 mg, 0.42 mmol), sodium ascorbate (167 mg, 0.84 mmol), AcOH (0.23 ml, 4.02 mmol) as yellowish solid (74 mg, 83%). Mp 168–169 °C. IR (film, cm<sup>-1</sup>)  $\nu_{\max}$ =1357 (S=O), 1166 (S=O); <sup>1</sup>H NMR (400 MHz, CDCl<sub>3</sub>)  $\delta$ =4.13 (dd, 2H, *J*=6.0, 1.1 Hz), 6.06–6.13 (m, 1H), 6.93 (d, 1H, *J*=11.3 Hz), 7.30–7.35 (m, 2H), 7.51 (d, 1H, *J*=8.8 Hz), 7.79 (dd, 1H, *J*=8.8, 2.5 Hz), 7.85 (d, 1H, *J*=2.5 Hz), 7.91–7.98 (m, 2H), 8.25 (s, 1H); <sup>13</sup>C NMR (100 MHz, CDCl<sub>3</sub>)  $\delta$ =51.8, 120.6 (q, *J*=257.9 Hz), 121.4, 121.7, 122.1, 122.9, 124.7, 127.5, 128.8, 130.0, 131.5, 135.6, 147.3,

149.5, 149.6; HRMS (ESI)  $m/z$   $[M+H]^+$  calcd for  $C_{18}H_{13}F_3N_3O_4S$ : 424.0579, found 424.0553.



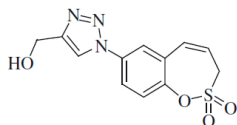
**1-(2,2-Dioxido-3H-1,2-benzoxathiepin-7-yl)-4-(3-fluorophenyl)-1H-1,2,3-triazole (14)**

Compound **14** was prepared according to the general procedure from 1-ethynyl-3-fluorobenzene (25 mg, 0.21 mmol), azide **8** (50 mg, 0.21 mmol),  $CuSO_4 \cdot 5H_2O$  (105 mg, 0.42 mmol), sodium ascorbate (166 mg, 0.84 mmol), AcOH (0.25 ml, 4.37 mmol) as brownish solid (56 mg, 74%). Mp 188–189 °C. IR (KBr,  $cm^{-1}$ )  $\nu_{max}$ =1354 (S=O), 1175 (S=O);  $^1H$  NMR (400 MHz, DMSO- $d_6$ )  $\delta$ =4.62 (dd, 2H,  $J$ =6.0, 1.3 Hz), 6.09–6.16 (m, 1H), 7.01 (d, 1H,  $J$ =11.6 Hz), 7.20–7.26 (m, 1H), 7.52–7.60 (m, 1H), 7.64 (d, 1H,  $J$ =8.8 Hz), 7.70–7.75 (m, 1H), 7.77–7.81 (m, 1H), 8.02 (dd, 1H,  $J$ =8.9, 2.7 Hz), 8.10 (d, 1H,  $J$ =2.7 Hz), 9.42 (s, 1H);  $^{13}C$  NMR (100 MHz, DMSO- $d_6$ )  $\delta$ =51.7, 111.9 (d,  $J$ =23.0 Hz), 115.1 (d,  $J$ =20.8 Hz), 120.7, 121.3 (d,  $J$ =2.5 Hz), 121.6, 122.1, 122.7, 124.1, 129.6, 130.0, 131.2 (d,  $J$ =8.7 Hz), 132.4 (d,  $J$ =8.4 Hz), 134.9, 146.3, 146.4, 162.6 (d,  $J$ =243.5 Hz); HRMS (ESI)  $m/z$   $[M+H]^+$  calcd for  $C_{17}H_{13}FN_3O_3S$ : 358.0662, found 358.0667.



**2-[1-(2,2-Dioxido-3H-1,2-benzoxathiepin-7-yl)-1H-1,2,3-triazol-4-yl]aniline (15)**

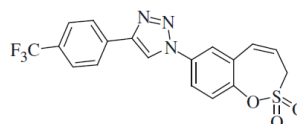
Compound **15** was prepared according to the general procedure from 2-ethynylaniline (25 mg, 0.21 mmol), azide **8** (50 mg, 0.21 mmol),  $CuSO_4 \cdot 5H_2O$  (105 mg, 0.42 mmol), sodium ascorbate (166 mg, 0.84 mmol), AcOH (0.25 ml, 4.37 mmol) as yellowish solid (43 mg, 57%). Mp 190–191 °C. IR (film,  $cm^{-1}$ )  $\nu_{max}$ =3430 (N–H), 3364 (N–H), 1365 (S=O), 1358 (S=O), 1167 (S=O), 1163 (S=O);  $^1H$  NMR (400 MHz, DMSO- $d_6$ )  $\delta$ =4.61 (dd, 2H,  $J$ =6.0, 1.2 Hz), 6.09–6.16 (m, 1H), 6.49–6.85 (m, 2H), 7.01 (d, 1H,  $J$ =11.3 Hz), 7.10–7.18 (m, 1H), 7.59–7.66 (m, 2H), 8.08 (dd, 1H,  $J$ =8.9, 2.4 Hz), 8.16 (d, 1H,  $J$ =2.4 Hz), 9.26 (s, 1H);  $^{13}C$  NMR (100 MHz, DMSO- $d_6$ )  $\delta$ =51.7, 112.1, 115.9, 116.1, 119.8, 121.8, 122.1, 122.8, 124.0, 127.9, 129.0, 129.6, 130.1, 135.0, 145.8, 146.3, 148.1; HRMS (ESI)  $m/z$   $[M+H]^+$  calcd for  $C_{17}H_{15}N_4O_3S$ : 355.0865, found 355.0869.



**[1-(2,2-dioxido-3H-1,2-benzoxathiepin-7-yl)-1H-1,2,3-triazol-4-yl]methanol (16)**

Compound **16** was prepared according to the general procedure from propargyl alcohol (0.012 ml, 0.21 mmol), azide **8** (50 mg,

0.21 mmol),  $CuSO_4 \cdot 5H_2O$  (105 mg, 0.42 mmol), sodium ascorbate (166 mg, 0.84 mmol), AcOH (0.25 ml, 4.37 mmol) as white solid (50 mg, 81%). Mp 144–145 °C. IR (KBr,  $cm^{-1}$ )  $\nu_{max}$ =1374 (S=O), 1167 (S=O);  $^1H$  NMR (400 MHz, DMSO- $d_6$ )  $\delta$ =4.59 (d, 2H,  $J$ =5.7 Hz), 4.62 (s, 2H), 6.05–6.13 (m, 1H), 6.98 (d, 1H,  $J$ =11.5 Hz), 7.56 (d, 1H,  $J$ =8.9 Hz), 7.99 (dd, 1H,  $J$ =8.9, 2.6 Hz), 8.09 (d, 1H,  $J$ =2.6 Hz), 8.74 (s, 1H);  $^{13}C$  NMR (100 MHz, DMSO- $d_6$ )  $\delta$ =51.8, 54.9, 121.3, 121.5, 121.9, 122.6, 123.9, 129.5, 130.1, 135.1, 146.1, 149.4; HRMS (ESI)  $m/z$   $[M+H]^+$  calcd for  $C_{12}H_{12}N_3O_4S$ : 294.0549, found 294.0553.

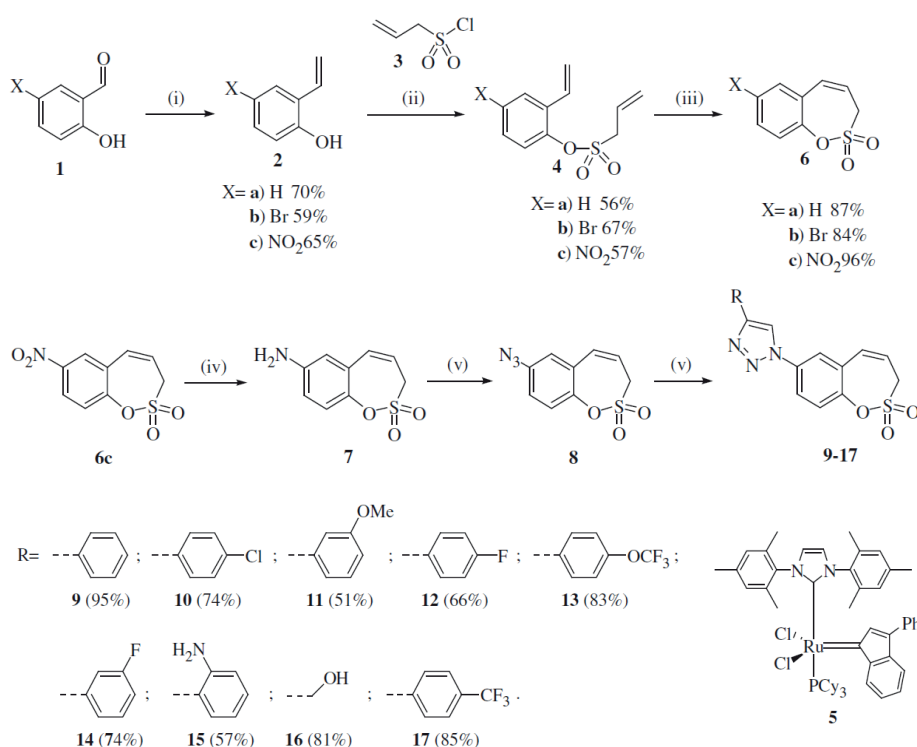


**4-(2,2-Dioxido-3H-1,2-benzoxathiepin-7-yl)-1-[4-(trifluoromethyl)phenyl]-1H-1,2,3-triazole (17)**

Compound **17** was prepared according to the general procedure from 4-(trifluoromethyl)phenylacetylene (36 mg, 0.21 mmol), azide **8** (50 mg, 0.21 mmol),  $CuSO_4 \cdot 5H_2O$  (105 mg, 0.42 mmol), sodium ascorbate (166 mg, 0.84 mmol), AcOH (0.25 ml, 4.37 mmol) as yellowish solid (73 mg, 85%). Mp 192–193 °C. IR (KBr,  $cm^{-1}$ )  $\nu_{max}$ =1358 (S=O), 1328 (S=O), 1174 (S=O), 1166 (S=O);  $^1H$  NMR (400 MHz, DMSO- $d_6$ )  $\delta$ =4.62 (dd, 2H,  $J$ =5.9, 1.0 Hz), 6.09–6.16 (m, 1H), 7.01 (d, 1H,  $J$ =11.5 Hz), 7.64 (d, 1H,  $J$ =8.8 Hz), 7.86–7.91 (m, 2H), 8.04 (dd, 1H,  $J$ =8.8, 2.7 Hz), 8.13 (d, 1H,  $J$ =2.7 Hz), 8.13–8.18 (m, 2H), 9.52 (s, 1H);  $^{13}C$  NMR (100 MHz, DMSO- $d_6$ )  $\delta$ =51.7, 121.2, 121.7, 122.1, 122.8, 124.1, 124.2 (q,  $J$ =272.0 Hz), 125.8, 126.1 (q,  $J$ =3.8 Hz), 128.4 (q,  $J$ =32.0 Hz), 129.6, 130.0, 134.0, 134.9, 146.0, 146.4; HRMS (ESI)  $m/z$   $[M+H]^+$  calcd for  $C_{18}H_{13}F_3N_3O_3S$ : 408.0630, found 408.0626.

**CA inhibition assay**

An SX.18 MV-R Applied Photophysics (Oxford, UK) stopped-flow instrument has been used to assay the catalytic/inhibition of various CA isozymes<sup>16</sup>. Phenol Red (at a concentration of 0.2 mM) has been used as indicator, working at the absorbance maximum of 557 nm, with 10 mM HEPES (pH 7.4) as buffer, 0.1 M  $Na_2SO_4$  or  $NaClO_4$  (for maintaining constant the ionic strength; these anions are not inhibitory in the used concentration),<sup>17</sup> following the CA-catalysed  $CO_2$  hydration reaction for a period of 5–10 s. Saturated  $CO_2$  solutions in water at 25 °C were used as substrate. Stock solutions of inhibitors were prepared at a concentration of 10 mM (in DMSO-water 1:1, v/v) and dilutions up to 1 nM done with the assay buffer mentioned above. At least seven different inhibitor concentrations have been used for measuring the inhibition constant. Inhibitor and enzyme solutions were preincubated together for 6 h at 4 °C prior to assay, in order to allow for the formation of the E-I complex. Triplicate experiments were done for each inhibitor concentration, and the values reported throughout the paper are the mean of such results. The inhibition constants were obtained by non-linear least-squares methods using the Cheng-Prusoff equation, as reported earlier<sup>17</sup>, and represent the mean from at least three different determinations. All CA isozymes used here were recombinant proteins obtained as reported earlier by our group<sup>18</sup>.



**Scheme 2.** Reagents and conditions: (i) MePPh<sub>3</sub>Br, tBuOK, THF, RT, 24 h; (ii) NEt<sub>3</sub>, CH<sub>2</sub>Cl<sub>2</sub>, RT, 20 h; (iii) **5**, toluene, 70 °C, 4 h; (iv) Fe, AcOH, EtOH, H<sub>2</sub>O, 70 °C, 1 h, 98%; (v) 1) NaNO<sub>2</sub>, H<sub>2</sub>O, TFA, 2) NaN<sub>3</sub>, H<sub>2</sub>O, 69%; (vi) alkyne, tBuOH/H<sub>2</sub>O (1:1), CuSO<sub>4</sub>, sodium ascorbate, acetic acid, 30 min.

### X-ray structure determination

X-Ray diffraction data for compound **6c** were collected using a *NoniusKappaCCD* diffractometer (MoK $\alpha$  radiation,  $\lambda = 0.71073$  Å), equipped with low temperature *Oxford CryosystemsCryostream Plus* device (Delft, the Netherlands). Data were collected using *KappaCCD Server Software*, cell refined by *SCALEPACK*<sup>19</sup>, data reduction performed by *DENZO*<sup>20</sup> and *SCALEPACK*<sup>19</sup>, structures solved by direct method using *SIR2004* and refined by *SHELXL97*<sup>21</sup> as implemented in the program package *WinGX*<sup>22</sup>. Software used to prepare CIF file was *SHELXL97*<sup>21</sup> and graphics-*ORTEP3*<sup>22</sup>.

*Crystal data for 6c*: C<sub>9</sub>H<sub>7</sub>NO<sub>3</sub>S (*M* = 241.22), monoclinic, *P*<sub>2</sub><sub>1</sub>/*a*, *a* = 7.3194(3), *b* = 14.9000(7) and *c* = 18.3387(8) Å,  $\beta = 101.325(1)^\circ$ , *V* = 1961.06(15) Å<sup>3</sup>, *T* = 173(2) K, *Z* = 2, *Z'* = 1,  $\mu$ (MoK $\alpha$ ) = 0.34 mm<sup>-1</sup>, 9545 reflections measured, 2150 independent reflections (*R*<sub>int</sub> = 0.083), *R*<sub>1</sub>(obs) = 0.058, *wR*<sub>1</sub>(obs) = 0.1500, *R*<sub>1</sub>(all) = 0.1893, *wR*<sub>1</sub>(all) = 0.1096, *S* = 0.94.

CCDC 1526002 contains the supplementary crystallographic data for this paper. These data can be obtained free of charge from The Cambridge Crystallographic Data Centre via <http://www.ccdc.cam.ac.uk>.

## Results and discussion

### Chemistry

The synthesis of homo-sulfocoumarins began with a Wittig reaction in which salicylic aldehydes **1** were converted to the corresponding mono-olefins **2a–c** in good yields (Scheme 2). Treatment of compounds **2a–c** with allyl sulfonyl chloride (**3**) provided bis-olefins **4a–c** as the key intermediates, again in good yields

(see Experimental for details). In the next step, olefin metathesis with the commercially available Ru-catalyst **5** was used, in which *bis*-olefins **4a–c** were converted to 3*H*-1,2-benzoxathiepine 2,2-dioxides **6a–b** in 84–96% yields. To obtain a series of 7-substituted homo-sulfocoumarins, the synthesis of 1,4-triazolyl derivatives **9–17** was thereafter performed. For this purpose, 7-nitro derivative **6c** was reduced by elemental iron to the corresponding amine **7** in nearly quantitative yield. Further diazotization of amine **7** followed by *in situ* treatment with sodium azide afforded the azide **8**. Treatment of azide **8** with alkynes under click chemistry condition provides a series of 1,4-triazolyl homo-sulfocoumarins **9–17** in good to excellent yields (see Experimental for details).

The structures of all synthesized 3*H*-1,2-benzoxathiepine 2,2-dioxides **6–17** were fully supported by <sup>1</sup>H, <sup>13</sup>C NMR and IR spectroscopy, MS or elemental analysis. Additionally, the final unequivocal identification of the scaffold of 3*H*-1,2-benzoxathiepine 2,2-dioxide was established by a single-crystal X-ray structure for compound **6c**, shown in Figure 2.

### Carbonic anhydrase inhibition

All the synthesized derivatives **6c–17** were evaluated for their efficacy in inhibiting four relevant CA isoforms, i.e. hCA I, II, IX and XII, by using the stopped flow carbon dioxide hydrase assay<sup>16</sup>, in comparison to the sulphonamide acetazolamide (**AAZ**, 5-acetamido-1,3,4-thiadiazole-2-sulfonamide) as a standard CAI.

Data of Table 1 show that the cytosolic isoforms hCA I and II (widely distributed enzymes, with important physiological roles in many tissues)<sup>9,10</sup> were generally not inhibited by the investigated homo-sulfocoumarins, up to 50  $\mu$ M concentration of inhibitors in

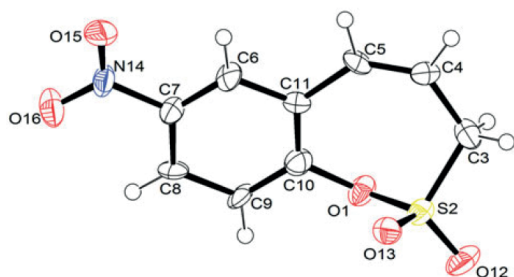


**Figure 2.** Single-crystal X-ray structure of **6c** (CCDC deposition number 1526002). Thermal ellipsoids are drawn at the 50% probability level (see Experimental for details).

**Table 1.** CA inhibition data against isoforms hCA I, II, IX and XII with homo-sulfocoumarins **6–17** and acetazolamide (AAZ) as standard, by a stopped-flow CO<sub>2</sub> hydrase assay<sup>14</sup>.

Compound	K <sub>i</sub> (μM) <sup>a</sup>			
	hCA I	hCA II	hCA IX	hCA XII
<b>6c</b>	>50	>50	0.027	0.64
<b>7</b>	>50	>50	3.57	>50
<b>9</b>	>50	>50	1.71	>50
<b>10</b>	>50	>50	3.59	>50
<b>11</b>	>50	>50	2.56	>50
<b>12</b>	>50	>50	1.75	>50
<b>13</b>	>50	5.77	0.34	1.72
<b>14</b>	>50	>50	1.15	>50
<b>15</b>	>50	>50	0.46	2.32
<b>16</b>	>50	>50	0.87	>50
<b>17</b>	>50	>50	0.43	>50
AAZ	0.25	0.012	0.025	0.006

<sup>a</sup>Errors in the range of ±5% of the reported values, from three different assays.

the assay system. Only one derivative, **13**, showed a moderate inhibitory profile against hCA II, with an inhibition constant of 5.77 μM.

The tumour associated isoform hCA IX, a validated drug target for antitumor/antimetastatic agents<sup>23,24</sup>, was on the other hand effectively inhibited by the investigated homo-sulfocoumarins, with K<sub>i</sub>s ranging between 27 nM and 3.59 μM (Table 1). The structure activity relationship (SAR) was very interesting, as the best inhibitor (**6c**) incorporated a compact, powerful electron attracting moiety (NO<sub>2</sub>) whereas the remaining derivatives, incorporating substituted 1,2,3-triazole moieties in position 7 of the homo-sulfocoumarin ring were less effective hCA IX inhibitors. Four submicromolar hCA IX inhibitors were however detected apart **6c**, derivatives **13**, **15**, **16** and **17**, which incorporate either the compact hydroxymethyl group at the triazole fragment of the molecule, or substituted phenyls with 4-trifluoromethoxy-, 2-amino-, or 4-trifluoromethyl substituents on the aryl fragment. These derivatives showed K<sub>i</sub>s ranging between 0.34 and 0.87 μM. The remaining homo-sulfocoumarins were low micromolar hCA IX inhibitors.

The SAR for inhibition of the second tumour-associated isoform, hCA XII, was more complex compared to what discussed above for hCA IX (Table 1). Thus, 8 out of 11 derivatives were inactive (K<sub>i</sub>s > 50 μM) whereas the remaining ones, **6c**, **13** and **15**, inhibited hCA XII with K<sub>i</sub>s in the range of 0.64–2.32 μM.

This inhibition profile is rather similar to the one of sulfocoumarins<sup>1–6</sup> and coumarins<sup>7,8</sup>, which are generally selective inhibitors for the tumour-associated over the cytosolic isoforms. However, some homo-sulfocoumarins showed a very specific, and unique up until now inhibition profile among all classes of CAIs known to

date<sup>9,10</sup>, as they are highly selective for hCA IX over hCA I, II and XII (e.g. **7–12**, **14**, **16** and **17**).

In conclusion, we report here a new chemotype with effective and isoform-selective CAIs, the homo-sulfocoumarins, which show a unique inhibition profile for the tumour-associated CA isoforms hCA IX (and XII) over the cytosolic ones. Although the CA inhibition mechanism with these new compounds is unknown for the moment, we hypothesize that it may be similar to that of the sulfocoumarins, i.e. hydrolysis to the corresponding sulfonic acids which thereafter anchor to the zinc-coordinated water molecule within the enzyme active site.

## Disclosure statement

No potential conflict of interest was reported by the authors.

## References

1. a) Grandane A, Belyakov S, Trapencieris P, et al. Facile synthesis of coumarin bioisosteres – 1,2-benzoxathiine 2,2-dioxides. *Tetrahedron* 2012;68:5541–6. b) Tars K, Vullo D, Kazaks A, et al. Sulfocoumarins (1,2-benzoxathiine-2,2-dioxides): a class of potent and isoform-selective inhibitors of tumor-associated carbonic anhydrases. *J Med Chem* 2013; 56:293–300.
2. Tanc M, Carta F, Bozdog M, et al. 7-Substituted-sulfocoumarins are isoform-selective, potent carbonic anhydrase II inhibitors. *Bioorg Med Chem* 2013;21:4502–10.
3. a) Grandane A, Tanc M, Zalubovskis R, et al. Synthesis of 6-tetrazolyl-substituted sulfocoumarins acting as highly potent and selective inhibitors of the tumor-associated carbonic anhydrase isoforms IX and XII. *Bioorg Med Chem* 2014;22:1522–8. b) Grandane A, Tanc M, Zalubovskis R, et al. 6-Triazolyl-substituted sulfocoumarins are potent, selective inhibitors of the tumor-associated carbonic anhydrases IX and XII. *Bioorg Med Chem Lett* 2014;24:1256–60.
4. Grandane A, Tanc M, Di Cesare Mannelli L, et al. 6-Substituted sulfocoumarins are selective carbonic anhydrase IX and XII inhibitors with significant cytotoxicity against colorectal cancer cells. *J Med Chem* 2015;58: 3975–83.
5. Grandane A, Tanc M, Žalubovskis R, et al. Synthesis of 6-aryl-substituted sulfocoumarins and investigation of their carbonic anhydrase inhibitory action. *Bioorg Med Chem* 2015;23:1430–6.
6. Nocentini A, Ceruso M, Carta F, et al. 7-Aryl-triazolyl-substituted sulfocoumarins are potent, selective inhibitors of the tumor-associated carbonic anhydrase IX and XII. *J Enzyme Inhib Med Chem* 2016;31:1226–33.
7. (a) Maresca A, Temperini C, Vu H, et al. Non-zinc mediated inhibition of carbonic anhydrases: coumarins are a new class of suicide inhibitors. *J Am Chem Soc* 2009;131:3057–62. b) Maresca A, Temperini C, Pochet L, et al. Deciphering the mechanism of carbonic anhydrase inhibition with coumarins and thiocoumarins. *J Med Chem* 2010;53:335–44. c) Maresca A, Supuran CT. Coumarins incorporating hydroxy- and chloro-moieties selectively inhibit the transmembrane, tumor-associated carbonic anhydrase isoforms IX and XII over the cytosolic ones I and II. *Bioorg Med Chem Lett* 2010;20:4511–14.
8. a) Maresca A, Scozzafava A, Supuran CT. 7,8-Disubstituted- but not 6,7-disubstituted coumarins selectively inhibit the

- transmembrane, tumor-associated carbonic anhydrase isoforms IX and XII over the cytosolic ones I and II in the low nanomolar/subnanomolar range. *Bioorg Med Chem Lett* 2010;20:7255–58. b) Touisni N, Maresca A, McDonald PC, et al. Glycosyl coumarin carbonic anhydrase IX and XII inhibitors strongly attenuate the growth of primary breast tumors. *J Med Chem* 2011;54:8271–7. c) Carta F, Maresca A, Scozzafava A, et al. Novel coumarins and 2-thioxo-coumarins as inhibitors of the tumor-associated carbonic anhydrases IX and XII. *Bioorg Med Chem* 2012;20:2266–73. d) Davis RA, Vullo D, Maresca A, et al. Natural product coumarins that inhibit human carbonic anhydrases. *Bioorg Med Chem* 2013;21:1539–43. e) Sharma A, Tiwari M, Supuran CT. Novel coumarins and benzocoumarins acting as isoform-selective inhibitors against the tumor-associated carbonic anhydrase IX. *J Enzyme Inhib Med Chem* 2014;29:292–6. f) Ferraroni M, Carta F, Scozzafava A, Supuran CT. Thioxocoumarins show an alternative carbonic anhydrase inhibition mechanism compared to coumarins. *J Med Chem* 2016;59:462–73.
9. a) Supuran CT. Carbonic anhydrases: novel therapeutic applications for inhibitors and activators. *Nat Rev Drug Discov* 2008;7:168–81. b) Neri D, Supuran CT. Interfering with pH regulation in tumours as a therapeutic strategy. *Nat Rev Drug Discov* 2011;10:767–77. c) Durdagi S, Vullo D, Pan P, et al. Protein-protein interactions: Inhibition of mammalian carbonic anhydrases I–XV by the murine inhibitor of carbonic anhydrase and other members of the transferrin family. *J Med Chem* 2012;55:5529–35. d) Di Cesare Mannelli L, Micheli L, Carta F, et al. Carbonic anhydrase inhibition for the management of cerebral ischemia: in vivo evaluation of sulfonamide and coumarin inhibitors. *J Enzyme Inhib Med Chem* 2016;31:894–9.
  10. a) Supuran CT. Structure and function of carbonic anhydrases. *Biochem J* 2016;473:2023–32. b) Supuran CT. How many carbonic anhydrase inhibition mechanisms exist? *J Enzyme Inhib Med Chem* 2016;31:345–60. c) Supuran CT. Carbonic anhydrases. *Bioorg Med Chem* 2013;21:1377–8. d) Supuran CT. Advances in structure-based drug discovery of carbonic anhydrase inhibitors. *Expert Opin Drug Discov* 2017;12:61–88. e) Alterio V, Di Fiore A, D'Ambrosio K, et al. Multiple binding modes of inhibitors to carbonic anhydrases: how to design specific drugs targeting 15 different isoforms? *Chem Rev* 2012;112:4421–68. f) Supuran CT. *Legionella pneumophila* carbonic anhydrases: underexplored antibacterial drug targets. *Pathogens* 2016;5:E44.
  11. (a) De Simone G, Alterio V, Supuran CT. Exploiting the hydrophobic and hydrophilic binding sites for designing carbonic anhydrase inhibitors. *Expert Opin Drug Discov* 2013;8:793–810. (b) Masini E, Carta F, Scozzafava A, et al. Antiglaucoma carbonic anhydrase inhibitors: a patent review. *Expert Opin Ther Pat* 2013;23:705–16. (c) Supuran CT. Carbonic anhydrase inhibitors. *Bioorg Med Chem Lett* 2010;2:3467–74. (d) Supuran CT. Carbonic anhydrases: from biomedical applications of the inhibitors and activators to biotechnological use for CO<sub>2</sub> capture. *J Enzyme Inhib Med Chem* 2013;28:229–30. e) D'Ambrosio K, Carradori S, Monti SM, et al. Out of the active site binding pocket for carbonic anhydrase inhibitors. *Chem Commun* 2015;51:302–5.
  12. a) Supuran CT. Structure-based drug discovery of carbonic anhydrase inhibitors. *J Enzyme Inhib Med Chem* 2012;27:759–72. b) Supuran CT. Carbonic anhydrase inhibitors: an editorial. *Expert Opin Ther Pat* 2013;23:677–9. c) Winum JY, Supuran CT. Recent advances in the discovery of zinc-binding motifs for the development of carbonic anhydrase inhibitors. *J Enzyme Inhib Med Chem* 2015;30:321–4. d) De Luca V, Del Prete S, Supuran CT, et al. Protonography, a new technique for the analysis of carbonic anhydrase activity. *J Enzyme Inhib Med Chem* 2015;30:277–82. e) Lomelino CL, Supuran CT, McKenna R. Non-classical inhibition of carbonic anhydrase. *Int J Mol Sci* 2016;17:E1150.
  13. a) Supuran CT. Acetazolamide for the treatment of idiopathic intracranial hypertension. *Expert Rev Neurother* 2015;15:851–6. b) Di Fiore A, De Simone G, Alterio V, et al. The anticonvulsant sulfamide JNJ-26990990 and its: S,S-dioxide analog strongly inhibit carbonic anhydrases: solution and X-ray crystallographic studies. *Org Biomol Chem* 2016;14:4853–8. c) Supuran CT. Drug interaction considerations in the therapeutic use of carbonic anhydrase inhibitors. *Expert Opin Drug Metab Toxicol* 2016;12:423–31.
  14. Albert S, Horbach R, Deising HB, et al. Synthesis and antimicrobial activity of (E) stilbene derivatives. *Bioorg Med Chem* 2011;19:5155–66.
  15. Dauban P, Dodd RH. Synthesis of cyclic sulfonamides via intramolecular copper-catalyzed reaction of unsaturated iminodinanones. *Org Lett* 2000;2:2327–9.
  16. Khalifah RG. The carbon dioxide hydration activity of carbonic anhydrase. I. Stop-flow kinetic studies on the native human isoenzymes B and C. *J Biol Chem* 1971;246:2561–73.
  17. Leitans J, Sprudza A, Tanc M, et al. 5-Substituted-(1,2,3-triazol-4-yl)thiophene-2-sulfonamides strongly inhibit human carbonic anhydrases I, II, IX and XII: solution and X-ray crystallographic studies. *Bioorg Med Chem* 2013;21:5130–8.
  18. a) Korkmaz N, Obaidi OA, Senturk M, et al. Synthesis and biological activity of novel thiourea derivatives as carbonic anhydrase inhibitors. *J Enzyme Inhib Med Chem* 2015;30:75–80. b) Abdel-Aziz AAM, El-Azab AS, Ekinci D, et al. Investigation of arenesulfonyl-2-imidazolidinones as potent carbonic anhydrase inhibitors. *J Enzyme Inhib Med Chem* 2015;30:81–4. c) Akdemir A, De Monte C, Carradori S, et al. Computational investigation of the selectivity of salen and tetrahydrosalen compounds towards the tumor-associated hCA XII isozyme. *J Enzyme Inhib Med Chem* 2015;3:114–18. d) Leitans J, Kazaks A, Balode A, et al. Efficient expression and crystallization system of cancer-associated carbonic anhydrase isoform IX. *J Med Chem* 2015;58:9004–9. e) Göçer H, Akincioglu AS, Gulcin GI, et al. Carbonic anhydrase and acetylcholinesterase inhibitory effects of carbamates and sulfamoylcarbamates. *J Enzyme Inhib Med Chem* 2015;30:316–20. f) Ceruso M, Bragagni M, AlOthman Z, et al. New series of sulfonamides containing amino acid moiety act as effective and selective inhibitors of tumor-associated carbonic anhydrase XII. *J Enzyme Inhib Med Chem* 2015;3:430–4. g) Zolfaghari Emameh R, Syrjänen L, Barker H, et al. *Drosophila melanogaster*: a model organism for controlling dipteran vectors and pests. *J Enzyme Inhib Med Chem* 2015;30:505–13.
  19. Otwinowski Z, Minor W. Processing of X-ray diffraction data collected in oscillation mode. *Methods Enzymol* 1997;276:307–26.
  20. Burla MC, Caliandro R, Camalli M, et al. SIR2004: an improved tool for crystal structure determination and refinement. *J Appl Crystallogr* 2005;38:381–8.
  21. Sheldrick GM. A short history of SHELX. *Acta Crystallogr* 2008;64:112–22.
  22. Farrugia LJ. WinGX and ORTEP for windows: an update. *J Appl Crystallogr* 2012;45:849–54.

23. a) Gieling RG, Babur M, Mamnani L, et al. Antimetastatic effect of sulfamate carbonic anhydrase IX inhibitors in breast carcinoma xenografts. *J Med Chem* 2012;55:5591–600. b) Winum JY, Maresca A, Carta F, et al. Polypharmacology of sulfonamides: pazopanib, a multitargeted receptor tyrosine kinase inhibitor in clinical use, potently inhibits several mammalian carbonic anhydrases. *Chem Commun* 2012;48:8177–9. c) Lock EF, McDonald PC, Lou Y, et al. Targeting carbonic anhydrase IX depletes breast cancer stem cells within the hypoxic niche. *Oncogene* 2013;32:5210–19. d) Ward C, Langdon SP, Mullen P, et al. New strategies for targeting the hypoxic tumour microenvironment in breast cancer. *Cancer Treat Rev* 2013;39:171–9.
24. a) Pan J, Lau J, Mesak F, et al. Synthesis and evaluation of  $^{18}\text{F}$ -labeled carbonic anhydrase IX inhibitors for imaging with positron emission tomography. *J Enzyme Inhib Med Chem* 2014;29:249–55. b) Pettersen EO, Ebbesen P, Gieling RG, et al. Targeting tumour hypoxia to prevent cancer metastasis. From biology, biosensing and technology to drug development: The METOXIA consortium. *J Enzyme Inhib Med Chem* 2015;30:689–721.




Pustenko, A., Nocentini, A., Balašova, A., Alafeefy, A., Krasavin, M., Žalubovskis, R., Supuran, C. T. Aryl derivatives of 3H-1,2-benzoxathiepine 2,2-dioxide as carbonic anhydrase inhibitors. *J. Enzyme Inhib. Med. Chem.* **2020**, *35*, 245–254.

Reprinted with permission from Taylor & Francis Group.

Copyright © 2020, Taylor & Francis Group.

## Aryl derivatives of 3H-1,2-benzoxathiepine 2,2-dioxide as carbonic anhydrase inhibitors

Aleksandrs Pustenko<sup>a,b</sup>, Alessio Nocentini<sup>c</sup>, Anastasija Balašova<sup>a</sup>, Ahmed Alafeefy<sup>d</sup>, Mikhail Krasavin<sup>e</sup>, Raivis Žalubovskis<sup>a,b</sup> and Claudiu T. Supuran<sup>c</sup> 

<sup>a</sup>Latvian Institute of Organic Synthesis, Riga, Latvia; <sup>b</sup>Institute of Technology of Organic Chemistry, Faculty of Materials Science and Applied Chemistry, Riga Technical University, Riga, Latvia; <sup>c</sup>Dipartimento Neurofarba, Sezione di Scienze Farmaceutiche e Nutraceutiche, Università degli Studi di Firenze, Florence, Italy; <sup>d</sup>Faculty of Pharmacy, University Technology MARA, UiTM, Bandar, Malaysia; <sup>e</sup>Chemistry Department, Saint Petersburg State University, Saint Petersburg, Russian Federation

### ABSTRACT

A new series of homosulfocoumarins (3H-1,2-benzoxathiepine 2,2-dioxides) possessing various substitution patterns and moieties in the 7, 8 or 9 position of the heterocyclic ring were prepared by original procedures and investigated for the inhibition of four physiologically relevant carbonic anhydrase (CA, EC 4.2.1.1) isoforms, the human (h) hCA I, II, IX and XII. The 8-substituted homosulfocoumarins were the most effective hCA IX/XII inhibitors followed by the 7-substituted derivatives, whereas the substitution pattern in position 9 led to less effective binders for the transmembrane, tumour-associated isoforms IX/XII. The cytosolic isoforms hCA I and II were not inhibited by these compounds, similar to the sulfocoumarins/coumarins investigated earlier. As hCA IX and XII are validated anti-tumour targets, with one sulphonamide (SLC-0111) in Phase Ib/II clinical trials, finding derivatives with better selectivity for the tumour-associated isoforms over the cytosolic ones, as the homosulfocoumarins reported here, is of crucial importance.

### ARTICLE HISTORY

Received 7 October 2019  
Revised 13 November 2019  
Accepted 14 November 2019

### KEYWORDS

Carbonic anhydrase; transmembrane isoforms; sulfocoumarin; homosulfocoumarin; isoform-selective inhibitor

### 1. Introduction



Carbonic anhydrases (CAs, EC 4.2.1.1) are metalloenzymes widespread in nature, being encoded by at least eight different genetic families, which have been identified in organisms all over the phylogenetic tree<sup>1–3</sup>. By catalysing a crucial physiologic reaction, by which CO<sub>2</sub> is hydrated with the formation of a weak base (bicarbonate) and a strong acid (hydronium ions), these enzymes are involved in a multitude of physiologic processes, starting with pH regulation and ending with metabolism<sup>1,3–6</sup>. As thus, CAs are drug targets for decades, with their inhibitors having pharmacological applications in a multitude of fields<sup>1,3–5</sup>. The primary sulphonamides were discovered as CA inhibitors (CAIs) in the 40s, and most of the drugs that were launched in the next decades as diuretics, antiepileptics, or antiglaucoma agents targeting CAs belonged to this class of compounds<sup>1,3–5</sup>. Although highly effective as CAIs<sup>1</sup>, the sulphonamides generally indiscriminately inhibit most  $\alpha$ -CA isoforms present in mammals (at least 15 in humans, and 16 in other vertebrates<sup>1</sup>) as well as CAs belonging to the other genetic families ( $\beta$ -,  $\gamma$ -,  $\delta$ -,  $\zeta$ -,  $\eta$ -,  $\theta$ - and  $i$ -CAs)<sup>2–5</sup> and for this reason alternative CAI classes were searched for. In fact, in the last 10 years, a multitude of new chemotypes as well as novel CA inhibition mechanisms were reported<sup>1,4,7–9</sup>, which highly enriched our understanding of these enzymes and also allowed for obtaining isoform-selective CAIs targeting all the mammalian isoforms<sup>4,7–9</sup>. Among the new such chemotypes, which also showed the highest levels of isoform selectivity, were the coumarins<sup>9</sup>, the

(3H-1,2-benzoxathiepine 2,2-dioxides)<sup>10</sup>. Considering the fact that this last chemotype was only recently reported and rather poorly investigated<sup>10</sup>, we report here a series of new aryl-3H-1,2-benzoxathiepine 2,2-dioxides substituted in various positions of the heterocyclic ring, which have been designed in order to explore the chemical space around this new CA inhibitory chemotype and to see whether the presence of various moieties in position 7, 8 or 9 of the heterocyclic system maintains the desired enzyme inhibitory activity and selectivity for the target isoforms.

### 2. Materials and methods

#### 2.1. Chemistry

Reagents, starting materials and solvents were obtained from commercial sources and used as received. Thin-layer chromatography was performed on silica gel, spots were visualised with UV light (254 and 365 nm). Melting points were determined on an OptiMelt automated melting point system. IR spectra were recorded on Shimadzu FTIR IR Prestige-21 spectrometer. NMR spectra were recorded on Bruker Advance Neo (400 MHz) spectrometer with chemical shifts values ( $\delta$ ) in ppm relative to TMS using the residual DMSO-d<sub>6</sub> signal (<sup>1</sup>H 2.50; <sup>13</sup>C 39.52) or CDCl<sub>3</sub> signal (<sup>1</sup>H 7.26; <sup>13</sup>C 77.16) as an internal standard. High-resolution mass spectra (HRMS) were recorded on a mass spectrometer with a Q-TOF micro mass analyser using the ESI technique. Elemental analyses were measured using Carlo Erba (EA1108) apparatus

CONTACT Claudiu T. Supuran  claudiu.supuran@unifi.it  Neurofarba Department, University of Florence, Firenze 50121, Italy

© 2019 The Author(s). Published by Informa UK Limited, trading as Taylor & Francis Group.

This is an Open Access article distributed under the terms of the Creative Commons Attribution License (<http://creativecommons.org/licenses/by/4.0/>), which permits unrestricted use, distribution, and reproduction in any medium, provided the original work is properly cited.

**2-Hydroxy-5-iodobenzaldehyde (2)**

To a solution of salicylaldehyde (**1**) (8.73 mL, 81.9 mmol) in AcOH (40 mL) iodine monochloride (4.92 mL, 98.3 mmol) was added<sup>11</sup>. Reaction mixture was stirred 24 h at 40 °C, then cooled to r.t. EtOH (60 mL) was added and all volatiles were removed in vacuum. CH<sub>2</sub>Cl<sub>2</sub> (60 mL) and water (100 mL) were added, the phases were separated and the aqueous phase was extracted with CH<sub>2</sub>Cl<sub>2</sub> (3 × 50 mL). The combined organic phases were washed with 10% Na<sub>2</sub>S<sub>2</sub>O<sub>3</sub> (1 × 60 mL), brine (1 × 60 mL), dried over Na<sub>2</sub>SO<sub>4</sub>, filtered and concentrated. The residue was purified by column chromatography on silica gel (PE/EtOAc 3:1), the crude product was re-crystallised from EtOH to afford product **2** (17.1 g, 84%) as yellowish solid. <sup>1</sup>H NMR (400 MHz, DMSO-d<sub>6</sub>) δ = 6.85 (d, 1H, *J* = 8.6 Hz), 7.77 (dd, 1H, *J* = 8.6, 2.4 Hz), 7.87 (d, 1H, *J* = 2.4 Hz), 10.16 (s, 1H), 10.92 (s, 1H) ppm. <sup>13</sup>C NMR (100 MHz, DMSO-d<sub>6</sub>) δ = 81.4, 120.1, 124.6, 136.7, 144.1, 160.3, 189.8 ppm.

**Prop-2-ene-1-sulphonyl chloride (4)**

Compound was synthesised using previously described procedure by our group<sup>10</sup>. To a solution of Na<sub>2</sub>SO<sub>3</sub> (30.2 g; 0.24 mol) in water (140 mL) allyl bromide (17.4 mL; 0.20 mol) was added and the reaction mixture was refluxed overnight. After cooling to room temperature, reaction mixture was washed with Et<sub>2</sub>O (3 × 50 mL). Aqueous phase was concentrated. Crude white solid was dried under high vacuum at 100 °C for 6 h. To the white solid at 0 °C POCl<sub>3</sub> (120 mL) was added, and mixture was refluxed for 4 h. After cooling to room temperature dry THF (60 mL) was added and reaction mixture was vigorously stirred for 10 min and filtered. Filter cake was suspended in dry THF (60 mL), suspension was vigorously stirred for 10 min and filtered. Filtrates were combined and solvent was carefully driven off on rotary evaporator. Residue was distilled in vacuum (10 mbar) and fraction with boiling point 38–42 °C was collected, to give prop-2-ene-1-sulfonyl chloride (**4**) as colourless oil (18.6 g, 66%), which was used in further reactions without additional purification.

**General procedure for the synthesis of ethenylphenoles (3, 14, 18, 27)**

To a stirred solution of methyltriphenylphosphonium bromide (2.60 eq) in dry THF (5 mL/1 mmol of methyltriphenylphosphonium bromide), was added tBuOK (3.2 eq) in several portions over 20 min. Reaction mixture was stirred for 1 h at r.t. Corresponding benzaldehyde (1 eq) was added and stirring continued at room temperature for 24 h. Reaction mixture was diluted with CH<sub>2</sub>Cl<sub>2</sub> (4 mL/1 mmol of methyltriphenylphosphonium bromide). Organic layer was washed with water (2 × 20 mL) and brine (2 × 20 mL), and dried over Na<sub>2</sub>SO<sub>4</sub>, filtered and concentrated. The crude product was purified by column chromatography on silica gel (PE/EtOAc 4:1).

**4-Iodo-2-ethenylphenol (3)**

Compound **3** was prepared according to the general procedure from methyltriphenylphosphonium bromide (14.98 g, 37.0 mmol), t-BuOK (5.79 g, 51.6 mmol) and 2-hydroxy-5-iodobenzaldehyde (**2**) (4.00 g, 16.1 mmol) as yellowish solid (3.29 g, 83%)<sup>12</sup>. <sup>1</sup>H NMR

(400 MHz, DMSO-d<sub>6</sub>) δ = 5.23 (dd, 1H, *J* = 11.3, 1.4 Hz), 5.80 (dd, 1H, *J* = 17.8, 1.4 Hz), 6.67 (d, 1H, *J* = 8.6 Hz), 6.77–6.87 (m, 1H), 7.38 (dd, 1H, *J* = 8.5, 2.3 Hz), 7.70 (d, 1H, *J* = 2.3 Hz), 9.94 (s, 1H) ppm. <sup>13</sup>C NMR (100 MHz, DMSO-d<sub>6</sub>) δ = 81.4, 115.1, 118.4, 126.9, 130.4, 134.4, 137.0, 154.6 ppm.

**3-Bromo-2-ethenylphenol (14)**

Compound **14** was prepared according to the general procedure from methyltriphenylphosphonium bromide (18.48 g; 51.7 mmol), t-BuOK (7.15 g; 63.7 mmol) and 2-bromo-5-hydroxybenzaldehyde (**13**) (4.00 g, 19.9 mmol) as yellowish solid (3.25 g; 82%). <sup>1</sup>H NMR (400 MHz, DMSO-d<sub>6</sub>) δ = 5.51 (dd, 1H, *J* = 12.0, 2.4 Hz), 6.06 (dd, 1H, *J* = 17.7, 2.4 Hz), 6.76 (dd, 1H, *J* = 17.7, 11.9 Hz), 6.86–6.91 (m, 1H), 6.98 (t, 1H, *J* = 8.0 Hz), 7.07 (dd, 1H, *J* = 8.0, 1.2 Hz), 10.18 (s, 1H) ppm. <sup>13</sup>C NMR (100 MHz, DMSO-d<sub>6</sub>) δ = 115.4, 120.9, 123.2, 123.4, 124.2, 129.1, 132.2, 157.1 ppm.

**5-Bromo-2-ethenylphenol (18)**

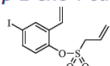
Compound **18** was prepared according to the general procedure from methyltriphenylphosphonium bromide (18.48 g; 51.7 mmol), t-BuOK (7.15 g; 63.7 mmol) and 4-bromo-2-hydroxybenzaldehyde (**17**) (4.00 g, 19.9 mmol) as yellowish solid (3.01 g; 76%)<sup>13</sup>. <sup>1</sup>H NMR (400 MHz, DMSO-d<sub>6</sub>) δ = 5.24 (dd, 1H, *J* = 11.3, 1.6 Hz), 5.79 (dd, 1H, *J* = 17.8, 1.6 Hz), 6.86 (dd, 1H, *J* = 17.8, 11.3 Hz), 6.93–6.97 (m, 1H), 7.00 (d, 1H, *J* = 2.0 Hz), 7.37 (d, 1H, *J* = 8.3 Hz), 10.13 (s, 1H) ppm. <sup>13</sup>C NMR (100 MHz, DMSO-d<sub>6</sub>) δ = 114.6, 118.3, 120.8, 122.0, 123.5, 128.0, 130.8, 155.7 ppm.

**2-Bromo-6-ethenylphenol (27)**

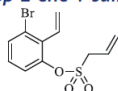
Compound **27** was prepared according to the general procedure from methyltriphenylphosphonium bromide (18.48 g; 51.7 mmol), t-BuOK (7.15 g; 63.7 mmol) and 3-bromo-2-hydroxybenzaldehyde (**26**) (4.00 g, 19.9 mmol) as yellowish solid (3.17 g; 80%)<sup>14</sup>. <sup>1</sup>H NMR (400 MHz, DMSO-d<sub>6</sub>) δ = 5.29 (dd, 1H, *J* = 11.2, 1.3 Hz), 5.78 (dd, 1H, *J* = 17.6, 1.4 Hz), 6.80 (t, 1H, *J* = 7.8 Hz), 7.02 (dd, 1H, *J* = 17.6, 11.2 Hz), 7.41–7.49 (m, 2H), 9.32 (s, 1H) ppm. <sup>13</sup>C NMR (100 MHz, DMSO-d<sub>6</sub>) δ = 112.2, 115.5, 121.3, 125.4, 127.5, 131.4, 132.1, 150.7 ppm.

**General procedure for diolefine (5, 15, 19, 28) synthesis**

To a stirred solution of corresponding ethenylphenol (**3**, **14**, **18**, **27**) (1 eq) in CH<sub>2</sub>Cl<sub>2</sub> (10 mL/1 mmol corresponding ethenylphenol) at 0 °C was added prop-2-ene-1-sulphonyl chloride (**4**) (1.39 eq) and Et<sub>3</sub>N (1.4 eq). Reaction mixture was stirred overnight (20 h) at room temperature. Water (30 mL) was added, reaction mixture was extracted with EtOAc (3 × 40 mL), combined organic extracts were washed with brine (2 × 40 mL), and dried over Na<sub>2</sub>SO<sub>4</sub>, filtered and concentrated. The crude product was purified by column chromatography on silica gel (EtOAc/PE 1:4).

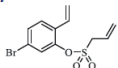
**4-Iodo-2-ethenylphenyl prop-2-ene-1-sulfonate (5)**

Compound **5** was prepared according to the general procedure from 4-iodo-2-ethenylphenol (**3**) (2.00 g; 8.13 mmol), prop-2-ene-1-sulphonyl chloride (**4**) (1.11 mL; 10.57 mmol) and  $\text{NEt}_3$  (1.58 mL; 11.38 mmol) as yellowish oil (2.36 g; 83%). IR (film,  $\text{cm}^{-1}$ )  $\nu_{\text{max}} = 1373$  (S=O), 1160 (S=O).  $^1\text{H}$  NMR (400 MHz,  $\text{DMSO-d}_6$ )  $\delta = 4.46\text{--}4.50$  (m, 2H), 5.44–5.55 (m, 2H), 5.56–5.63 (m, 1H), 5.85–5.97 (m, 1H), 6.02 (d, 1H,  $J = 17.6$  Hz), 6.84 (dd, 1H,  $J = 17.8$ , 11.2 Hz), 7.15 (d, 1H,  $J = 8.6$  Hz), 7.72 (dd, 1H,  $J = 8.6$ , 2.2 Hz), 8.10 (d, 1H,  $J = 2.2$  Hz) ppm.  $^{13}\text{C}$  NMR (100 MHz,  $\text{DMSO-d}_6$ )  $\delta = 54.9$ , 93.0, 119.0, 124.6, 125.0, 125.3, 128.4, 133.1, 134.9, 137.9, 145.7 ppm. HRMS (ESI)  $[\text{M} + \text{H}]^+$ :  $m/z$  calcd for  $\text{C}_{11}\text{H}_{12}\text{O}_3\text{SI}$ : 350.9552. Found 350.9542.

**3-Bromo-2-vinylphenyl prop-2-ene-1-sulfonate (15)**

Compound **15** was prepared according to the general procedure from 3-bromo-2-ethenylphenol (**14**) (2.00 g; 10.05 mmol), prop-2-ene-1-sulphonyl chloride (**4**) (1.37 mL; 13.06 mmol) and  $\text{NEt}_3$  (1.96 mL; 14.07 mmol) as yellowish oil (2.01 g; 66%). IR (film,  $\text{cm}^{-1}$ )  $\nu_{\text{max}} = 1368$  (S=O), 1174 (S=O), 1160 (S=O).

$^1\text{H}$  NMR (400 MHz,  $\text{DMSO-d}_6$ )  $\delta = 4.41$  (dt, 2H,  $J = 7.2$ , 1.0 Hz), 5.49–5.53 (m, 1H), 5.55–5.61 (m, 1H), 5.69–5.76 (m, 2H), 5.83–5.94 (m, 1H), 6.63 (dd, 1H,  $J = 17.9$ , 11.7 Hz), 7.30–7.35 (m, 1H), 7.43–7.46 (m, 1H), 7.67 (dd, 1H,  $J = 8.0$ , 1.1 Hz) ppm.  $^{13}\text{C}$  NMR (100 MHz,  $\text{DMSO-d}_6$ )  $\delta = 55.4$ , 122.4, 123.5, 123.7, 124.5, 125.2, 129.8, 130.6, 131.6, 131.9, 146.9 ppm. HRMS (ESI)  $[\text{M} + \text{H}]^+$ :  $m/z$  calcd for  $\text{C}_{11}\text{H}_{12}\text{O}_3\text{SBr}$ : 302.9691. Found 302.9681.

**5-Bromo-2-vinylphenyl prop-2-ene-1-sulfonate (19)**

Compound **19** was prepared according to the general procedure from 5-bromo-2-ethenylphenol (**18**) (2.00 g; 10.05 mmol), prop-2-ene-1-sulphonyl chloride (**4**) (1.37 mL; 13.06 mmol) and  $\text{NEt}_3$  (1.96 mL; 14.07 mmol) as yellowish oil (1.65 g; 54%). IR (film,  $\text{cm}^{-1}$ )  $\nu_{\text{max}} = 1377$  (S=O), 1161 (S=O).  $^1\text{H}$  NMR (400 MHz,  $\text{DMSO-d}_6$ )  $\delta = 4.54$  (dt, 2H,  $J = 7.2$ , 1.0 Hz), 5.48 (dd, 1H,  $J = 11.2$ , 0.8 Hz), 5.52–5.56 (m, 1H), 5.58–5.64 (m, 1H), 5.86–5.98 (m, 1H), 5.99 (dd, 1H,  $J = 17.6$ , 0.9 Hz), 6.89 (dd, 1H,  $J = 17.8$ , 11.2 Hz), 7.55–7.59 (m, 2H), 7.73–7.77 (m, 1H) ppm.  $^{13}\text{C}$  NMR (100 MHz,  $\text{DMSO-d}_6$ )  $\delta = 55.1$ , 118.4, 120.8, 124.5, 125.4, 125.6, 128.1, 128.7, 130.3, 130.5, 146.1 ppm. HRMS (ESI)  $[\text{M} + \text{H}]^+$ :  $m/z$  calcd for  $\text{C}_{11}\text{H}_{12}\text{O}_3\text{SBr}$ : 302.9691. Found 302.9684.

**2-Bromo-6-vinylphenyl prop-2-ene-1-sulfonate (28)**

Compound **28** was prepared according to the general procedure from 2-bromo-6-ethenylphenol (**27**) (2.00 g; 10.05 mmol), prop-2-ene-1-sulphonyl chloride (**4**) (1.37 mL; 13.06 mmol) and  $\text{NEt}_3$  (1.96 mL; 14.07 mmol) as yellowish oil (2.62 g; 86%). IR (film,  $\text{cm}^{-1}$ )  $\nu_{\text{max}} = 1367$  (S=O), 1179 (S=O), 1165 (S=O).  $^1\text{H}$  NMR (400 MHz,  $\text{CDCl}_3$ )  $\delta = 4.31$  (dt, 2H,  $J = 7.2$ , 1.0 Hz), 5.45 (dd, 1H,  $J = 11.0$ ,

0.80 Hz), 5.57–5.65 (m, 2H), 5.81 (dd, 1H,  $J = 17.5$ , 0.8 Hz), 6.03–6.15 (m, 1H), 7.07–7.17 (m, 2H), 7.52–7.59 (m, 2H) ppm.  $^{13}\text{C}$  NMR (100 MHz,  $\text{CDCl}_3$ )  $\delta = 57.9$ , 117.7, 118.4, 123.9, 125.7, 126.0, 128.3, 130.9, 133.1, 135.1, 144.4 ppm. HRMS (ESI)  $[\text{M} + \text{H}]^+$ :  $m/z$  calcd for  $\text{C}_{11}\text{H}_{12}\text{O}_3\text{SBr}$ : 302.9691. Found 302.9681.

**General method for 3H-1,2-benzoxathiepine 2,2-dioxide halogen derivative (7, 20, 29) synthesis**

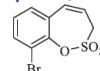
To a solution of corresponding diolefine (**5**, **15**, **19**, **28**) (1.0 eq) in dry, degassed toluene (15 mL/1 mmol corresponding diolefine) ruthenium catalyst **6** (5 mol %) was added. Reaction mixture was bubbled with argon for 5 min and sealed, stirred at 70 °C for 4 h. After cooling to r.t. it was concentrated, and the crude product was purified by column chromatography on silica gel (EtOAc/PE 1:4). Products were re-crystallised from EtOH.

**7-Iodo-3H-1,2-benzoxathiepine 2,2-dioxide (7)**

Compound **7** was prepared according to the general procedure from diolefine (**5**) (1.00 g; 2.86 mmol) and ruthenium catalyst **6** (0.14 g; 0.14 mmol) as yellowish solid (0.82 g; 89%). Mp 127–128 °C. IR (film,  $\text{cm}^{-1}$ )  $\nu_{\text{max}} = 1370$  (S=O), 1164 (S=O), 1155 (S=O).  $^1\text{H}$  NMR (400 MHz,  $\text{DMSO-d}_6$ )  $\delta = 4.52$  (dd, 2H,  $J = 5.8$ , 1.3 Hz), 5.97–6.04 (m, 1H), 6.82–6.87 (m, 1H), 7.14 (d, 1H,  $J = 8.5$  Hz), 7.79 (dd, 1H,  $J = 8.5$ , 2.2 Hz), 7.88 (d, 1H,  $J = 2.2$  Hz) ppm.  $^{13}\text{C}$  NMR (100 MHz,  $\text{DMSO-d}_6$ )  $\delta = 51.6$ , 92.3, 121.5, 124.5, 129.8, 130.4, 138.7, 139.6, 146.7 ppm. Anal. Calcd for  $\text{C}_9\text{H}_7\text{IO}_3\text{S}$ : C, 33.56; H, 2.19. Found: C, 33.55; H, 2.21.

**8-Bromo-3H-1,2-benzoxathiepine 2,2-dioxide (20)**

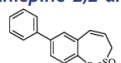
Compound **20** was prepared according to the general procedure from diolefine (**19**) (1.23 g; 4.06 mmol) and ruthenium catalyst **6** (0.19 g; 0.20 mmol) as white solid (1.0 g; 90%). Mp 144–145 °C. IR (film,  $\text{cm}^{-1}$ )  $\nu_{\text{max}} = 1359$  (S=O), 1182 (S=O), 1165 (S=O).  $^1\text{H}$  NMR (400 MHz,  $\text{DMSO-d}_6$ )  $\delta = 4.54$  (dd, 2H,  $J = 5.8$ , 1.0 Hz), 5.95–6.05 (m, 1H), 6.87 (d, 1H,  $J = 11.4$  Hz), 7.42–7.47 (m, 1H), 7.58–7.66 (m, 2H) ppm.  $^{13}\text{C}$  NMR (100 MHz,  $\text{DMSO-d}_6$ )  $\delta = 51.9$ , 120.9, 122.0, 125.2, 127.5, 130.1, 130.3, 133.0, 147.1 ppm. Anal. Calcd for  $\text{C}_9\text{H}_7\text{BrO}_3\text{S}$ : C, 39.29; H, 2.56. Found: C, 39.28; H, 2.59.

**9-Bromo-3H-1,2-benzoxathiepine 2,2-dioxide (29)**

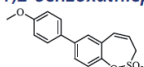
Compound **29** was prepared according to the general procedure from diolefine (**28**) (2.20 g; 7.26 mmol) and ruthenium catalyst **6** (0.34 g; 0.36 mmol) as yellowish solid (1.55 g; 78%). Mp 113–114 °C. IR (film,  $\text{cm}^{-1}$ )  $\nu_{\text{max}} = 1364$  (S=O), 1177 (S=O).  $^1\text{H}$  NMR (400 MHz,  $\text{CDCl}_3$ )  $\delta = 4.10$  (dd, 2H,  $J = 6.0$ , 1.2 Hz), 5.95–6.03 (m, 1H), 6.82–6.87 (m, 1H), 7.18 (t, 1H,  $J = 7.8$  Hz), 7.24–7.28 (m, 1H), 7.66 (dd, 1H,  $J = 7.9$ , 1.6 Hz) ppm.  $^{13}\text{C}$  NMR (100 MHz,  $\text{CDCl}_3$ )  $\delta = 51.8$ , 117.7, 120.1, 128.0, 130.0, 130.1, 132.2, 134.2, 144.9 ppm. Anal. Calcd for  $\text{C}_9\text{H}_7\text{BrO}_3\text{S}$ : C, 39.29; H, 2.56. Found: C, 39.28; H, 2.58.

**General method for 3H-1,2-benzoxathiepine 2,2-dioxide aryl derivative (8–12, 21–25 and 30–34) synthesis**

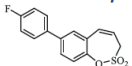
In a pressure tube corresponding 3H-1,2-benzoxathiepine 2,2-dioxide halogen derivative (**7**, **20**, **29**) (1.0 eq) was dissolved in dry toluene (6 mL/1 mmol corresponding 3H-1,2-benzoxathiepine 2,2-dioxide halogen derivative), degassed water was added (5% from toluene volume), corresponding boronic acid (1.5 eq),  $K_3PO_4$  (2.0 eq) and  $Pd(PPh_3)_4$  (0.1 eq). Reaction mixture was bubbled with argon 5 min, tube was sealed and heated for 16 h at 100 °C temperature. Reaction mixture was cooled to r.t., filtered through celite was washed with EtOAc (40 mL). Mixture was evaporated and crude product was purified by column chromatography on silica gel (EtOAc/PE 1:3). Products were re-crystallised from EtOH.

**7-Phenyl-3H-1,2-benzoxathiepine 2,2-dioxide (8)**

Compound **8** was prepared according to the general procedure from 7-iodo-3H-1,2-benzoxathiepine 2,2-dioxide (**7**) (0.20 g; 0.62 mmol) phenylboronic acid (0.11 g; 0.93 mmol),  $K_3PO_4$  (0.26 g; 1.24 mmol) and  $Pd(PPh_3)_4$  (72 mg; 0.062 mmol) as white solid (95 mg; 56%). Mp 144–145 °C. IR (film,  $cm^{-1}$ )  $\nu_{max}$ =1366 (S=O), 1363 (S=O), 1172 (S=O), 1164 (S=O).  $^1H$  NMR (400 MHz,  $CDCl_3$ )  $\delta$ =4.06 (dd, 2H,  $J$ =6.2, 0.8 Hz), 5.99–6.07 (m, 1H), 6.95 (d, 1H,  $J$ =11.0 Hz), 7.38–7.43 (m, 2H), 7.44–7.52 (m, 3H), 7.54–7.58 (m, 2H), 7.62 (dd, 1H,  $J$ =8.4, 2.2 Hz) ppm.  $^{13}C$  NMR (100 MHz,  $CDCl_3$ )  $\delta$ =51.4, 119.8, 123.3, 127.3, 128.1, 128.5, 129.1, 129.3, 129.4, 132.9, 139.4, 140.6, 147.1 ppm. Anal. Calcd for  $C_{15}H_{12}O_3S$ : C, 66.16; H, 4.44. Found: C, 66.06; H, 4.45.

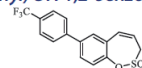
**7-(4-Methoxyphenyl)-3H-1,2-benzoxathiepine 2,2-dioxide (9)**

Compound **9** was prepared according to the general procedure from 7-iodo-3H-1,2-benzoxathiepine 2,2-dioxide (**7**) (0.20 g; 0.62 mmol) 4-methoxyphenylboronic acid (0.14 g; 0.93 mmol),  $K_3PO_4$  (0.26 g; 1.24 mmol) and  $Pd(PPh_3)_4$  (72 mg; 0.062 mmol) as yellowish solid (115 mg; 61%). Mp 162–163 °C. IR (film,  $cm^{-1}$ )  $\nu_{max}$ =1395 (S=O), 1375 (S=O), 1179 (S=O), 1156 (S=O).  $^1H$  NMR (400 MHz,  $DMSO-d_6$ )  $\delta$ =3.80 (s, 3H), 4.50 (dd, 2H,  $J$ =5.8, 1.0 Hz), 5.98–6.06 (m, 1H), 6.97 (d, 1H,  $J$ =11.2 Hz), 7.02–7.07 (m, 2H), 7.38 (d, 1H,  $J$ =8.4 Hz), 7.62–7.67 (m, 2H), 7.69 (dd, 1H,  $J$ =8.4, 2.4 Hz), 7.73 (d, 1H,  $J$ =2.4 Hz) ppm.  $^{13}C$  NMR (100 MHz,  $DMSO-d_6$ )  $\delta$ =51.6, 55.2, 114.5, 120.5, 122.7, 127.9, 128.0, 128.4, 129.0, 130.8, 131.2, 138.7, 145.8, 159.3 ppm. Anal. Calcd for  $C_{16}H_{14}O_4S$ : C, 63.56; H, 4.67. Found: C, 63.38; H, 4.68.

**7-(4-Fluorophenyl)-3H-1,2-benzoxathiepine 2,2-dioxide (10)**

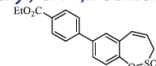
Compound **10** was prepared according to the general procedure from 7-iodo-3H-1,2-benzoxathiepine 2,2-dioxide (**7**) (0.20 g; 0.62 mmol) (4-fluorophenyl)boronic acid (0.13 g; 0.93 mmol),  $K_3PO_4$  (0.26 g; 1.24 mmol) and  $Pd(PPh_3)_4$  (72 mg; 0.062 mmol) as white solid (79 mg; 44%). Mp 117–118 °C. IR (film,  $cm^{-1}$ )  $\nu_{max}$ =1373 (S=O), 1181 (S=O), 1168 (S=O).  $^1H$  NMR (400 MHz,  $CDCl_3$ )  $\delta$ =4.06 (dd, 2H,  $J$ =6.2, 1.2 Hz), 5.99–6.06 (m, 1H), 6.93 (d, 1H,  $J$ =11.0 Hz), 7.12–7.18 (m, 2H), 7.39 (d, 1H,  $J$ =8.4 Hz), 7.45 (d, 1H,  $J$ =2.3 Hz), 7.49–7.55 (m, 2H), 7.57 (dd, 1H,  $J$ =8.4, 2.3 Hz) ppm.

$^{13}C$  NMR (100 MHz,  $CDCl_3$ )  $\delta$ =51.4, 116.1 (d,  $J$ =21.6 Hz), 119.9, 123.4, 128.6, 128.9, 129.0, 129.2, 129.3, 132.8, 135.6 (d,  $J$ =3.4 Hz), 139.6, 147.1, 163.0 (d,  $J$ =247.0 Hz) ppm. Anal. Calcd for  $C_{15}H_{11}FO_3S$ : C, 62.06; H, 3.82. Found: C, 62.34; H, 3.83.

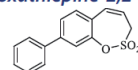
**7-(4-(Trifluoromethyl)phenyl)-3H-1,2-benzoxathiepine 2,2-dioxide (11)**

Compound **11** was prepared according to the general procedure from 7-iodo-3H-1,2-benzoxathiepine 2,2-dioxide (**7**) (0.20 g; 0.62 mmol) (4-(trifluoromethyl)phenyl)boronic acid (0.18 g; 0.93 mmol),  $K_3PO_4$  (0.26 g; 1.24 mmol) and  $Pd(PPh_3)_4$  (72 mg; 0.062 mmol) as white solid (140 mg; 66%). Mp 166–168 °C.

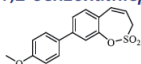
IR (film,  $cm^{-1}$ )  $\nu_{max}$ =1357 (S=O), 1332 (S=O), 1166 (S=O).  $^1H$  NMR (400 MHz,  $DMSO-d_6$ )  $\delta$ =4.56 (dd, 2H,  $J$ =5.8, 1.0 Hz), 6.00–6.08 (m, 1H), 6.99 (d, 1H,  $J$ =11.4 Hz), 7.47 (d, 1H,  $J$ =8.4 Hz), 7.81–7.86 (m, 3H), 7.88 (d, 1H,  $J$ =2.2 Hz), 7.94 (d, 2H,  $J$ =8.2 Hz) ppm.  $^{13}C$  NMR (100 MHz,  $DMSO-d_6$ )  $\delta$ =51.8, 120.8, 123.0, 124.3 (q,  $J$ =273.0 Hz), 125.9 (q,  $J$ =3.7 Hz), 127.7, 128.3 (q,  $J$ =32.0 Hz), 128.6, 128.9, 130.3, 130.8, 137.4, 142.5, 146.9 ppm. Anal. Calcd for  $C_{16}H_{11}F_3O_3S$ : C, 56.47; H, 3.26. Found: C, 56.46; H, 3.28.

**7-(4-(Ethoxycarbonyl)phenyl)-3H-1,2-benzoxathiepine 2,2-dioxide (12)**

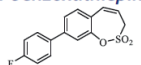
Compound **12** was prepared according to the general procedure from 7-iodo-3H-1,2-benzoxathiepine 2,2-dioxide (**7**) (0.20 g; 0.62 mmol) (4-(ethoxycarbonyl)phenyl)boronic acid (0.18 g; 0.93 mmol),  $K_3PO_4$  (0.26 g; 1.24 mmol) and  $Pd(PPh_3)_4$  (72 mg; 0.062 mmol) as yellowish solid (96 mg; 44%). Mp 141–142 °C. IR (film,  $cm^{-1}$ )  $\nu_{max}$ =1701 (C=O), 1380 (S=O), 1184 (S=O), 1170 (S=O).  $^1H$  NMR (400 MHz,  $DMSO-d_6$ )  $\delta$ =1.34 (t, 3H,  $J$ =7.1 Hz), 4.34 (q, 2H,  $J$ =7.1 Hz), 4.55 (dd, 2H,  $J$ =5.8, 1.2 Hz), 6.00–6.08 (m, 1H), 6.99 (d, 1H,  $J$ =11.5 Hz), 7.46 (d, 1H,  $J$ =8.5 Hz), 7.83 (dd, 1H,  $J$ =8.5, 2.3 Hz), 7.85–7.90 (m, 3H), 8.03–8.08 (m, 2H) ppm.  $^{13}C$  NMR (100 MHz,  $DMSO-d_6$ )  $\delta$ =14.2, 51.7, 60.8, 120.8, 123.0, 127.1, 128.6, 128.8, 129.2, 129.8, 130.1, 130.8, 137.7, 142.9, 146.9, 165.4 ppm. Anal. Calcd for  $C_{18}H_{16}O_5S$ : C, 62.78; H, 4.68. Found: C, 62.76; H, 4.71.

**8-Phenyl-3H-1,2-benzoxathiepine 2,2-dioxide (21)**

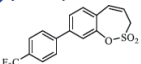
Compound **21** was prepared according to the general procedure from 8-bromo-3H-1,2-benzoxathiepine 2,2-dioxide (**20**) (0.25 g; 0.91 mmol) phenylboronic acid (0.17 g; 1.36 mmol),  $K_3PO_4$  (0.39 g; 1.82 mmol) and  $Pd(PPh_3)_4$  (105 mg; 0.091 mmol) as yellowish solid (109 mg; 44%). Mp 103–104 °C. IR (film,  $cm^{-1}$ )  $\nu_{max}$ =1376 (S=O), 1177 (S=O).  $^1H$  NMR (400 MHz,  $CDCl_3$ )  $\delta$ =4.08 (dd, 2H,  $J$ =6.1, 1.2 Hz), 5.94–6.01 (m, 1H), 6.88–6.93 (m, 1H), 7.36–7.43 (m, 2H), 7.44–7.50 (m, 2H), 7.55–7.63 (m, 4H) ppm.  $^{13}C$  NMR (100 MHz,  $CDCl_3$ )  $\delta$ =51.6, 119.2, 121.3, 125.7, 126.8, 127.2, 128.5, 129.2, 131.3, 132.5, 138.9, 144.0, 148.1 ppm. Anal. Calcd for  $C_{15}H_{12}O_3S$ : C, 66.16; H, 4.44. Found: C, 66.15; H, 4.46.

**8-(4-Methoxyphenyl)-3H-1,2-benzoxathiepine 2,2-dioxide (22)**

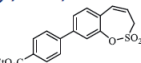
Compound **22** was prepared according to the general procedure from 8-bromo-3H-1,2-benzoxathiepine 2,2-dioxide (**20**) (0.25 g; 0.91 mmol) 4-methoxyphenylboronic acid (0.21 g; 1.36 mmol),  $K_3PO_4$  (0.39 g; 1.82 mmol) and  $Pd(PPh_3)_4$  (105 mg; 0.091 mmol) as yellowish solid (121 mg; 44%). Mp 142–143 °C. IR (film,  $cm^{-1}$ )  $\nu_{max}$  = 1369 (S=O), 1177 (S=O), 1164 (S=O).  $^1H$  NMR (400 MHz,  $CDCl_3$ )  $\delta$  = 3.86 (s, 3H), 4.07 (dd, 2H,  $J$  = 6.1, 1.1 Hz), 5.92–5.99 (m, 1H), 6.88 (d, 1H,  $J$  = 11.1 Hz), 6.97–7.02 (m, 2H), 7.32–7.36 (m, 1H), 7.50–7.58 (m, 4H) ppm.  $^{13}C$  NMR (100 MHz,  $CDCl_3$ )  $\delta$  = 51.6, 55.5, 114.6, 118.8, 120.6, 125.2, 126.1, 128.3, 131.3, 132.6, 143.6, 148.2, 160.1 ppm. Anal. Calcd for  $C_{16}H_{14}O_4S$ : C, 63.56; H, 4.67. Found: C, 63.20; H, 4.69.

**8-(4-Fluorophenyl)-3H-1,2-benzoxathiepine 2,2-dioxide (23)**

Compound **23** was prepared according to the general procedure from 8-bromo-3H-1,2-benzoxathiepine 2,2-dioxide (**20**) (0.25 g; 0.91 mmol) (4-fluorophenyl)boronic acid (0.19 g; 1.36 mmol),  $K_3PO_4$  (0.39 g; 1.82 mmol) and  $Pd(PPh_3)_4$  (105 mg; 0.091 mmol) as white solid (108 mg; 41%). Mp 111–112 °C. IR (film,  $cm^{-1}$ )  $\nu_{max}$  = 1371 (S=O), 1168 (S=O).  $^1H$  NMR (400 MHz,  $CDCl_3$ )  $\delta$  = 4.08 (dd, 2H,  $J$  = 6.1, 1.2 Hz), 5.94–6.01 (m, 1H), 6.90 (d, 1H,  $J$  = 11.0 Hz), 7.12–7.19 (m, 2H), 7.35–7.40 (m, 1H), 7.50–7.53 (m, 2H), 7.54–7.60 (m, 2H) ppm.  $^{13}C$  NMR (100 MHz,  $CDCl_3$ )  $\delta$  = 51.7, 116.2 (d,  $J$  = 21.6 Hz), 119.3, 121.2, 125.6, 126.9, 128.9, 129.0, 131.5, 132.4, 135.0 (d,  $J$  = 3.3 Hz), 142.9, 148.1, 163.2 (d,  $J$  = 248.0 Hz) ppm. Anal. Calcd for  $C_{15}H_{11}FO_3S$ : C, 62.06; H, 3.82. Found: C, 62.04; H, 3.86.

**8-(4-(Trifluoromethyl)phenyl)-3H-1,2-benzoxathiepine 2,2-dioxide (24)**

Compound **24** was prepared according to the general procedure from 8-bromo-3H-1,2-benzoxathiepine 2,2-dioxide (**20**) (0.25 g; 0.91 mmol) (4-(trifluoromethyl)phenyl)boronic acid (0.26 g; 1.36 mmol),  $K_3PO_4$  (0.39 g; 1.82 mmol) and  $Pd(PPh_3)_4$  (105 mg; 0.091 mmol) as white solid (142 mg; 46%). Mp 121–122 °C. IR (film,  $cm^{-1}$ )  $\nu_{max}$  = 1366 (S=O), 1324 (S=O), 1172 (S=O).  $^1H$  NMR (400 MHz,  $CDCl_3$ )  $\delta$  = 51.8, 119.7, 121.6, 124.2 (q,  $J$  = 273.0 Hz), 125.9, 126.2 (q,  $J$  = 3.8 Hz), 127.6, 127.8, 130.5 (q,  $J$  = 32.9 Hz), 131.7, 132.2, 142.3, 142.4, 148.1 ppm. Anal. Calcd for  $C_{16}H_{11}F_3O_3S$ : C, 56.47; H, 3.26. Found: C, 56.23; H, 3.23.

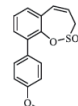
**8-(4-(Ethoxycarbonyl)phenyl)-3H-1,2-benzoxathiepine 2,2-dioxide (25)**

Compound **25** was prepared according to the general procedure from 8-bromo-3H-1,2-benzoxathiepine 2,2-dioxide (**20**) (0.25 g; 0.91 mmol) (4-(ethoxycarbonyl)phenyl)boronic acid (0.26 g; 1.36 mmol),  $K_3PO_4$  (0.39 g; 1.82 mmol) and  $Pd(PPh_3)_4$  (105 mg; 0.091 mmol) as white solid (119 mg; 38%). Mp 151–152 °C. IR (film,  $cm^{-1}$ )  $\nu_{max}$  = 1703 (C=O), 1366 (S=O), 1175 (S=O).  $^1H$  NMR (400 MHz,  $CDCl_3$ )  $\delta$  = 1.42 (t, 3H,  $J$  = 7.1 Hz), 4.10 (dd, 2H,  $J$  = 6.1,

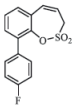
1.2 Hz), 4.41 (q, 2H,  $J$  = 7.1 Hz), 5.96–6.03 (m, 1H), 6.90 (d, 1H,  $J$  = 11.2 Hz), 7.39–7.43 (m, 1H), 7.57–7.62 (m, 2H), 7.65–7.70 (m, 2H), 8.11–8.16 (m, 2H) ppm.  $^{13}C$  NMR (100 MHz,  $CDCl_3$ )  $\delta$  = 14.5, 51.7, 61.3, 119.6, 121.5, 125.9, 127.1, 127.7, 130.4, 131.6, 132.3, 142.7, 143.0, 148.1, 166.3 ppm. Anal. Calcd for  $C_{18}H_{16}O_5S$ : C, 62.78; H, 4.68. Found: C, 62.50; H, 4.70.

**9-Phenyl-3H-1,2-benzoxathiepine 2,2-dioxide (30)**

Compound **30** was prepared according to the general procedure from 9-bromo-3H-1,2-benzoxathiepine 2,2-dioxide (**29**) (0.25 g; 0.91 mmol) phenylboronic acid (0.17 g; 1.36 mmol),  $K_3PO_4$  (0.39 g; 1.82 mmol) and  $Pd(PPh_3)_4$  (105 mg; 0.091 mmol) as white solid (104 mg; 42%). Mp 135–136 °C. IR (film,  $cm^{-1}$ )  $\nu_{max}$  = 1370 (S=O), 1162 (S=O).  $^1H$  NMR (400 MHz,  $CDCl_3$ )  $\delta$  = 4.08 (dd, 2H,  $J$  = 5.8, 1.3 Hz), 5.87–5.94 (m, 1H), 6.85–6.90 (m, 1H), 7.29 (dd, 1H,  $J$  = 7.6, 1.8 Hz), 7.35–7.42 (m, 2H), 7.43–7.49 (m, 3H), 7.51–7.55 (m, 2H) ppm.  $^{13}C$  NMR (100 MHz,  $CDCl_3$ )  $\delta$  = 52.1, 118.9, 127.1, 128.1, 128.5, 128.6, 129.6, 130.5, 132.1, 132.5, 136.3, 136.5, 144.7 ppm. Anal. Calcd for  $C_{15}H_{12}O_3S$ : C, 66.16; H, 4.44. Found: C, 66.15; H, 4.46.

**9-(4-Methoxyphenyl)-3H-1,2-benzoxathiepine 2,2-dioxide (31)**

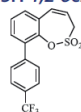
Compound **31** was prepared according to the general procedure from 9-bromo-3H-1,2-benzoxathiepine 2,2-dioxide (**29**) (0.25 g; 0.91 mmol) 4-methoxyphenylboronic acid (0.21 g; 1.36 mmol),  $K_3PO_4$  (0.39 g; 1.82 mmol) and  $Pd(PPh_3)_4$  (105 mg; 0.091 mmol) as white solid (110 mg; 40%). Mp 113–114 °C. IR (film,  $cm^{-1}$ )  $\nu_{max}$  = 1369 (S=O), 1181 (S=O), 1154 (S=O).  $^1H$  NMR (400 MHz,  $CDCl_3$ )  $\delta$  = 3.85 (s, 3H), 4.08 (dd, 2H,  $J$  = 5.8, 1.3 Hz), 5.86–5.94 (m, 1H), 6.84–6.89 (m, 1H), 6.97–7.02 (m, 2H), 7.23–7.27 (m, 1H), 7.34 (t, 1H,  $J$  = 7.6 Hz), 7.42 (dd, 1H,  $J$  = 7.6, 1.8 Hz), 7.45–7.50 (m, 2H) ppm.  $^{13}C$  NMR (100 MHz,  $CDCl_3$ )  $\delta$  = 52.0, 55.4, 114.0, 118.9, 127.1, 128.6, 128.7, 130.1, 130.8, 132.0, 132.6, 136.2, 144.7, 159.5 ppm. Anal. Calcd for  $C_{16}H_{14}O_4S$ : C, 63.56; H, 4.67. Found: C, 63.58;

**9-(4-Fluorophenyl)-3H-1,2-benzoxathiepine 2,2-dioxide (32)**

Compound **32** was prepared according to the general procedure from 9-bromo-3H-1,2-benzoxathiepine 2,2-dioxide (**29**) (0.25 g; 0.91 mmol) (4-fluorophenyl)boronic acid (0.19 g; 1.36 mmol),  $K_3PO_4$  (0.39 g; 1.82 mmol) and  $Pd(PPh_3)_4$  (105 mg; 0.091 mmol) as white solid (103 mg; 39%). Mp 130–131 °C. IR (film,  $cm^{-1}$ )  $\nu_{max}$  = 1370 (S=O), 1154 (S=O).  $^1H$  NMR (400 MHz,  $CDCl_3$ )  $\delta$  = 4.08 (dd, 2H,  $J$  = 5.8, 1.3 Hz), 5.88–5.95 (m, 1H), 6.85–6.90 (m, 1H), 7.10–7.18 (m, 2H), 7.30 (dd, 1H,  $J$  = 7.5, 2.0 Hz), 7.37 (t, 1H,  $J$  = 7.5 Hz), 7.41 (dd, 1H,  $J$  = 7.5, 2.0 Hz), 7.47–7.53 (m, 2H) ppm.  $^{13}C$  NMR (100 MHz,  $CDCl_3$ )  $\delta$  = 52.1, 115.5 (d,  $J$  = 21.6 Hz), 119.1, 127.2, 128.7, 130.6, 131.3, 131.4, 132.0, 132.3 (d,  $J$  = 3.3 Hz), 132.5, 135.6, 144.7, 162.8

(d,  $J = 247.0$  Hz) ppm. Anal. Calcd for  $C_{15}H_{11}FO_3S$ : C, 62.06; H, 3.82. Found: C, 62.05; H, 3.84.

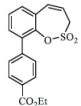
#### 9-(4-(Trifluoromethyl)phenyl)-3H-1,2-benzoxathiepine 2,2-dioxide (33)



Compound **33** was prepared according to the general procedure from 9-bromo-3H-1,2-benzoxathiepine 2,2-dioxide (**29**) (0.25 g; 0.91 mmol) 4-(trifluoromethyl)phenylboronic acid (0.26 g; 1.36 mmol),  $K_3PO_4$  (0.39 g; 1.82 mmol) and  $Pd(PPh_3)_4$  (105 mg; 0.091 mmol) as white solid (136 mg; 44%). Mp 115–116 °C.

IR (film,  $cm^{-1}$ )  $\nu_{max} = 1333$  (S=O), 1166 (S=O).  $^1H$  NMR (400 MHz,  $CDCl_3$ )  $\delta = 4.10$  (dd, 2H,  $J = 5.8, 1.3$  Hz), 5.90–5.97 (m, 1H), 6.86–6.91 (m, 1H), 7.35 (dd, 1H,  $J = 7.0, 2.6$  Hz), 7.38–7.45 (m, 2H), 7.62–7.67 (m, 2H), 7.70–7.74 (m, 2H) ppm.  $^{13}C$  NMR (100 MHz,  $CDCl_3$ )  $\delta = 52.2, 119.2, 124.5$  (q,  $J = 273.0$  Hz), 125.5 (q,  $J = 3.8$  Hz), 127.3, 128.9, 130.0, 130.2 (q,  $J = 32.0$  Hz), 131.3, 131.9, 132.3, 135.2, 140.0 (q,  $J = 1.5$  Hz), 144.6 ppm. Anal. Calcd for  $C_{16}H_{11}F_3O_3S$ : C, 56.47; H, 3.26. Found: C, 56.21; H, 3.29.

#### 9-(4-(Ethoxycarbonyl)phenyl)-3H-1,2-benzoxathiepine 2,2-dioxide (34)



Compound **34** was prepared according to the general procedure from 9-bromo-3H-1,2-benzoxathiepine 2,2-dioxide (**29**) (0.25 g; 0.91 mmol) 4-(ethoxycarbonyl)phenylboronic acid (0.26 g; 1.36 mmol),  $K_3PO_4$  (0.39 g; 1.82 mmol) and  $Pd(PPh_3)_4$  (105 mg; 0.091 mmol) as white solid (113 mg; 36%). Mp 105–106 °C.

IR (film,  $cm^{-1}$ )  $\nu_{max} = 1714$  (C=O), 1375 (S=O), 1157 (S=O).  $^1H$  NMR (400 MHz,  $CDCl_3$ )  $\delta = 1.41$  (t, 3H,  $J = 7.1$  Hz), 4.08 (dd, 2H,  $J = 5.8, 1.1$  Hz), 4.40 (q, 2H,  $J = 7.1$  Hz), 5.89–5.97 (m, 1H), 6.88 (d, 1H,  $J = 11.4$  Hz), 7.31–7.46 (m, 3H), 7.58–7.63 (m, 2H), 8.11–8.16 (m, 2H) ppm.  $^{13}C$  NMR (100 MHz,  $CDCl_3$ )  $\delta = 14.5, 52.1, 61.1, 119.2, 127.2, 128.8, 129.6, 129.7, 130.1, 131.1, 131.8, 132.4, 135.6, 140.9$ .

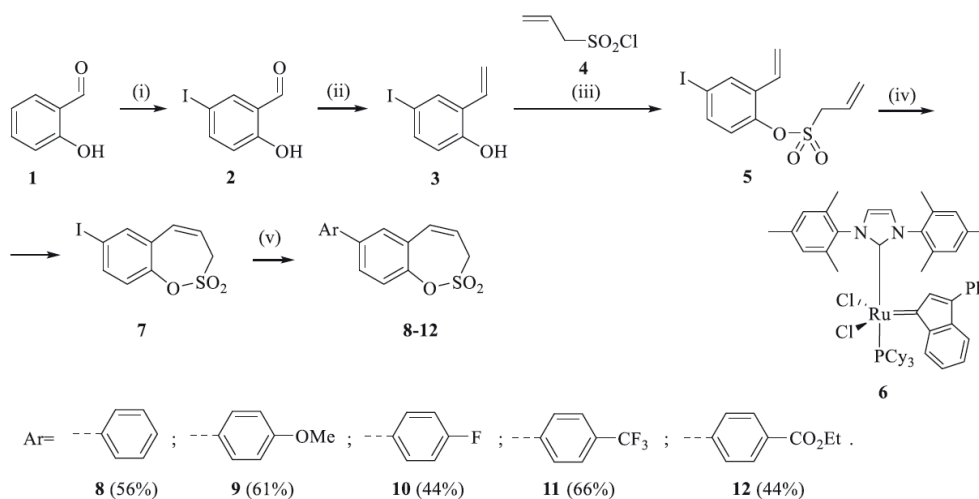
#### 2.2. CA inhibitory assay

An Applied Photophysics stopped-flow instrument has been used for assaying the CA catalysed  $CO_2$  hydration activity<sup>15</sup>. Phenol red (at a concentration of 0.2 mM) was used as indicator, working at the absorbance maximum of 557 nm, with 20 mM Hepes (pH 7.5) as buffer and 20 mM  $Na_2SO_4$  (for maintaining constant the ionic strength), following the initial rates of the CA-catalysed  $CO_2$  hydration reaction for a period of 10–100 s. The  $CO_2$  concentrations ranged from 1.7 to 17 mM for the determination of the kinetic parameters and inhibition constants. For each inhibitor, at least six traces of the initial 5–10% of the reaction have been used for determining the initial velocity. The uncatalysed rates were determined in the same manner and subtracted from the total observed rates. Stock solutions of inhibitor (0.1 mM) were prepared in distilled–deionised water, and dilutions up to 0.01 nM were done thereafter with the assay buffer. Inhibitor and enzyme solutions were preincubated together for 6 h at room temperature prior to assay in order to allow for the formation of the E–I complex. The inhibition constants were obtained by non-linear least-squares methods using PRISM 3 and the Cheng–Prusoff equation, as reported earlier<sup>16–19</sup>, and represent the mean from at least three different determinations. All CA isoforms were recombinant ones obtained in-house as reported earlier<sup>19,20</sup>.

### 3. Results and discussion

#### 3.1. Chemistry

The synthesis of desired compounds is partly based on the strategy previously developed by our groups<sup>10</sup>. The synthesis of 7-aryl 3H-1,2-benzoxathiepine 2,2-dioxides starts with the iodination of salicylaldehyde (**1**) by iodine monochloride and corresponding iodo derivative **2** was isolated in good yield (Scheme 1)<sup>11</sup>. Under Wittig reaction conditions aldehyde **2** was converted to olefin **3**, which was treated by sulphonyl chloride **4** thus providing bis-olefin **5** in 83% yield. To obtain the key intermediate **7**, the ring closure in compound **5** was performed in olefin metathesis



Scheme 1. Reagents and conditions for the preparation of derivatives 8–12: (i) ICl, AcOH, 40 °C, 24 h, 84%; (ii) K<sub>2</sub>CO<sub>3</sub>, CH<sub>3</sub>P(C<sub>6</sub>H<sub>5</sub>)<sub>3</sub>Br, THF, RT, 18 h, 83%; (iii) NEt<sub>3</sub>, CH<sub>2</sub>Cl<sub>2</sub>, 0 °C to RT, 4 h, 83%; (iv) toluene, 70 °C, 4 h, 89%; (v) Ar-B(OH)<sub>2</sub>, Pd(PPh<sub>3</sub>)<sub>4</sub>, K<sub>3</sub>PO<sub>4</sub>, toluene/H<sub>2</sub>O, 100 °C, 16 h.

conditions, using Ru-catalyst **6**. The key intermediate **7** was reacted with a series of aryl boronic acids under Suzuki reaction conditions and the desired 7-aryl 3H-1,2-benzoxathiepine 2,2-dioxides **8–12** were isolated in acceptable yields (44–66%) (Scheme 1).

In an attempt to prepare 6-aryl 3H-1,2-benzoxathiepine 2,2-dioxides, the commercially available bromo salicylaldehyde **13** was first converted to olefin **14** under Wittig reaction conditions, followed by treatment with sulphonyl chloride **4**, thus providing bis-olefin **15** for olefin metathesis ring closure reaction (Scheme 2). Utilisation of the Ru-catalyst **6** as described above did not provide the formation of the desired key intermediate 6-bromo 3H-1,2-benzoxathiepine 2,2-dioxide (**16**) even at prolonged reaction times. By doubling catalyst **6** amount (10 mol%) only traces of compound **16** were observed after 40 h. No product formation was observed also when using Schrock and Schrock–Hoveyda Mo-catalysts. Probably olefin metathesis ring closure reaction did not take place due to sterical constraints due to the bulky Br atom at 3-position of bis-olefin **15**.

The synthesis of 8-bromo intermediate **20** was started from commercially available aldehyde **17**, when under Wittig reaction conditions olefin **18** was obtained, which was thereafter treated with sulphonyl chloride **4** and provided the bis-olefin **19** in good yield (Scheme 3). Ru-catalysed olefin metathesis afforded the key intermediate **20** which in turn, by reaction with a series of aryl boronic acids under Suzuki reaction condition, provided the desired compounds **21–25**.

The same strategy was successfully utilised for the synthesis of a series of 9-aryl 3H-1,2-benzoxathiepine 2,2-dioxides starting by

the treatment of aldehyde **26** with methyltriphenylphosphonium bromide under Wittig reaction conditions (Scheme 4). The obtained phenol **27** was reacted with sulphonyl chloride **4** and ring closure of isolated **28** was successfully performed in Ru-catalysed olefin metathesis conditions, providing bromide **29**. Further reaction of compound **9** with aryl boronic acids provided the desired derivatives **30–34** in moderate yields.

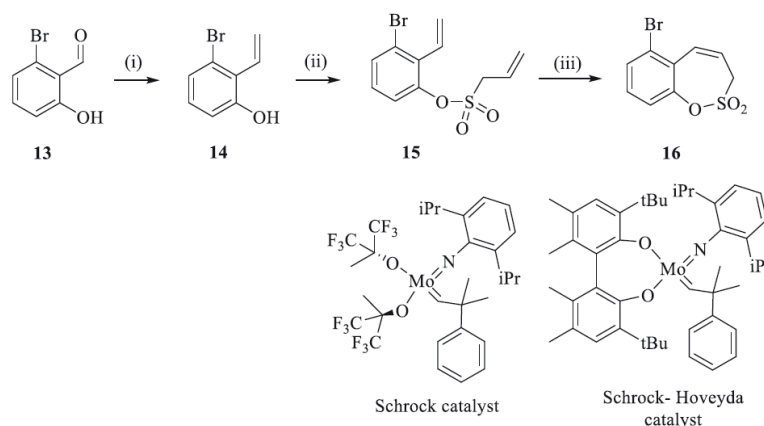
### 3.2. Carbonic anhydrase inhibition

The obtained homosulfocoumarins **7–34** were investigated for their CA inhibitory properties by using a stopped-flow CO<sub>2</sub> hydrase assay<sup>15</sup> and four human CA isoforms (hCA I, II, IX and XII) known to be drug targets<sup>1</sup> (Table 1).

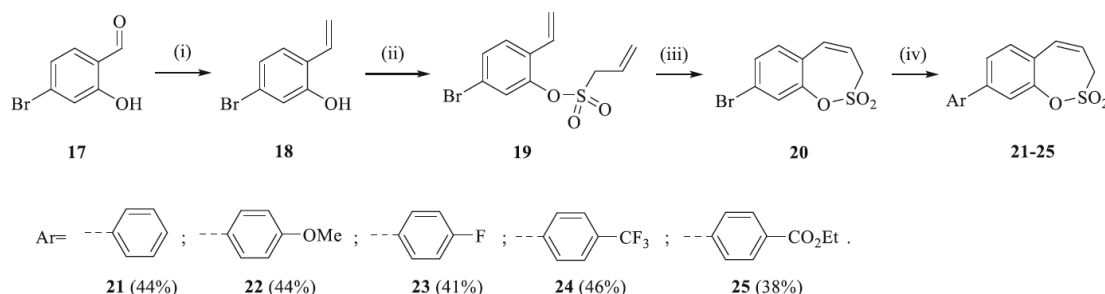
The following structure-activity relationship (SAR) can be observed from the inhibition data of Table 1.

(i) as the previously reported homosulfocoumarins<sup>10</sup> and similar to sulfocoumarins<sup>7–9</sup>, also the derivatives reported here did not significantly inhibit the cytosolic isoforms hCA I and II, unlike the sulphonamide acetazolamide (used as standard CAI), which has a very good affinity (in the nanomolar range) for hCA II and a micromolar one for hCA I (Table 1).

(ii) the transmembrane, tumour-associated isoforms hCA IX and XII were effectively inhibited by derivatives **7–29** reported here (in the low – medium nanomolar range) and were poorly inhibited, in the micromolar range by the 9-substituted-homosulfocoumarins **30–34** (K<sub>i</sub>s in the range of 16.4–60.9 μM against hCA IX and >100 μM

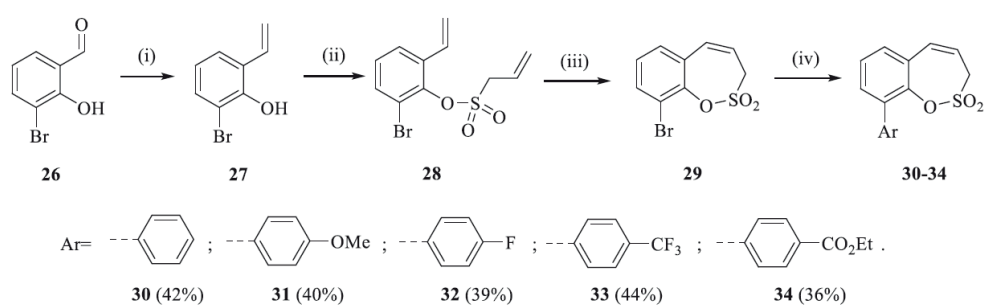


**Scheme 2.** Reagents and conditions: (i) KOtBu, CH<sub>3</sub>P(C<sub>6</sub>H<sub>5</sub>)<sub>3</sub>Br, THF, RT, 18 h, 82%; (ii) **4**, NEt<sub>3</sub>, CH<sub>2</sub>Cl<sub>2</sub>, 0 °C to RT, 4 h, 66%; (iii) a) **6** (5 mol% and 10 mol%), toluene, 70 °C, 40 h, 0%; b) Schrock catalyst [Mo] (10 mol%), toluene, 70 °C, 16 h, 0%; c) Schrock–Hoveyda [Mo] (10 mol%), toluene, 70 °C, 16 h, 0%;



**Scheme 3.** Reagents and conditions: (i) KOtBu, CH<sub>3</sub>P(C<sub>6</sub>H<sub>5</sub>)<sub>3</sub>Br, THF, RT, 18 h, 76%; (ii) **4**, NEt<sub>3</sub>, CH<sub>2</sub>Cl<sub>2</sub>, 0 °C to RT, 4 h, 54%; (iii) **6**, toluene, 70 °C, 4 h, 90%; (iv) Ar-B(OH)<sub>2</sub>, Pd(PPh<sub>3</sub>)<sub>4</sub>, K<sub>3</sub>PO<sub>4</sub>, toluene/H<sub>2</sub>O, 100 °C, 16 h.





**Scheme 4.** Reagents and conditions: (i)  $\text{KOtBu}$ ,  $\text{CH}_3\text{P}(\text{C}_6\text{H}_5)_3\text{Br}$ , THF, RT, 18 h, 80%; (ii) **4**,  $\text{NEt}_3$ ,  $\text{CH}_2\text{Cl}_2$ , 0 °C to RT, 4 h, 86%; (iii) **6**, toluene, 70 °C, 4 h, 78%; (iv)  $\text{Ar-B(OH)}_2$ ,  $\text{Pd}(\text{PPh}_3)_4$ ,  $\text{K}_3\text{PO}_4$ , toluene/ $\text{H}_2\text{O}$ , 100 °C, 16 h.

**Table 1.** Inhibition data of human CA isoforms CA I, II, IX and XII with 3H-1,2-benzoxathiepine 2,2-dioxides **7–34** using AAZ as a standard drug.

Cmpd	7 / 8 / 9	R	$K_i$ (nM)*			
			CA I	CA II	CA IX	CA XII
<b>7</b>	7	H	>100 $\mu\text{M}$	>100 $\mu\text{M}$	66.2	455.5
<b>8</b>	7	H	>100 $\mu\text{M}$	>100 $\mu\text{M}$	654.8	1376
<b>9</b>	7	$\text{OCH}_3$	>100 $\mu\text{M}$	>100 $\mu\text{M}$	407.6	2934
<b>10</b>	7	F	>100 $\mu\text{M}$	>100 $\mu\text{M}$	330.8	890.5
<b>11</b>	7	$\text{CF}_3$	>100 $\mu\text{M}$	>100 $\mu\text{M}$	221.4	4017
<b>12</b>	7	$\text{CO}_2\text{CH}_2\text{CH}_3$	>100 $\mu\text{M}$	>100 $\mu\text{M}$	620.8	2398
<b>20</b>	8	Br	>100 $\mu\text{M}$	>100 $\mu\text{M}$	47.5	132.9
<b>21</b>	8	H	>100 $\mu\text{M}$	>100 $\mu\text{M}$	104.8	473.2
<b>22</b>	8	$\text{OCH}_3$	>100 $\mu\text{M}$	>100 $\mu\text{M}$	63.1	168.6
<b>23</b>	8	F	>100 $\mu\text{M}$	>100 $\mu\text{M}$	95.2	77.9
<b>24</b>	8	$\text{CF}_3$	>100 $\mu\text{M}$	>100 $\mu\text{M}$	44.0	247.8
<b>25</b>	8	$\text{CO}_2\text{CH}_2\text{CH}_3$	>100 $\mu\text{M}$	>100 $\mu\text{M}$	79.8	289.3
<b>29</b>	9	Br	>100 $\mu\text{M}$	>100 $\mu\text{M}$	754.8	3824
<b>30</b>	9	H	>100 $\mu\text{M}$	>100 $\mu\text{M}$	21.1 $\mu\text{M}$	>100 $\mu\text{M}$
<b>31</b>	9	$\text{OCH}_3$	>100 $\mu\text{M}$	>100 $\mu\text{M}$	60.9 $\mu\text{M}$	>100 $\mu\text{M}$
<b>32</b>	9	F	>100 $\mu\text{M}$	>100 $\mu\text{M}$	33.7 $\mu\text{M}$	>100 $\mu\text{M}$
<b>33</b>	9	$\text{CF}_3$	>100 $\mu\text{M}$	>100 $\mu\text{M}$	47.1 $\mu\text{M}$	>100 $\mu\text{M}$
<b>34</b>	9	$\text{CO}_2\text{CH}_2\text{CH}_3$	>100 $\mu\text{M}$	>100 $\mu\text{M}$	16.4 $\mu\text{M}$	>100 $\mu\text{M}$
AAZ	–	–	250	12	25	5.7

\*Mean from three different assays, by a stopped flow technique (errors were in the range of  $\pm 5$ –10% of the reported values).

against hCA XII). Thus, although weak inhibitors, these sulfocoumarins are anyhow highly selective for the inhibition of hCA IX, whereas their activity against hCA I, II and XII is absent (Table 1). As already anticipated above, the most important factors associated with CA IX/XII inhibitory activity are the position and the nature of the moieties present on the six-membered ring of the homosulfocoumarin. Indeed, for 9-substituted derivatives, the presence of bulky, substituted aryls as in **30–34** leads to low activity, as mentioned above. Only the 9-bromo-derivative **29** had a medium potency inhibitory action against the two isoforms, with  $K_i$ s in the range of 754.8 – 3824 nM. On the contrary, the 8-substituted derivatives **20–25** showed a much better inhibitory power against both isoforms, being generally more potent than the corresponding 7-substituted derivatives **7–12**. Indeed, for the 7-substituted homosulfocoumarins the  $K_i$ s were in the range of 66.2 – 620.8 nM against hCA IX and of 455.5 –

2934 nM against hCA XII. On the contrary, for the 8-substituted homosulfocoumarins, the  $K_i$ s were in the range of 44.0 – 104.8 nM against hCA IX and in the range of 77.9 – 473.2 nM for hCA XII (Table 1). The 8-(4-trifluoromethyl)phenyl-substituted homosulfocoumarin **24** was the most effective hCA IX inhibitor (potency in the same range as AAZ), whereas the corresponding 4-fluorophenyl derivative **23** was the best hCA XII inhibitor in the new series of compounds investigated here but it was an order of magnitude less effective compared to acetazolamide.

#### 4. Conclusions

A new series of homosulfocoumarins (3H-1,2-benzoxathiepine 2,2-dioxides) possessing various moieties in the 7, 8 or 9 position of the heterocyclic ring were prepared by original procedures and investigated for the inhibition of four physiologically relevant CA isoforms, hCA I, II, IX and XII. The 8-substituted homosulfocoumarins were the most effective hCA IX/XII inhibitors followed by the 7-substituted derivatives, whereas the substitution pattern in position 9 led to less effective inhibitors for these transmembrane, tumour-associated isoforms. The cytosolic isoforms hCA I and II were not inhibited by these compounds, similar to the sulfocoumarins/coumarins investigated earlier. As hCA IX and XII are validated anti-tumour targets<sup>5</sup>, with one sulphonamide (SLC-0111) in Phase Ib/II clinical trials, finding derivatives with a better selectivity for inhibiting the tumour-associated isoforms over the cytosolic ones, as the homosulfocoumarins reported here, is of crucial importance.

#### Disclosure statement

No potential conflict of interest was reported by the authors.

#### Funding

This work was supported by ERA.Net RUS plus joint programme project THIOREDIN (State Education Development Agency of Republic of Latvia) [grant number RUS\_ST2017-309] and the Russian Foundation for Basic Research [grant number 18–515-76001].

#### ORCID

Claudiu T. Supuran <http://orcid.org/0000-0003-4262-0323>

## References

- (a) Supuran CT. Carbonic anhydrases: novel therapeutic applications for inhibitors and activators. *Nature Rev Drug Discov* 2008;7:168–81.(b) Alterio V, Di Fiore A, D'Ambrosio K, et al. Multiple binding modes of inhibitors to carbonic anhydrases: how to design specific drugs targeting 15 different isoforms? *Chem Rev* 2012;112:4421–68.(c) Supuran CT. Structure and function of carbonic anhydrases. *Biochem J* 2016;473:2023–32.
- (a) Xu Y, Feng L, Jeffrey PD, et al. Structure and metal exchange in the cadmium carbonic anhydrase of marine diatoms. *Nature* 2008;452:56–61.(b) Del Prete S, Vullo D, Fisher GM, et al. Discovery of a new family of carbonic anhydrases in the malaria pathogen *Plasmodium falciparum* – the  $\eta$ -carbonic anhydrases. *Bioorg Med Chem Lett* 2014;24:4389–96.(c) Jensen EL, Clement R, Kosta A, et al. A new widespread subclass of carbonic anhydrase in marine phytoplankton. *ISME J* 2019;13:2094–106.
- (a) Capasso C, Supuran CT. Anti-infective carbonic anhydrase inhibitors: a patent and literature review. *Expert Opin Ther Pat* 2013;23:693–704.(b) Capasso C, Supuran CT. An overview of the alpha-, beta- and gamma-carbonic anhydrases from bacteria: can bacterial carbonic anhydrases shed new light on evolution of bacteria? *J Enzyme Inhib Med Chem* 2015;30:325–32.(c) Capasso C, Supuran CT. Bacterial, fungal and protozoan carbonic anhydrases as drug targets. *Expert Opin Ther Targets* 2015;19:1689–704.(d) Supuran CT, Capasso C. Biomedical applications of prokaryotic carbonic anhydrases. *Expert Opin Ther Pat* 2018;28:745–54.
- (a) Supuran CT. How many carbonic anhydrase inhibition mechanisms exist? *J Enzyme Inhib Med Chem* 2016;31:345–60.(b) Nocentini A, Supuran CT. Advances in the structural annotation of human carbonic anhydrases and impact on future drug discovery. *Expert Opin Drug Discov* 2019;14:1175–97.(c) Supuran CT. Advances in structure-based drug discovery of carbonic anhydrase inhibitors. *Expert Opin Drug Discov* 2017;12:61–88.(d) De Simone G, Supuran CT. (In)organic anions as carbonic anhydrase inhibitors. *J Inorg Biochem* 2012;111:117–29.
- (a) Supuran CT. Carbonic anhydrase inhibitors as emerging agents for the treatment and imaging of hypoxic tumors. *Expert Opin Investig Drugs* 2018;27:963–70.(b) Supuran CT. Carbonic anhydrase inhibitors and their potential in a range of therapeutic areas. *Expert Opin Ther Pat* 2018;28:709–12.(c) Supuran CT. Applications of carbonic anhydrases inhibitors in renal and central nervous system diseases. *Expert Opin Ther Pat* 2018; 28:713–21.(d) Neri D, Supuran CT. Interfering with pH regulation in tumours as a therapeutic strategy. *Nat Rev Drug Discov* 2011;10:767–77.(e) Supuran CT, Alterio V, Di Fiore A, et al. Inhibition of carbonic anhydrase IX targets primary tumors, metastases, and cancer stem cells: three for the price of one. *Med Res Rev* 2018;38:1799–836.
- (a) Supuran CT. Carbonic anhydrases and metabolism. *Metabolites* 2018;8:25.(b) Supuran CT. Carbonic anhydrase inhibition and the management of hypoxic tumors. *Metabolites* 2017;7:E48.(c) Da'dara AA, Angeli A, Ferraroni M, et al. Crystal structure and chemical inhibition of essential schistosome host-interactive virulence factor carbonic anhydrase SmCA. *Commun Biol* 2019;2:333.
- Tars K, Vullo D, Kazaks A, et al. Sulfofumarins (1,2-benzoxathiine 2,2-dioxides): a class of potent and isoform-selective inhibitors of tumor-associated carbonic anhydrases. *J Med Chem* 2013;56:293–300.
- (a) Tanc M, Carta F, Bozdag M, et al. 7-Substituted-sulfofumarins are isoform-selective, potent carbonic anhydrase II inhibitors. *Bioorg Med Chem* 2013;21:4502–10.(b) Nocentini A, Ceruso M, Carta F, Supuran CT. 7-Aryl-triazolyl-substituted sulfofumarins are potent, selective inhibitors of the tumor-associated carbonic anhydrase IX and XII. *J Enzyme Inhib Med Chem* 2016;31:1226–33.(c) Grandane A, Tanc M, Mannelli LDC, et al. Substituted sulfofumarins are selective carbonic anhydrase IX and XII inhibitors with significant cytotoxicity against colorectal cancer cells. *J. Med. Chem* 2015;58:3975–83.
- (a) Maresca A, Temperini C, Vu H, et al. Non-zinc mediated inhibition of carbonic anhydrases: coumarins are a new class of suicide inhibitors. *J Am Chem Soc* 2009;131:3057–62.(b) Maresca A, Temperini C, Pochet L, et al. Deciphering the mechanism of carbonic anhydrase inhibition with coumarins and thiocoumarins. *J Med Chem* 2010;53:335–44.(c) Temperini C, Innocenti A, Scozzafava A, et al. The coumarin-binding site in carbonic anhydrase accommodates structurally diverse inhibitors: the antiepileptic lacosamide as an example. *J Med Chem* 2010;53:850–4.(d) Touisni N, Maresca A, McDonald PC, et al. Glycosylcoumarin carbonic anhydrase IX and XII inhibitors strongly attenuate the growth of primary breast tumors. *J Med Chem* 2011;54:8271–7.
- Pustenko A, Stepanovs D, Zalubovskis R, et al. 3H-1,2-benzoxathiepine 2,2-dioxides: a new class of isoform-selective carbonic anhydrase inhibitors. *J Enzyme Inhib Med Chem* 2017;32:767–75.
- Yin H, Zhang B, Yu H, et al. Two-photon fluorescent probes for biological Mg<sup>2+</sup> detection based on 7-substituted coumarin. *J Org Chem* 2015;80:4306–12.
- Gillis EP, Burke MD. A simple and modular strategy for small molecule synthesis: iterative Suzuki–Miyaura coupling of B-protected haloboronic acid building blocks. *J Am Chem Soc* 2007;129:6716–7.
- Seoane A, Casanova N, Quinones N, et al. Straightforward assembly of benzoxepines by means of a rhodium(III)-catalyzed C–H functionalization of o-vinylphenols. *J Am Chem Soc* 2014;136:834–7.
- Hoveyda HR, Marsault E, Gagnon R, et al. Optimization of the potency and pharmacokinetic properties of a macrocyclic ghrelin receptor agonist (Part I): development of ulimorelin (TZP-101) from hit to clinic. *J Med Chem* 2011;54:8305–20.
- Khalifah RG. The carbon dioxide hydration activity of carbonic anhydrase. *J Biol Chem* 1971;246:2561–73.
- (a) Nocentini A, Bua S, Del Prete S, et al. *Malassezia globosa*: activity and modeling studies. *ChemMedChem* 2018;13:816–23.(b) D'Ascenzio M, Guglielmi P, Carradori S, et al. Open saccharin-based secondary sulfonamides as potent and selective inhibitors of cancer-related carbonic anhydrase IX and XII isoforms. *J Enzyme Inhib Med Chem* 2017;32:51–9.(c) Nocentini A, Ceruso M, Bua S, et al. Discovery of  $\beta$ -adrenergic receptors blocker-carbonic anhydrase inhibitor hybrids for multitargeted antiglaucoma therapy. *J Med Chem* 2018;61:5380–94.(d) Köhler K, Hillebrecht A, Schulze Wischeler J, et al. Saccharin inhibits carbonic anhydrases: possible explanation for its unpleasant metallic aftertaste. *Angew Chem Int Ed Engl* 2007;46:7697–9.
- (a) Vermelho AB, da Silva Cardoso V, Ricci Junior E, et al. Nanoemulsions of sulfonamide carbonic anhydrase inhibitors strongly inhibit the growth of *Trypanosoma cruzi*. *J*


- Enzyme Inhib Med Chem 2018;33:139–46.(b) Nocentini A, Carta F, Tanc M, et al. Deciphering the mechanism of human carbonic anhydrases inhibition with sulfocoumarins: computational and experimental studies. *Chemistry* 2018;24:7840–4.(c) Awadallah FM, Bua S, Mahmoud WR, et al. Inhibition studies on a panel of human carbonic anhydrases with N1-substituted secondary sulfonamides incorporating thiazolinone or imidazolone-indole tails. *J Enzyme Inhib Med Chem* 2018;33:629–38.
18. (a) Bua S, Bozdog M, Del Prete S, et al. Mono- and di-thio-carbamate inhibition studies of the  $\delta$ -carbonic anhydrase TweCA $\delta$  from the marine diatom *Thalassiosira weissflogii*. *J Enzyme Inhib Med Chem* 2018;33:707–13.(b) Ferraroni M, Gaspari R, Scozzafava A, et al. Dioxygen, an unexpected carbonic anhydrase ligand. *J Enzyme Inhib Med Chem* 2018;33:999–1005.(c) El-Gazzar MG, Nafie NH, Nocentini A, et al. Carbonic anhydrase inhibition with a series of novel benzenesulfonamide-triazole conjugates. *J Enzyme Inhib Med Chem* 2018;33:1565–74.(d) Akocak S, Lolak N, Bua S, Supuran CT. Discovery of novel 1,3-diaryltriazene sulfonamides as carbonic anhydrase I, II, VII, and IX inhibitors. *J Enzyme Inhib Med Chem* 2018;33:1575–80.
19. (a) Nocentini A, Bonardi A, Gratteri P, et al. Steroids interfere with human carbonic anhydrase activity by using alternative binding mechanisms. *J Enzyme Inhib Med Chem* 2018;33:1453–9.(b) Nocentini A, Trallori E, Singh S, et al. 4-Hydroxy-3-nitro-5-ureido-benzenesulfonamides selectively target the tumor-associated carbonic anhydrase isoforms IX and XII showing hypoxia-enhanced antiproliferative profiles. *J Med Chem* 2018;61:10860–74.(c) Chohan ZH, Munawar A, Supuran CT. Transition metal ion complexes of Schiff bases. Synthesis, characterization and antibacterial properties. *Met Based Drugs* 2001;8:137–43.(d) Oztürk Sarikaya SB, Topal F, Sentürk M, et al. In vitro inhibition of  $\alpha$ -carbonic anhydrase isozymes by some phenolic compounds. *Bioorg Med Chem Lett* 2011;21:4259–62.
20. (a) Supuran CT, Clare BW. Carbonic anhydrase inhibitors. Part 57. Quantum chemical QSAR of a group of 1,3,4-thiadiazole and 1,3,4-thiadiazoline disulfonamides with carbonic anhydrase inhibitory properties. *Eur J Med Chem* 1999;34:41–50.(b) Supuran CT, Ilies MA, Scozzafava A. Carbonic anhydrase inhibitors. Part 29. Interaction of isozymes I, II and IV with benzolamide-like derivatives. *Eur J Med Chem* 1998;33:739–52.(c) Sentürk M, Gülçin I, Daştan A, et al. Carbonic anhydrase inhibitors. Inhibition of human erythrocyte isozymes I and II with a series of antioxidant phenols. *Bioorg Med Chem* 2009;17:3207–11.

Pustenko, A., Nocentini, A., Balašova, A., Krasavin, M., Žalubovskis, R., Supuran, C. T. 7-acylamino-3H-1,2-benzoxathiepine 2,2-dioxides as new isoform-selective carbonic anhydrase IX and XII inhibitors. *J. Enzyme Inhib. Med. Chem.* **2020**, *35*, 650–656.

Reprinted with permission from Taylor & Francis Group.

Copyright © 2020, Taylor & Francis Group.

## 7-Acylamino-3H-1,2-benzoxathiepine 2,2-dioxides as new isoform-selective carbonic anhydrase IX and XII inhibitors

Aleksandrs Pustenko<sup>a,b</sup>, Alessio Nocentini<sup>c</sup>, Anastasija Balašova<sup>a</sup>, Mikhail Krasavin<sup>d</sup>, Raivis Žalubovskis<sup>a,b</sup> and Claudiu T. Supuran<sup>c</sup> 

<sup>a</sup>Latvian Institute of Organic Synthesis, Riga, Latvia; <sup>b</sup>Institute of Technology of Organic Chemistry, Faculty of Materials Science and Applied Chemistry, Riga Technical University, Riga, Latvia; <sup>c</sup>Dipartimento Neurofarba, Sezione di Scienze Farmaceutiche e Nutraceutiche, Università degli Studi di Firenze, Florence, Italy; <sup>d</sup>Department of Chemistry, Saint Petersburg State University, Saint Petersburg, Russian Federation

### ABSTRACT

A series of 3H-1,2-benzoxathiepine 2,2-dioxides incorporating 7-acylamino moieties were obtained by an original procedure starting from 5-nitrosalicylaldehyde, which was treated with propenylsulfonyl chloride followed by Wittig reaction of the bis-olefin intermediate. The new derivatives, belonging to the homosulfocoumarin chemotype, were assayed as inhibitors of the zinc metalloenzyme carbonic anhydrase (CA, EC 4.2.1.1). Four pharmacologically relevant human (h) isoforms were investigated, the cytosolic hCA I and II and the transmembrane, tumour-associated hCA IX and XII. No relevant inhibition of hCA I and II was observed, whereas some of the new derivatives were effective, low nanomolar hCA IX/XII inhibitors, making them of interest for investigations in situations in which the activity of these isoforms is overexpressed, such as hypoxic tumours, arthritis or cerebral ischaemia.

### ARTICLE HISTORY

Received 26 December 2019  
Revised 21 January 2020  
Accepted 23 January 2020





### KEYWORDS

Carbonic anhydrase;  
transmembrane isoforms;  
sulfocoumarin; homosulfocoumarin; isoform-selective inhibitor

### 1. Introduction

Sulfocoumarins (1,2-benzoxathiepine 2,2-dioxides) and homosulfocoumarins (3H-1,2-benzoxathiepine 2,2-dioxides)<sup>1–5</sup> are among the most investigated new classes of carbonic anhydrase (CA, EC 4.2.1.1) inhibitors, which have been designed considering the structurally similar coumarins<sup>6–8</sup> as lead molecules. Indeed, CAs are widely spread enzymes in organisms of all types, from simple to complex ones<sup>9–15</sup>, and are involved in crucial physiological processes, among which carbon fixation in diatoms and other marine organisms in which several genetic families of such metalloenzymes were reported<sup>9</sup>. In protozoans, CAs are involved in biosynthetic reactions<sup>9</sup> whereas in bacteria, where at least three genetic families were described ( $\alpha$ -,  $\beta$ -, and  $\gamma$ -CAs) these enzymes play crucial roles related both to metabolism but also virulence and survival in various niches<sup>10</sup>. In vertebrates, including humans, a high number of different CA isoforms belonging to the  $\alpha$ -CA class were described<sup>11,12</sup>, which by hydrating CO<sub>2</sub> to a weak base (bicarbonate) and a strong acid (hydronium ions), are involved in a multitude of processes, starting with pH regulation and ending with metabolism<sup>13,14</sup>. As thus, CAs are drug targets for decades, with their inhibitors having pharmacological applications in a multitude of fields<sup>11–16</sup>. The primary sulphonamides were discovered as CA inhibitors (CAIs) in the '40s, and most of the drugs that were launched in the next decades as diuretics, antiepileptics, or anti-glaucoma agents belonged to this class of compounds or to their isosteres such as the sulfamates and sulfamides<sup>11</sup>. An important drawback of such first generation CA inhibitors (CAIs) was their lack of isoform selectivity, considering the fact that in humans at

least 12 catalytically active and three acatalytic isoforms are present<sup>11,12</sup>. However, the new generation CAIs to which coumarins and sulfocoumarins belong, show significant isoform-selective inhibition profiles, as demonstrated in a considerable number of studies<sup>1–8</sup>. This is principally due to the fact that these compounds possess a distinct inhibition mechanism compared to the sulphonamides, which coordinate to the zinc ion from the CA active site as anions<sup>11,12</sup>. In fact, coumarins and sulfocoumarins act as prodrug inhibitors, undergoing an active site mediated hydrolysis, which leads to the formation of 2-hydroxy-cinnamic acids in the case of the coumarins, and ethane-sulphonates in the case of the sulfocoumarins, which subsequently bind in different active site regions, different of those where the classical sulphonamide CAIs bind<sup>1–8</sup>. As shown by X-ray crystallography, the hydrolysed coumarins occlude the entrance of the CA active site cavity<sup>6</sup>, whereas the sulfocoumarins bind deeper within the active site, but still do not coordinate to the metal ion. Instead, the formed sulphonates anchor to the zinc-coordinated water molecule, as shown again by means of X-ray crystallographic techniques<sup>2</sup>. As these regions of the CA active site are the most variable ones, a straightforward explanation of the isoform selectivity of these new generation CAIs was furnished by using a combination of crystallographic and kinetic studies, which also allowed the development of compounds showing a higher degree of selectivity<sup>15,16</sup>. This allowed for the development of inhibitors useful for new pharmacological applications such as antitumor/antimetastatic compounds<sup>13</sup>, CAIs useful for the management of arthritis<sup>17</sup>, neuropathic pain<sup>18</sup>, and cerebral ischaemia<sup>19</sup>.

**CONTACT** Raivis Žalubovskis  raivis@osi.lv  Latvian Institute of Organic Synthesis, 21 Aizkraukles Str, Riga, LV-1006, Latvia; Claudiu T. Supuran  claudiu.supuran@unifi.it  Dipartimento Neurofarba, Sezione di Scienze Farmaceutiche e Nutraceutiche, Università degli Studi di Firenze, Sesto Fiorentino, Florence, Italy

© 2020 The Author(s). Published by Informa UK Limited, trading as Taylor & Francis Group.

This is an Open Access article distributed under the terms of the Creative Commons Attribution License (<http://creativecommons.org/licenses/by/4.0/>), which permits unrestricted use, distribution, and reproduction in any medium, provided the original work is properly cited.

Considering our interest in designing non-sulphonamide CAls with various potential applications, we report here a new series of homosulfocoumarins and their inhibitory profiles against the major human (h) CA isoforms, hCA I, II, IX, and XII, involved in many pathologies, including cancer.

## 2. Experimental part

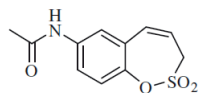
### 2.1. Chemistry

Reagents, starting materials/intermediates **1–7** and solvents were obtained from commercial sources (Sigma-Aldrich, St. Louis, MO) and used as received. Anhydrous  $\text{CH}_2\text{Cl}_2$  and toluene were obtained by passing commercially available solvents through activated alumina columns. Thin-layer chromatography was performed on silica gel, spots were visualised with UV light (254 and 365 nm). Melting points were determined on an OptiMelt automated melting point system. IR spectra were recorded on Shimadzu FTIR IR Prestige-21 spectrometer. NMR spectra were recorded on Bruker Avance Neo (400 MHz) spectrometer with chemical shifts values ( $\delta$ ) in ppm relative to TMS using the residual  $\text{DMSO-d}_6$  signal ( $^1\text{H}$  2.50;  $^{13}\text{C}$  39.52) or  $\text{CDCl}_3$  signal ( $^1\text{H}$  7.26;  $^{13}\text{C}$  77.16) as an internal standard. High-resolution mass spectra (HRMS) were recorded on a mass spectrometer with a Q-TOF micro mass analyser using the ESI technique.

#### General procedure for synthesis of acyl compound 8–17

To a solution of amino derivative **7** (1.0 eq.) in dry  $\text{CH}_2\text{Cl}_2$  (20 ml per mmol of compound **7**) at  $0^\circ\text{C}$  appropriate acyl chloride (1.1 eq.) and  $\text{Net}_3$  (1.1 eq.) were added. The resulting mixture was stirred at room temperature under an argon atmosphere for 2 h. Water was added (20 ml per mmol of compound **7**). Layers were separated, water layer was washed with  $\text{EtOAc}$  ( $2 \times 40$  ml). Combined organic layers were washed with brine, dried over anhydrous  $\text{Na}_2\text{SO}_4$ , filtered, evaporated. The crude solids were recrystallised from  $\text{EtOAc}$ /petrol ether mixture to afford product.

#### N-(2,2-Dioxido-3H-1,2-benzoxathiepin-7-yl)acetamide (8).



Compound **8a** was prepared according to the general procedure from amino derivative **7** (150 mg; 0.71 mmol), acetyl chloride (56  $\mu\text{L}$ ; 0.78 mmol) and  $\text{Et}_3\text{N}$  (110  $\mu\text{L}$ ; 0.78 mmol) as white solid (127 mg; 70%). Mp  $164\text{--}165^\circ\text{C}$ .

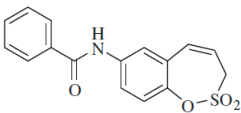
IR (film,  $\text{cm}^{-1}$ )  $\nu_{\text{max}} = 3276$  (N-H), 1670 (C=O), 1370 (S=O), 1361 (S=O), 1166 (S=O), 1162 (S=O);

$^1\text{H}$  NMR (400 MHz,  $\text{DMSO-d}_6$ )  $\delta = 2.06$  (s, 3H), 4.37–4.41 (m, 2H), 5.96–5.604 (m, 1H), 6.89 (d, 1H,  $J = 11.3$  Hz), 7.28 (d, 1H,  $J = 8.9$  Hz), 7.58 (dd, 1H,  $J = 8.9, 2.5$  Hz), 7.69 (d, 1H,  $J = 2.5$  Hz), 10.16 (s, 1H) ppm.

$^{13}\text{C}$  NMR (100 MHz,  $\text{DMSO-d}_6$ )  $\delta = 24.0, 51.0, 120.6, 120.8, 122.7, 128.4, 131.5, 138.0, 142.2, 168.6$  ppm.

HRMS (ESI)  $[\text{M} + \text{H}]^+$ :  $m/z$  calcd for ( $\text{C}_{11}\text{H}_{12}\text{NO}_4\text{S}$ ) 254.0487. Found 254.0498.

#### N-(2,2-Dioxido-3H-1,2-benzoxathiepin-7-yl)benzamide (9).



Compound **9** was prepared according to the general procedure from amino derivative **7** (150 mg; 0.71 mmol), benzoyl chloride (90  $\mu\text{L}$ ; 0.78 mmol) and

$\text{Et}_3\text{N}$  (110  $\mu\text{L}$ ; 0.78 mmol) as white solid (162 mg; 72%). Mp  $174\text{--}175^\circ\text{C}$ .

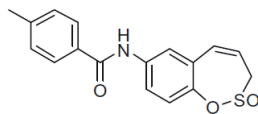
IR (film,  $\text{cm}^{-1}$ )  $\nu_{\text{max}} = 3289$  (N-H), 1652 (C=O), 1370 (S=O), 1363 (S=O), 1163 (S=O);

$^1\text{H}$  NMR (400 MHz,  $\text{DMSO-d}_6$ )  $\delta = 4.43$  (dd, 2H,  $J = 6.0, 0.9$  Hz), 5.99–6.06 (m, 1H), 6.93 (d, 1H,  $J = 11.2$  Hz), 7.35 (d, 1H,  $J = 8.8$  Hz), 7.52–7.58 (m, 2H), 7.59–7.64 (m, 1H), 7.82 (dd, 1H,  $J = 8.8, 2.5$  Hz), 7.91 (d, 1H,  $J = 2.5$  Hz), 7.94–7.99 (m, 2H), 10.46 (s, 1H) ppm.

$^{13}\text{C}$  NMR (100 MHz,  $\text{DMSO-d}_6$ )  $\delta = 51.1, 120.9, 122.0, 122.1, 122.6, 127.7, 128.3, 128.5, 131.4, 131.8, 134.6, 137.9, 142.7, 165.7$  ppm

HRMS (ESI)  $[\text{M} + \text{H}]^+$ :  $m/z$  calcd for ( $\text{C}_{16}\text{H}_{14}\text{NO}_4\text{S}$ ) 316.0644. Found 316.0654.

#### N-(2,2-Dioxido-3H-1,2-benzoxathiepin-7-yl)-4-methyl benzamide (10).



Compound **10** was prepared according to the general procedure from amino derivative **7** (150 mg; 0.71 mmol), 4-methylbenzoyl chloride (103  $\mu\text{L}$ ; 0.78 mmol) and  $\text{Et}_3\text{N}$  (110  $\mu\text{L}$ ; 0.78 mmol) as white crystals (170 mg; 73%). Mp  $197\text{--}198^\circ\text{C}$ .

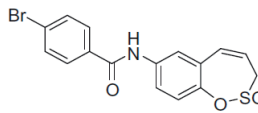
IR (film,  $\text{cm}^{-1}$ )  $\nu_{\text{max}} = 3324$  (N-H), 1646 (C=O), 1378 (S=O), 1363 (S=O), 1177 (S=O), 1169 (S=O);

$^1\text{H}$  NMR (400 MHz,  $\text{DMSO-d}_6$ )  $\delta = 2.39$  (s, 3H), 4.41–4.45 (m, 2H), 5.99–6.06 (m, 1H), 6.92 (d, 1H,  $J = 11.2$  Hz), 7.32–7.37 (m, 3H), 7.82 (dd, 1H,  $J = 8.9, 2.6$  Hz), 7.86–7.92 (m, 3H), 10.37 (s, 1H) ppm

$^{13}\text{C}$  NMR (100 MHz,  $\text{DMSO-d}_6$ )  $\delta = 21.0, 51.1, 120.8, 121.9, 122.1, 122.6, 127.7, 128.3, 129.0, 131.4, 131.6, 138.0, 141.9, 142.6, 165.5$  ppm

HRMS (ESI)  $[\text{M} + \text{H}]^+$ :  $m/z$  calcd for ( $\text{C}_{17}\text{H}_{16}\text{NO}_4\text{S}$ ) 330.0800. Found 330.0815.

#### N-(2,2-Dioxido-3H-1,2-benzoxathiepin-7-yl)-4-bromobenzamide (11).



Compound **11** was prepared according to the general procedure from amino derivative **7** (150 mg; 0.71 mmol), 4-bromobenzoyl chloride (171 mg; 0.78 mmol) and  $\text{Et}_3\text{N}$  (110  $\mu\text{L}$ ; 0.78 mmol) as white solid (166 mg; 59%). Mp  $185\text{--}186^\circ\text{C}$ .

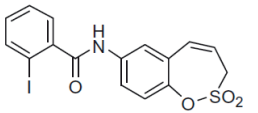
IR (film,  $\text{cm}^{-1}$ )  $\nu_{\text{max}} = 3260$  (N-H), 1653 (C=O), 1375 (S=O), 1363 (S=O), 1167 (S=O);

$^1\text{H}$  NMR (400 MHz,  $\text{DMSO-d}_6$ )  $\delta = 4.42\text{--}4.46$  (m, 2H), 5.99–6.06 (m, 1H), 6.92 (d, 1H,  $J = 11.3$  Hz), 7.35 (d, 1H,  $J = 8.8$  Hz), 7.74–7.83 (m, 3H), 7.88–7.94 (m, 3H), 10.52 (s, 1H) ppm

$^{13}\text{C}$  NMR (100 MHz,  $\text{DMSO-d}_6$ )  $\delta = 51.2, 120.9, 122.0, 122.2, 122.7, 125.6, 128.3, 129.8, 131.4, 131.5, 133.6, 137.7, 142.8, 164.7$  ppm

HRMS (ESI)  $[\text{M} + \text{H}]^+$ :  $m/z$  calcd for ( $\text{C}_{16}\text{H}_{13}\text{BrNO}_4\text{S}$ ) 393.9749. Found 393.9736.

#### N-(2,2-Dioxido-3H-1,2-benzoxathiepin-7-yl)-2-iodobenzamide (12).



Compound **12** was prepared according to the general procedure from amino derivative **7** (150 mg; 0.71 mmol), 2-iodobenzoyl chloride

(208 mg; 0.78 mmol) and  $\text{Et}_3\text{N}$  (110  $\mu\text{L}$ ; 0.78 mmol) as white solid (276 mg; 88%). Mp  $188\text{--}189^\circ\text{C}$ .

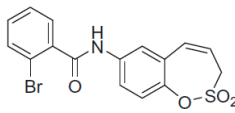
IR (film,  $\text{cm}^{-1}$ )  $\nu_{\text{max}} = 3240$  (N-H), 1641 (C=O), 1374 (S=O), 1362 (S=O), 1156 (S=O);

<sup>1</sup>H NMR (400 MHz, DMSO-d<sub>6</sub>) δ = 4.41–4.45 (m, 2H), 6.00–6.08 (m, 1H), 6.94 (d, 1H, *J* = 11.2 Hz), 7.22–7.28 (m, 1H), 7.36 (d, 1H, *J* = 8.8 Hz), 7.47–7.55 (m, 2H), 7.72 (dd, 1H, *J* = 8.8, 2.5 Hz), 7.87 (d, 1H, *J* = 2.5 Hz), 7.9–7.97 (m, 1H), 10.67 (s, 1H) ppm

<sup>13</sup>C NMR (100 MHz, DMSO-d<sub>6</sub>) δ = 51.0, 93.6, 121.0, 121.2, 121.3, 122.9, 128.1, 128.2, 128.5, 131.2, 131.5, 137.7, 139.1, 142.7, 142.8, 167.7 ppm

HRMS (ESI) [M + H]<sup>+</sup>: *m/z* calcd for (C<sub>16</sub>H<sub>13</sub>INO<sub>4</sub>S) 441.9610  
Found 441.9609.

#### N-(2,2-Dioxido-3H-1,2-benzoxathiepin-7-yl)-2-bromobenzamide (13).



Compound **13** was prepared according to the general procedure from amino derivative **7** (150 mg; 0.71 mmol), 2-bromobenzoyl chloride

(102 μL; 0.78 mmol) and Et<sub>3</sub>N (110 μL; 0.78 mmol) as white solid (230 mg; 82%). Mp 177–178 °C.

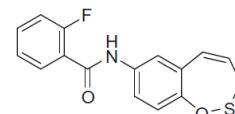
IR (film, cm<sup>-1</sup>) ν<sub>max</sub> = 3288 (N–H), 1653 (C=O), 1371 (S=O), 1176 (S=O), 1156 (S=O);

<sup>1</sup>H NMR (400 MHz, DMSO-d<sub>6</sub>) δ = 4.43 (dd, 2H, *J* = 6.0, 0.9 Hz), 6.00–6.07 (m, 1H), 6.94 (d, 1H, *J* = 11.2 Hz), 7.36 (d, 1H, *J* = 8.9 Hz), 7.41–7.47 (m, 1H), 7.51 (dt, 1H, *J* = 7.4, 1.1 Hz), 7.55–7.59 (m, 1H), 7.69–7.76 (m, 2H), 7.87 (d, 1H, *J* = 2.6 Hz), 10.73 (s, 1H) ppm

<sup>13</sup>C NMR (100 MHz, DMSO-d<sub>6</sub>) δ = 51.0, 118.9, 121.1, 121.2, 122.9, 127.8, 128.6, 128.9, 131.4, 131.5, 132.8, 137.6, 138.8, 142.8, 166.0 ppm

HRMS (ESI) [M + H]<sup>+</sup>: *m/z* calcd for (C<sub>16</sub>H<sub>13</sub>BrNO<sub>4</sub>S) 393.9749  
Found 393.9766.

#### N-(2,2-Dioxido-3H-1,2-benzoxathiepin-7-yl)-2-fluorobenzamide (14).



Compound **14** was prepared according to the general procedure from amino derivative **7** (150 mg; 0.71 mmol), 2-fluorobenzoyl chloride

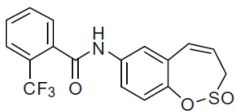
(93 μL; 0.78 mmol) and Et<sub>3</sub>N (110 μL; 0.78 mmol) as white solid (188 mg; 79%). Mp 173–174 °C.

IR (film, cm<sup>-1</sup>) ν<sub>max</sub> = 1671 (C=O), 1371 (S=O), 1365 (S=O), 1164 (S=O), 1156 (S=O);

<sup>1</sup>H NMR (400 MHz, DMSO-d<sub>6</sub>) δ = 4.41–4.45 (m, 2H), 6.00–6.07 (m, 1H), 6.93 (d, 1H, *J* = 11.2 Hz), 7.32–7.40 (m, 3H), 7.56–7.63 (m, 1H), 7.65–7.71 (m, 1H), 7.74 (dd, 1H, *J* = 8.8, 2.5 Hz), 7.86 (d, 1H, *J* = 2.5 Hz), 10.65 (s, 1H) ppm

- <sup>13</sup>C NMR (100 MHz, DMSO-d<sub>6</sub>) δ = 51.1, 116.2 (d, *J* = 21.7 Hz), 121.0, 121.4, 121.5, 122.8, 124.6 (d, *J* = 5.5 Hz), 124.7 (d, *J* = 6.3 Hz), 128.5, 129.9 (d, *J* = 2.6 Hz), 131.4, 132.8 (d, *J* = 8.5 Hz), 137.5, 142.8, 159.9 (d, *J* = 249 Hz), 163.0 ppm
- HRMS (ESI) [M + H]<sup>+</sup>: *m/z* calcd for (C<sub>16</sub>H<sub>13</sub>FNO<sub>4</sub>S) 334.0549  
Found 334.0554.

#### N-(2,2-Dioxido-3H-1,2-benzoxathiepin-7-yl)-2-(trifluoromethyl)benzamide (15).



Compound **15** was prepared according to the general procedure from amino derivative **7** (150 mg; 0.71 mmol), 2-(trifluoromethyl)benzoyl chloride (115 μL; 0.78 mmol)

and Et<sub>3</sub>N (110 μL; 0.78 mmol) as white solid (236 mg; 87%). Mp 192–193 °C.

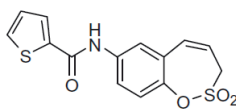
IR (film, cm<sup>-1</sup>) ν<sub>max</sub> = 3195 (N–H), 1666 (C=O), 1377 (S=O), 1316 (S=O), 1164 (S=O);

<sup>1</sup>H NMR (400 MHz, DMSO-d<sub>6</sub>) δ = 4.42–4.45 (m, 2H), 6.00–6.08 (m, 1H), 6.94 (d, 1H, *J* = 11.2 Hz), 7.36 (d, 1H, *J* = 8.8 Hz), 7.67–7.76 (m, 3H), 7.78–7.89 (m, 3H), 10.81 (s, 1H) ppm

<sup>13</sup>C NMR (100 MHz, DMSO-d<sub>6</sub>) δ = 51.0, 121.1, 121.3, 122.9, 123.8 (q, *J* = 274 Hz), 125.8 (q, *J* = 31.2 Hz), 126.4 (q, *J* = 4.6 Hz), 128.5, 128.6, 130.3, 131.4, 132.7, 135.8 (q, *J* = 2.3 Hz), 137.6, 142.8, 165.8 ppm

HRMS (ESI) [M + H]<sup>+</sup>: *m/z* calcd for (C<sub>17</sub>H<sub>13</sub>NO<sub>4</sub> F<sub>3</sub>S) 384.0517  
Found 384.0519.

#### N-(2,2-Dioxido-3H-1,2-benzoxathiepin-7-yl)thiophene-2-carboxamide (16).



Compound **16** was prepared according to the general procedure from amino derivative **7** (150 mg; 0.71 mmol), 2-thiophenecarbonyl chloride (84 μL; 0.78 mmol) and Et<sub>3</sub>N

(110 μL; 0.78 mmol) as white solid (185 mg; 81%). Mp 162–163 °C.

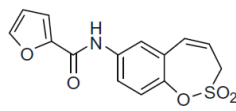
IR (film, cm<sup>-1</sup>) ν<sub>max</sub> = 3357 (N–H), 1648 (C=O), 1372 (S=O), 1356 (S=O), 1178 (S=O), 1165 (S=O);

<sup>1</sup>H NMR (400 MHz, DMSO-d<sub>6</sub>) δ = 4.44 (dd, 2H, *J* = 6.0, 1.1 Hz), 5.99–6.06 (m, 1H), 6.92 (d, 1H, *J* = 11.2 Hz), 7.23–7.26 (m, 1H), 7.35 (d, 1H, *J* = 8.8 Hz), 7.78 (dd, 1H, *J* = 8.8, 2.6 Hz), 7.84 (d, 1H, *J* = 2.6 Hz), 7.88 (dd, 1H, *J* = 5.0, 1.1 Hz), 8.04 (dd, 1H, *J* = 3.8, 1.1 Hz), 10.43 (s, 1H) ppm

<sup>13</sup>C NMR (100 MHz, DMSO-d<sub>6</sub>) δ = 51.2, 120.9, 121.9, 122.1, 122.7, 128.2, 128.4, 129.5, 131.3, 132.3, 137.5, 139.5, 142.7, 160.0 ppm

HRMS (ESI) [M + H]<sup>+</sup>: *m/z* calcd for (C<sub>14</sub>H<sub>12</sub>NO<sub>4</sub>S<sub>2</sub>) 322.0208  
Found 322.0221.

#### N-(2,2-Dioxido-3H-1,2-benzoxathiepin-7-yl)furan-2-carboxamide (17).



Compound **17** was prepared according to the general procedure from amino derivative **7** (150 mg; 0.71 mmol), 2-furoyl chloride (84 μL; 0.78 mmol) and Et<sub>3</sub>N (110 μL; 0.78 mmol) as white solid

(185 mg; 81%). Mp 162–163 °C.

IR (film, cm<sup>-1</sup>) ν<sub>max</sub> = 3299 (N–H), 1663 (C=O), 1367 (S=O), 1363 (S=O), 1165 (S=O), 1158 (S=O);

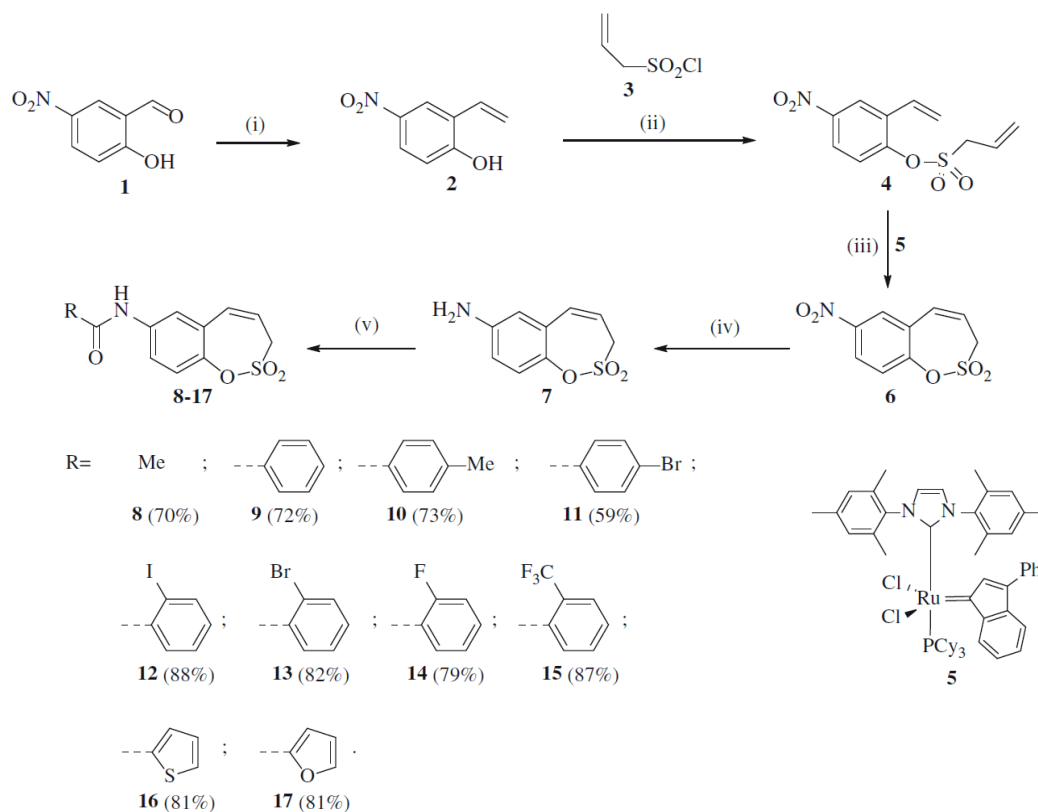
<sup>1</sup>H NMR (400 MHz, DMSO-d<sub>6</sub>) δ = 4.41–4.45 (m, 2H), 5.98–6.06 (m, 1H), 6.70–6.74 (m, 1H), 6.90 (d, 1H, *J* = 11.2 Hz), 7.32–7.38 (m, 2H), 7.80 (dd, 1H, *J* = 8.8, 2.6 Hz), 7.87 (d, 1H, *J* = 2.6 Hz), 7.95–7.97 (m, 1H), 10.41 (s, 1H) ppm

<sup>13</sup>C NMR (100 MHz, DMSO-d<sub>6</sub>) δ = 51.2, 112.3, 115.2, 120.9, 122.0, 122.2, 122.6, 128.3, 131.4, 137.3, 142.7, 146.0, 147.2, 156.3 ppm

HRMS (ESI) [M + H]<sup>+</sup>: *m/z* calcd for (C<sub>14</sub>H<sub>12</sub>NO<sub>5</sub>S) 306.0436  
Found 306.0463.

## 2.2. CA inhibitory assay

An applied photophysics stopped-flow instrument has been used for assaying the CA catalysed CO<sub>2</sub> hydration activity<sup>20</sup>. Phenol red (at a concentration of 0.2 mM) was used as indicator, working at the absorbance maximum of 557 nm, with 20 mM HEPES (pH 7.5) as buffer and 20 mM Na<sub>2</sub>SO<sub>4</sub> (for maintaining constant the ionic strength), following the initial rates of the CA-catalysed CO<sub>2</sub> hydration reaction for a period of 10–100 s. The CO<sub>2</sub> concentrations ranged from 1.7 to 17 mM for the determination of the kinetic parameters and inhibition constants. For each inhibitor, at least six traces of the initial 5–10% of the reaction have been used for



**Scheme 1.** Reagents and conditions: (i) MePPh<sub>3</sub>Br, tBuOK, THF, RT, 18 h, 65%; (ii) Net<sub>3</sub>, CH<sub>2</sub>Cl<sub>2</sub>, 0 °C to RT, 4 h, 57%; (iii) **5**, toluene, 70 °C, 4 h, 96%; (iv) Fe, AcOH, EtOH, H<sub>2</sub>O, 75 °C, 1 h, 98%; (v) RCOCl, Net<sub>3</sub>, CH<sub>2</sub>Cl<sub>2</sub>, 0 °C to RT, 4 h.

determining the initial velocity. The uncatalysed rates were determined in the same manner and subtracted from the total observed rates. Stock solutions of inhibitor (0.1 mM) were prepared in distilled–deionised water, and dilutions up to 0.01 nM were done thereafter with the assay buffer. Inhibitor and enzyme solutions were preincubated together for 6 h at room temperature prior to assay in order to allow for the formation of the E–I complex. The inhibition constants were obtained by nonlinear least-squares methods using PRISM 3 and the Cheng–Prusoff equation, as reported earlier<sup>21–23</sup>, and represent the mean from at least three different determinations. All CA isoforms were recombinant ones obtained in-house as reported earlier<sup>21,24</sup>.

### 3. Results and discussion

#### 3.1. Chemistry

Starting from the benzaldehyde derivative **1**, the synthesis of the key intermediate **7** was reported earlier by our groups<sup>1</sup>. Briefly, the synthesis of 7-amino-3H-1,2-benzoxathiepine 2,2-dioxide (**7**) was started with a Wittig reaction in which 5-nitrosalicylic aldehyde **1** was converted to the corresponding mono-olefin **2** in 65% yield (Scheme 1). Treatment of compound **2** with allyl sulphonyl chloride (**3**) provided the bisolefin **4** in 65% yield. In the next step, the olefin metathesis reaction with Ru-catalyst **5** was employed, leading to the conversion of compound **4** to 7-nitro-3H-1,2-benzoxathiepine 2,2-dioxide **6** in 96% yield. The nitro derivative **6** was thereafter reduced with iron in acidic medium to

**Table 1.** Inhibition data of human CA isoforms CA I, II, IX and XII with 3H-1,2-benzoxathiepine 2,2-dioxide **8–17** using acetazolamide (AAZ) as a standard drug.

Cmpd	R	K <sub>i</sub> (nM) <sup>a,b</sup>			
		hCA I	hCA II	hCA IX	hCA XII
<b>8</b>	CH <sub>3</sub>	>100 μM	>100 μM	61.8	162.5
<b>9</b>	C <sub>6</sub> H <sub>5</sub>	>100 μM	>100 μM	208.6	370.1
<b>10</b>	4-CH <sub>3</sub> -C <sub>6</sub> H <sub>4</sub>	>100 μM	>100 μM	83.0	309.3
<b>11</b>	4-Br-C <sub>6</sub> H <sub>4</sub>	>100 μM	>100 μM	353.3	140.7
<b>12</b>	2-I-C <sub>6</sub> H <sub>4</sub>	>100 μM	>100 μM	45.4	643.7
<b>13</b>	2-Br-C <sub>6</sub> H <sub>4</sub>	>100 μM	>100 μM	66.8	96.2
<b>14</b>	2-F-C <sub>6</sub> H <sub>4</sub>	>100 μM	>100 μM	74.6	40.3
<b>15</b>	2-CF <sub>3</sub> -C <sub>6</sub> H <sub>4</sub>	>100 μM	>100 μM	19.7	8.7
<b>16</b>	thien-2-yl	>100 μM	>100 μM	177.5	73.2
<b>17</b>	furan-2-yl	>100 μM	>100 μM	210.1	134.4
AAZ	–	250	12	25	5.7

<sup>a</sup>Mean from three different assays, by a stopped flow technique (errors were in the range of ±5–10% of the reported values).

<sup>b</sup>Incubation time 6 h.

the corresponding amine **7** in nearly quantitative yield (98%). The key intermediate **7** was subsequently reacted with a series of acyl chlorides to afford the desired compounds **8–17** in good to



excellent yields (see Experimental for details). The nature of moieties R was chosen in such a way to assure chemical diversity. Apart R=Me in compound **8**, the remaining derivatives **9–17** incorporated aromatic or heterocyclic moieties, such as phenyl, 2- or 4-substituted phenyls, thienyl and furyl. We found out in previous papers<sup>1–3</sup> that aryl or hetaryl moieties on the sulfocoumarin, homosulfocoumarin or coumarin ring<sup>6</sup> systems lead to compounds with an effective inhibition profile against CA isoforms of pharmacologic interest, such as the tumour-associated ones CA IX and XII.

### 3.2. Carbonic anhydrase inhibition

The obtained homosulfocoumarins **8–17** were investigated for their CA inhibitory properties by using a stopped-flow CO<sub>2</sub> hydrase assay<sup>20</sup> and four human CA isoforms (hCA I, II, IX, and XII) known to be drug targets<sup>1</sup> (Table 1).

As seen from data of Table 1, derivatives **8–17** did not significantly inhibit the cytosolic isoforms hCA I and II, similar to other homosulfocoumarins, sulfocoumarins or coumarins investigated earlier<sup>1–8</sup>. On the other hand, the transmembrane, tumour-associated isoforms hCA IX and XII were inhibited by all these compounds in the nanomolar range. For hCA IX the K<sub>S</sub> were in the range of 19.7–353.3 nM whereas for hCA XII in the range of 8.7–643.7 nM (Table 1). The nature of the R moiety on the carboxamide functionality greatly influenced the inhibitory power. For hCA IX/XII the optimal substitution was that present in compound **15**, 2-trifluoromethylphenyl, whereas the one leading to the least effective inhibitor was the one with 4-bromophenylcarboxamide moiety (compound **9**) for hCA IX and 2-iodophenylcarboxamide (compound **12**) for hCA XII. Overall, all these new homosulfocoumarins act as isoform IX/XII selective CAs over hCA I and II, which is highly desirable for these new chemotypes with enzyme inhibitory properties.

### 4. Conclusions

A series of 3H-1,2-benzoxathiepine 2,2-dioxides incorporating 7-acylamino moieties were obtained by an original procedure starting from 5-nitrosalicylaldehyde which was treated with propenylsulfonyl chloride followed by cyclisation through a Wittig reaction of the bis-olefin intermediate. The new derivatives, belonging to the homosulfocoumarin chemotype, were assayed as inhibitors of the zinc metalloenzyme CA. Four pharmacologically relevant human (h) isoforms were investigated, the cytosolic hCA I and II, and the transmembrane, tumour-associated hCA IX and XII. No relevant inhibition of hCA I and II was observed, whereas some of the new derivatives were effective, low nanomolar hCA IX/XII inhibitors, making them of interest for investigations in situations in which the activity of these isoforms is overexpressed, such as hypoxic tumours, arthritis or cerebral ischaemia.

### Disclosure statement

The author(s) do not declare any conflict of interest.

### Funding

This work was partly supported by ERA.Net RUS plus joint programme project THIOREDIN (State Education Development Agency of Republic of Latvia) and the Russian Foundation for

Basic Research [project grant 18–515-76001] under ERA.Net RUS plus joint programme grant RUS\_ST2017-309.

### ORCID

Claudiu T. Supuran  <http://orcid.org/0000-0003-4262-0323>

### References

- (a) Pustenko A, Stepanovs D, Žalubovskis R, et al. 3H-1,2-benzoxathiepine 2,2-dioxides: a new class of isoform-selective carbonic anhydrase inhibitors. *J Enzyme Inhib Med Chem* 2017;32:767–75.;(b) Pustenko A, Nocentini A, Balašova A, et al. Aryl derivatives of 3H-1,2-benzoxathiepine 2,2-dioxide as carbonic anhydrase inhibitors. *J Enzyme Inhib Med Chem* 2020;35:245–54.
- Tars K, Vullo D, Kazaks A, et al. Sulfocoumarins (1,2-benzoxathiine 2,2-dioxides): a class of potent and isoform-selective inhibitors of tumor-associated carbonic anhydrases. *J Med Chem* 2013;56:293–300.
- Tanc M, Carta F, Bozdag M, et al. 7-Substituted-sulfocoumarins are isoform-selective, potent carbonic anhydrase II inhibitors. *Bioorg Med Chem* 2013;21:4502–10.
- Nocentini A, Ceruso M, Carta F, Supuran CT. 7-Aryl-triazolyl-substituted sulfocoumarins are potent, selective inhibitors of the tumor-associated carbonic anhydrase IX and XII. *J Enzyme Inhib Med Chem* 2016;31:1226–33.
- Grandane A, Tanc M, Mannelli LDC, et al. Substituted sulfocoumarins are selective carbonic anhydrase IX and XII inhibitors with significant cytotoxicity against colorectal cancer cells. *J Med Chem* 2015;58:3975–83.
- (a) Maresca A, Temperini C, Vu H, et al. Non-zinc mediated inhibition of carbonic anhydrases: coumarins are a new class of suicide inhibitors. *J Am Chem Soc* 2009;131:3057–62; (b) Maresca A, Temperini C, Pochet L, et al. Deciphering the mechanism of carbonic anhydrase inhibition with coumarins and thiocoumarins. *J Med Chem* 2010;53:335–44; (c) Temperini C, Innocenti A, Scozzafava A, et al. The coumarin-binding site in carbonic anhydrase accommodates structurally diverse inhibitors: the antiepileptic lacosamide as an example. *J Med Chem* 2010;53:850–4; (d) Touisni N, Maresca A, McDonald PC, et al. Glycosylcoumarin carbonic anhydrase IX and XII inhibitors strongly attenuate the growth of primary breast tumors. *J Med Chem* 2011;54:8271–7.
- Zengin Kurt B, Sonmez F, Durdagi S, et al. Synthesis, biological activity and multiscale molecular modeling studies for coumaryl-carboxamide derivatives as selective carbonic anhydrase IX inhibitors. *J Enzyme Inhib Med Chem* 2017;32:1042–52.
- (a) Maresca A, Scozzafava A, Supuran CT. 7,8-disubstituted-but not 6,7-disubstituted coumarins selectively inhibit the transmembrane, tumor-associated carbonic anhydrase isoforms IX and XII over the cytosolic ones I and II in the low nanomolar/subnanomolar range. *Bioorg Med Chem Lett* 2010;20:7255–8; (b) Maresca A, Supuran CT. Coumarins incorporating hydroxy- and chloro-moieties selectively inhibit the transmembrane, tumor-associated carbonic anhydrase isoforms IX and XII over the cytosolic ones I and II. *Bioorg Med Chem Lett* 2010;20:4511–4.
- (a) Xu Y, Feng L, Jeffrey PD, et al. Structure and metal exchange in the cadmium carbonic anhydrase of marine

- diatoms. *Nature* 2008;452:56–61; (b) Del Prete S, Vullo D, Fisher GM, et al. Discovery of a new family of carbonic anhydrases in the malaria pathogen *Plasmodium falciparum*—the  $\eta$ -carbonic anhydrases. *Bioorg Med Chem Lett* 2014;24:4389–96; (c) Jensen EL, Clement R, Kosta A, et al. A new widespread subclass of carbonic anhydrase in marine phytoplankton. *ISME J* 2019;13:2094–106.
10. (a) Capasso C, Supuran CT. Anti-infective carbonic anhydrase inhibitors: a patent and literature review. *Expert Opin Ther Pat* 2013;23:693–704; (b) Capasso C, Supuran CT. An overview of the alpha-, beta- and gamma-carbonic anhydrases from Bacteria: can bacterial carbonic anhydrases shed new light on evolution of bacteria? *J Enzyme Inhib Med Chem* 2015;30:325–32; (c) Capasso C, Supuran CT. Bacterial, fungal and protozoan carbonic anhydrases as drug targets. *Expert Opin Ther Targets* 2015;19:1689–704; (d) Supuran CT, Capasso C. Biomedical applications of prokaryotic carbonic anhydrases. *Expert Opin Ther Pat* 2018;28:745–54; (e) Nishimori I, Minakuchi T, Morimoto K, et al. Carbonic anhydrase inhibitors: DNA cloning and inhibition studies of the alpha-carbonic anhydrase from *Helicobacter pylori*, a new target for developing sulfonamide and sulfamate gastric drugs. *J Med Chem* 2006;49:2117–26.
  11. (a) Supuran CT. Carbonic anhydrases: novel therapeutic applications for inhibitors and activators. *Nature Rev Drug Discov* 2008;7:168–81; (b) Alterio V, Di Fiore A, D'Ambrosio K, et al. Multiple binding modes of inhibitors to carbonic anhydrases: how to design specific drugs targeting 15 different isoforms? *Chem Rev* 2012;112:4421–68; (c) Supuran CT. Structure and function of carbonic anhydrases. *Biochem J* 2016;473:2023–32; (d) Innocenti A, Gülçin I, Scozzafava A, Supuran CT. Carbonic anhydrase inhibitors. Antioxidant polyphenols effectively inhibit mammalian isoforms I–XV. *Bioorg Med Chem Lett* 2010;20:5050–3.
  12. (a) Supuran CT. How many carbonic anhydrase inhibition mechanisms exist? *J Enzyme Inhib Med Chem* 2016;31:345–60; (b) Nocentini A, Supuran CT. Advances in the structural annotation of human carbonic anhydrases and impact on future drug discovery. *Expert Opin Drug Discov* 2019;14:1175–97; (c) Supuran CT. Advances in structure-based drug discovery of carbonic anhydrase inhibitors. *Expert Opin Drug Discov* 2017;12:61–88; (d) De Simone G, Supuran CT. (In)organic anions as carbonic anhydrase inhibitors. *J Inorg Biochem* 2012;111:117–29.
  13. (a) Supuran CT. Carbonic anhydrase inhibitors as emerging agents for the treatment and imaging of hypoxic tumors. *Expert Opin Investig Drugs* 2018;27:963–70; (b) Supuran CT. Carbonic anhydrase inhibitors and their potential in a range of therapeutic areas. *Expert Opin Ther Pat* 2018;28:709–12; (c) Supuran CT. Applications of carbonic anhydrases inhibitors in renal and central nervous system diseases. *Expert Opin Ther Pat* 2018;28:713–21; (d) Neri D, Supuran CT. Interfering with pH regulation in tumours as a therapeutic strategy. *Nature Rev Drug Discov* 2011;10:767–77; (e) Supuran CT, Alterio V, Di Fiore A, et al. Inhibition of carbonic anhydrase IX targets primary tumors, metastases, and cancer stem cells: three for the price of one. *Med Res Rev* 2018;38:1799–836.
  14. (a) Supuran CT. Carbonic anhydrases and metabolism. *Metabolites* 2018;8:25; (b) Supuran CT. Carbonic anhydrase inhibition and the management of hypoxic tumors. *Metabolites* 2017;7:E48; (c) Da'dara AA, Angeli A, Ferraroni M, et al. Crystal structure and chemical inhibition of essential schistosome host-interactive virulence factor carbonic anhydrase SmCA. *Commun Biol* 2019;2:333.
  15. (a) Supuran CT, Ilies MA, Scozzafava A. Carbonic anhydrase inhibitors. Part 29. Interaction of isozymes I, II and IV with benzamide-like derivatives. *Eur J Med Chem* 1998;33:739–52; (b) Köhler K, Hillebrecht A, Schulze Wischeler J, et al. Saccharin inhibits carbonic anhydrases: possible explanation for its unpleasant metallic aftertaste. *Angew Chem Int Ed Engl* 2007;46:7697–9; (c) Scozzafava A, Menabuoni L, Mincione F, et al. Carbonic anhydrase inhibitors: perfluoroalkyl/aryl-s substituted derivatives of aromatic/heterocyclic sulfonamides as topical intraocular pressure-lowering agents with prolonged duration of action. *J Med Chem* 2000;43:4542–51; (d) Sentürk M, Gülçin I, Daştan A, et al. Carbonic anhydrase inhibitors. Inhibition of human erythrocyte isozymes I and II with a series of antioxidant phenols. *Bioorg Med Chem* 2009;17:3207–11.
  16. (a) Supuran CT, Altamimi ASA, Carta F. Carbonic anhydrase inhibition and the management of glaucoma: a literature and patent review 2013–2019. *Expert Opin Ther Pat* 2019;29:781–92; (b) Supuran CT. Carbon-versus sulphur-based zinc binding groups for carbonic anhydrase inhibitors? *J Enzyme Inhib Med Chem* 2018;33:485–95; (c) Bilginer S, Gul HI, Erdal FS, et al. Synthesis, cytotoxicities, and carbonic anhydrase inhibition potential of 6-(3-aryl-2-propenyl)-2(3H)-benzoxazolones. *J Enzyme Inhib Med Chem* 2019;34:1722–9.
  17. (a) Margheri F, Ceruso M, Carta F, et al. Overexpression of the transmembrane carbonic anhydrase isoforms IX and XII in the inflamed synovium. *J Enzyme Inhib Med Chem* 2016;31:60–3; (b) Bua S, Di Cesare Mannelli L, Vullo D, et al. Design and synthesis of novel nonsteroidal anti-inflammatory drugs and carbonic anhydrase inhibitors hybrids (NSAIDs-CAIs) for the treatment of rheumatoid arthritis. *J Med Chem* 2017;60:1159–70; (c) Akgul O, Di Cesare Mannelli L, Vullo D, et al. Discovery of novel nonsteroidal anti-inflammatory drugs and carbonic anhydrase inhibitors hybrids (NSAIDs-CAIs) for the management of rheumatoid arthritis. *J Med Chem* 2018;61:4961–77.
  18. (a) Carta F, Di Cesare Mannelli L, Pinard M, et al. A class of sulfonamide carbonic anhydrase inhibitors with neuropathic pain modulating effects. *Bioorg Med Chem* 2015;23:1828–40; (b) Supuran CT. Carbonic anhydrase inhibition and the management of neuropathic pain. *Expert Rev Neurother* 2016;16:961–8.
  19. Di Cesare Mannelli L, Micheli L, Carta F, et al. Carbonic anhydrase inhibition for the management of cerebral ischemia: in vivo evaluation of sulfonamide and coumarin inhibitors. *Enzyme Inhib Med Chem* 2016;31:894–9.
  20. Khalifah RG. The carbon dioxide hydration activity of carbonic anhydrase. I. Stop-flow kinetic studies on the native human isoenzymes B and C. *J Biol Chem* 1971;246:2561–73.
  21. (a) Vermelho AB, da Silva Cardoso V, Ricci Junior E, et al. Nanoemulsions of sulfonamide carbonic anhydrase inhibitors strongly inhibit the growth of *Trypanosoma cruzi*. *J Enzyme Inhib Med Chem* 2018;33:139–46; (b) Nocentini A, Carta F, Tanc M, et al. Deciphering the mechanism of human carbonic anhydrases inhibition with sulfocoumarins: computational and experimental studies. *Chemistry* 2018;24:7840–4; (c) Awadallah FM, Bua S, Mahmoud WR, et al. Inhibition studies on a panel of human carbonic anhydrases with N1-substituted secondary sulfonamides incorporating thiazolinone or imidazolone-indole tails. *J Enzyme Inhib Med Chem* 2018;33:629–38.

22. (a) Bua S, Bozdog M, Del Prete S, et al. Mono- and di-thio-carbamate inhibition studies of the  $\delta$ -carbonic anhydrase TweCA $\delta$  from the marine diatom *Thalassiosira weissflogii*. *J Enzyme Inhib Med Chem* 2018;33:707–13; (b) Ferraroni M, Gaspari R, Scozzafava A, et al. Dioxygen, an unexpected carbonic anhydrase ligand. *J Enzyme Inhib Med Chem* 2018;33:999–1005; (c) El-Gazzar MG, Nafie NH, Nocentini A, et al. Carbonic anhydrase inhibition with a series of novel benzenesulfonamide-triazole conjugates. *J Enzyme Inhib Med Chem* 2018;33:1565–74; (d) Akocak S, Lolak N, Bua S, Supuran CT. Discovery of novel 1,3-diaryltriazene sulfonamides as carbonic anhydrase I, II, VII, and IX inhibitors. *J Enzyme Inhib Med Chem* 2018;33:1575–80.
23. (a) Nocentini A, Bonardi A, Gratteri P, et al. Steroids interfere with human carbonic anhydrase activity by using alternative binding mechanisms. *J Enzyme Inhib Med Chem* 2018;33:1453–9; (b) Nocentini A, Trallori E, Singh S, et al. 4-Hydroxy-3-nitro-5-ureido-benzenesulfonamides selectively target the tumor-associated carbonic anhydrase isoforms IX and XII showing hypoxia-enhanced antiproliferative profiles. *J Med Chem* 2018;61:10860–74; (c) Chohan ZH, Munawar A, Supuran CT. Transition metal ion complexes of Schiff bases. Synthesis, characterization and antibacterial properties. *Met Based Drugs* 2001;8:137–43; (d) Oztürk Sarikaya SB, Topal F, Sentürk M, et al. In vitro inhibition of  $\alpha$ -carbonic anhydrase isozymes by some phenolic compounds. *Bioorg Med Chem Lett* 2011;21:4259–62.
24. (a) Awadallah FM, Bua S, Mahmoud WR, et al. Inhibition studies on a panel of human carbonic anhydrases with N1-substituted secondary sulfonamides incorporating thiazolone or imidazolone-indole tails. *J Enzyme Inhib Med Chem* 2018;33:629–38; (b) Supuran CT, Clare BW. Carbonic anhydrase inhibitors. Part 57. Quantum chemical QSAR of a group of 1,3,4-thiadiazole and 1,3,4-thiadiazoline disulfonamides with carbonic anhydrase inhibitory properties. *Eur J Med Chem* 1999;34:41–50.

Pustenko, A., Nocentini, A., Gratteri, P., Bonardi, A., Vozny, I., Žalubovskis, R., Supuran, C. T. The antibiotic furagin and its derivatives are isoform-selective human carbonic anhydrase inhibitors. *J. Enzyme Inhib. Med. Chem.* **2020**, *35*, 1011–1020.

Reprinted with permission from Taylor & Francis Group.

Copyright © 2020, Taylor & Francis Group.

## The antibiotic furagin and its derivatives are isoform-selective human carbonic anhydrase inhibitors

Aleksandrs Pustenko<sup>a,b</sup>, Alessio Nocentini<sup>c,d</sup>, Paola Gratter<sup>d</sup>, Alessandro Bonardi<sup>c,d</sup>, Igor Vozny<sup>a</sup>, Raivis Žalubovskis<sup>a,b</sup> and Claudiu T. Supuran<sup>c</sup> 

<sup>a</sup>Latvian Institute of Organic Synthesis, Riga, Latvia; <sup>b</sup>Institute of Technology of Organic Chemistry, Faculty of Materials Science and Applied Chemistry, Riga Technical University, Riga, Latvia; <sup>c</sup>Department of NEUROFARBA, Section of Pharmaceutical and Nutraceutical Sciences, University of Florence, Firenze, Italy; <sup>d</sup>Department of NEUROFARBA, Section of Pharmaceutical and Nutraceutical Sciences, Laboratory of Molecular Modeling Cheminformatics & QSAR, University of Florence, Firenze, Italy

### ABSTRACT

The clinically used antibiotic Furagin and its derivatives possess inhibitory activity on human (h) carbonic anhydrases (CA, EC 4.2.1.1), some of which are highly expressed in various tissues and malignancies (hCA IX/XII). Furagin exhibited good hCA IX and XII inhibition with  $K_i$ s of 260 and 57 nM, respectively. It does not inhibit off-target CA I and poorly inhibited CA II ( $K_i = 9.6 \mu\text{M}$ ). Some synthesised Furagin derivatives with aminohydantoin moieties as zinc binding group exhibited weak inhibition of CA I/II, and good inhibition of CA IX/XII with  $K_i$ s ranging from 350 to 7400 and 150 to 5600 nM, respectively. Docking and molecular dynamics simulations suggest that selectivity for the cancer-associated CA IX/XII over CA II is due to strong H-bond interactions in CA IX/XII, involving the tail orientated towards hydrophobic area of the active site. These results suggest a possible drug repurposing of Furagin as anti-cancer agent.

### ARTICLE HISTORY

Received 6 March 2020  
Revised 31 March 2020  
Accepted 1 April 2020

### KEYWORDS

Carbonic anhydrase inhibitors; molecular dynamics; furagin; hydantoin; synthesis

### 1. Introduction

Carbonic anhydrases (CAs, EC 4.2.1.1) are ubiquitous metalloenzymes, being encoded by at least eight different genetic families, which have been found in organisms all over the phylogenetic tree<sup>1–10</sup>. CAs catalyse a crucial physiologic reaction, where by hydration of  $\text{CO}_2$  is formed a weak base (bicarbonate) and a strong acid (hydronium ions). These enzymes are involved in a multitude of physiologic processes, starting with pH regulation and ending with metabolism<sup>1–3,7–10,11–22</sup>.

CAs are also involved in various pathological processes and therefore are drug targets for decades, with their inhibitors having pharmacological applications in many fields<sup>1–3,7–19</sup>. The primary sulphonamides were discovered as CA inhibitors (CAIs) already in the 40s, and most of the drugs that were launched in the next decades as diuretics, antiepileptics, or antiglaucoma agents targeting CAs belonged to this class of compounds<sup>1–3,7–19</sup>. Although highly potent as CAIs<sup>1–3</sup>, the sulphonamides generally non-selectively inhibit most  $\alpha$ -CA isoforms present in humans and mammals in general<sup>1–3</sup> as well as CAs from the other genetic families ( $\beta$ -,  $\gamma$ -,  $\delta$ -,  $\zeta$ -,  $\eta$ -,  $\theta$ - and  $\iota$ -CAs)<sup>4–19</sup>, therefore alternative, isoform selective CAI classes were searched. A multitude of new chemotypes as well as novel CA inhibition mechanisms were reported in the last decade<sup>1–3,11–14,23–30</sup>.





That has highly enriched our understanding of these enzymes and also allowed obtaining of isoform-selective CAIs targeting physiologically relevant isoforms<sup>11–14,23–27</sup>. Among the new chemotypes, which also exhibited the highest levels of isoform


selectivity, were the coumarins<sup>27</sup>, the sulfocoumarins<sup>23–26</sup> and their congeners, homosulfocoumarins (3H-1,2-benzoxathiepine 2,2-dioxides)<sup>31</sup>, and saccharin derivatives<sup>32–34</sup>. Considering the fact that this last chemotype was somewhat chemically similar to hydantoin (imidazolidine-2,4-dione) that may serve as zinc binding group (ZBG) we investigated clinically used antibiotic **Furagin** (Figure 1), also known under names Furazidine, Furamags or Furazidin<sup>35</sup>, that contains hydantoin moiety, as well as newly prepared its derivatives.

### 2. Materials and methods

#### 2.1. Chemical syntheses – general

Reagents, starting materials and solvents were obtained from commercial sources and used as received. Thin-layer chromatography was performed on silica gel, spots were visualised with UV light (254 and 365 nm). Melting points were determined on an OptiMelt automated melting point system. IR spectra were recorded on Shimadzu FTIR IR Prestige-21 spectrometer. NMR spectra were recorded on Bruker Avance Neo (400 MHz) spectrometer with chemical shifts values ( $\delta$ ) in ppm relative to TMS using the residual DMSO- $d_6$  signal ( $^1\text{H}$  2.50;  $^{13}\text{C}$  39.52) or  $\text{CDCl}_3$  signal ( $^1\text{H}$  7.26;  $^{13}\text{C}$  77.16) as an internal standard, or  $\text{D}_2\text{O}$  signal and dioxane ( $^1\text{H}$  4.79;  $^{13}\text{C}$  67.19). High-resolution mass spectra (HRMS) were recorded on a mass spectrometer with a Q-TOF micro mass

CONTACT Raivis Žalubovskis  [raivis@osi.lv](mailto:raivis@osi.lv)  Riga Technical University, Riga, Latvia; Claudiu T. Supuran  [claudiu.supuran@unifi.it](mailto:claudiu.supuran@unifi.it)  University of Florence, Firenze, Italy

 Supplemental data for this article can be accessed [here](#).

© 2020 The Author(s). Published by Informa UK Limited, trading as Taylor & Francis Group.

This is an Open Access article distributed under the terms of the Creative Commons Attribution License (<http://creativecommons.org/licenses/by/4.0/>), which permits unrestricted use, distribution, and reproduction in any medium, provided the original work is properly cited.

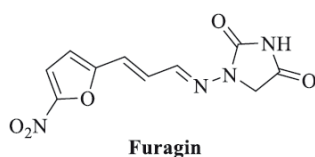


Figure 1. Structure of Furagin.

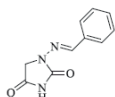
analyser using the ESI technique. Examples of spectral data are furnished in the Supporting Information to the article.

## 2.2. General procedure for compound 2–17 synthesis

To a solution of 1-aminoimidazolidine-2,4-dione hydrochloride (**1**) (1.0 eq.) in EtOH (15 ml per 1 mmol of compound **1**) appropriate aldehyde (1.05 eq.) was added. The resulting mixture was stirred at room temperature overnight.

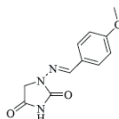
The solvent was removed under vacuum and the crude product was re-crystallized from EtOH to afford product.

### 2.2.1. 1-(Benzylideneamino)imidazolidine-2,4-dione (**2**)<sup>36</sup>



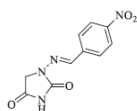
Compound **2** was prepared according to the general procedure from compound **1** (0.5 g; 3.30 mmol) and benzaldehyde (0.35 ml; 3.46 mmol) as white solid (0.60 g; 90%). Mp 252 – 253 °C. IR (film,  $\text{cm}^{-1}$ )  $\nu_{\text{max}}$  = 1778 (C=O), 1717 (C=O); <sup>1</sup>H NMR (400 MHz, DMSO-*d*<sub>6</sub>)  $\delta$  = 4.36 (s, 2H), 7.38–7.48 (m, 3H), 7.68–7.72 (m, 2H), 7.80 (s, 1H), 11.25 (s, 1H) ppm <sup>13</sup>C NMR (100 MHz, DMSO-*d*<sub>6</sub>)  $\delta$  = 48.9, 126.8, 128.8, 129.8, 134.3, 143.0, 153.4, 169.0 ppm HRMS (ESI) [M + H]<sup>+</sup>: *m/z* calcd for (C<sub>10</sub>H<sub>10</sub>N<sub>3</sub>O<sub>2</sub>) 204.0773. Found 204.0783.

### 2.2.2. 1-((4-Methoxybenzylidene)amino)imidazolidine-2,4-dione (**3**)



Compound **3** was prepared according to the general procedure from compound **1** (0.5 g; 3.30 mmol) and 4-methoxybenzaldehyde (0.42 ml; 3.46 mmol) as white solid (0.62 g; 80%). Mp 242 – 244 °C. IR (film,  $\text{cm}^{-1}$ )  $\nu_{\text{max}}$  = 1768 (C=O), 1718 (C=O); <sup>1</sup>H NMR (400 MHz, DMSO-*d*<sub>6</sub>)  $\delta$  = 3.80 (s, 3H), 4.33 (s, 2H), 6.99–7.04 (m, 2H), 7.62–7.66 (m, 2H), 7.75 (s, 1H), 11.18 (s, 1H) ppm <sup>13</sup>C NMR (100 MHz, DMSO-*d*<sub>6</sub>)  $\delta$  = 48.9, 55.3, 114.3, 126.9, 128.4, 142.9, 153.4, 160.6, 169.1 ppm HRMS (ESI) [M + H]<sup>+</sup>: *m/z* calcd for (C<sub>11</sub>H<sub>12</sub>N<sub>3</sub>O<sub>3</sub>) 234.0879. Found 234.0885.

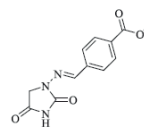
### 2.2.3. 1-((4-Nitrobenzylidene)amino)imidazolidine-2,4-dione (**4**)<sup>37</sup>



Compound **4** was prepared according to the general procedure

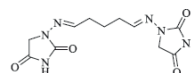
from compound **1** (0.5 g; 3.30 mmol) and 4-nitrobenzaldehyde (0.52 g; 3.46 mmol) as yellowish solid (0.68 g; 82%). Mp 280 °C dec. IR (film,  $\text{cm}^{-1}$ )  $\nu_{\text{max}}$  = 1780 (C=O), 1714 (C=O); <sup>1</sup>H NMR (400 MHz, DMSO-*d*<sub>6</sub>)  $\delta$  = 4.38 (s, 2H), 7.90–7.96 (m, 3H), 8.28–8.33 (m, 2H), 11.39 (s, 1H) ppm <sup>13</sup>C NMR (100 MHz, DMSO-*d*<sub>6</sub>)  $\delta$  = 49.1, 124.2, 127.7, 140.6, 140.7, 147.6, 153.4, 168.9 ppm HRMS (ESI) [M + H]<sup>+</sup>: *m/z* calcd for (C<sub>10</sub>H<sub>9</sub>N<sub>4</sub>O<sub>4</sub>) 249.0624. Found 249.0616.

### 2.2.4. Methyl 4-(((2,4-dioximidazolidin-1-yl)imino)methyl)benzoate (**5**)



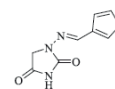
Compound **5** was prepared according to the general procedure from compound **1** (0.5 g; 3.30 mmol) and methyl 4-formylbenzoate (0.57 g; 3.46 mmol) as white solid (0.82 g; 95%). Mp 280 °C dec. IR (film,  $\text{cm}^{-1}$ )  $\nu_{\text{max}}$  = 1763 (C=O), 1717 (C=O); <sup>1</sup>H NMR (400 MHz, DMSO-*d*<sub>6</sub>)  $\delta$  = 3.86 (s, 3H), 4.37 (s, 2H), 7.80–7.87 (m, 3H), 8.00–8.05 (m, 2H), 11.33 (s, 1H) ppm <sup>13</sup>C NMR (100 MHz, DMSO-*d*<sub>6</sub>)  $\delta$  = 49.0, 52.2, 127.0, 129.7, 130.2, 138.8, 141.6, 153.4, 165.9, 168.9 ppm HRMS (ESI) [M + H]<sup>+</sup>: *m/z* calcd for (C<sub>12</sub>H<sub>12</sub>N<sub>3</sub>O<sub>4</sub>) 262.0828. Found 262.0834.

### 2.2.5. 1,1'-((Pentane-1,5-diylidene)bis(azaneylylidene))bis(imidazolidine-2,4-dione) (**6**)



Compound **6** was prepared according to the general procedure from compound **1** (0.5 g; 3.30 mmol) and glutaraldehyde 50 wt % solution in H<sub>2</sub>O (0.31 ml; 3.46 mmol) as white solid (0.49 g; 50%). Mp 237 °C dec. IR (film,  $\text{cm}^{-1}$ )  $\nu_{\text{max}}$  = 1768 (C=O), 1734 (C=O); <sup>1</sup>H NMR (400 MHz, DMSO-*d*<sub>6</sub>)  $\delta$  = 1.72 (p, 2H, *J* = 7.4 Hz), 2.28–2.36 (m, 4H), 4.17 (s, 4H), 7.06 (t, 2H, *J* = 5.2 Hz), 11.07 (s, 2H) ppm <sup>13</sup>C NMR (100 MHz, DMSO-*d*<sub>6</sub>)  $\delta$  = 23.1, 31.3, 48.5, 146.7, 153.4, 169.1 ppm HRMS (ESI) [M + Na]<sup>+</sup>: *m/z* calcd for (C<sub>11</sub>H<sub>14</sub>N<sub>6</sub>O<sub>4</sub>Na) 317.0974. Found 317.0978.

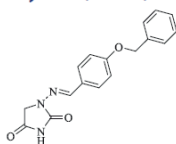
### 2.2.6. 1-((Furan-3-ylmethylene)amino)imidazolidine-2,4-dione (**7**)



Compound **7** was prepared according to the general procedure from compound **1** (0.5 g; 3.30 mmol) and 3-furaldehyde (0.33 g; 3.46 mmol) as yellowish solid (0.57 g; 89%). Mp 235 °C dec. IR (film,  $\text{cm}^{-1}$ )  $\nu_{\text{max}}$  = 1780 (C=O), 1714 (C=O);

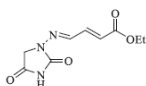
<sup>1</sup>H NMR (400 MHz, DMSO-*d*<sub>6</sub>)  $\delta$  = 4.30 (s, 2H), 6.74–6.76 (m, 1H), 7.73–7.77 (m, 2H), 8.05–8.07 (m, 1H), 11.18 (s, 1H) ppm <sup>13</sup>C NMR (100 MHz, DMSO-*d*<sub>6</sub>)  $\delta$  = 48.8, 107.0, 122.5, 136.1, 144.8, 144.9, 153.3, 169.1 ppm HRMS (ESI) [M + H]<sup>+</sup>: *m/z* calcd for (C<sub>8</sub>H<sub>8</sub>N<sub>3</sub>O<sub>3</sub>) 194.0566. Found 194.0570.

## 2.2.7. 1-((4-(Benzyloxy)benzylidene)amino)imidazolidine-2,4-dione (8)



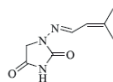
Compound **8** was prepared according to the general procedure from compound **1** (0.5 g; 3.30 mmol) and 4-benzyloxybenzaldehyde (0.73 g; 3.46 mmol) as white solid (0.92 g; 90%). Mp 258–260 °C. IR (film,  $\text{cm}^{-1}$ )  $\nu_{\text{max}}$ =1790 (C=O), 1730 (C=O);  $^1\text{H}$  NMR (400 MHz,  $\text{DMSO-d}_6$ )  $\delta$ =4.33 (s, 2H), 5.15 (s, 2H), 7.07–7.12 (m, 2H), 7.31–7.36 (m, 1H), 7.37–7.43 (m, 2H), 7.44–7.49 (m, 2H), 7.62–7.67 (m, 2H), 7.75 (s, 1H), 11.19 (s, 1H) ppm  $^{13}\text{C}$  NMR (100 MHz,  $\text{DMSO-d}_6$ )  $\delta$ =48.9, 69.4, 115.1, 127.1, 127.8, 127.9, 128.4, 128.5, 136.8, 142.8, 153.4, 159.7, 169.1 ppm HRMS (ESI)  $[\text{M} + \text{H}]^+$ :  $m/z$  calcd for ( $\text{C}_{17}\text{H}_{16}\text{N}_3\text{O}_3$ ) 310.1192. Found 310.1194.

## 2.2.8. Ethyl (2E)-4-((2,4-dioxoimidazolidin-1-yl)imino)but-2-enoate (9)



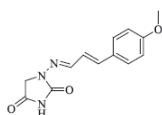
Compound **9** was prepared according to the general procedure from compound **1** (0.5 g; 3.30 mmol) and ethyl trans-4-oxo-2-butenate (0.42 ml; 3.46 mmol) as white solid (0.60 g; 81%). Mp 210–211 °C. IR (film,  $\text{cm}^{-1}$ )  $\nu_{\text{max}}$ =1772 (C=O), 1721 (C=O);  $^1\text{H}$  NMR (400 MHz,  $\text{DMSO-d}_6$ )  $\delta$ =1.24 (t, 3H,  $J=7.1$  Hz), 4.17 (q, 2H,  $J=7.1$  Hz), 4.27 (s, 2H), 7.37 (d, 1H,  $J=15.6$  Hz), 7.16–7.24 (m, 1H), 7.60 (d, 1H,  $J=9.3$  Hz), 11.39 (s, 1H) ppm  $^{13}\text{C}$  NMR (100 MHz,  $\text{DMSO-d}_6$ )  $\delta$ =14.1, 49.0, 60.4, 126.5, 140.3, 141.7, 153.2, 165.4, 168.7 ppm HRMS (ESI)  $[\text{M} + \text{H}]^+$ :  $m/z$  calcd for ( $\text{C}_9\text{H}_{12}\text{N}_3\text{O}_4$ ) 226.0828. Found 226.0834.

## 2.2.9. 1-((3-Methylbut-2-en-1-ylidene)amino)imidazolidine-2,4-dione (10)



Compound **10** was prepared according to the general procedure from compound **1** (0.5 g; 3.30 mmol) and 3-methyl-2-butenal (0.33 ml; 3.46 mmol) as white solid (0.43 g; 72%). Mp 186–187 °C. IR (film,  $\text{cm}^{-1}$ )  $\nu_{\text{max}}$ =1768 (C=O), 1717 (C=O);  $^1\text{H}$  NMR (400 MHz,  $\text{DMSO-d}_6$ )  $\delta$ =1.84–1.89 (m, 6H), 4.28 (s, 2H), 5.93–5.99 (m, 1H), 7.57 (d, 1H,  $J=9.5$  Hz), 11.11 (s, 1H) ppm  $^{13}\text{C}$  NMR (100 MHz,  $\text{DMSO-d}_6$ )  $\delta$ =18.7, 26.2, 48.9, 121.9, 142.4, 144.3, 153.3, 169.2 ppm HRMS (ESI)  $[\text{M} + \text{H}]^+$ :  $m/z$  calcd for ( $\text{C}_8\text{H}_{12}\text{N}_3\text{O}_2$ ) 182.0930. Found 182.0938.

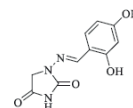
## 2.2.10 1-(((2E)-3-(4-methoxyphenyl)allylidene)amino)imidazolidine-2,4-dione (11)



Compound **11** was prepared according to the general procedure from compound **1** (0.5 g; 3.30 mmol) and

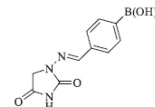
trans-4-methoxycinnamaldehyde (0.56 g; 3.46 mmol) as white solid (0.61 g; 71%). Mp 250 °C dec. IR (film,  $\text{cm}^{-1}$ )  $\nu_{\text{max}}$ =1770 (C=O), 1731 (C=O);  $^1\text{H}$  NMR (400 MHz,  $\text{DMSO-d}_6$ )  $\delta$ =3.78 (s, 3H), 4.29 (s, 2H), 6.85–7.00 (m, 4H), 7.51–7.59 (m, 3H), 11.18 (s, 1H) ppm  $^{13}\text{C}$  NMR (100 MHz,  $\text{DMSO-d}_6$ )  $\delta$ =48.8, 55.2, 114.3, 123.1, 128.5, 128.6, 138.5, 145.5, 153.3, 159.9, 169.1 ppm HRMS (ESI)  $[\text{M} + \text{H}]^+$ :  $m/z$  calcd for ( $\text{C}_{13}\text{H}_{14}\text{N}_3\text{O}_3$ ) 260.1035. Found 260.1047.

## 2.2.11. 1-((2,4-Dihydroxybenzylidene)amino)imidazolidine-2,4-dione (12)



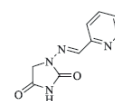
Compound **12** was prepared according to the general procedure from compound **1** (0.5 g; 3.30 mmol) and 2,4-dihydroxybenzaldehyde (0.48 g; 3.46 mmol) as white solid (0.72 g; 93%). Mp >300 °C. IR (film,  $\text{cm}^{-1}$ )  $\nu_{\text{max}}$ =3260 (OH), 3188 (OH), 1780 (C=O), 1717 (C=O);  $^1\text{H}$  NMR (400 MHz,  $\text{DMSO-d}_6$ )  $\delta$ =4.34 (s, 2H), 6.31 (d, 1H,  $J=2.3$  Hz), 6.35 (dd, 1H,  $J=8.5, 2.3$  Hz), 7.33 (d, 1H,  $J=8.5$  Hz), 7.90 (s, 1H), 9.90 (br s, 1H), 10.73 (s, 1H), 11.23 (br s, 1H) ppm  $^{13}\text{C}$  NMR (100 MHz,  $\text{DMSO-d}_6$ )  $\delta$ =48.5, 102.6, 107.8, 110.7, 130.5, 144.0, 153.3, 158.6, 160.5, 169.1 ppm HRMS (ESI)  $[\text{M} + \text{H}]^+$ :  $m/z$  calcd for ( $\text{C}_{10}\text{H}_{10}\text{N}_3\text{O}_4$ ) 236.0671. Found 236.0677.

## 2.2.12. 4-(((2,4-Dioxoimidazolidin-1-yl)imino)methyl)phenylboronic acid (13)

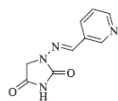


Compound **13** was prepared according to the general procedure from compound **1** (0.5 g; 3.30 mmol) and 4-formylphenylboronic acid (0.52 g; 3.46 mmol) as white solid (0.72 g; 88%). Mp >300 °C. IR (film,  $\text{cm}^{-1}$ )  $\nu_{\text{max}}$ =3349 (OH), 3173 (OH), 1780 (C=O), 1716 (C=O);  $^1\text{H}$  NMR (400 MHz,  $\text{DMSO-d}_6$ )  $\delta$ =4.37 (s, 2H), 7.64–7.68 (m, 2H), 7.79 (s, 1H), 7.83–7.87 (m, 2H), 8.12 (s, 2H), 11.26 (s, 1H) ppm  $^{13}\text{C}$  NMR (100 MHz,  $\text{DMSO-d}_6$ )  $\delta$ =48.9, 125.8, 134.5, 135.7, 136.0 (br) 143.0, 153.4, 169.1 ppm HRMS (ESI)  $[\text{M} + \text{H}]^+$ :  $m/z$  calcd for ( $\text{C}_{10}\text{H}_{11}\text{BN}_3\text{O}_4$ ) 248.0843. Found 248.0847.

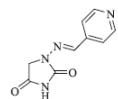
## 2.2.13. 1-((Pyridin-2-ylmethylene)amino)imidazolidine-2,4-dione (14)



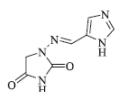
Compound **14** was prepared according to the general procedure from compound **1** (0.5 g; 3.30 mmol) and pyridine-2-carbaldehyde (0.33 ml; 3.46 mmol) as white solid (0.64 g; 95%). Mp 280 °C dec. IR (film,  $\text{cm}^{-1}$ )  $\nu_{\text{max}}$ =1770 (C=O), 1730 (C=O);  $^1\text{H}$  NMR (400 MHz,  $\text{DMSO-d}_6$ )  $\delta$ =4.43 (s, 2H), 7.61–7.66 (m, 1H), 7.89 (s, 1H), 8.02–8.06 (m, 1H), 8.16 (dt, 1H,  $J=7.7, 1.4$  Hz), 8.68–8.72 (m, 1H), 11.50 (s, 1H) ppm  $^{13}\text{C}$  NMR (100 MHz,  $\text{DMSO-d}_6$ )  $\delta$ =49.0, 121.6, 125.2, 139.3, 140.6, 146.8, 150.5, 153.3, 168.7 ppm HRMS (ESI)  $[\text{M} + \text{H}]^+$ :  $m/z$  calcd for ( $\text{C}_9\text{H}_9\text{N}_4\text{O}_2$ ) 205.0726. Found 205.0732.

**2.2.14. 1-((Pyridin-3-ylmethylene)amino)imidazolidine-2,4-dione (15)**

Compound **15** was prepared according to the general procedure from compound **1** (0.5 g; 3.30 mmol) and pyridine-3-carbaldehyde (0.33 ml; 3.46 mmol) as white solid (0.60 g; 90%). Mp 280 °C dec. IR (film,  $\text{cm}^{-1}$ )  $\nu_{\text{max}}$ =1764 (C=O), 1722 (C=O);  $^1\text{H}$  NMR (400 MHz,  $\text{D}_2\text{O}$  + NaOH + dioxane)  $\delta$ =7.46–7.51 (*m*, 1H), 7.56 (*s*, 1H), 8.18 (*td*, 1H, *J*=8.0, 1.8 Hz), 8.48 (*dd*, 1H, *J*=4.9, 1.6 Hz), 8.74 (*d*, 1H, *J*=1.8 Hz) ppm  $^{13}\text{C}$  NMR (100 MHz,  $\text{D}_2\text{O}$  + NaOH + dioxane)  $\delta$ =49.3 (*br*), 125.1, 131.6, 135.1, 138.9, 148.1, 149.7, 170.0, 186.3 ppm HRMS (ESI)  $[\text{M} + \text{H}]^+$ : *m/z* calcd for ( $\text{C}_9\text{H}_9\text{N}_4\text{O}_2$ ) 205.0726. Found 205.0731.

**2.2.15. 1-((Pyridin-4-ylmethylene)amino)imidazolidine-2,4-dione (16)**

Compound **16** was prepared according to the general procedure from compound **1** (0.5 g; 3.30 mmol) and pyridine-4-carbaldehyde (0.33 ml; 3.46 mmol) as white solid (0.61 g; 91%). Mp 280 °C dec. IR (film,  $\text{cm}^{-1}$ )  $\nu_{\text{max}}$ =1750 (C=O), 1723 (C=O);  $^1\text{H}$  NMR (400 MHz,  $\text{D}_2\text{O}$  + NaOH + dioxane)  $\delta$ =7.46 (*s*, 1H), 7.62–7.66 (*m*, 2H), 8.47–8.51 (*m*, 2H) ppm  $^{13}\text{C}$  NMR (100 MHz,  $\text{D}_2\text{O}$  + NaOH + dioxane)  $\delta$ =49.3 (*br*), 121.9, 139.2, 143.5, 149.7, 170.0, 186.4 ppm HRMS (ESI)  $[\text{M} + \text{H}]^+$ : *m/z* calcd for ( $\text{C}_9\text{H}_9\text{N}_4\text{O}_2$ ) 205.0726. Found 205.0730.

**2.2.16. 1-(((1*h*-Imidazol-5-yl)methylene)amino)imidazolidine-2,4-dione (17)**

Compound **17** was prepared according to the general procedure from compound **1** (0.5 g; 3.30 mmol) and 1*H*-imidazole-5-carbaldehyde (0.33 g; 3.46 mmol) as white solid (0.62 g; 97%). Mp 270 °C dec. IR (film,  $\text{cm}^{-1}$ )  $\nu_{\text{max}}$ =1764 (C=O), 1715 (C=O);  $^1\text{H}$  NMR (400 MHz,  $\text{D}_2\text{O}$  + NaOH + dioxane)  $\delta$ =7.45–7.48 (*m*, 1H), 7.67 (*s*, 1H), 7.72–7.76 (*m*, 1H) ppm  $^{13}\text{C}$  NMR (100 MHz,  $\text{D}_2\text{O}$  + NaOH + dioxane)  $\delta$ =49.5 (*br*), 125.1, 134.2, 136.5, 140.8, 170.3, 186.7 ppm HRMS (ESI)  $[\text{M} + \text{H}]^+$ : *m/z* calcd for ( $\text{C}_7\text{H}_8\text{N}_5\text{O}_2$ ) 194.0678. Found 194.0687.

**2.3. Ca inhibitory assay**

An Applied Photophysics stopped-flow instrument has been used for assaying the CA catalysed  $\text{CO}_2$  hydration activity, as reported earlier<sup>38,39</sup>. The inhibition constants were obtained by non-linear least-squares methods using PRISM 3 and the Cheng-Prusoff equation as reported earlier<sup>40</sup> and represent the mean from at least

three different determinations. The four tested CA isoforms were recombinant ones obtained in-house as reported earlier<sup>41–43</sup>.

**2.4. Computational studies**

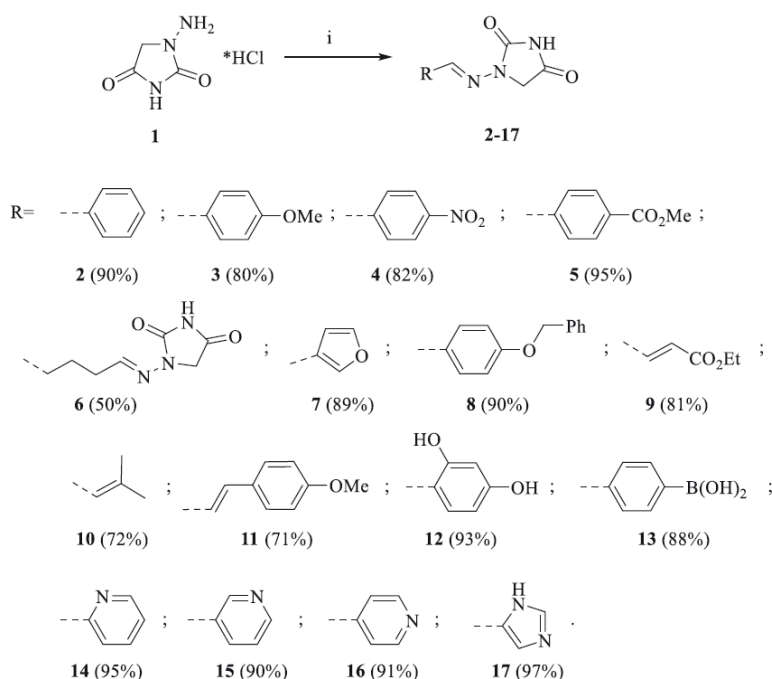
The crystal structure of CA II (pdb 5LJT)<sup>43</sup>, CA IX (pdb 5FL4)<sup>44</sup> and CA XII (pdb JLD0)<sup>45</sup> were prepared using the Protein Preparation Wizard tool implemented in Maestro - Schrödinger suite, assigning bond orders, adding hydrogens, deleting water molecules, and optimising H-bonding networks<sup>46</sup>. Energy minimisation protocol with a root mean square deviation (RMSD) value of 0.30 was applied using an Optimised Potentials for Liquid Simulation (OPLS3e) force field. 3D ligand structures were prepared by Maestro<sup>46a</sup> and evaluated for their ionisation states at pH 7.4 ± 0.5 with Epik<sup>46b</sup>. Additionally, the imidic nitrogen of the hydantoin nucleus was negatively charged in simulations. OPLS3e force field in Macromodel<sup>46e</sup> was used for energy minimisation for a maximum number of 2500 conjugate gradient iteration and setting a convergence criterion of 0.05 kcal mol<sup>-1</sup> Å<sup>-1</sup>. The docking grid was centred on the centre of mass of the co-crystallized ligands and Glide used with default settings. Ligands were docked with the standard precision mode (SP) of Glide<sup>46e</sup> and the best 5 poses of each molecule retained as output. The best pose for each compound, evaluated in terms of coordination, hydrogen bond interactions and hydrophobic contacts, was refined with Prime<sup>46d</sup> with a VSGB solvation model considering the target flexible within 3 Å around the ligand<sup>47–49</sup>.

The best poses of Furagin and **12** to CA II, CA IX and CA XII were submitted to a MD simulation using Desmond<sup>50</sup> and the OPL3e force field. Specifically, the system was solvated in an orthorhombic box using TIP4PEW water molecules, extended 15 Å away from any protein atom. It was neutralised adding chlorine and sodium ions. The simulation protocol included a starting relaxation step followed by a final production phase of 100 ns. In particular, the relaxation step comprised the following: (a) a stage of 100 ps at 10 K retaining the harmonic restraints on the solute heavy atoms (force constant of 50.0 kcal mol<sup>-1</sup> Å<sup>-2</sup>) using the NPT ensemble with Brownian dynamics; (b) a stage of 12 ps at 10 K with harmonic restraints on the solute heavy atoms (force constant of 50.0 kcal mol<sup>-1</sup> Å<sup>-2</sup>), using the NVT ensemble and Berendsen thermostat; (c) a stage of 12 ps at 10 K and 1 atm, retaining the harmonic restraints and using the NPT ensemble and Berendsen thermostat and barostat; (f) a stage of 12 ps at 300 K and 1 atm, retaining the harmonic restraints and using the NPT ensemble and Berendsen thermostat and barostat; (g) a final 24 ps stage at 300 K and 1 atm without harmonic restraints, using the NPT Berendsen thermostat and barostat. The final production phase of MD was run using a canonical NPT Berendsen ensemble at temperature 300 K. During the MD simulation, a time step of 2 fs was used while constraining the bond lengths of hydrogen atoms with the M-SHAKE algorithm. The atomic coordinates of the system were saved every 100 ps along the MD trajectory. Protein and ligand RMSD values, ligand torsions evolution and occupancy of intermolecular hydrogen bonds and hydrophobic contacts were computed along the production phase of the MD simulation with the Simulation Interaction Diagram tools implemented in Maestro.

**3. Results and discussion****3.1. Chemistry**

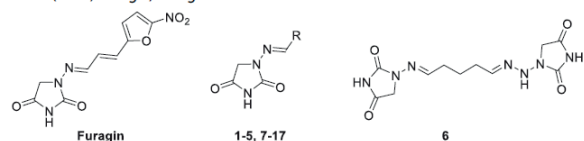
A series of Furagin derivatives **2–17** were prepared in reaction between 1-aminohydantoin hydrochloride (**1**) and various





Scheme 1. Reagents and conditions: i. RCHO, EtOH, RT, 16 h

Table 1. Inhibition data of human CA isoforms CA I, II, IX, and XII with aminohydantoin derivatives (2–17, Furagin) using AAZ as a standard inhibitor.



Comp.	R	$K_i$ (nM)*			
		CA I	CA II	CA IX	CA XII
2	C <sub>6</sub> H <sub>5</sub>	39 600	900	3500	5600
3	4-OCH <sub>3</sub> -C <sub>6</sub> H <sub>4</sub>	57 600	6400	1200	4700
4	4-NO <sub>2</sub> -C <sub>6</sub> H <sub>4</sub>	>100 000	11 100	7400	2800
5	4-(CO <sub>2</sub> CH <sub>3</sub> )-C <sub>6</sub> H <sub>4</sub>	>100 000	8300	4900	930
6	-	19 100	4000	1100	160
7	3-furanyl	16 800	710	850	1700
8	4-(OCH <sub>2</sub> C <sub>6</sub> H <sub>5</sub> )-C <sub>6</sub> H <sub>4</sub>	>100 000	540	350	910
9	CHCH(CO <sub>2</sub> C <sub>2</sub> H <sub>5</sub> )	45 900	23 600	810	440
10	CHC(CH <sub>3</sub> ) <sub>2</sub>	28 800	16 500	2900	880
11	CHCH(4-OCH <sub>3</sub> -C <sub>6</sub> H <sub>4</sub> )	>100 000	3100	400	360
12	2,4-(OH) <sub>2</sub> -C <sub>6</sub> H <sub>3</sub>	>100 000	59 900	5800	150
13	4-(B(OH) <sub>2</sub> )-C <sub>6</sub> H <sub>4</sub>	90 700	14 200	7300	230
14	2-pyridyl	51 800	4200	4500	1300
15	3-pyridyl	45 600	620	2300	3200
16	4-pyridyl	26 600	3300	1600	810
17	5-imidazolyl	9600	12 400	560	350
Furagin	-	>100 000	9600	260	57
AAZ	-	250	12	25	6

\*Mean from 3 different assays, by a stopped flow technique (errors were in the range of  $\pm$  5–10% of the reported values).

aldehydes (Scheme 1). Compounds 2–17 were isolated in good to excellent yields, all new structure were proven by <sup>1</sup>H and <sup>13</sup>C NMR and IS spectroscopy as well as high-resolution mass spectra. The purity of all compounds was greater than 95% according UPLC analysis.

### 3.2. Biological evaluation

The CA inhibitory profiles of Furagin and synthesised aminohydantoin derivatives were evaluated by applying a stopped flow carbon dioxide hydrase assay<sup>51</sup>, in comparison to acetazolamide (AAZ) as a standard CAI against four physiologically significant isoforms CA I, II, IX, and XII. The following structure–activity relationship (SAR) can be concluded from the inhibition data presented in Table 1.

- All the tested aminohydantoin exhibited weak inhibitory effect on the slow cytosolic isoform, hCA I, where the binding affinity constant ( $K_i$ ) values fluctuating in the thousands nM range ( $K_i$  16 800–>100 000 nM).
- The physiologically relevant isoform, hCA II, was better inhibited by most of the tested compounds ( $K_i$ s: 620–59 000 nM). It is observed that, the aminohydantoin compounds (2, 7, 8 and 15) were more potent hCA II inhibitors with  $K_i$ s in range from 540–900 nM. These compounds have unsubstituted Ph or hetaryl moieties. Rest of the compounds showed weaker inhibitory effect of CA II with  $K_i$ s in range from 3100–59 900 nM. It is interesting to note, that compound 12 having dihydroxyphenyl substituent stood out by nearly three times weaker inhibition compare to the second weakest inhibitor 9.
- The tumour associated isoform hCA IX was inhibited in nanomolar range by compounds 7–9, 11, 17 and Furagin ( $K_i$ s: 260–850 nM), where the strongest inhibition was observed for Furagin. Rest of the aminohydantoin derivatives showed one order weaker inhibition with  $K_i$ s in range from 1100–7 300 nM. Certain pattern can be observed, where better CA IX inhibition can be observed for compounds with vinyl substituents (9, 11, 17 and Furagin) or small hetaryl substituents (7 and 17), with exception in case of compound 8, containing ester moiety on phenyl ring.

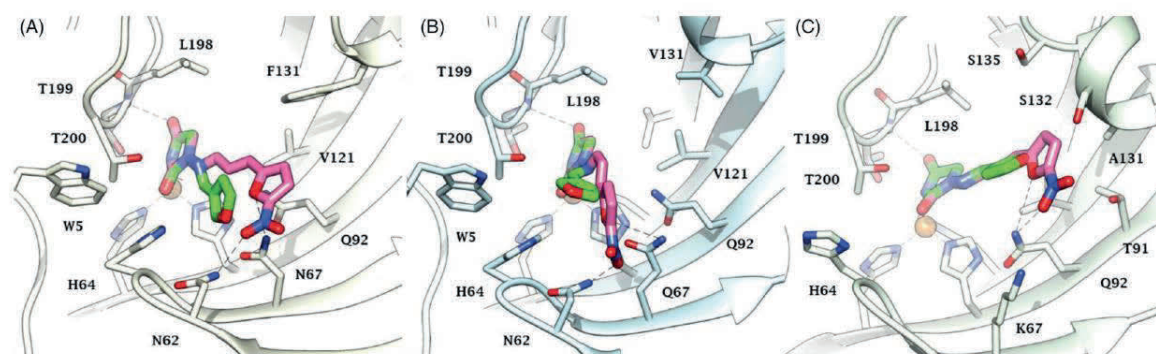


Figure 2. Predicted docking orientations of **7** (green) and Furagin (pink) to (A) CA II, (B) CA IX and (C) CA XII.

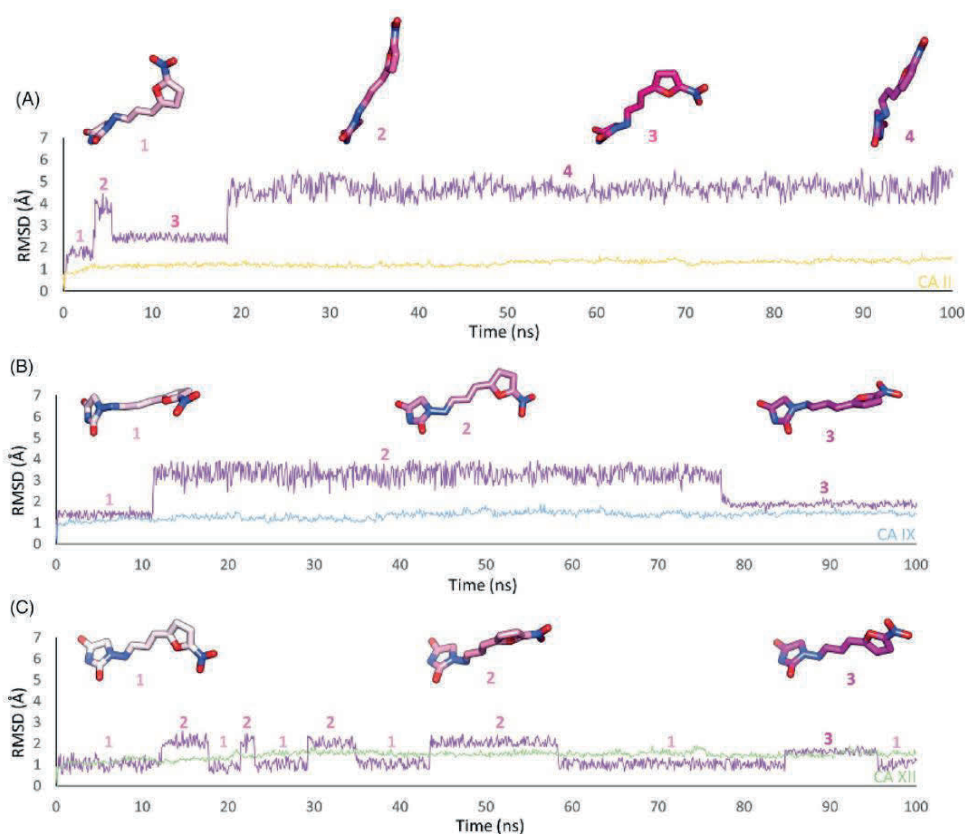


Figure 3. RMSD analysis of Furagin heavy atoms and (A) CA II, (B) CA IX and (C) CA XII backbone over the 100 ns MD simulation. The ligand colour darkens over the dynamic simulation.

- d. The other tumour associated isoform hCA XII was best inhibited among all isoforms studied. The best compound of this series was Furagin with  $K_i = 57$  nM. It was followed by vinyl substituted aminohydantoin derivatives **6**, **9** and **10** with  $K_S$  160, 360 and 880 nM, respectively. One order weaker CA XII inhibition compare to Furagin was also observed for aryl (**5**, **8** and **12**) and hetaryl (**16** and **17**) derivatives ranging  $K_S$  from 150 to 930 nM.

In general good selectivity against cancer associated CA isoforms (CA IX and CA XII) compare to off-target ones (CA I and CA II) was observed for three compounds Furagin, **9** and **12**.

### 3.3. Computational studies

Docking studies were used to investigate the binding mode of Furagin and aminohydantoin derivatives **2-17** within the active site of CA II (pdb 5LJT)<sup>44</sup>, IX (pdb 5FL4)<sup>43</sup> and XII (pdb JLD0)<sup>45</sup>. Similarly to benzenesulfonamides (pKa 10.1) which binds to the CA Zn ion in the deprotonated form, the imidic nitrogen of the hydantoin nucleus as well as considered negatively charged (pKa 9.16)<sup>52</sup> in the docking experiments and resulted to coordinate the zinc ion in all the obtained poses with CAs II, IX and XII. Furthermore, the oxygen atom of the CO in position 4 of the hydantoin core acts as a bifurcated acceptor establishing two H-bonds with T199, that

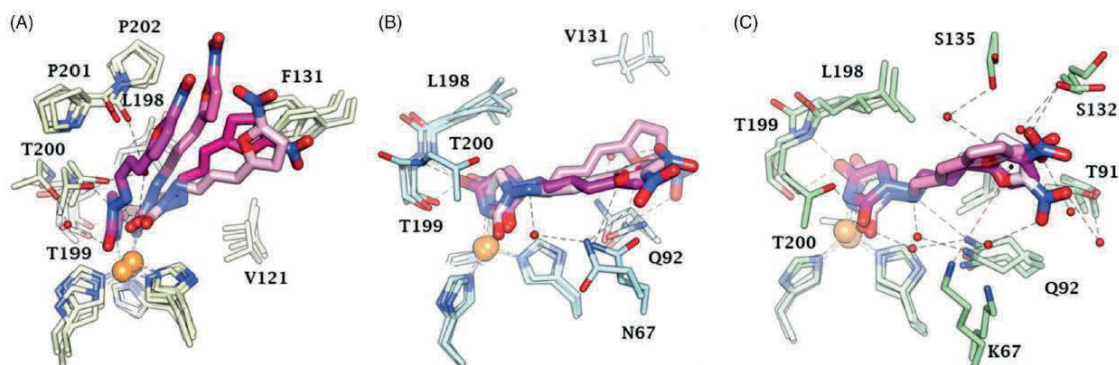


Figure 4. Dynamics evolution of the binding mode of Furagin to (A) CA II, (B) CA IX and (C) CA XII over the course of 100 ns. Water molecules are represented as red spheres. The ligand colour darkens over the dynamic simulation.

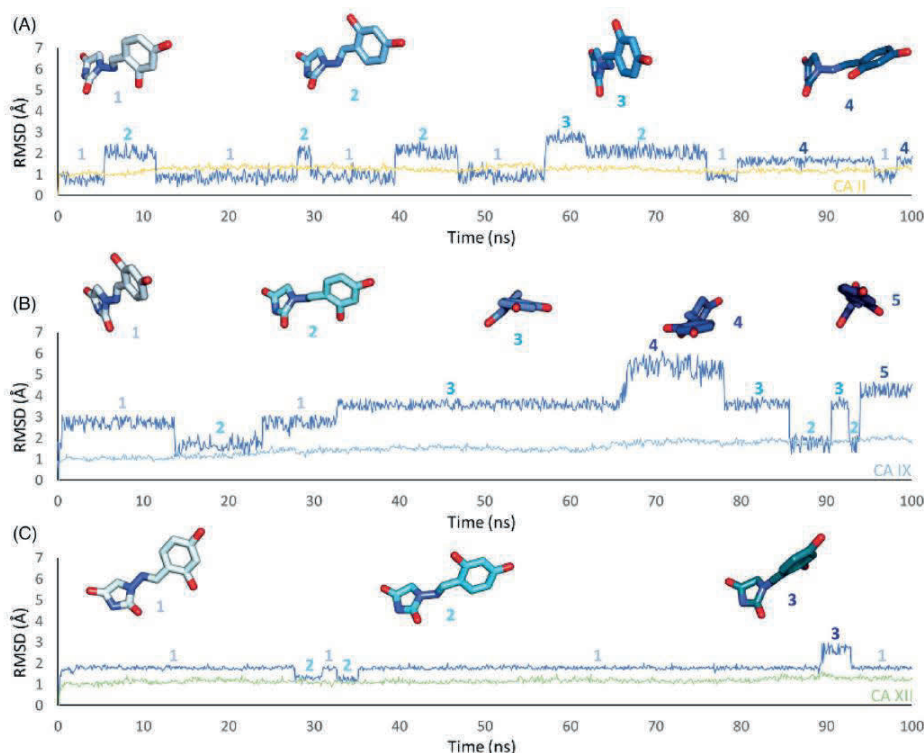


Figure 5. RMSD analysis of 12 heavy atoms and (A) CA II, (B) CA IX and (C) CA XII backbone over the 100 ns MD simulation. The ligand colour darkens over the dynamic simulation.

is,  $O \cdots (H-N, HG1-O)$ , whereas overall the heterocycle forms VdW contacts with residues H94, H96, H119, L198, T200 and W209 (Figure 2).

In CA II and CA IX, the  $N_1$  pendants of all ligands are oriented towards a hydrophilic cleft defined by H4, W5, N62, N67 and H64, except **8** and **9**, whose  $N_1$  tails are housed, in CA II, into a hydrophobic pocket formed by I91, V121 and F131 (Figure 2(A–B)). Amino acids T91, Q92, A131, S132 and S135 are instead targeted by the pendants on the aminohydantoin of the ligands in all docking solutions with CA XII (Figure 2(C)). The docking procedure was complemented with 100 ns long molecular dynamic (MD)

simulations on the predicted binding conformations of Furagin and **12**, the most potent CA XII inhibitors also showing significant CA XII over CA II selectivity. The structure of the three investigated CA isoforms was stable during the computation with the backbone atom RMSDs exhibiting small fluctuations over the 100 ns (Figures 3 and 5). Additionally, the ZBG of the ligands remains stably anchored to the metal ion all over the MD, with the hydantoin core receiving H-bonds by the amidic NH and side chain OH of Thr199 (Figures 4 and 6).

After an initial equilibration, mainly occurring in CA II and IX, the molecular tail of Furagin undergoes minor conformational

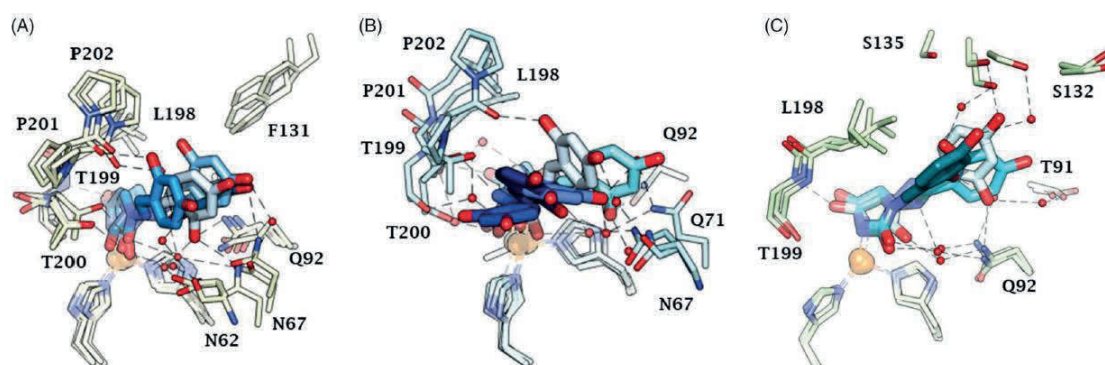


Figure 6. Dynamics evolution of the binding mode of **12** to (A) CA II, (B) CA IX and (C) CA XII over the course of 100 ns. Water molecules are represented as red spheres. The ligand colour darkens over the dynamic simulation.

fluctuations during simulation approaching to stable binding conformations within the three CA isoforms (Figures 3 and 4). In CA IX and XII, the ligand accommodates the N1-pendant in the hydrophilic half of the active sites where it makes VdW contacts and both direct and water mediated H-bond interactions with the enzymes (Figure 4(B,C)). In the CA II, the ligand-bound conformation of Furagin orients the tail towards the hydrophobic area of the target and does not form persistent H-bond interactions over the 100 ns (Figure 4(A)). The hydrogen bond persistence within the three CA isoforms is in good agreement with the inhibitory profile of the ligand (CAXII > CA IX > CA II).

An ensemble of few conformations is representative of the binding of **12** within CA II and IX (Figures 5 and 6). Here, the ligand approaches the hydrophobic regions of the enzymes and, coming next to the end of the simulation, the N<sub>1</sub> tails lose direct or water-bridged H-bonds with glutamine and asparagine residues, progressively moving towards T199 or T200, that is, the area of the enzyme that undergoes to the greatest residue displacement. In CA XII, the docked pose of **12** remains firmly anchored to the residues of the hydrophilic portion of the enzyme throughout the dynamic. A wide network of direct and water mediated H-bonds stabilise the binding of the ligand. This is consistent with the inhibition profile exhibited by **12** in CA XII as compared with the other two CA isoforms.

#### 4. Conclusions

In summary, we have demonstrated that clinically used antibiotic – Furagin and its derivatives **2-17** are potential CA inhibitors. Furagin and all newly synthesised hydantoin derivative were examined for their inhibitory activities towards hCA I, II, IX and XII. The four studied hCA isoforms were inhibited by Furagin and its derivatives at various degrees. In particular, Furagin and prepared compounds **2-17** did not inhibit or poorly inhibited off-target hCA I with  $K_i$ s ranging from >100  $\mu$ M (compounds **4**, **5**, **8**, **11**, **12** and Furagin) to 9.6  $\mu$ M. Ubiquitous hCA II was poorly inhibited by compounds **3-6**, **9-14**, **16**, **17** and Furagin ( $K_i$ s from 59.9 to 3.1  $\mu$ M). Rest of the compounds significantly inhibited hCA II ( $K_i$ s from 900 nM to 540 nM). Remarkable inhibition of cancer associated hCA IX was observed for Furagin ( $K_i$ =260 nM) and compounds **7-9**, **11** and **17** with  $K_i$ s ranging from 350 to 850 nM. The rest of compounds exhibited slightly weaker inhibition of hCA IX with  $K_i$ s ranging from 1100 to 7400 nM. Other cancer associated isoform – hCA XII also was significantly inhibited by Furagin ( $K_i$ =57 nM) and compounds **5**, **6**, **8-13**, **16** and **17** ( $K_i$ s from 160 to

910 nM). The rest of the compounds exhibited slightly weaker inhibition with  $K_i$ s ranging from 1300 to 5600 nM. Docking and molecular dynamics simulations shed light on the ligands selectivity for the cancer-associated CAs over ubiquitous CA II. The significant inhibition activity and especially selectivity of Furagin against hCA IX and XII was attributed due to the strong H-bond interactions, whereas in case of hCA II no persistent H-bond interactions are formed due to Furagin's tails orientation towards hydrophobic area of the enzyme.

The knowledge obtained gives the solid base for both – investigation of drug repurposing of clinically used antibiotic Furagin for anti-cancer therapy and further studies of new chemotype of inhibitors of CAs.

#### Disclosure statement

The authors have no relevant affiliations of financial involvement with any organisation or entity with a financial interest in or financial conflict with the subject matter or materials discussed in the manuscript.

#### ORCID

Claudiu T. Supuran  <http://orcid.org/0000-0003-4262-0323>

#### References

- Supuran CT. Structure and function of carbonic anhydrases. *Biochem J* 2016;473:2023–32.
- Alterio V, Di Fiore A, D'Ambrosio K, et al. Multiple binding modes of inhibitors to carbonic anhydrases: how to design specific drugs targeting 15 different isoforms. *Chem Rev* 2012;112:4421–68.
- Supuran CT. Carbonic anhydrases: novel therapeutic applications for inhibitors and activators. *Nature Rev Drug Discov* 2008;7:168–81.
- Jensen EL, Clement R, Kosta A, et al. A new widespread subclass of carbonic anhydrase in marine phytoplankton. *Isme J* 2019;13:2094–106.
- Del Prete S, Vullo D, Fisher GM, et al. Discovery of a new family of carbonic anhydrases in the malaria pathogen *Plasmodium falciparum* – the  $\eta$ -carbonic anhydrases. *Bioorg Med Chem Lett* 2014;24:4389–96.

6. Xu Y, Feng L, Jeffrey PD, et al. Structure and metal exchange in the cadmium-carbonic anhydrase of marine diatoms. *Nature* 2008;452:56–61.
7. Supuran CT, Capasso C. Biomedical applications of prokaryotic carbonic anhydrases. *Expert Opin Ther Pat* 2018;28:745–54.
8. Capasso C, Supuran CT. An overview of the alpha-, beta- and gamma-carbonic anhydrases from bacteria: can bacterial carbonic anhydrases shed new light on evolution of bacteria?. *J Enzyme Inhib Med Chem* 2015;30:325–32.
9. Capasso C, Supuran CT. Bacterial, fungal and protozoan carbonic anhydrases as drug targets. *Expert Opin Ther Targets* 2015;19:1689–704.
10. Capasso C, Supuran CT. Anti-infective carbonic anhydrase inhibitors: a patent and literature review. *Expert Opin Ther Pat* 2013;23:693–704.
11. Nocentini A, Supuran CT. Advances in the structural annotation of human carbonic anhydrases and impact on future drug discovery. *Expert Opin Drug Discov* 2019;14:1175–97.
12. Supuran CT. Advances in structure-based drug discovery of carbonic anhydrase inhibitors. *Expert Opin Drug Discov* 2017;12:61–88.
13. Supuran CT. How many carbonic anhydrase inhibition mechanisms exist?. *J Enzyme Inhib Med Chem* 2016;31:345–60.
14. De Simone G, Supuran CT. (In)organic anions as carbonic anhydrase inhibitors. *J Inorg Biochem* 2012;111:117–29.
15. Supuran CT. Carbonic anhydrase inhibitors as emerging agents for the treatment and imaging of hypoxic tumors. *Expert Opin Investig Drugs* 2018;27:963–70.
16. Supuran CT. Carbonic anhydrase inhibitors and their potential in a range of therapeutic areas. *Expert Opin Ther Pat* 2018;28:709–12.
17. Supuran CT. Applications of carbonic anhydrases inhibitors in renal and central nervous system diseases. *Expert Opin Ther Pat* 2018;28:713–21.
18. Supuran CT, Alterio V, Di Fiore A, et al. Inhibition of carbonic anhydrase IX targets primary tumors, metastases, and cancer stem cells: three for the price of one. *Med Res Rev* 2018;38:1799–836.
19. Neri D, Supuran CT. Interfering with pH regulation in tumours as a therapeutic strategy. *Nat Rev Drug Discov* 2011;10:767–77.
20. Da'dara AA, Angeli A, Ferraroni M, et al. Crystal structure and chemical inhibition of essential schistosome host-interactive virulence factor carbonic anhydrase SmCA. *Commun Biol* 2019;2:333.
21. Supuran CT. Carbonic anhydrases and metabolism. *Metabolites* 2018;8:25.
22. Supuran CT. Carbonic anhydrase inhibition and the management of hypoxic tumors. *Metabolites* 2017;7:E48.
23. Tars K, Vullo D, Kazaks A, et al. Sulfocoumarins (1,2-benzoxathiine 2,2-dioxides): a class of potent and isoform-selective inhibitors of tumor-associated carbonic anhydrases. *J Med Chem* 2013;56:293–300.
24. Nocentini A, Ceruso M, Carta F, et al. 7-Aryl-triazolyl-substituted sulfocoumarins are potent, selective inhibitors of the tumor-associated carbonic anhydrase IX and XII. *J Enzyme Inhib Med Chem* 2016;31:1226–33.
25. Grandane A, Tanc M, Di Cesare Mannelli L, et al. Substituted sulfocoumarins are selective carbonic anhydrase IX and XII inhibitors with significant cytotoxicity against colorectal cancer cells. *J Med Chem* 2015;58:3975–83.
26. Tanc M, Carta F, Bozdog M, et al. 7-Substituted-sulfocoumarins are isoform-selective, potent carbonic anhydrase II inhibitors. *Bioorg Med Chem* 2013;21:4502–10.
27. Touisni N, Maresca A, McDonald PC, et al. Glycosylcoumarin carbonic anhydrase IX and XII inhibitors strongly attenuate the growth of primary breast tumors. *J Med Chem* 2011;54:8271–7.
28. Maresca A, Temperini C, Pochet L, et al. Deciphering the mechanism of carbonic anhydrase inhibition with coumarins and thiocoumarins. *J Med Chem* 2010;53:335–44.
29. Temperini C, Innocenti A, Scozzafava A, et al. The coumarin binding site in carbonic anhydrase accommodates structurally diverse inhibitors: the antiepileptic lacosamide as an example. *J Med Chem* 2010;53:850–4.
30. Maresca A, Temperini C, Vu H, et al. Non-zinc mediated inhibition of carbonic anhydrases: coumarins are a new class of suicide inhibitors. *J Am Chem Soc* 2009;131:3057–62.
31. Pustenko A, Stepanovs D, Žalubovskis R, et al. 3H-1,2-benzoxathiepine 2,2-dioxides: a new class of isoform-selective carbonic anhydrase inhibitors. *J Enzyme Inhib Med Chem* 2017;32:767–75.
32. Ivanova J, Carta F, Vullo D, et al. N-Substituted and ring opened saccharin derivatives selectively inhibit transmembrane, tumor-associated carbonic anhydrases IX and XII. *Bioorg Med Chem* 2017;25:3583–9.
33. Alterio V, Tanc M, Ivanova J, et al. X-ray crystallographic and kinetic investigations of 6-sulfamoyl-saccharin as a carbonic anhydrase inhibitor. *Org Biomol Chem* 2015;13:4064–9.
34. Ivanova J, Leitans J, Tanc M, et al. X-ray crystallography-promoted drug design of carbonic anhydrase inhibitors. *Chem Commun (Camb)* 2015;51:7108–11.
35. Chernov NM, Koshevenko AS, Yakovlev IP, et al. Synthesis and antimicrobial activity of 4-hydroxy-2-[5-nitrofur(then)-2-yl]-6h-1,3-oxazin-6-ones. *Pharm Chem J* 2017;51:644–7.
36. Gut J, Novacek A, Fiedler P. Reaction of six-membered cyclic hydrazides with aromatic aldehydes. *Collect Czechoslovak Chem Comm* 1968;33:2087–96.
37. Wang Q, Liu Y-C, Chen Y-J, et al. Development of a direct competitive chemiluminescent ELISA for the detection of nitrofurantoin metabolite 1-amino-hydantoin in fish and honey. *Anal Methods* 2014;6:4414–20.
38. Nocentini A, Ceruso M, Bua S, et al. Discovery of  $\beta$ -adrenergic receptors blocker-carbonic anhydrase inhibitor hybrids for multitargeted antiglaucoma therapy. *J Med Chem* 2018;61:5380–94.
39. Köhler K, Hillebrecht A, Schulze Wischeler J, et al. Saccharin inhibits carbonic anhydrases: possible explanation for its unpleasant metallic aftertaste. *Angew Chem Int Ed Engl* 2007;46:7697–9.
40. Eldehna WM, Nocentini A, Bonardi A, et al. 3-Hydrazinoisatin-based benzenesulfonamides as novel carbonic anhydrase inhibitors endowed with anticancer activity: Synthesis, *in vitro* biological evaluation and *in silico* insights. *Eur J Med Chem* 2019;184:111768.
41. Eldehna WM, Nocentini A, Al-Rashood ST, et al. Tumor-associated carbonic anhydrase isoform IX and XII inhibitory properties of certain isatin-bearing sulfonamides endowed with *in vitro* antitumor activity towards colon cancer. *Bioorg Chem* 2018;81:425–32.
42. Al-Sanea MM, Elkamhaway A, Paik S, et al. Synthesis and biological evaluation of novel 3-(quinolin-4-ylamino)benzenesulfonamides as carbonic anhydrase isoforms I and II inhibitors. *J Enzyme Inhib Med Chem* 2019;34:1457–64.

43. Leitans J, Kazaks A, Balode A, et al. Efficient expression and crystallization system of cancer-associated carbonic anhydrase isoform IX. *J Med Chem* 2015;58:9004–9.
44. Nocentini A, Ferraroni M, Carta F, et al. Benzenesulfonamides incorporating flexible Triazole moieties are highly effective carbonic anhydrase inhibitors: synthesis and kinetic, crystallographic, computational, and intraocular pressure lowering investigations. *J Med Chem* 2016;59:10692–704.
45. Whittington DA, Waheed A, Ulmasov B, et al. Crystal structure of the dimeric extracellular domain of human carbonic anhydrase XII, a bitopic membrane protein overexpressed in certain cancer tumor cells. *Proc Natl Acad Sci USA* 2001;98:9545–50.
46. Schrödinger Suite Release 2019-1, Schrödinger, LLC, New York, NY, 2019: (a) Prime, v.5.5; Maestro v.11.9; (b) Epik, v.4.7; (c) Impact, v.8.2; (d) Macromodel v.12.3. (e) Glide, v.8.2.
47. (a) Nocentini A, Gratteri P, Supuran CT. Phosphorus versus Sulfur: Discovery of Benzenephosphonamidates as Versatile Sulfonamide-Mimic Chemotypes Acting as Carbonic Anhydrase Inhibitors. *Chemistry* 2019;25:1188–92. (b) Supuran CT. Carbon- versus sulphur-based zinc binding groups for carbonic anhydrase inhibitors? *J Enzyme Inhib Med Chem* 2018;33:485–95. 33: 1453–9.
48. Nocentini A, Bonardi A, Gratteri P, et al. Steroids interfere with human carbonic anhydrase activity by using alternative binding mechanisms. *J Enzyme Inhib Med Chem* 2018;33: 1453–9.
49. Nocentini A, Carta F, Tanc M, et al. Deciphering the mechanism of human carbonic anhydrases inhibition with sulfocoumarins: computational and experimental studies. *Chemistry* 2018;24:7840–4.
50. Schrödinger Release 2019-2: Desmond Molecular Dynamics System, D. E. Shaw Research, New York, NY, 2019, v.5.7.
51. Khalifah RG. The carbon dioxide hydration activity of carbonic anhydrase. I. Stop-flow kinetic studies on the native human isoenzymes B and C. *J Biol Chem* 1971;246:2561–73.
52. Verdolino V, Cammi R, Munk BH, et al. Calculation of pKa values of nucleobases and the guanine oxidation products guanidinohydantoin and spiroiminodihydantoin using density functional theory and a polarizable continuum model. *J Phys Chem B* 2008;112:16860–73.